ACTA MINERALOGICA PAKISTANICA

ISSN 0257-3660

Volume 11 2000

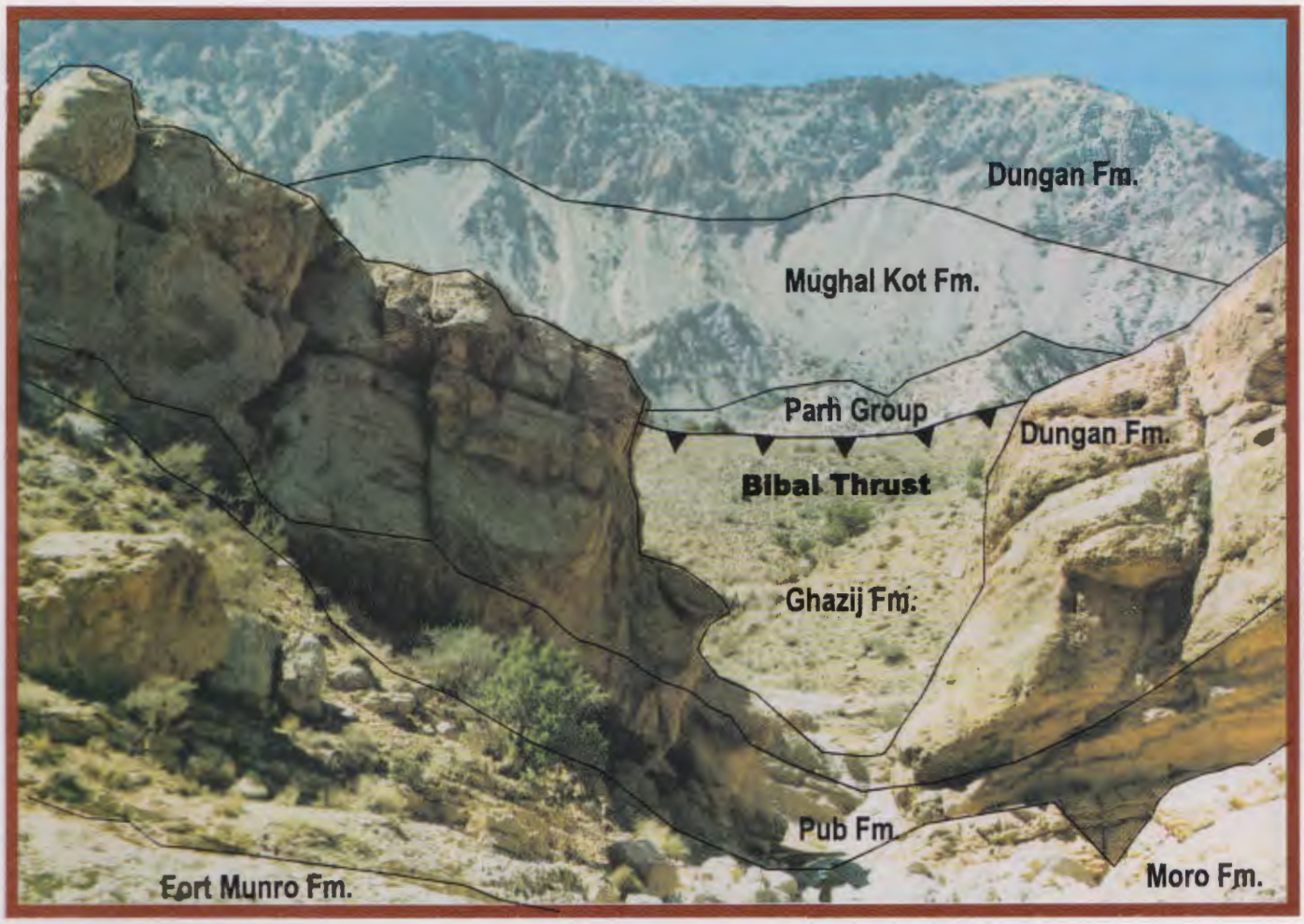

NATIONAL CENTRE OF EXCELLENCE IN MINERALOGY
UNIVERSITY OF BALOCHISTAN,
QUETTA, PAKISTAN

ACTA MINERALOGICA PAKISTANICA

An annual publication of the National Centre of Excellence in Mineralogy, Quetta Pakistan

VOLUME 11 **2000**

On Cover *Upper Cretaceous-Paleocene succession of the Spera Ragha-Chinjun Valley in the foreground and Urghargai-Mazu Ghar in the background. The two successions have been juxtaposed by Bibai Thrust. Photo looking to southwest from Lel Gat (Grid Ref. 628622). The stratigraphy and geological structures of the area are described in this volume by Kassi and others. Photo courtesy of M.A.Farooqui, labelled by A.M.* Kassi.

Address for correspondence	Editor, *Acta Mineralogica Pakistanica*, National Centre of Excellence in Mineralogy, University of Balochistan, Quetta. Pakistan. Phone No. (081) 9211323, Fax No. (081) 9211285 cem@minerals.qta.sdnpk.undp.org cem@uob.qta.sdnpk.undp.org
ISSN	0257-3660
Copyright	©Centre of Excellence in Mineralogy, University of Balochistan, Quetta.
Price for volume 11	Rs. 200.00, US$12.00, UK£8.00 (includes postage and handling)
Type setting and composing	Mohammad Ahmad Farooqui
Printed at	United Printers, Zonki Ram Road, Quetta.

Published in June 2001

ACTA MINERALOGICA PAKISTANICA

VOLUME 11

2000

CONTENTS

ARTICLES

ABSTRACTS

REPORTS

ACTA MINERALOGICA PAKISTANICA
Volume 11 (2000)

Article Reference AMP11.2000/001-024/ISSN0257-3660

THE UPPER CRETACEOUS BIBAI SUBMARINE FAN (BIBAI FORMATION), KACH ZIATRAT VALLEY, WESTERN SULAIMAN THRUST-FOLD BELT, PAKISTAN

ABDUL TAWAB KHAN[1], *AKHTAR MOHAMMAD KASSI*[1] *and ABDUL SALAM KHAN*[2]
[1]Department of Geology University of Balochistan, Quetta, Pakistan
[2]Centre of Excellence in Mineralogy, University of Balochistan, Quetta, Pakistan

ABSTRACT

The Upper Cretaceous Bibai Formation is exposed in Kach-Ziarat and Spera Ragha-Chinjun valleys and near Muslimbagh, within the western part of the Sulaiman Thrust-Fold Belt. The formation generally comprises basic volcanic rocks, volcanic conglomerate and breccia, sandstone, mudstone and ash beds. Within the Kach-Ziarat valley it is dominantly composed of volcaniclastic sediments and rarely lava flows, while, within the Spera Ragha-Chinjun valley dominantly the in-situ basaltic volcanic rocks. Volcaniclastic succession of the Kach-Ziarat valley may be categorized into various facies like volcanic conglomerate (VC), volcanic breccia (VB), sandstone (SS), sandstone rhythmically interbedded with mudstone (SSMS), mudstone (MS), limestone (LS) and lava flows (VOL). These facies posses characters which indicate deposition by sediment gravity flows and slumping. Volcanic conglomerate and sandstone (VC-SS) association of facies, their stacking pattern, erosive bases and fining-upward trends suggest deposition within a channelized complex anastomosing on a submarine fan system. The SSMS facies of sandstone rhythmically interbedded with mudstone, is characterized by grading, Bouma Tabcde, Tbcde, Tcde and Tde sequences, sole marks, soft sediment deformation, pinch-and-swell and general thinning- and fining-upward trends of 2nd-order cycles. It indicates deposition by turbidity currents in overbank (-levee) complex between channels. The mudstone (MS) facies, possessing occasional thin sandstone and siltstone beds in lower part and profusion of shallow marine fauna in upper part, indicate deposition in lower fan / basin plane conditions and also an overall shallowing-up trend of the succession. Limestone (LS) facies, interbedded with volcaniclastic facies in lower part of the formation, is very finely crystalline (bio-micritic) possessing foraminifera of the Globotruncana family suggest deposition during calm periods when gravity flows had been suspended intermittently. Paleocurrent pattern indicate a south-southwest paleo-flow direction and a source area to the north-northeast of Bibai Peak.

Based on characters of various facies associations, their vertical and lateral organization, paleocurrent pattern and composition of detritus, it is proposed that the Bibai formation comprises a special category of "channel (-levee) -overbank complex", we name it the Bibai Submarine Fan, which developed on the slope of a series of seamounts (hotspot volcanos). Lithofacies and their associations clearly define the mid-fan, overbank (-levee) and lower-fan/ basin plane components of the submarine fan. Seamounts developed on sea floor of the northwestern margin of the Indo-Pakistan Plate, which later on emerged and provided detritus

to the Bibai Submarine Fan. It is proposed that he present trend of paleocurrents, generally southward, has been rotated anticlockwise along with the north and northeastward drift and anticlockwise rotation of the Indo-Pakistan Plate towards Eurasia during the Upper Cretaceous and later periods till present time. Its clockwise rotation back to its Upper Cretaceous (71.4±3.4 My) position would give its original west-northwestward paleoslope at the northwestern margin of the Indo-Pakistan Plate.

INTRODUCTION

The Upper Cretaceous Bibai formation (Kazmi 1955, 1979) is widely exposed at Kach-Ziarat valley, western Sulaiman Thrust-Fold Belt, east of the Quetta Syntaxes (Fig.1). Within the Kach-Ziarat valley the formation mainly comprises volcanic conglomerate, breccia, sandstone and mudstone, whereas, within the Spera Ragha-Chinjun valley, mainly the *in-situ* volcanic rocks. Initially the formation was included within the Mughal Kot Formation (Kahan Conglomerate member) by Williams (1959). The Hunting Survey Corporation (1960) referred to it as "Parh-related volcanics" and considered it as part of the Parh Group. Shah (1977) included these "Parh-related volcanics" and volcaniclastic succession of the Kach-Ziarat valley in the Bela Volcanic Group. Within the Kach-Ziarat valley, the formation conformably and transitionally overlies the Cretaceous Parh Limestone and conformably and transitionally underlies the Maestrichtian Pab Sandstone and Paleocene Dungan Formation.

Kazmi (1955, 1979) provided lithological details of the volcaniclastic succession of the formation and proposed the name Bibai formation for the volcanic and volcaniclastic succession. McCormick (1985), Khan (1986), Otsuki et al. (1989), Kassi et al. (1993) and Siddiqui et al. (1994, 1996) studied the formation within the Chinjun, Spera Ragha, Kach-Ziarat and surrounding areas. Kassi et al. (1993), initiated study of the volcaniclastic succession and have shown that volcaniclastic succession of the Bibai formation in Kach-Ziarat valley comprises turbidites. DeJong and Subhani (1979) and Otsuki et al. (1989) studied these rocks around Muslimbagh area and considered them as Andean-Type volcanics formed at the northwestern margin of the Indian Plate. Petrology and petro-chemistry of the *in-situ* volcanic rocks (basaltic lava flows) have been studied in Spera-Ragha-Chinjun valley and Muslimbagh region by Khan (1986), McCormick (1986), Sawada et al. (1992), Siddiqui et al. (1994) and Baloch and McCormick (1995). McCormick (1985), Sawada et al. (1992) and Siddiqui et al. (1994, 1996) interpreted the Bibai Volcanics as within-plate hotspot volcanics. K-Ar age dating of the Bibai Volcanics has been carried out by Sawada et al. (1995) who have proposed an age of 71.4+3.4 My for the Bibai Volcanics. Determination of age based on paleomagnetic studies have been carried out by Khadim et al. (1992) and Yoshida et al. (1995) who assigned Campanian to Maestrichtian age to the Bibai formation.

This paper presents the description and interpretation of the sedimentary facies of volcaniclastic succession of the Bibai formation in Kach-Ziarat valley. Also depositinal model has been proposed on the basis of various facies associations and their vertical and lateral organization.

SEDIMENTARY FACIES

Sedimentary facies in 14 sections were studied within the Kach-Ziarat valley (Fig. 1) near Kach, Ahmadun, Gogai, Spina Khaizai, Shina Khawra, north of Kawasa, Varchoom and Allahdad (near Bibai Peak) and 2 sections in Spera Ragha-Chinjun valley. Interpretations of facies and facies associations are mainly based on facies classification and description by Mutti and Ricci Luchi (1975), Pickering et al. (1986) and Shanmugam and Moiola (1988). A summary of the facies classification after Pickering et al. (1986), to which facies of the volcaniclastic succession of the Bibai formation have been compared, is given in Table 1.

VOLCANIC CONGLOMERATE (VC)

The volcanic conglomerate is mostly very poorly to moderately sorted and generally sub-angular to sub-rounded (Fig. 2, 3). Particles are mostly pebbly with minor proportion of cobble and boulder size. They are mostly clast-supported and subordinately matrix-supported. Imbrication, though not very common, is observed. Clast size is mostly within the range of pebble. Maximum clast sizes range between 2 and 80 cm. Beds are typically lenticular, frequently pinch out laterally, have concave-up channel morphology and strongly erosive bases, truncating the underlying rocks of various facies (Fig. 4, 5). Also they are frequently amalgamated. Some comparatively thinner beds (approx. 120 cm) were seen to pinch out laterally within a distance of 5 meters. Rip-up mudstone, siltstone and sandstone clasts of the same formation, and limestone and mudstone clasts of the underlying Parh Group are commonly present. In some cases they are amalgamated.

Erosive bases of the volcanic conglomerate horizons possess very large size, up to 2 m wide and 1 m deep elongate ridge-and-furrows, flute marks and load casts. Orientation of the ridge-and-furrow structures at the base of conglomerate horizons is quite consistent and parallel to the paleocurrent directions. An overall fining-upward trend is commonly observed within the VC facies, whereby the particle size generally decreases upward from cobble and/or pebble size to grit, sand and even

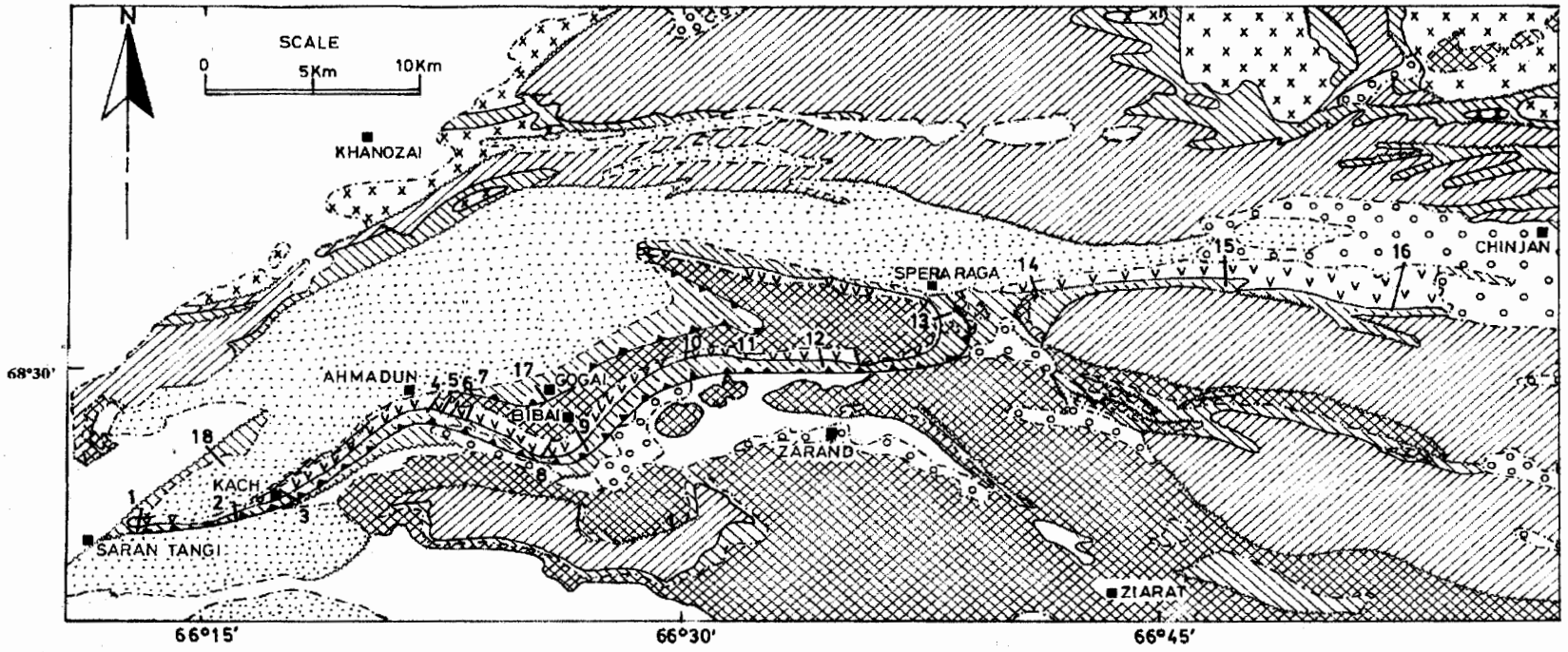

Recent/Sub-Recent

Siwalik Geroup (Mio-Pliocene)

Ghazij Fm./Spintangi Lst./Nasai Group (Eocene)

Dungan Fm (Paleocene)

Muslim Bagh Ophiolite (Cretaceous)

Bibai Fm. (Upper Cretaceous)

Parh Group (Cretaceous)

Allozai Group/Shirinab Fm. (Tri-Jurassic)

Contact Unconformable

Contact Conformable

Contact Faulted

Figure 1. Geological Map of the study area (modified after HSC 1960) showing positions of various studied sections and localities mentioned in text.

Table 1. Sedimentary facies of the Bibai formation and their comparison with the classes, groups and facies of Pickering et al. (1986).

The Bibai Facies	Pickering et al. (1986)'s Class, Group and Facies	Transport / Depositional Processes
VCP, VCC	A 1.1- Disorganized gravel	Debris flows or high concentration turbidity currents. Freezing on decreasing bottom slopes due to inter granular friction and cohesion.
	A2.1- Stratified gravel	High concentration turbidity currents. Grain-by-grain deposition from suspension and then traction transport as bed-load.
	A 2.2 and A 2.3- Multiple inversely and normally graded gravel	High concentration turbidity currents. Intense grain interaction accompanied by rapid grain-by-grain deposition from suspension and successively minor traction.
	A 2.4 - Graded-stratified gravel	High concentration turbidity currents. Grain-by-grain deposition by suspension followed by traction during deposition of upper part of the bed.
SS	A 2.5 - Stratified pebbly sand	High concentration turbidity currents. Grain-by-grain deposition from suspension followed by traction transport as bed load.
	A 2.6 and A 2.7 - Multiple inversely and normally graded pebbly sand	High concentration turbidity currents. Rapid deposition by frictional freezing of a traction carpet followed by grain-by-grain deposition from suspension with little traction transport.
	A 2.8 - Graded stratified pebbly sand	High concentration turbidity currents becoming more dilute with time at single locality. Grain-by-grain deposition from suspension and later on as bed load by traction.
	B 1.1 Thick / medium bedded disorganized sand	High concentration turbidity currents. Rapid mass deposition due to inter-granular friction in a concentrated dispersion near the bed.
	B 2.1- Parallel stratified sand	High concentration turbidity currents. Freezing of successively generated traction carpets at the base of flow. Structure less divisions record rapid grain-by-grain fall-out from suspension or freezing of a thicker and unsorted layer.
SSMS	C 2.2 and C 2.3 - Organized sand-mud couplets	Dilute to moderately high concentrated turbidity currents. Grain-by-grain deposition from suspension followed by traction transport. Muddy upper divisions are deposited in the same manner as mud turbidites of Facies Class D.
MS	D 2.1 - Graded stratified silt	Low concentration turbidity currents. Grain-by-grain deposition from suspension followed by traction along the bottom to produce lamination. Clay-grade tops are produced by suspension.
	D 2.3 - Thin regular silt and mud laminae	Low concentration turbidity currents. Slow uniform deposition from suspension (Stow and Bowen 1980).
	E 1.1 - Structure less muds	Likely to be mud-rich turbidity currents and lateral transfer of hemipelagic material by ocean currents. Rapid deposition by ponding of mud-rich turbidity currents in confined basins (Pickering and Hiscott 1985).
	E 1.3 - Mottled muds	Transported as suspended load in bottom currents. Settling of particles or flocs from suspension.
	E 2.1- Graded muds	Low and high concentration turbidity currents. Grain-by-grain or floc settling during flow deceleration.
VB	F 1.1 - Exotic clasts (rubble)	Submarine rock-falls, avalanching along over pressured glide planes, ?debris flow. Cessation of movement on increased friction due to decreasing bottom slopes because gravity forces no longer exceed or balance basal and internal friction.
SS, SSMS (conto-rted)	F 2.1- Coherent folded and contorted strata	Slides and rotational slumps either due to depositional overloading of weakly lithified sediments or to cyclic or single shocks (earthquakes, tsunamis). Cessation of movement on decreasing bottom slopes because gravity forces no longer exceed or balance basal and internal friction.
LS	Very finely crystalline (bio-micritic) limestone	Pelagic (deep marine) sedimentation with planktonic foraminifera.

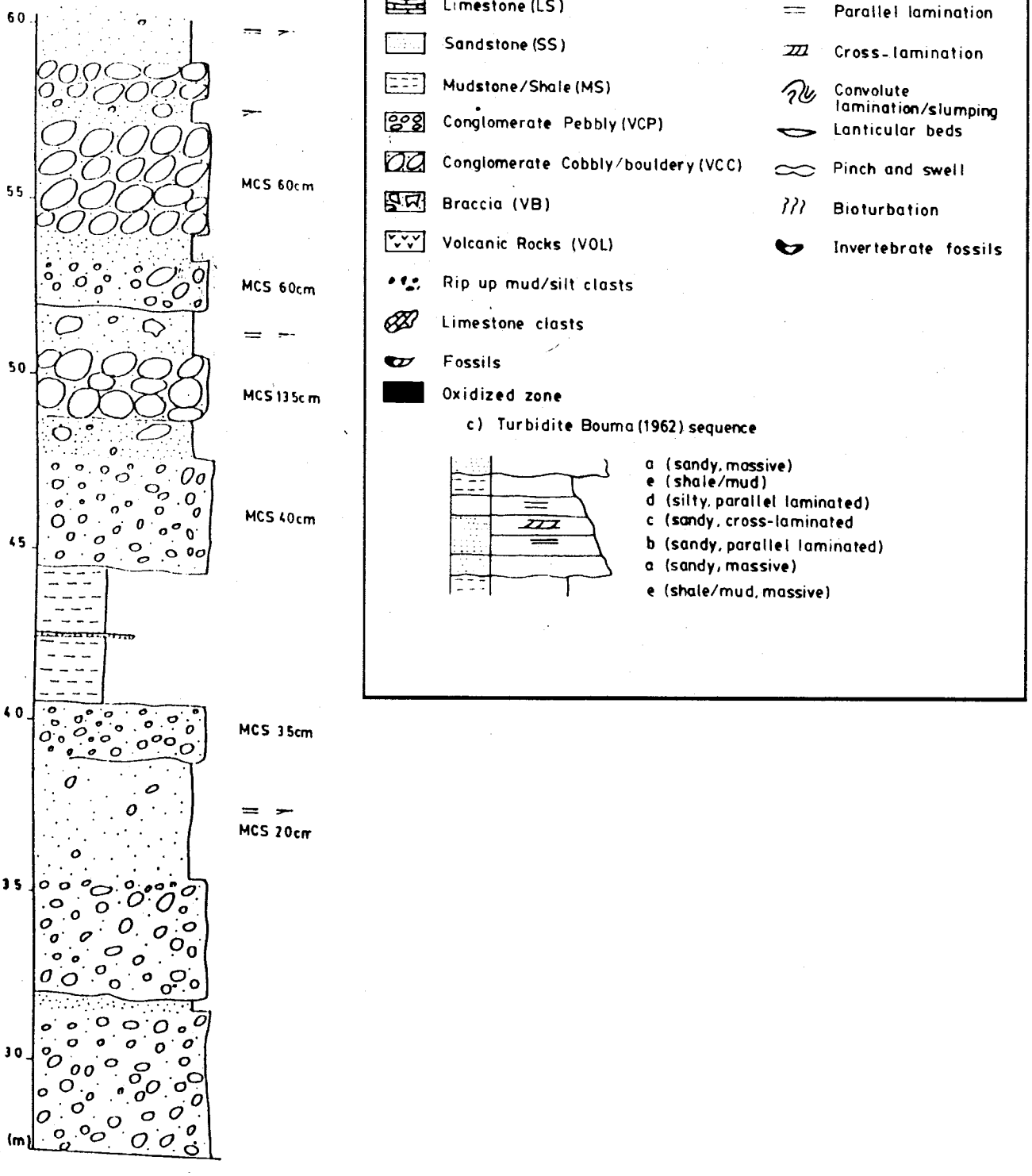

Figure 2. Part of the columnar profile of the Shina Khawra (Grid Ref. 892 880) Section showing Volcanic Conglomerate (VC) and SS facies.

Figure 3. Photograph showing a close-up of the Volcanic Conglomerate (VC) facies at Narai Section (Grid Ref. 893 937). Note that almost all the clasts are those of the basic volcanic rock types.

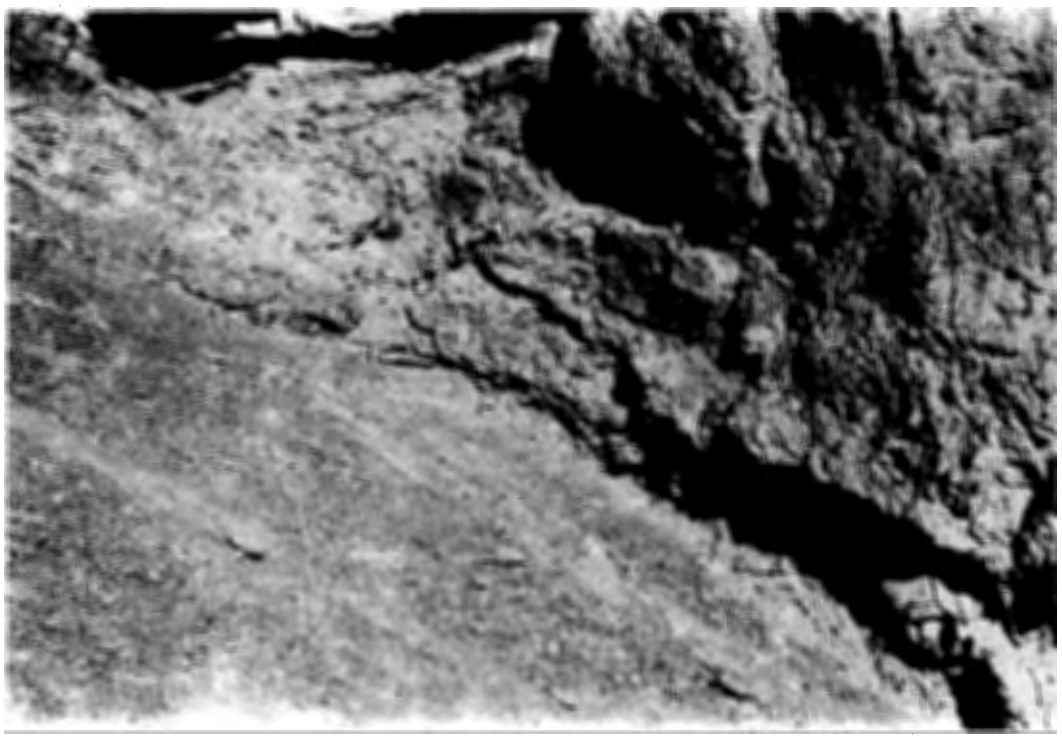

Figure 4. Photograph of the Narai Section (Grid Ref. 893 937) showing concave-up morphology, erosive base and truncation of the underlying SSMS facies by the VC facies. Note sole marks and load casts at the base.

Figure 5. Photograph of the Shina Khawra Section (Grid Ref. 892 880) showing stacking and anastomosing channelized facies. The SSMS facies inter digitate with channelized (VC-SS) facies. Note the erosive base and concave-up morphology of the channelized facies.

mud size. Multiple grading of successively normal and reverse type within the sand-pebble range may also be seen.

The VC facies are normally present in the form of stacking pattern in which each horizon of general fining-upward trend would truncate the underlying horizons of the similar or different facies and in turn would be truncated by the overlying horizon (Fig. 4, 5). However, they may be found separately within the fine grained facies, normally SSMS.

The VC facies usually contains sandstone lenses which may be up to 75 cm thick, normally parallel laminated, low-angle cross-laminated (<10°) and rarely massive. Lower contacts of the sandstone with conglomerate are usually gradational and upper contacts sharp, either truncated by the overlying VC and SS facies and/or overlain by the SSMS facies. Multiple grading within the sand size and/or pebble size may frequently be seen.

Interpretation

Characters of the VC facies resemble with the facies class A and its groups of Pickering et al. (1986). Textural and structural characters like sub-rounded to rounded, clast supported and rarely matrix supported nature, poor sorting, elongate ridges and furrows, sole marks and imbrication indicate deposition by gravity flows in the form of high concentration debris flows (Table1). Lenticular morphology, erosive bases, truncation of the underlying facies, presence of rip-up clasts, amalgamation, elongate ridges-and-furrows and flute marks, association of this facies with the SSMS facies, which possesses characters of turbidites indicate deposition within submarine channels. The general thickening- and fining-upward trend within this facies is characteristic of channels (Mutti and Ricci Luchi 1972, Ricci Luchi 1975) indicating a general upward-widening of the channel section and/or progressive channel abandonment. However, multiple grading suggest episodic phases of fluctuatary flows. Associated sandstone lenses which possess parallel and low-angle cross-bedding, however, indicate high concentration turbidity currents and traction transport as bed load. Multiple normal and reverse grading indicate intense grain interaction accompanied by repeated influxes of suspension and minor traction. Stacking of the channelized facies indicate that channel complex was anastomosing on a submarine fan system and truncating the channels and the inter-channel fine grained turbidite facies (SSMS). Some isolated channels also occur within the inter-channel fine grained turbidite facies which are represented by isolated lenticular conglomerate horizons of similar character.

SANDSTONE (SS)

The SS facies (Fig. 2) comprises sandstones of light

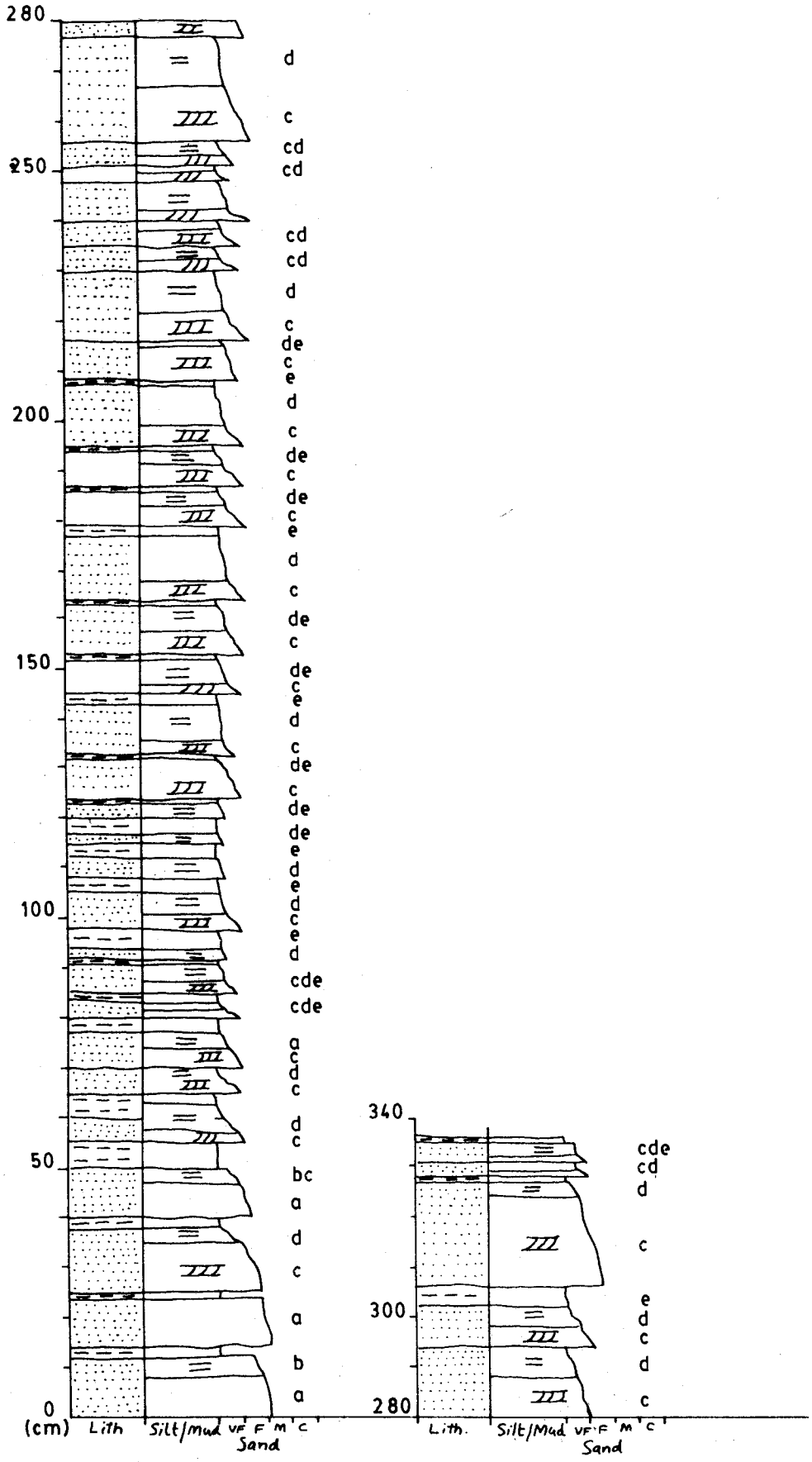

Figure 6. Part of the columnar profile of the Spina Khezai Section (Grid Ref. 837 907) showing typical SSMS facies.

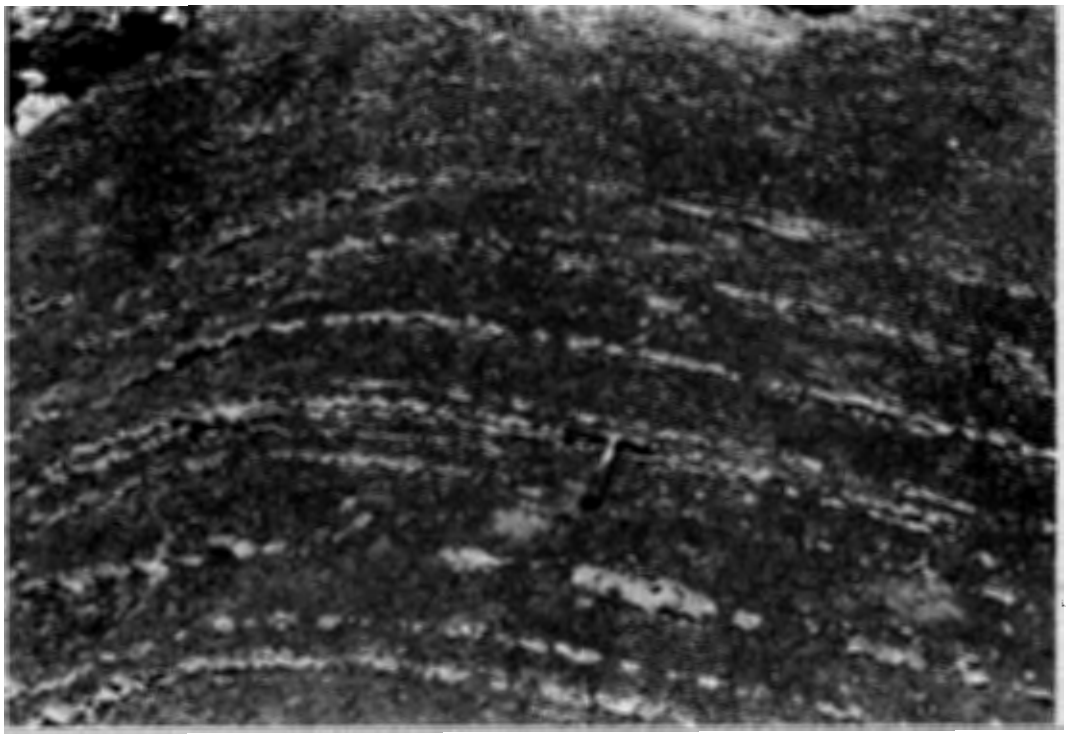

Figure 7. Photograph of the Gogai Section (Grid Ref. 880 920) showing typical SSMS facies. Note lateral continuity and rhythmic pattern of the sandstone and shale beds.

grey and light greenish grey colour which is poorly sorted, medium to very coarse grained, mostly pebbly and rarely containing cobbles and even boulders. Maximum clast sizes in pebbly sandstone range between 2 and 80 cm. Beds are mostly lenticular and frequently pinche out laterally within short distances e.g. a 2 m thick bed may pinch out laterally within a distance of 15 m. They commonly show concave-up erosive bases, and possess rip-up mudstone and siltstone clasts of the underlying facies and also limestone and shale clasts of the underlying Parh Group (Fig. 2). They usually truncate the underlying facies and in some localities even the intercalated Parh-type (micritic) limestone and shale. Sandstone is mostly low-angle cross-laminated ($<10^0$), parallel laminated and partly massive. Multiple grading of normal and reverse type is commonly present, although a general fining-upward trend is characteristic of this facies. Sandstone (SS) facies occurs within the VC facies or as isolated horizons. Where they occur as part of the VC facies their lower contacts are usually gradational, however, upper contacts may be sharp or gradational with the VC facies but usually sharp with other facies like SSMS. In situations where they occur as independent horizons, their lower and upper contacts are usually sharp with any other type of facies and truncates the underlying facies. In some cases they also truncate facies of the same kind and laterally amalgamate with them. Their erosive bases normally possess flute marks, longitudinal ridges and load casts. Soft sediment deformation, slumping and convolute lamination may also be observed within the SS facies.

Interpretation

Characters of the SS facies resemble with the facies class A and B of (Mutti and Ricci Luchi 1975 and Pickering et al. 1986) and its various groups and sub groups. Collectively, they are the product of high concentration turbidity currents. Facies groups of Pickering et al. (1986) like stratified pebbly sand (A 2.5), some showing normal and reverse grading (A 2.6, A 2.7), graded stratified pebbly sand (A 2.8), thick to medium bedded disorganized sand (B 1.1) and parallel stratified sand (B 2.1) are included within the SS facies. Transport and depositional mechanisms are mainly suspension, traction, frictional "freezing" of traction carpets and grain-by-grain deposition from suspension (Pickering et al. 1986). Lenticular morphology, erosive bases, truncation of the underlying facies, amalgamation, rip-up clasts, sole marks and occurrence of parallel and low-angle ($<10^0$) cross-lamination suggest deposition within the submarine channels and high energy conditions at upper flow regime. Frequent association of this facies with the conglomerate facies (VC) also confirms conditions of high gradient and upper flow regime. Association of the coherent folded and contorted strata (facies class F of Pickering et al. 1986) indicate

Figure 8.
Photograph of the Gogai Section (Grid Ref. 880920) showing close-up of sandstone within the SSMS facies in which an overall grading and Bouma Tab sequences are clearly seen.

slides, slumps and soft sediment deformation at high gradient, depositional overloading of weakly lithified sediments or events of seismic activity.

SANDSTONE INTERBEDDED WITH MUDSTONE (SSMS)

The SSMS facies (Fig. 4-9) is represented by rhythmically interbedded sandstone and mudstone, whereby sandstone to mudstone ratio change variously from 3:1 to 1:20. Sandstone is mostly very thin bedded, fine to very fine grained and rarely medium to coarse grained. Thickness of the sandstone beds vary generally between a few cm to 10 cm, however, rarely sandstone beds reach up to 50 cm. They are normally of dark grey and dark brownish grey colour.

Sandstone usually possesses characters of turbidites like grading, sole marks and parallel and cross-lamination. Sole marks include flute cas s, groove marks, longitudinal ridges, load casts and associated flame structures. They commonly show lenticular morphology and pinch-and-swell of the beds. Bouma sequences (Bouma 1962) such as Tabcde, Tbcde, Tcde, Ta(?bc)de, in which Tbc (?d)e and Tcde sequences are common (Fig. 6-7). Some of the thicker beds show concave-up erosive bases, rip-up clasts, lenticular morphology and lateral pinching within very short distances. Lateral pinching may be very rapid e.g. a 13 cm thick bed and pinch out laterally within a distance of 30 cm. Soft sediment deformation including load casts and associated flame structures and slumping (Fig. 9), which in some localities involve several horizons, is commonly present. Slumped succession may be several meters thick (Fig. 9).

A general thinning- and fining-upward trend is characteristic of these facies in which the frequency and/or thickness of sandstone beds gradually decreases

upward causing gradual decrease of sandstone to mudstone ratio from 3:1 to 1:20 or even lower, so that in some cases the upper part becomes dominantly mudstone (MS) containing only occasional sandstone and siltstone beds. Interbedded mudstone is dark grey to dark brownish grey, blocky, partly fissile and rarely fossiliferous.

Interpretation

Rhythmic alternations of the sandstone and mudstone beds and the range of the associated sedimentary structures like grading, sole marks and Bouma sequences (Bouma, 1962) indicate their deposition by turbidity currents. These characters resemble with the facies C 2.3 of the organized sand-mud couplets of Pickering et al. (1986), indicating deposition by dilute to moderately high concentrated turbidity currents and grain-by-grain deposition from suspension and traction transport. Muddy upper divisions are the product of low concentration turbidity currents and/or hemipelagic in overbank (-levee) complex. The thicker lenticular beds with concave-up erosive bases are crevasse splays within the inter-channel fine grained turbidite succession.

Slumping, soft sediment deformation (Fig. 9), as represented by asymmetrical folds, normal faults, load casts and associated flame structures, which represent facies F of Pickering et al. (1986), indicate down-slope gravity-related movements that occurred shortly after the deposition in response to over loading at high gradient and may have been triggered by seismic activity which was also associated with the eruptive and/or tectonic activities.

MUDSTONE (MS)

This is the most common facies which predominates in Kach Section (Fig. 10, 13) and further southwestward, Pusha Section and further northeastward, Urghargai Section west of Spera Ragha, Pinakai Section and Malkhozun Section northwest of Kach. Also it is frequently found almost in all sections in upper parts of the succession and in between. The MS facies comprises dominantly mudstone with very minor proportion of siltstone and thin bedded sandstone (Fig. 10). Occasional sandstone beds are mostly less then 10 cm thick, however, rarely up to 30 cm thick beds may be found. Sandstone to mudstone ratio is less than 1:20. The sandstone beds are of dark grey and dark brownish grey. They are graded, having sharp erosional bases, showing pinch-and-swell, load casts and sole marks Bouma Tcd, Tbc and rarely Tabc successions may be observed. Mudstone is dark brownish grey, mostly blocky, in places fissile, silty and sandy. It is mostly barren, in places highly fossiliferous, however, the occurrence of fossils tend to increase upward. Upper part of the section near Kach is highly fossiliferous and possesses gastropods, cephalopods, bivalves, brachiopods, echinoderms and trace fossils.

Interpretation

This facies represents the facies classes D and E of Mutti and Ricci Luchi (1975), and Pickering et al. (1986). Facies D is deposited partly by low-concentration turbidity currents, and partly grain-by-grain deposition and traction. Facies E which comprises the structure less and mottled mud is deposited by mud-rich very low-concentration turbidity currents and lateral transfer of hemipelagic/ pelagic material by ocean currents where settling occurs from suspension. This facies indicate deposition of mudstone away from the centers of volcanic activity and source area. The presence of bivalves, gastropods, echinoderms and brachiopods, which increase upward within the succession, suggest shallow marine environments in upper part of the succession.

VOLCANIC BRECCIA (VB)

This facies (Fig. 11-12) is composed of angular to sub-angular, very poorly sorted, gritty to pebbly, occasionally cobble to boulder-size, fragments of mostly basic volcanic rocks. Limestone and shale fragments of the underlying Parh Limestone and small (a few meters across) lumps of basaltic lava flows may also be associated with this facies. Maximum clast size in such facies reaches up to 1.5 m. This facies is not very common, however, found in lowermost part of the succession in Tora Khaizai, Shina Khawra, Allahdad, Takarai, Pusha and Narai sections. In these sections, volcanic breccia clearly truncates the uppermost part of the Parh Limestone. In Takarai Section this facies is highly distorted and slumped in which distorted lumps of basaltic lava flows and underlying Parh Limestone, up to a few meters across, are present.

Interpretation

Sub-angular to angular nature, very poor sorting, association of lava flows and large angular fragments of the underlying Parh Limestone indicate down slope transportation in the form of debris flows associated with frequent slumping. Characters of this facies resemble with the debrite facies model of Stow (1985) or F1 (exotic clasts) of the chaotic deposits of Pickering et al. (1986). These indicate submarine rock fall, avalanching and sliding along over-pressured glide planes, debris flow and their subsequent cessation because of basal friction. Angular fragments and lumps of lava flows indicate very short distance of transport and deposition next to the source i.e. near the volcanic crater. This, along with the associated facies, represents the most proximal succession of the volcaniclastic sediments.

LIMESTONE (LS)

Limestone is found intercalated with the volcaniclastic succession of VC, VB and SSMS facies within lower part of the Bibai formation (Fig. 11). It is white and cream colored, very finely crystalline (micritic, biomicritic) possessing grey specs of

Figure 9. Photograph of the Tora Khezai Section (Grid Ref. 859 897) showing slumping and soft sediment deformation within the SSMS facies.

Figure 10. Photograph of the Spina Khezai Section (Grid Ref. 837 907) showing typical mudstone MS facies with occasional thin sandstone beds.

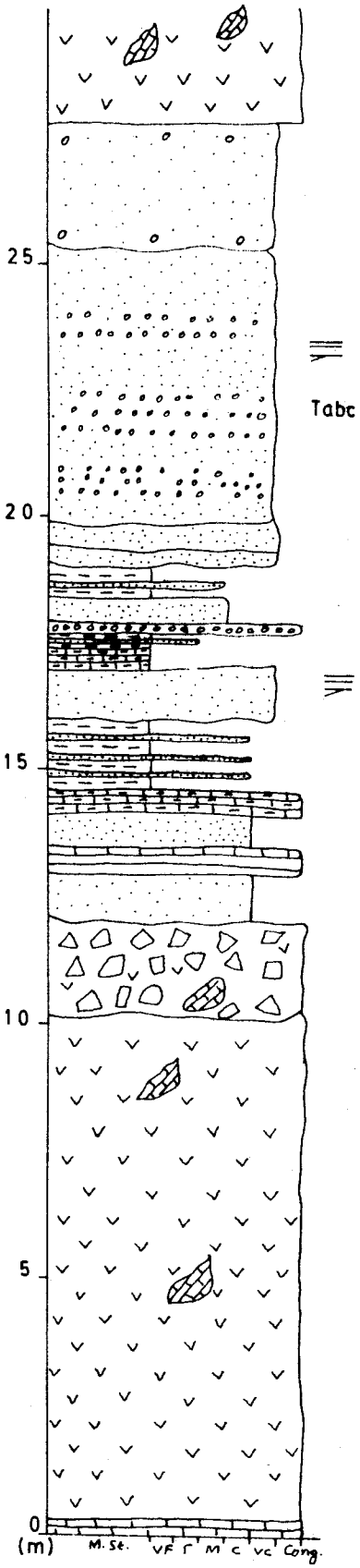

Figure 11. Columnar profile of part of the Pusha Section (Grid Ref. 019937) showing VB, VOL, LS and SS facies.

microfossils which mostly belong to *Globotruncana* (Kazmi 1995, 1988). They are porcelaineous and breaks with concoidal fracture. These characters clearly resemble with the underlying Parh Limestone (Hunting Survey Corporation 1960, Shah 1977, Allemann 1979). In places pink shale and limestone, resembles to that of Goru Formation are also intercalated.

Interpretation

The LS facies, by virtue of their resemblance with those of the Parh Limestone, are interpreted to have been deposited by pelagic sedimentation in lower shelf or upper slope conditions (Kazmi 1955, Allemann 1979). At places these limestone and marl beds, which are interbedded with the volcaniclastic sediments, have been truncated by conglomeratic and sandy channels (VC and SS facies) suggesting that during calm periods, when deposition of coarse volcaniclastic material had stopped, deposition of the LS facies (Parh-type limestone) resumed. The LS facies is also associated with the inter-channel (overbank-levee) deposits. This also suggest deposition by pelagic sedimentation and its subsequent truncation by the coarse volcaniclastic channels in response to the renewed influx of volcanism.

VOLCANIC ROCKS (VOL)

The basic volcanic (basaltic) rocks (Fig. 11) are mentioned here because in some sections it is frequently interbedded with Parh-type limestone (LS) and volcaniclastic sediments (VB and VC facies). Lava flows are very common and thick in the Spera Ragha-Chinjun valley and have been described by early workers (McCormick 1985, Khan 1986, 1994, Siddiqui et al. 1994, 1996).

Interpretation

Interpretation of the genesis and origin of volcanic rocks is described by earlier workers (McCormick 1985, Khan 1986, Siddiqui et al.1994, 1996, Khan 1986, Khan et al. 1999) who suggest the "Reunion hotspot" origin for the volcanic rocks.

FACIES ASSOCIATIONS

Facies VC and SS are mostly found intercalated and best developed in proximal part of the study area near Ahmadun, Shina Khawra, Allahdad, Bibai and Narai (Fig. 13). Although VC is the most commonly occurring facies in this association, SS is also interbedded. This association, in general, represents the channelized complex of the middle fan of Mutti and Ricci Lucchi (1972, 1975) and Shanmugam and Moiola (1988).

The SSMS facies is usually associated as distinct inter-fingering successions (Fig. 5-7) which are mostly clearly truncated by the VC-SS association. This association is lenticular and usually pinches laterally. Also it may be found within the MS facies in distal part of the succession. Characters of the facies resembles with the facies classes C and D of the Mutti and Ricci Lucchi

Figure 12 Photograph of the Narai Section (Grid Ref. 983 937) showing Volcanic Breccia (VB) facies. Note angularity of the basic volcanic fragments.

(1972, 1975) and Pickering et al. (1986) which are characteristic of inter-channel overbank deposits of the submarine fan.

The VOL-VB-LS association of facies is present within lower most part of the succession. These are found intercalated (Fig. 11) and usually slumped, however, VOL may also be found independently. The LS facies, which represents Parh-type limestone, indicates a transitional change from deposition of pelagic (micritic) limestone in calm conditions to eruptive volcanic activity and related coarse volcaniclastic material of high-concentration turbidity currents and debris flow deposits. High gradient, induced by volcanic activity, provided conditions favorable for slumping, debris flows, inter-mixing of the associated facies and high concentration turbidity currents. In Spera Ragha-Chinjun valley, thick succession of the basic volcanic rocks (VOL) with very minor proportion of volcaniclastic sediments, indicate *in-situ* lava flows at or near the volcanic crater.

Association of the facies MS, comprises mostly mudstone / siltstone with occasional very thin bedded (<10 cm thick) sandstone (Fig. 10). However, rarely 5-10 m thick successions of SSMS facies may also be associated. The MS facies is dominant in the distal areas like Kach and further southwestward and near Pusha and further northeastward. Also near the Bibai Peak, several tens of meters of this facies association is found in upper part of the Bibai formation (Fig. 13) and above the SSMS and VC-SS associations within the proximal area. In such cases their thickness varies from a few meters up to over 50 m. This association represents the lower fan / basin plane component of the submarine fan (Mutti and Ricci Lucchi 1972, 1975, Shanmugam and Moiola 1985, 1988).

The VOL association is found within Spera Ragha and Chinjun and the area in between. Very minor proportion of VC- SS association is present within an oxidized succession above the *in-situ* volcanic rocks in Spera Ragha Section.

COMPARISON OF VARIOUS SECTIONS

Comparison and correlation of various sections (Fig. 13) shows systematic lateral variations. The Allahdad Section (near Bibai Peak) is the thickest, and the most proximal, comprising dominantly the VC-SS and minor proportion of VB-VOL-LS facies association in lower part where the coarse volcaniclastic succession is over 1000 m thick. The Pinakai Section towards SW and Urghargai Section towards NE being the most distal comprising dominantly the MS facies. Proportion of VC-SS-SSMS facies decreases from proximal to distal areas towards SW and NE (Fig. 13), where only MS facies are dominant. Similarly, the overall thickness of volcaniclastic succession of the Bibai formation also

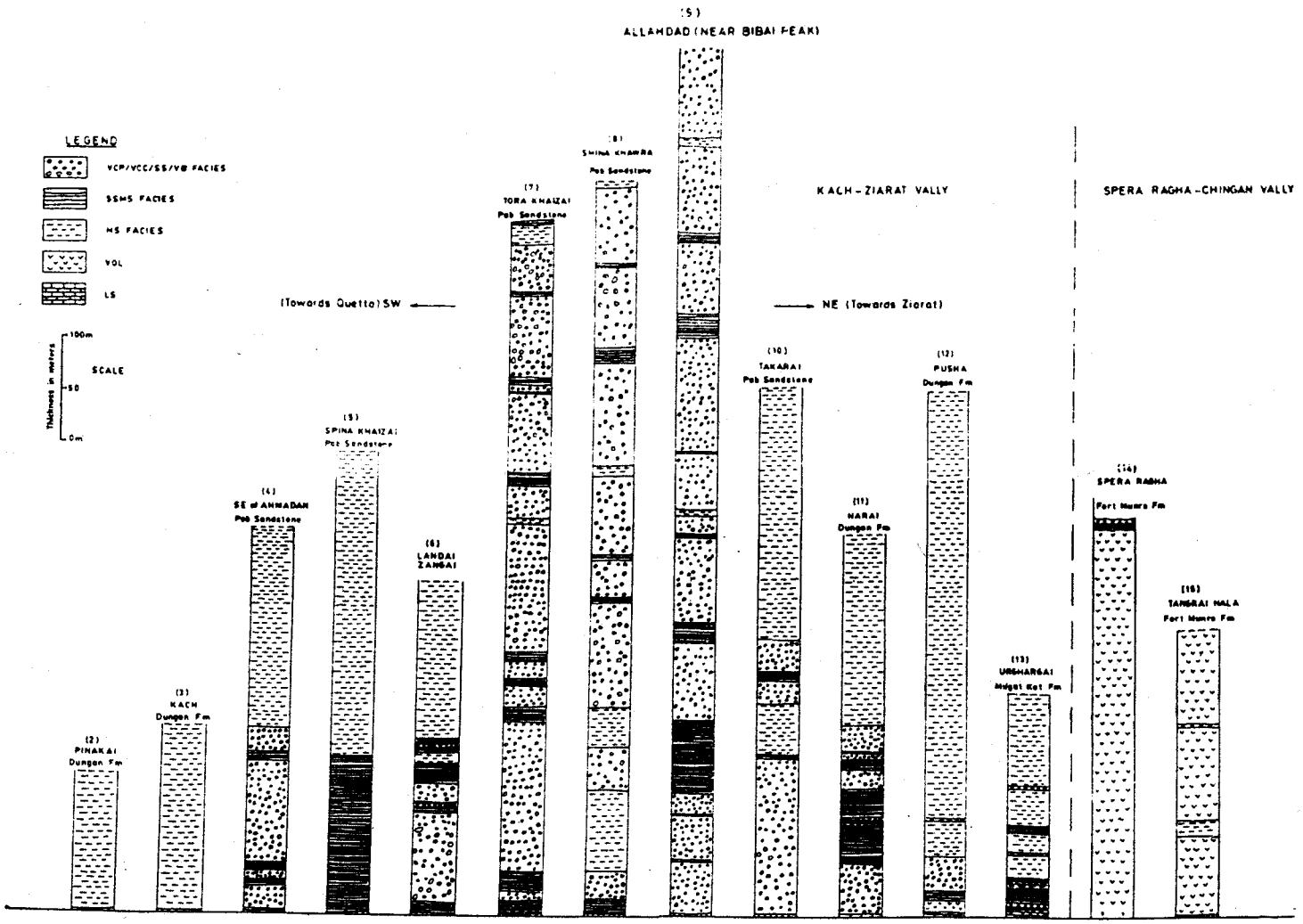

Figure 13. Figure showing comparison of columnar profiles of the studied sections and vertical and lateral variations within the studied area.

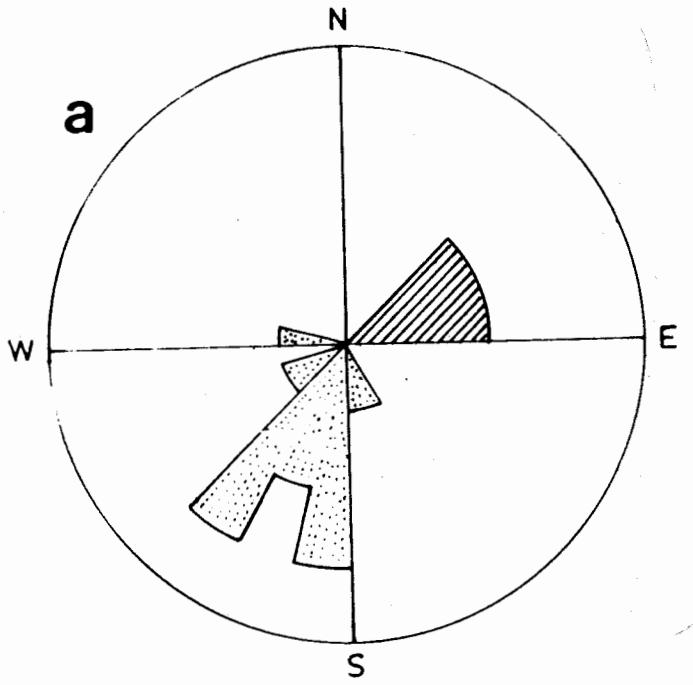

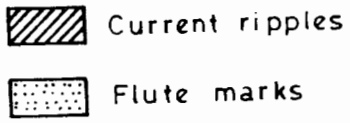

Figure 14.
Rose diagram of paleocurrent pattern; a) based on flute marks and current ripples within the SSMS facies; Scale: 2 cm = 1 reading; n = 12; b) based on longitudinal ridges and flute marks; Scale: 1cm = 4 readings; n = 83.

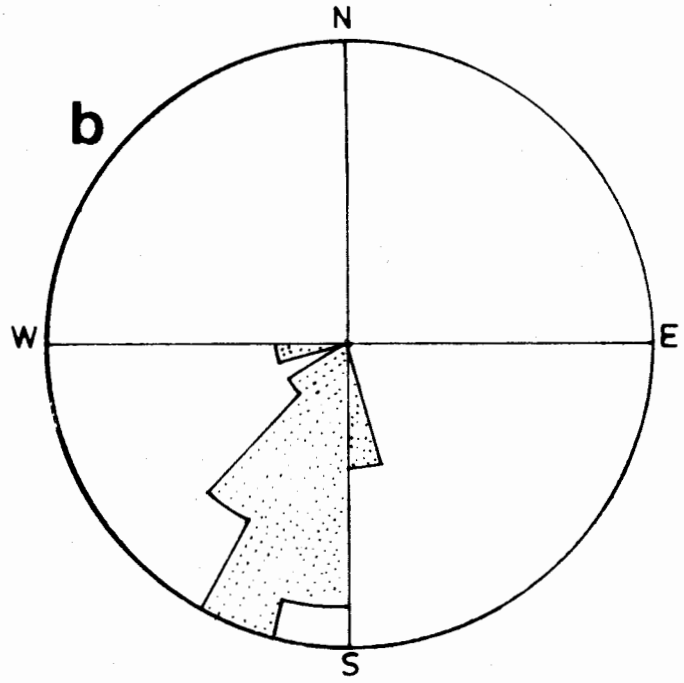

decreases from proximal to distal areas.

Comparison of the facies associations of Bibai formation in Kach-Ziarat valley with those of the Spera Ragha-Chinjun valley (Fig. 13) shows marked contrasts. Within the Kach-Ziarat valley volcaniclastic succession predominates, whereas, within the Spera Ragha-Chinjun valley the *in-situ* volcanic rocks predominate.

Comparison of the studied sections (Fig. 13), paleocurrent pattern and composition of volcaniclastic detritus indicate that source area was somewhere to the north of Bibai, probably westward extinction of the *in-situ* v olcanics of the Spera Ragha-Chinjun valley. This suggestion is also supported by the presence of contrasting characters of detritus including acidic igneous fragments of rhyolite, granite and dolerite. Such rock types have not been reported elsewhere from the Bibai volcanics of the Spera Ragha-Chinjun valley.

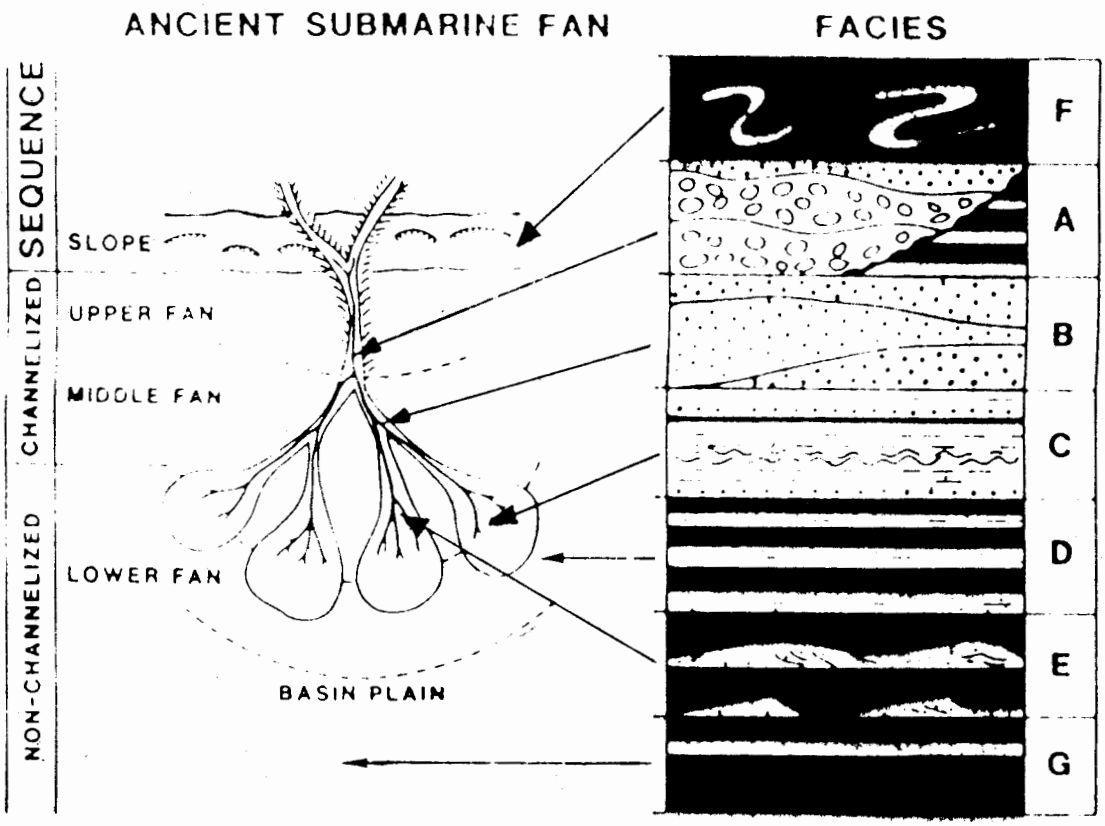

Figure 15. Figure showing the components of ancient submarine fan and distribution of related turbidite facies. Facies nomenclature used is from Mutti and Ricci Lucchi (1972, 1975) and Pickering et al. (1986).

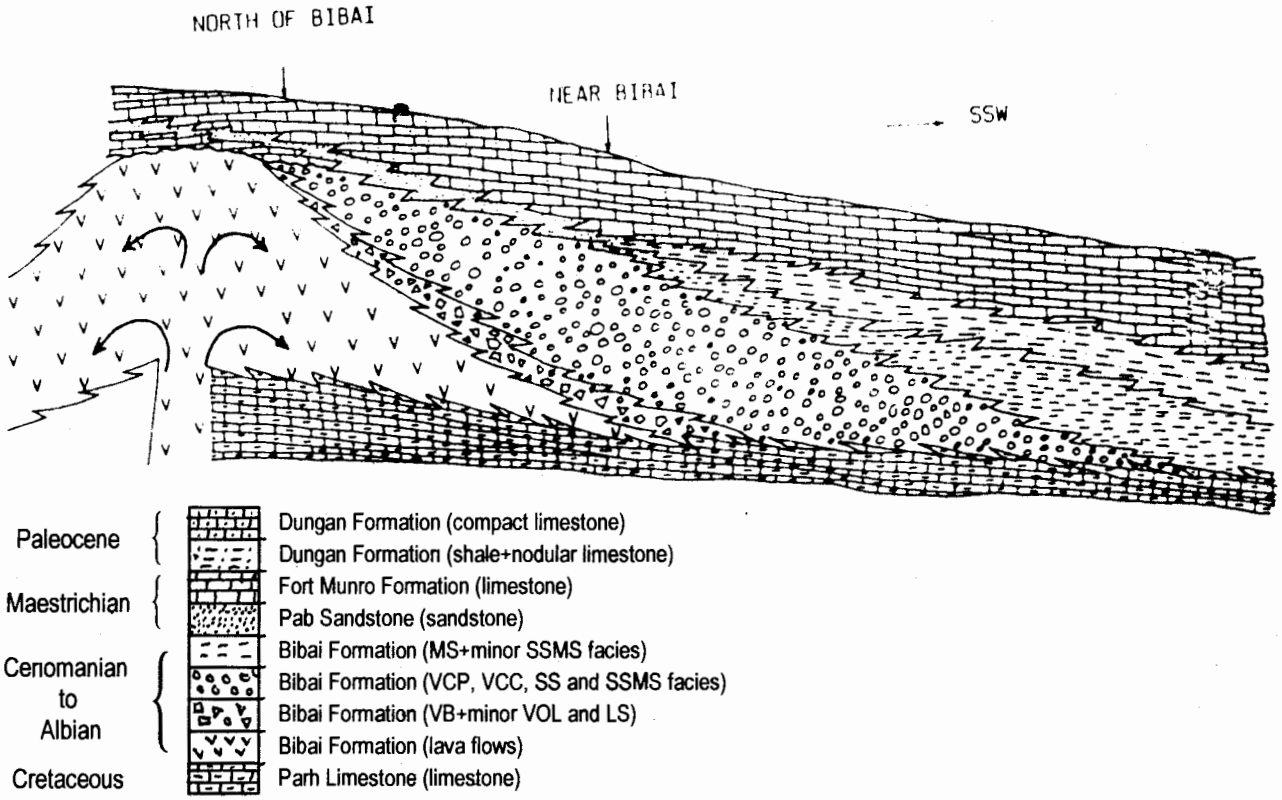

Figure 16. Idealized section showing lateral variations with the stratigraphic section of Kach-Ziarat and Spera Ragha-Chingun valleys.

PALEOCURRENT DIRECTIONS

Orientations of the paleocurrent directions were measured directly with the help of compass because dip angle of the beds are usually below 40°. Paleocurrents were measured based on flute marks and longitudinal ridges at the bases of VC and SS facies and flute marks and ripple marks within the SSMS facies. Plots of the paleocurrent directions in the form of rose diagrams (Fig. 14) suggest that paleocurrent directions were dominantly from NE to SW and subordinately from NW to SE. Variability in the paleocurrent directions is noticeable from one section to the other and also from channel to channel. Paleocurrent directions within the SSMS facies were observed in the Shina Khawra Section (Fig. 14a). These, representing the inter-channel (-levee) complex, show similar but a higher range of current directions. Directions roughly normal to those shown by channel facies are also present which indicate a probable influence of the crevasse channels. Paleocurrent pattern based on current ripples within the SSMS facies in Shina Khawra Section (Fig. 14a) indicates directions normal to those shown by flute marks i.e. from SW to NE.

In the light of comprehensive plot of the paleocurrents obtained in the area, it is concluded that source area was somewhere to the north of Bibai Peak. Variability in paleocurrent patterns, within and between the sections, supports the pattern of diverging channels on a submarine fan.

THE BIBAI SUBMARINE FAN

Submarine fan has been defined (Bouma et al. 1985) as "a channel (-levee) -overbank system". Shanmugam and Moiola (1988) defined fan as "channel-lobe complex" which formed from sediment gravity flows in deep-sea environment commonly beyond the continental shelf. According to these definitions recognition of both channel, overbank (-levee) and lobe deposits are essential in establishing the existence of submarine fan system in either modern or ancient settings. In theory, the submarine fans are considered to be fan/cone-shaped (Fig. 15), but as fans vary greatly in size and shape, shape is not a useful criteria for classifying fans (Barnes and Normark 1985). Sediment gravity flows i.e. the channelized turbidity currents and associated debris flows (Middleton and Hampton 1973), are the most important deep-sea processes in developing the submarine fans. Slumps and liquified flows are also important which require high gradients (over 18°). The most common mechanism that triggers the sediment gravity flows are over steepening, earthquakes and pore-water pressure. Major positions of submarine fan successions comprise turbidites that occur as channel-fill, overbank (-levee), lobes and sheet sands. Paleocurrent patterns are also a major source of information for interpreting the radial shape of the ancient submarine fans. In general, components of the ancient fans (Fig. 15) may be recognized using the following criteria:

1) The Upper Fan: by the presence of major feeder channel.
2) The Middle Fan: by a network of distributary channels and associated overbank (-levee) deposits.
3) The Lower Fan: by depositional lobes and sheet sands.

Fan components are recognized using the turbidite facies associations schemes (Table 1) of Mutti and Ricci Lucchi (1972, 1975) and Pickering et al. (1986). Channels may be recognized by thinning- (finning-) upward trends (Mutti and Ricci Lucchi 1972, Ricci Lucchi 1975) because an upward-widening channel section results in deposition of successively thinner beds. In most cases the thinning-upward trends may be due to progressive channel abandonment. Channels are mostly filled with the conglomerate, sandstone and mudstone (A and B facies of Mutti and Ricci Lucchi 1975) and have erosive bases, profusion of rip-up clasts and lenticular morphology. Depositional lobes (Fig. 15) are considered (Shanmugam and Moiola 1988) to be an important component in most submarine fans. General characters of depositional lobes include (Mutti and Ricci Licchi 1972, 1975, Ricci Lucchi, 1975, Mutti and Normark 1988) absence of channeling, thickening-upward cycles composed dominantly of coarse to fine sandstone (facies C) and laterally continuous beds (sheet-like geometry) extending for several kilometers and enclosed in fine grained thin bedded turbidite facies (facies D) of the basin plane setting.

Based on facies and facies associations recognized in various sections (Fig. 2-13) and their lateral organization (Fig. 13) we propose a submarine fan environment for the volcaniclastic succession of the Bibai formation which comprises "channel (-levee) - overbank complex" that developed on slope of a series of sea mounts (hotspot volcanoes) whereby its material has been derived from the same volcanic terrain. We name it the "Bibai Submarine Fan". These volcaniclastic sediments show various characters that are typical of deposition by sediment gravity flows (Middeton and Hampton 1973). The most common mechanism for triggering them were over steepening, earthquakes and volcanic eruptions. Lateral facies variations (Fig. 13) and paleocurrent directions (Fig. 14) within the formation also suggest fan-shaped morphology of the Bibai Submarine Fan. The proximal area, near the Bibai Peak, shows anastomosing and interfingering pattern of the channel and inter-channel facies (Fig. 13), whereas, distal area is dominated by the MS facies of basin plane deposits. The identified Lithofacies and their associations clearly define the following major components of the submarine fan:

a) Distributory channel deposits (middle fan)
b) Inter-channel deposits (overbank-levee)
c) Lower fan plane deposits (lower fan/basin plane).

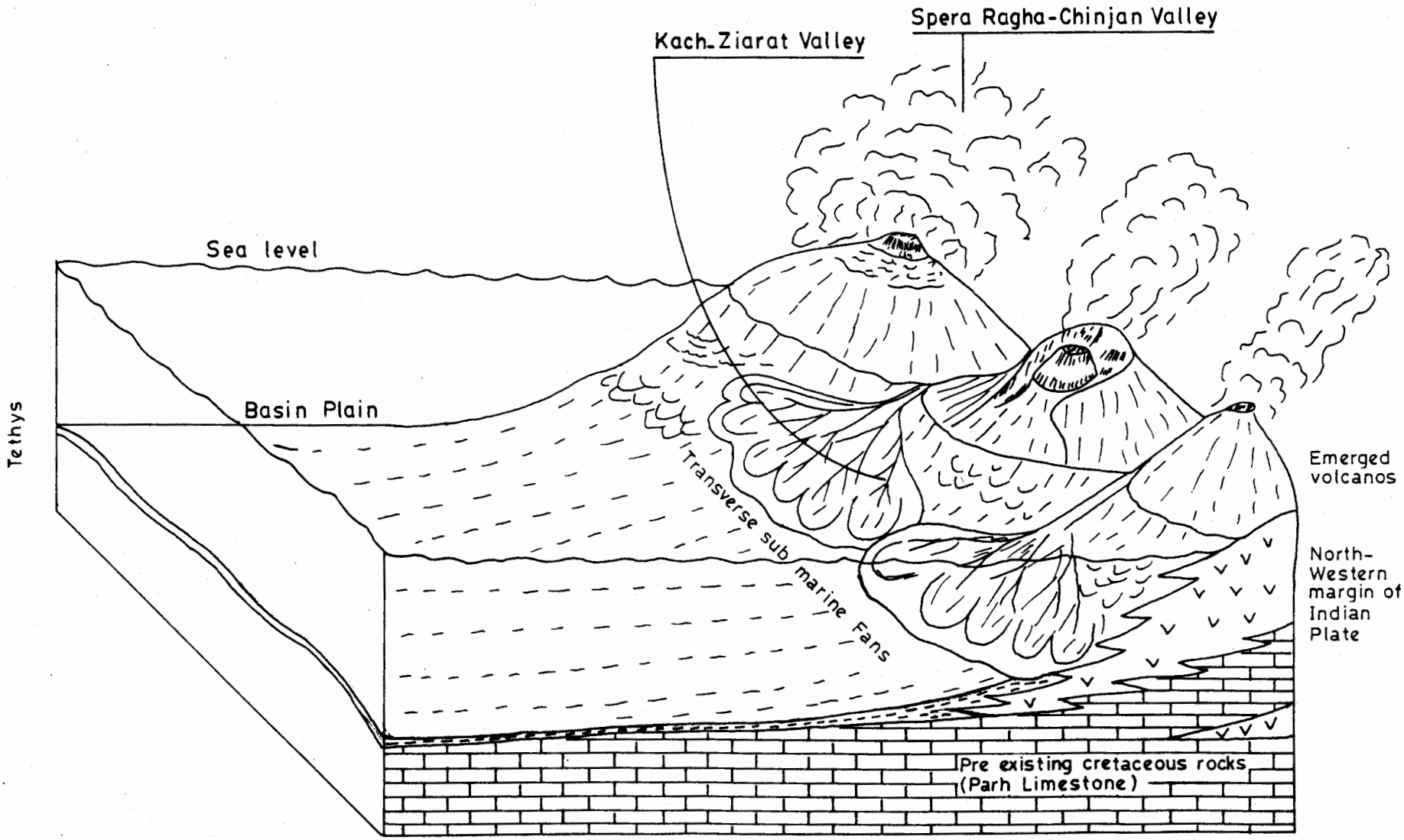

Figure 17. Proposed paleogeographic model showing development of the submarine fans on the slope of sea mounts at northwestern margin of Indo-Pakistan plate during Late Cretaceous.

DISTRIBUTARY CHANNEL DEPOSITS (MIDDLE FAN)

Channelized deposits are clearly recognizable within the Bibai formation at Allahdad, Shina Khawra, Ahmadun and Narai sections. They are characterized by their erosive bases, truncating the underlying facies (Fig. 4) and profusion of rip-up clasts, lenticular concave-up morphology, thinning (-fining) -upward trends and association of VC and SS facies (A and B facies classes of Mutti and Ricci Lucchi 1975, Pickering et al. 1986). Within the Bibai Submarine Fan channels are mostly filled with pebble to boulder size conglomerate, pebbly sandstone and rarely coarse sand.

Although depositional lobes are considered to be important parts of the submarine fans, not all submarine fans possess depositional lobes (Shanmugam and Moiola 1988). Within the Bibai Submarine Fan the thickening-upward cycles, which are characteristic of progradational trend of the fan lobes (Mutti and Ricci Lucchi 1975), have not been observed.

INTER-CHANNEL (OVERBANK-LEVEE) DEPOSITS

These deposits in the Bibai formation are represented by SSMS facies (facies C of Mutti and Ricci Lucchi 1975, Pickering et al.1986) of organized sand-mud couplets. No clear thickening-upward cycles may be seen. Beds are laterally continuous unless otherwise truncated by channels. Repeated truncation of these facies by distributory channels, lateral pinching and lack of clear 2nd and 3rd-order thickening-upward cycles (Mutti and Ricci Lucchi 1972, 1975) suggest that they are inter-channel (overbank-levee) deposits rather than the depositional lobes.

LOWER FAN (BASIN PLANE) DEPOSITS

Within the Kach-Ziarat valley the Bibai formation at certain levels, and also increasingly towards northeast and southwest of the Bibai Peak, contain the MS facies (Fig. 10) of mudstone and siltstone (facies D and E of Mutti and Ricci Lucchi 1975 and Pickering et al. 1986). These facies are characteristic of lower fan and basin plane areas. Near Kach and Pinakai, facies MS (Facies E of Pickenring et al. 1986) dominates which represent the the lower fan deposits at distal part of the Bibai Submarine Fan.

The Bibai Submarine Fan resembles with the Type-III system of the three types of "models" of Mutti (1985) which is composed of channel-levee complex. It is because the Bibai Submarine Fan does not possess any thickening-upward succession which are characteristic of the depositional lobes. Type I and II systems represent detached and attached lobe models, respectively, of Mutti (1985). Among the four types of submarine fans of Shanmugam and Moiola (1988), the Bibai Submarine Fan resembles with that of the "mixed setting", as it has particularly developed on the basinward slope of seamounts (hotspot volcanos) on passive northwestern (and northward drifting) margin of Indo-Pakistan Plate (Fig. 18). Hence, the Bibai Submarine Fan may not be attributed to any of the remaining three types of settings of Shanmugam and Moiola (1988), i.e. the "Immature Passive Margin Setting (North Sea Type)", "Passive Margin Setting (Atlantic Type)" and "Active Margin Setting (Pacific Type)". However, the very coarse (conglomeratic) nature of the Bibai Submarine Fan is a character comparable with the steep, short and radial character of the active margin fans.

DISCUSSION

Lateral variations of facies and paleocurrent directions (Fig. 13) show that distinctive proximal-distal variations exist in a systematic manner. The range of processes involved in development of the submarine fan include the sediment gravity flows, slumps, slides, debris flows, grain flows and turbidity currents (Suturn 1985). In areas of active explosive volcanism sediment supply rates are high and slopes often very steep so that gravity flows are common phenomena. Slopes on sea mounts are commonly concave-up, reaching up to 40° and on average about 20° (Cas and Wright 1987). Similar sort of slope conditions and dimensions of sea mounts can be envisaged on the Bibai Volcanics. Volcanic turbidites are particularly common in submarine volcanic settings and may be deposited in the form of submarine fans (Mitchell 1970, Bailes 1980, Fischer 1984, Suturn 1988). Sediments are mainly supplied from pyroclastic eruptions, although well rounded nature of the conglomerate suggests longer distance of transport and emergence of the sea mounts. There is close interaction between volcanic and sedimentary processes and volcanic activity is a vital control on sedimentation. Although autoclastic, hydroclastic (hyaloclastic) and pyroclastic processes have their own share in the overall composition of the volcaniclastic succession, epiclastic processes i.e. sedimentary erosion, transport and deposition seem to be most dominant. In oceanic sea mounts, due to the presence of volcanic vents at great depth, the hydrostatic pressure of water column prevents the explosive eruption of basalt, although hyaloclastite could form (Cas and Wright 1987). Formation of the pillow structures, as commonly observed within the Bibai Volcanics, would generally be regarded as the most distinctive feature of the basaltic lava erupted in submarine conditions.

The underlying rocks in both the Spera Ragha-Chinjun and Kach-Ziarat valleys are the pelagic succession of the Parh Limestone and overlying rocks, the shallow marine succession of the Fort Munro Formation, Pab Sandstone and Dungan Limestone. It indicates that during the periods of volcanic eruption and development of Bibai Submarine Fan there was an overall shallowing-up trend suggesting a sea-level fall and/or tectonic uplift. Shallowing-up trend is also evidenced from the association of pelagic limestone in

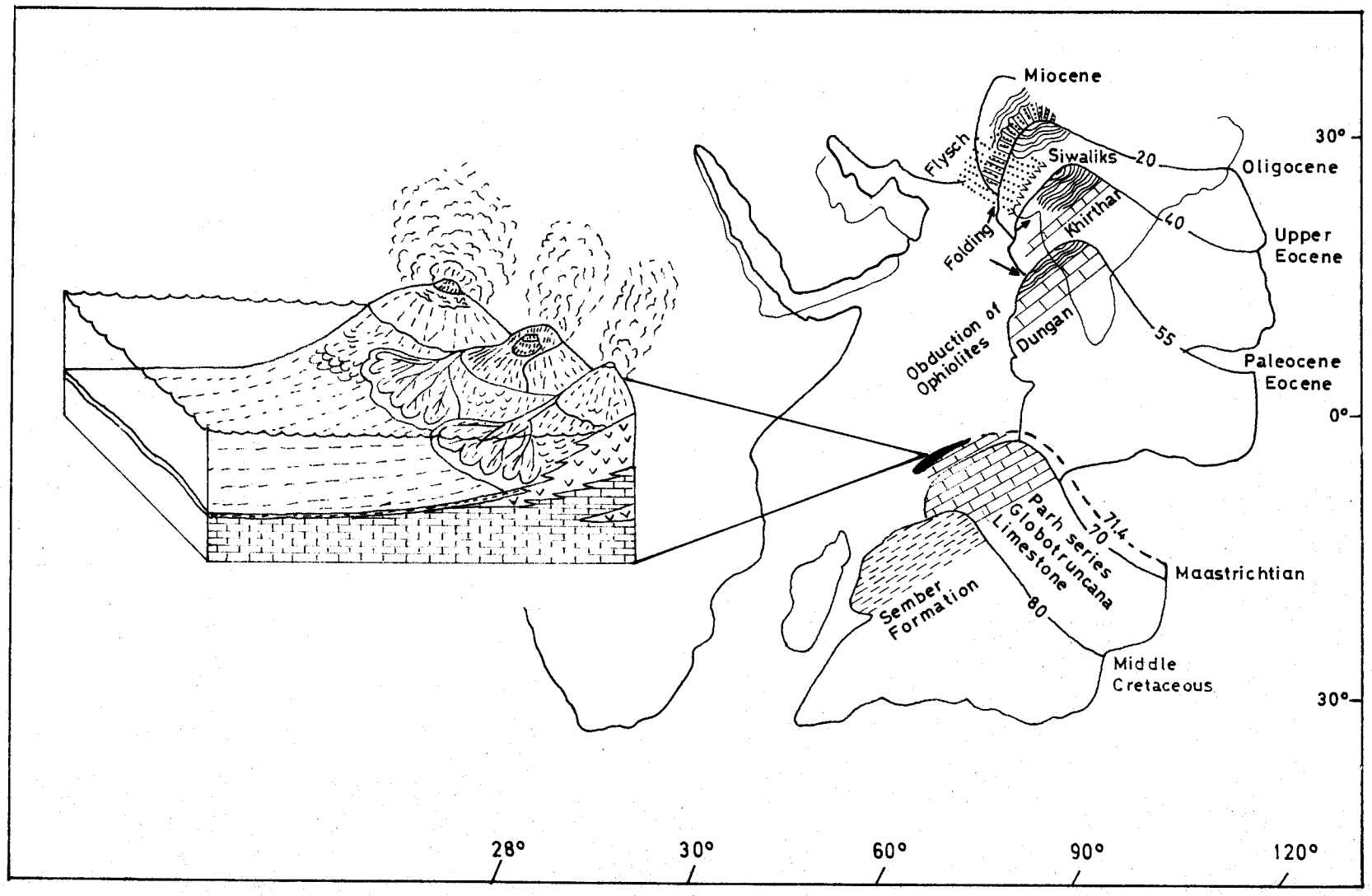

Figure 18. Sketch showing northward drift and anticlockwise rotation of the Indo-Pakistan plate during Middle Cretaceous through Recent (modified after Powell 1979). Position of the seamount along with its westward paleocurrent directions is shown which have been rotated anticlockwise along with the northward drift and anticlockwise rotation of the Indo-Pakistan Plate.

lower part and shallow marine fauna in upper part of the volcaniclastic succession of the Bibai formation in Kach-Ziarat valley. Continued volcanic eruption, along with the sea-level fall and /or tectonic uplift, ultimately caused emergence of the volcanic craters (Fig. 16-18). Evidence of the emergence can be observed in Spera Ragha valley in the form of a well developed oxidation zone (Fig. 13) on top of the *in-situ* volcanic succession of the Bibai formation. Paleocurrent directions also support this notion by indicating a northward source area for the volcaniclastic succession in Kach-Ziarat valley (Fig. 14).

The proposed paleogeographic model (Fig. 16-18) suggests development of submarine fans on slopes of the sea mounts (hotspot volcanos) that developed on the north-western margin of the Indian Ocean. The submarine fans developed in response to the emergence of these volcanos which provided volcaniclastic detritus to the submarine fans. Vail et al. (1977) suggested that accumulation of major sequences of coarse grained turbidites require periods of relative sea-level fall (lowstand) and/or tectonic uplift. Retrogressive slides, produced either by tectonic uplift, eustatic sea-level fall or their combination, appear to be basic factors in controlling the occurrence of predominantly coarse grained turbidite facies i.e. sandstone and conglomerate deposited by high concentration gravity flows (Facies A and B of Mutti and Ricci Lucchi 1972, 1975 and Pickering et al. 1986). Lowering of sea-level and/or tectonic uplift caused by northward drift of Indo-Pakistani Plate towards Eurasia as well as volcanic activity, i.e. development of sea mounts (the Bibai volcanics), led to conditions suitable for deposition by gravity flows. The present trend of paleocurrent directions observed within the Bibai Submarine Fan, generally from north-northeast to south-southwest (Fig. 13) showing derivation of detritus from north-northeast, must have been considerably rotated anticlockwise in response to the overall anticlockwise rotation of the Indo-Pakistani Plate along with its continued north-northeastward drift (Powell 1979) during the Upper Cretaceous and later periods till present time (Fig. 18). General restoration of the Indo-Pakistani continent in a clockwise direction back to its 71.4±3.4 My position would bring the presently south-southwest trend of paleocurrents to its original west-northwest direction which justifies a west-northwestward original paleoslope of the Indo-Pakistani Plate during the Upper Cretaceous.

Petrogenetic study of the Bibai Volcanics (Siddiqui et al. 1994, 1996) clearly suggests that they represent 71.4±3.4 My old alkali basalt of the hotspot-related volcanic activity. Also the petrogenetic study of the volcaniclastic detritus of the Bibai Submarine Fan in Kach-Ziarat valley suggests its derivation from volcanic terrain of hotspot origin (Khan 1998, Khan et al. 1999).

The paleo-position of the northwestern margin of Indo-Pakistani Plate during Upper Cretaceous was around 5° ± 5° south latitude and 70° east longitude (Powell 1979, Fig. 18). A more recent paleomagnetic study by Khadim et al. (1992) have given a 17° ± 8° south paleo-latitude for the Bibai Volcanics which roughly coincides with the present position of the Reunion Island in the Indian Ocean, a sea mount postulated (Dietz and Holden 1970, Whitemarsh 1974, Wilson 1989) to have formed in a hotspot related setting. Hotspot origin has also been suggested for the Chagos-Laccadive Ridge and Duccan Basalt, the lateral equivalents of the Bibai volcanics, which represent manifestation of the Reunion hotspot formed by passage of Indo-Pakistan continent and Indian Ocean floor during 68-66 Ma and 57-49 Ma, respectively (Siddiqui et al. 1996). The 71.4±3.4 My Bibai volcanics, therefore, represent manifestation of the Reunion hotspot formed by the passage of Neo-Tethys ocean floor and northwestern margin of Indian continent respectively, as perceived by Siddiqui et al. (1996).

The paleogeographic model suggests growth of the Late Cretaceous (71.4 ± 3.4 My) sea mounts over the pelagic (Parh) limestone succession over which the Bibai Submarine Fan developed (Fig. 18). The Bibai Submaine Fan extends from Saran Tangai (NE of Quetta) to Urghargai to the East of Ziarat (Fig. 1). These seamounts were actually the *in-situ* volcanic rocks of the Bibai volcanics which extend further westward to the north of Bibai Peak. Source area was the westward lateral extension of the *in-situ* Bibai volcanics of Spera Ragha-Chinjun valley which now unconformably underlies the Miocene-Pliocene Siwalik Group. Development of the sea mounts possibly on lower shelf or upper slope of the Tethyan sea floor caused high-angle sea-ward slope (toward west) over which the Bibai Submarine Fan developed. Development of the submarine fan, associated with the emergence and denudation of the sea mounts, was followed by submergence and deposition of shallow marine succession along with folding, thrusting and obduction of ophiolites.

CONCLUSIONS

1) Volcaniclastic succession of the Upper Cretaceous Bibai formation comprises various sedimentary facies and facies associations that are characteristic of gravity flow deposits such as slides, slumps, debris flows and high to low concentration turbidity currents.

2) Vertical and lateral organization of the facies and facies associations, paleocurrent pattern and paleogeographic position of the volcaniclastic succession of the Bibai formation suggest that it developed in a "channel-overbank (-levee) complex" for which the name Bibai Submarine Fan is proposed.

3) Paleocurrent pattern and volcanic nature of the detritus suggest that source area was a volcanic terrain to the north of Bibai Peak (Kach-Ziarat valley), i.e. westward extension of the *in-situ* volcanic rocks of the Spera Ragha-Chinjun valley.

4) The Bibai Submarine Fan formed on slope of a series of sea mounts (hotspot volcanos) that grew on the northwestern margin of the Indo-Pakistan Plate over the pelagic limestone succession on the Tethyan sea-floor and which later-on emerged and provided volcaniclastic detritus to the submarine fan.

5) The present trend of paleocurrent directions observed within the Bibai Submarine Fan (from north-northeast to south-southwest) indicate considerable north-northeastward drift and anticlockwise rotation of the Indo-Pakistan Plate which continued during the Upper Cretaceous and later periods till present time.

REFERENCES

Allemann, F., 1979. Time of emplacement of the Zhob Valley Ophiolites and Bela Ophiolites, Balochistan, *In* Farah, A. and DeJong, K. A., (eds.), Geodynamics of Pakistan: Geological Survey of Pakistan, Quetta, p. 215-242.

Baloch, W. K. and McCormick, G. R., 1995. Late Cretaceous volcanism in northwestern Balochistan, Pakistan: Abstract, International Symposium on Himalayan Suture Zones of Pakistan: 11-12, Pakistan Museum of Natural History, Islamabad, p. 27.

Bailes, A. H., 1980. Origin of early Proterozoic volcaniclastic turbidites, south margin of the Kisseynew sedimentary gneiss belt, File Lake, Manitoba: Precambrian Res., 12, p. 197-225.

Barnes, A. E. and Normark, W. R., 1985. Diagnostic parameters for comparing modern submarine fans and ancient turbidite systems: *In* Bouma, A. H., Normark, W. R. and Barnes, N. E., (eds.), Submarine fans and related turbidite systems: Springer-Verlag, New York, p. 13-14 and Wall Chart.

Bouma, A. H., 1962. Sedimentology of some flysch deposits - a graphic approach to the facies interpretation: Elservier, Amsterdam, 165 p.

Bouma, A. H., Normark, W. R. and Barnes, N. E., (eds.), 1985, Submarine fans and related turbidite systems: Springer-Verlag, New York. 352 p.

Cas, R. A. F. and Wright, J. V., 1987. Volcanic succession modern and ancient - A geological approach to processes, products and succession: Allen andUnwine, London.

DeJong, K. A. and Subhani, A. M., 1979. Note on the Bela Ophiolites with special reference to the Kanar area, *In* Farah, A. and DeJong, K. A., (eds.), Geodynamics of Pakistan: Geological Survey of Pakistan, Quetta, p. 263-270.

Dietz, R. S. and Holdon, J. C., 1970. The break-up of Pangaea: Geol. Soc. Am. Bull., 221, p. 126-137.

Fisher, R.V., 1984. A review of submarine volcanism, transport processes and deposits: *In* Kokelaar, B. P. and Howells, M. F., (eds.), Marginal Basin Geology - Volcanic and Associated Sedimentary and Tectonic Processes in Modern and Ancient Marginal Basins. Spec. Publ. Geol. Soc. London. No. 16, 5-28, Blackwell Scientific Publications, Oxford.

HSC: Hunting Survey Corporation, 1960, Reconnaissance Geology of part of West Pakistan: A Colombo Plan Cooperation Project, Toronto, Canada. 550 p.

Kassi, A. M., Khan, A. S., Kakar, D. M., Qureshi, A. R., Durrani, K. H. and Khan, H., 1993. Preliminary Sedimentology of part of the Bibai formation, Ahmadun-Gogai Area, Ziarat District, Balochistan: Geol. Bull. Punjab Univ., 28, p. 73-80.

Kazmi, A. H., 1955. Geology of the Ziarat-Kach-Zardalu area of Balochistan: D.I.C. thesis, Imperial College of Science andTechnology, London (unpubl.), 157 p.

Kazmi, A. H., 1979. The Bibai and Gogai Nappes in the Kach-Ziarat area of northeastern Balochistan: *In* Farah, A. and DeJong, K. A., (eds.), Geodynamics of Pakistan: Geological Survey of Pakistan, Quetta, p. 333-340.

Kazmi, A. H., 1984. Petrology of the Bibai Volcanics, northeastern Balochistan: Geol. Bull. Univ. Peshawar, 17, p. 34-51.

Kazmi, A. H., 1988. Stratigraphy of the Dungan Group in Kach-Ziarat area, northeastern Balochistan: Geol. Bull. Univ. Peshawar, 21, p. 117-130.

Kazmi, A. H., 1995. Sedimentary Sequence: *In* Bender, F. K. and Raza, H. A., (eds.), Geology of Pakistan: Gebruder Borntraeger.

Khadim, I. M., Yoshida, M. and Zaman, H., 1992. Paleomagnetic study of Late Cretaceous basaltic rocks in Calcareous Zone, Muslim Bagh area: Proc. Geosci. Colloq., 1, p. 99-114.

Khan, W., 1986. Geology and petrochemistry of part of the Parh Group Volcanics near Chinjun: M. Phil. dissertation, Centre of Excellence in Mineralogy, University of Balochistan, Quetta (unpubl.).

Khan, W., 1994. Geology, geochemistry and tectonic setting of the volcanic rocks of Chinjun and Ghunda Manra areas, northeastern Balochistan, Pakistan: Ph.D. dissertation (unpubl.), University of Iowa, 257p.

Khan, A. T., 1998. Sedimentology and petrology of volcaniclastic rocks of the Bibai formation, Ziarat District, Balochistan, Pakistan: Ph.D. thesis, Centre of Excellence in Mineralogy, University of Balochistan, Quetta.

Khan, A. T., Khan, A. S. and Kassi, A. M., 1999. Petrology, geochemistry and provenance of rock fragments of the volcanic conglomerate of the Bibai formation, Kach-Ziarat valley, western Sulaiman Thrust-Fold Belt, Pakistan: Abstract, 3rd South Asia Geological Congress (GEOSAS-III), Lahore, Pakistan.

McCormick, G. R., 1985. Preliminary study of the volcanic rocks of the South Tethyan suture in Balochistan, Pakistan: Acta Minralogica Pakistanica, I, p. 2-9.

Middleton, G. V. and Hampton, M. A., 1973. Sediment gravity flows - Mechanics of flow and deposition: *In* Middleton, G. V. and Bouma, A. H., (eds.), Turbidites and Deep-Water Sedimentation, Pacific Section: Soc. Econ. Paleontol. Mineral., Los Angeles, California, p. 1-38.

Mitchell, A. H. G., 1970. Facies of an early Miocene volcanic arc, Male Kula Island, New Hebrides: Sedimentology, 14, p. 201-43.

Mutti, E., 1985, Turbidite system and their relations to depositional sequences: *In* Zuffa, G. G., (ed.), Provenance of arenites: D. Reidel Publishing Company, Dordrecht, p. 65-93.

Mutti, E. and Normark, W. R., 1987. Comparing examples of modern and ancient turbidite systems - Problems and concepts: *In* Leggett, J. K. and Zuffa, G. G., (eds.), Marine Clastic Sedimentology - Concepts and Case Studies: Graham and Trotman,

London, p. 1-37.
Mutti, E. and Ricci Lucchi, F., 1972. Turbidites of the Northern Apennine - introduction to facies analysis: Int. Geol. Rev., 20, p. 125-166.
Mutti, E. and Ricci Lucchi, F., 1975. Turbidite facies and facies associations: *in* Examples of turbidite facies and facies associations from selected formations of the Northern Apennines: Field Trip Guide Book, A-11. Int. Sediment. Congr., IX, Nice, p. 21-36.
Otsuki, K., Anwar, M., Mengal, J. M., Brohi, J. A., Hohino, K., Fatmi, A. N. and Okimura, Y., 1989. Break-up of Gondwanaland and emplacement of ophiolitic complex in Muslim Bagh area of Balochistan: Geol. Bull. Univ. Peshawar, 22, p. 103-126.
Pickering, K. T., Stow, D. A. V., Watson, M. and Hiscott, R. N., 1986. Deep-water facies, processes and models - a review and classification scheme for modern and ancient sediments: Earth Sci. Rev., 22, p. 75-174.
Pickering, K. T. and Hiscott, R. N., 1985. Contained (reflected) turbidity currents from the Middle Odovician Cloridorme Formation, Quebec, Canada - an alternative to the antidune hypothesis: Sedimentology, 32, p. 373-394.
Powell, C. M. A., 1979. A Speculative Tectonic History of Pakistan and Surroundings - some constraints from the Indian Ocean: *In* Farah, A. and DeJong, K. A., (eds.), Geodynamics of Pakistan, Geological Survey of Pakistan, Quetta, p. 5-24.
Ricci Lucchi, F., 1975. Depositional cycles in two turbidite formations of Northern Apennines (Italy): Jour. Sediment. Petrol., 45, p. 3-43.
Sawada, Y., Siddiqui, R. H., Khan, S. R. and Aziz, A., 1992. Mesozoic igneous activity in Muslim Bagh area, Pakistan with special reference to hotspot magmatism related to break-up of Gondwanaland: Proc. Geosci. Colloq., 1, p. 21-70.
Sawada, Y., Siddiqui, R. H. and Khan, S. R., 1995. K-Ar Ages of the Mesozoic Igneous and Metamorphic Rocks from the Muslim Bagh area, Pakistan: Proc. Geosci. Colloq., 12, p. 73-90.
Shah, S. M. I., (ed.), 1977. Stratigraphy of Pakistan: Geological Survey of Pakistan, Mem. 12, 138 p.
Shanmugam, G. and Moiola, R. J., 1985. Submarine fan models: Proc. Annu. Conf. Nigerian Assoc. Pet. Explor., 1, p. 18-39.
Shanmugam, G. and Moiola, R. J., 1988. Submarine fans - characteristics, models, classification and reservoir potential: Earth Science Reviews, 24, p. 383-428.
Siddiqui, R. H., Khan, I. H. and Aziz, A., 1994. Petrogenetic study of hotspot related magmatism on the northwestern margin of Indian continent and its stratigraphic significance: Proc. Geosci. Colloq. Geosci. Lab, GSP, 8, p. 100-128.
Siddiqui, R. H., Khan, I. H. and Aziz, A., 1996. Geology and Petrogenesis of Hotspot Related Magmatism on the Northwestern Margin of the Indian continent: Proc. Geosci. Colloq. Geosci. Lab. GSP, 16, p. 115-48.
Stow, D. A. V., 1985. Deep sea clastics - Where are we and where we are going ?: *In* Brenchley, P. S. and Williams, B. P. J., (eds.) Sedimentology - recent developments and applied aspects: Geol. Soc. (London), Spec. Publn., 18,p. 67-93.
Stow, D. A. V. and Bowen, A. J., 1980. A physical model for the transportation and sorting of fine grained sediments by turbidity currents: Sedimentology, 27, p. 36-46.
Suturn, R. J., 1985. Facies analysis of volcaniclastic sediments - a review: *In* Brenchley, P. J. and Williams, B. P. J., (eds.), Sedimentology - Recent Developments and Applied Aspects: Geol. Soc. London, Spec. Publn., 18, p. 123-146.
Vail, P. R., Mitchum, R. M. and Thompson, III, S., 1977. Seismic stratigraphy and global changes of sea-level, Part 4 - Global cycles of relative changes of sea-level: *In* Payton, C. E., (ed.), Seismic Stratigraphy - application to Hydrocarbon Exploration: AAPG Memoir 26, p. 83-97.
Whitemarsh, R. B., 1974. Summary of general features of Arabian Sea and Red Sea Cenozoic History based on Leg 23 cores: Init. Rep. DSDP, 23, p. 377-390.
Williams, M. D., 1959. Stratigraphy of the lower Indus basin, West Pakistan: Proc. 5th World Petroleum Congress, Sec. New York, 1, 19, p. 337-391.
Wilson, J. T., 1989. Mantle plumes and plate motions: Tectonophysics, 19, p. 149-164.
Yoshida, M., Khadim, I. M. and Zaman, H., 1995. Paleomagnetism of pillow basalt in the Muslim Bagh area, Balochistan, Pakistan - Late Cretaceous trace of Re-Union Hotspot: Geologica, Res. Bull. Geosci. Lab., GSP, 1, p. 77-90.

Manuscript received Nov. 12, 1999
Revised Manuscript received April 15, 2000
Accepted May 20, 2000

ACTA MINERALOGICA PAKISTANICA
Volume 11 (2000)

Article Reference AMP11.2000/025-034/ISSN0257-3660

PETROGRAPHY AND GEOCHEMISTRY OF THE ARCHEAN BASEMENT COMPLEX OF MADHYAPARA AREA, DINAJPUR, BANGLADESH

MOHAMMAD NAZIM ZAMAN, SYED SAMSUDDIN AHMED AND MD. BADRUL ISLAM
Department of Geology and Mining, University of Rajshahi, Rajshahi 6205, Bangladesh.

ABSTRACT

At Madhyapara area the Basement Complex comprises tonalites, granodiorites, granodiorite gneiss with granite, adamellite and quartz-monzonite intrusions. The tonalite-granodiorite (TG) suite is the dominant rock type of the Basement Complex and characterized by typical granitoid texture and calc-alkaline in nature. This suite is mainly composed of feldspar, quartz, hornblende, biotite and a few accessories. Sericitic alteration of plagioclase feldspar and chloritization of hornblende and biotite are common. The ferromagnesian phase gradually decrease from tonalite to granodiorite implying fractionated nature of magma where clinopyroxene, hornblende and biotite played the dominant role. The granite, adamellite and quartz-monzonite are the intruded rocks having thickness of 1 to 5 meter and sharp contact with the TG suite. The intruded rocks are characterized by alkali feldspar, microcline-perthite, quartz and a few accessory minerals. The TG suite is of metaluminous, I-type granitoid formed in continental arc granitoid environment with a subduction related magmatism, derived by partial melting of a mafic source magma from lower crust to upper mantle and the intruded rocks are peraluminous, S-type formed in post orogenic granitoid environment derived by partial melting of pre-existing metasediments from upper crust to lower crust.

INTRODUCTION

Mineralogical study is a documentation of the observable facts about a rock, in terms of its mineralogy and texture. This study is of great importance in elucidating the genetic history of an igneous suite because it takes into account the mineralogical composition of the rocks of the suite and its cooling behavior as reflected by the texture. The Archean basement rocks are exposed as Indian Shield close to the Bangladesh territory but no exposure occurs in the extended Indian Shield of Bangladesh. Geologically the Indian Shield covers the basement rocks in the northwestern part of Bangladesh which extends to the east up to the Shillong Plateau (Fig. 1). Geophysical and drilling data indicate that at Madhyapara area the basement rocks occur at the shallowest depth of 128 meter with a thin cover of Pliocene Dupi Tila Formation, Pleistocene Barind Clay Formation and Alluvium of Recent age. Several boreholes have been drilled for exploration of the Basement Complex and to develop the hard rock mine in this area. Underground mining of the rocks for commercial purposes is now on the way. In the present research detailed mineralogical and geochemical study of core samples of the basement rocks encountered in the boreholes BH-1, BH-2, BH-5 and GDH-35 has been carried out in order to classify and to ascertain the possible origin of the studied rocks.

CLASSIFICATION

Rock types of the Archean Basement Complex in the study are classified according to their modal composition on the basis of classification scheme of Streckeisen (1973) in Table 1 and Fig. 2. Considering the relative abundance of quartz, alkali feldspar and

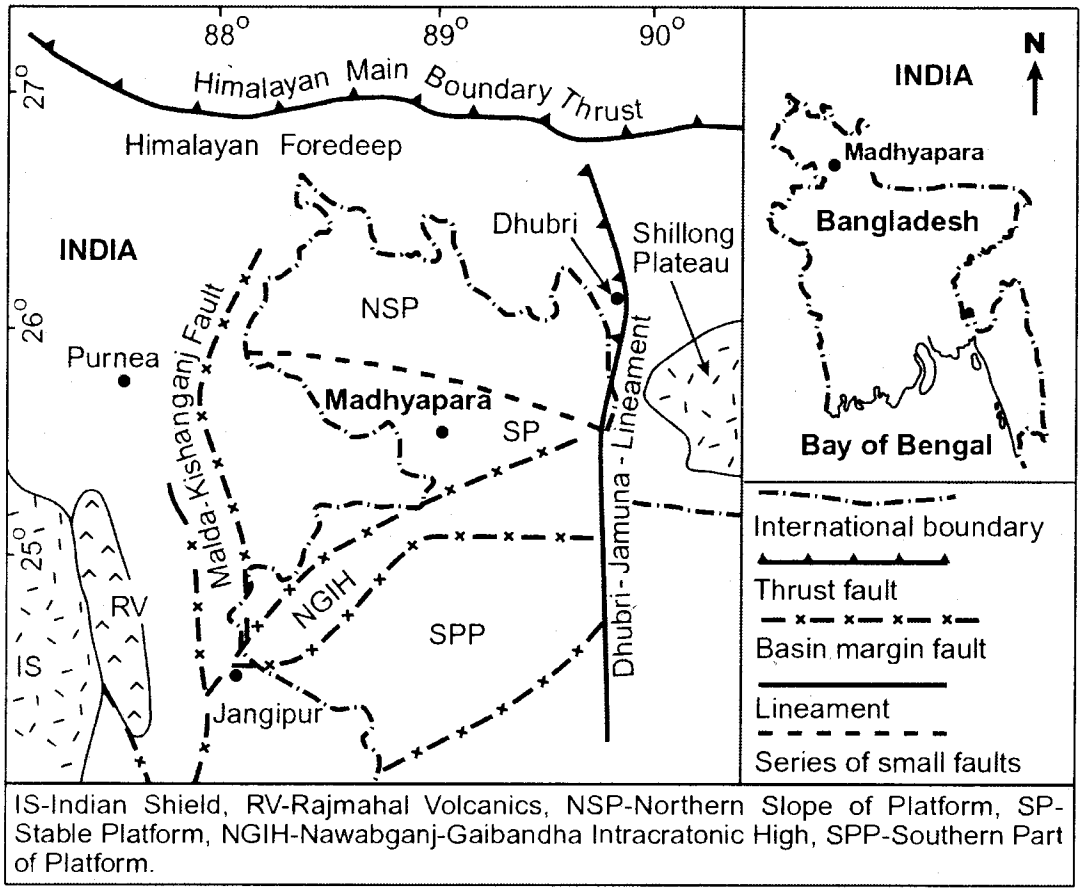

Figure 1. Location map of Madhyapara area, Dinajpur, Bangladesh.

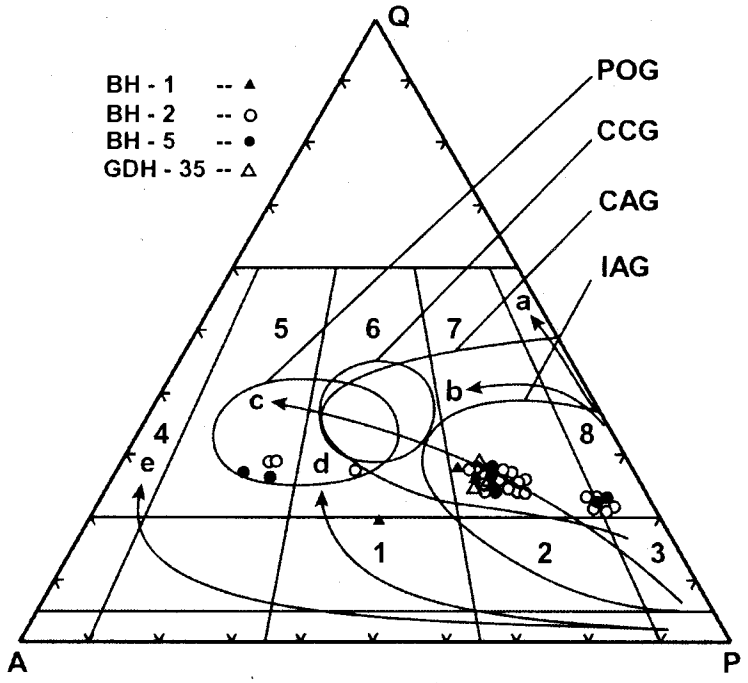

Figure 2.
Modal A-P-Q diagram for the basement rocks of Madhyapara area. **Fields**: 1. Quartz-monzonite 2. Quartz-monzodiorite 3. Quartz-diorite 4. Alkali-feldspar granite 5. Granite 6. Adamellite 7. Granodiorite 8. Tonalite, (after Streckeisen 1973). **Trends**: a-tholeiitte, b-calc-alkaline trondhjemite (low-K), c- calc-alkaline granodiorite (medium-K), d- calc alkaline (high-K), e-alkaline, (after Lameyre and Bowden, 1982). **POG** - Post orogenic granitoids, **CCG** - Continental collision granitoids, **CAG** - Continental arc granitoids, **IAG** - Island arc granitoids, (after Maniar and Piccoli, 1989).

Table 1. Modal composition of the basement rocks of Madhyapara area

BH. No.	Depth (m)	Sample No.	Plagioclase	Alkali Feldspar	Quartz	Horn-blende	Biotite	Chlorite	Apatite	Sericite	Epidote	Clino-zoisite	Pyroxene	Zircon	Garnet	Sphene	Opaque	C.I.	Comment
1	264.94	SB-01	42.00	21.00	23.00	9.00	3.00	0.80	0.10	0.10	0.20	0.10	0.40	0.10	0.05	0.00	0.15	14	Granodiorite
1	297.56	SB-02	39.00	36.00	19.00	0.60	2.40	1.20	0.10	0.45	0.10	0.00	0.00	0.00	0.00	0.30	0.85	05	Quartz-Monzonite
1	300.00	SB-03	44.00	19.00	21.00	9.00	3.00	1.00	0.50	0.20	0.70	0.20	0.45	0.15	0.15	0.03	0.62	15	Granodiorite
2	160.67	SB-06	54.00	5.00	16.00	12.00	5.80	2.00	1.00	0.80	1.50	0.00	0.90	0.30	0.40	0.10	0.20	23	Tonalite
2	165.85	SB-08	41.00	21.00	23.00	8.00	4.00	2.00	0.30	0.10	0.10	0.00	0.30	0.05	0.10	0.00	0.05	15	Granodiorite
2	177.90	SB-10	42.00	15.00	22.00	8.00	5.00	2.00	0.96	0.30	1.30	0.40	0.80	0.20	0.20	0.60	1.24	19	Granodiorite
2	187.04	SB-12	41.00	19.00	23.00	8.00	4.00	1.00	0.50	0.20	0.80	0.20	0.90	0.20	0.30	0.20	0.70	16	Granodiorite
2	210.37	SB-13	45.00	17.00	21.00	9.00	3.00	1.60	0.06	0.20	0.10	0.00	0.85	0.20	0.10	0.09	1.80	17	Granodiorite
2	228.05	SB-15	52.00	6.00	17.00	16.00	4.00	1.00	0.60	0.20	0.30	0.40	1.70	0.10	0.20	0.10	0.40	24	Tonalite
2	232.62	SB-16	21.00	46.00	28.00	0.60	2.00	0.70	0.00	0.60	0.00	0.00	0.00	0.10	0.00	0.20	0.80	04	Granite
2	235.67	SB-17	44.00	19.00	22.00	7.00	3.00	1.00	0.60	0.20	0.90	0.30	1.10	0.20	0.10	0.00	0.60	14	Granodiorite
2	240.55	SB-20	46.00	18.00	20.00	8.00	4.00	1.00	0.96	0.20	0.30	0.10	0.50	0.30	0.20	0.10	0.34	15	Granodiorite
2	257.01	SB-23	33.00	37.00	27.00	0.80	1.00	0.40	0.00	0.06	0.00	0.00	0.00	0.15	0.10	0.20	0.29	03	Adamellite
2	262.50	SB-24	43.00	16.00	22.00	10.00	5.00	0.80	0.20	1.00	0.50	0.00	0.90	0.10	0.10	0.00	0.40	18	Granodiorite
2	263.72	SB-25	42.00	17.00	21.00	9.00	4.00	2.60	0.60	0.80	0.40	0.20	1.10	0.20	0.15	0.00	0.95	19	Granodiorite
2	266.46	SB-26	45.00	15.00	21.00	9.00	5.00	1.00	0.40	0.60	0.50	0.20	1.10	0.30	0.20	0.20	0.50	18	Granodiorite
2	281.10	SB-30	56.00	5.00	16.00	13.00	5.00	1.00	0.70	0.40	0.30	0.30	1.50	0.10	0.10	0.00	0.60	22	Tonalite
2	283.84	SB-31	42.00	19.00	22.00	10.00	3.00	0.60	0.40	0.30	0.30	0.00	1.00	0.30	0.20	0.20	0.70	16	Granodiorite
2	292.38	SB-32	44.00	15.00	19.00	11.00	5.00	1.00	0.86	0.80	0.60	0.20	0.70	0.30	0.50	0.10	0.94	20	Granodiorite
2	300.00	SB-34	44.00	18.00	21.00	9.00	4.00	0.80	0.60	0.30	0.70	0.20	0.90	0.10	0.20	0.00	0.20	16	Granodiorite
2	300.91	SB-35	43.00	16.00	21.00	11.00	5.00	1.00	0.10	0.40	0.30	0.00	0.95	0.15	0.20	0.00	0.90	20	Granodiorite
2	314.33	SB-36	22.00	46.00	26.00	0.80	2.65	0.80	0.00	1.00	0.00	0.00	0.00	0.10	0.00	0.25	0.40	05	Granite
2	318.29	SB-38	43.00	17.00	23.00	9.00	3.60	0.80	0.50	0.80	0.60	0.20	0.90	0.20	0.10	0.10	0.20	16	Granodiorite
2	341.16	SB-40	45.00	18.00	21.00	8.00	3.50	1.00	0.30	1.30	0.60	0.20	0.80	0.10	0.10	0.10	0.00	14	Granodiorite
5	158.54	SB-42	22.00	48.00	25.00	0.70	3.00	0.00	0.00	0.00	0.00	0.00	0.00	0.10	0.00	0.10	1.10	05	Granite
5	162.80	SB-43	54.00	6.00	17.00	13.00	5.00	1.00	0.90	0.70	0.30	0.40	1.00	0.30	0.40	0.00	0.00	21	Tonalite
5	236.28	SB-46	43.00	18.00	21.00	11.00	5.00	0.50	0.20	0.30	0.20	0.00	0.40	0.10	0.10	0.00	0.20	18	Granodiorite
5	273.78	SB-47	56.00	5.00	18.00	12.00	5.00	1.00	0.70	0.40	0.20	0.10	0.90	0.20	0.25	0.00	0.25	20	Tonalite
5	280.49	SB-48	44.00	17.00	21.00	11.00	4.60	0.80	0.20	0.40	0.10	0.10	0.50	0.10	0.20	0.00	0.00	17	Granodiorite
5	297.56	SB-49	18.00	52.00	25.00	1.00	2.60	0.40	0.00	0.00	0.00	0.00	0.00	0.10	0.00	0.10	0.80	05	Granite
35	153.05	SB-50	41.00	17.00	22.00	9.00	5.00	1.40	0.80	0.20	0.40	0.10	1.40	0.20	0.30	0.10	1.10	19	Granodiorite Gneiss
35	159.45	SB-51	43.00	18.00	21.00	9.00	6.00	0.60	0.60	0.20	0.20	0.00	0.90	0.10	0.10	0.00	0.30	17	Granodiorite Gneiss
35	160.67	SB-52	44.00	19.00	20.00	8.50	4.50	0.80	0.70	0.30	0.40	0.10	0.90	0.20	0.15	0.10	0.35	16	Granodiorite Gneiss

plagioclase and texture, the studied rocks are grouped into tonalite, granodiorite, granodiorite gneiss, granite, adamellite and quartz-monzonite. The granodiorite, tonalite, granodiorite gneiss are the country rocks while granite, adamellite and quartz-monzonite are the intruded rocks (1-5m thick), having sharp contact with the tonalite-granodiorite (TG) suite of the Basement Complex at Madhyapara area. Granodiorite gneisses occur at depth of 153.05 to 160.67m in the borehole GDH-35, which show weakly developed fabric.

PETROGRAPHY

GRANODIORITE

Granodiorite is the dominant rock type of the Archean Basement Complex at Madhyapara area which is medium-coarse-grained, holocrystalline, hypidiomorphic to allitriomorphic granular texture having an interlocking arrangement of the mineral grains. Plagioclase (41-46%) occurs as anhedral to subhedral phase. In is the most dominant phase with anorthite content ranging from 16 to 24%. Few zoned plagioclase grains are also noticed. Plagioclase also shows sericitic alteration at places. Anhedral to subhedral quartz (19-24%) grains are generally fractured and exhibit undolose extinction. Both orthoclase and microcline (14-21%) are anhedral to subhedral by having occasional perthitic and graphic intergrowth.

Hornblende (7-11%) is the most abundant mafic mineral dominant over biotite. Both hornblende and biotite are anhedral to subhedral and are spatially closely associated. Apatite inclusions are also noticed in some of the hornblende grains. Biotite (3-5%) is light to dark brown in color. Some grains are locally bent and twisted. Many of the grains are altered to chlorite and some are partially altered along the cleavage plane. Epidote is an accessory mineral and dark brown in color. Augite (0.25%) and hypersthene (0.52%) are the two main pyroxene phases in this rock. Sphene, zircon, garnet and opaque occur as accessories.

TONALITE

Tonalites are holocrystalline, hypidiomorphic granular, fine to medium grained rocks having an interlocking arrangement of the mineral constituents. Plagioclase (51-56%) is the dominant phase. It is generally anhedral to subhedral having normal zoning and is generally sericitized. Myrmekitic intergrowths are observed along the quartz and plagioclase feldspar boundary. Quartz (16-18%) occurs as fine to medium and anhedral to subhedral grain. Some of the grains are fractured and strained showing undolose extinction. Alkali feldspar (5-7%) occurs both as orthoclase and microcline. Orthoclase is, however, the dominant alkali feldspar.

Hornblende (12-16%) occurs as light green to dark green pleochroic grains. Alteration of hornblende to chlorite and epidote is very prominent as compare to that of granodiorites. The hornblende grain usually contains inclusions of apatite and garnet. Biotites (4-7%) are anhedral to subhedral, light to dark brown in color and show occasional alteration to chlorite. It also exhibits twisting and bending at places. Pyroxene (0.9-1.7%) is also present as anhedral to subhedral individual grains. Zircon, sphene, garnet, rutile and opaque occur as accessories.

GRANODIORITE GNEISS

Granodiorite gneiss is medium-coarse-grained, holocrystalline and hypidiomorphic granular texture. Granoblastic texture is also common. Plagioclase (41-44%) is generally sodic (An_{22}- An_{24}%) in composition and exhibit sericitic alteration at places. Few grains of plagioclases show normal zoning and having inclusions of fine-grained quartz. Some of the plagioclase grains are fractured and stained. Quartz (20-22%) is the second dominant felsic phase of the granodiorite gneisses. It is anhedral to subhedral, highly fractured having undolose extinction suggesting that the rock has undergone intense tectonic pressure. Both orthoclase and microcline are the common alkali feldspar. However, orthoclase (17-19%) is dominating the microcline.

Hornblende (upto 9%) is the most abundant mafic phases. It is anhedral to subhedral with green to greenish brown pleochroism. Inclusions of apatite are also noticed in some hornblende grains. Brown and greenish brown biotite (5-6%) is the second abundant mafic phase in the rock. It is twisted and bent around quartz grains exhibiting the fabric development in the rock. Biotite at places also exhibits chlorite tint. Pyroxene constitutes 1.07% (average) of the rock and is generally anhedral to subhedral. Garnet, sphene, zircon and opaque occur as accessories.

GRANITE

Granite is inequigranular, coarse-grained, holocrystalline and hypidiomorphic granular in texture. Alkali feldspar (46-52%) is the dominant phase. It is generally microcline, microcline-perthite and orthoclase. It commonly occurs as subhedral megacrysts. Microcline shows perfect hatched twining while orthoclase is colorless, generally turbid. Quartz (25-28%) is anhedral to subhedral and an essential mineral of the granites is the second dominant phase. Plagioclase (18-22%) is medium-coarse-grained and is sodic (An_4-An_6%) in composition. It is sericitized at places.

Biotite (2-3%) is the dominant mafic phase having light brown to dark brown pleochroism. Some of the biotite grains are twisted and bent at places. Few grains of green to greenish brown hornblende are also noticed.

ADAMELLITE

Adamellite is medium-coarse-grained, holocrystalline and hypidiomorphic granular in texture.

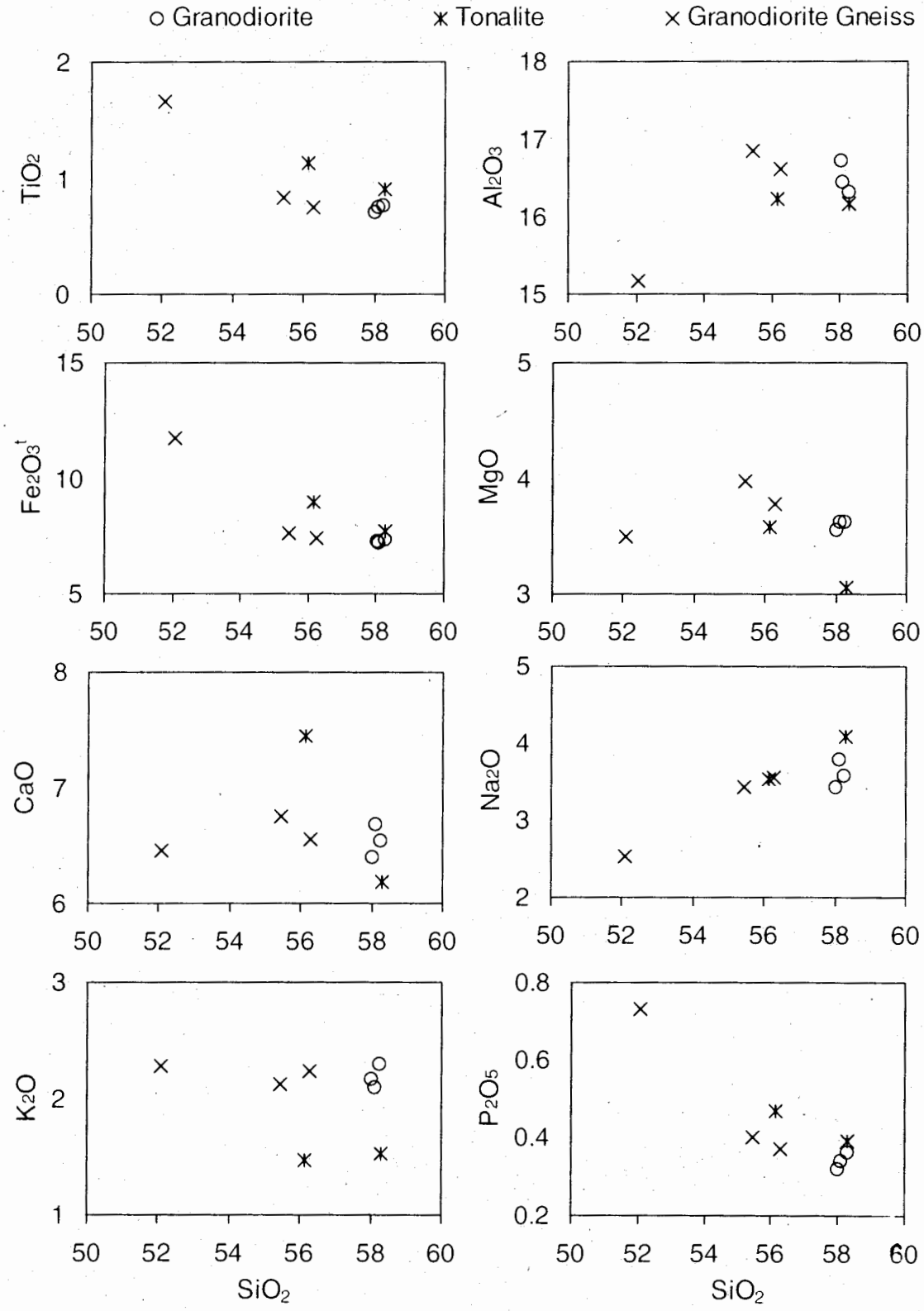

Figure 3. Variation diagram of major elements vs. SiO_2 (after Harker, 1909).

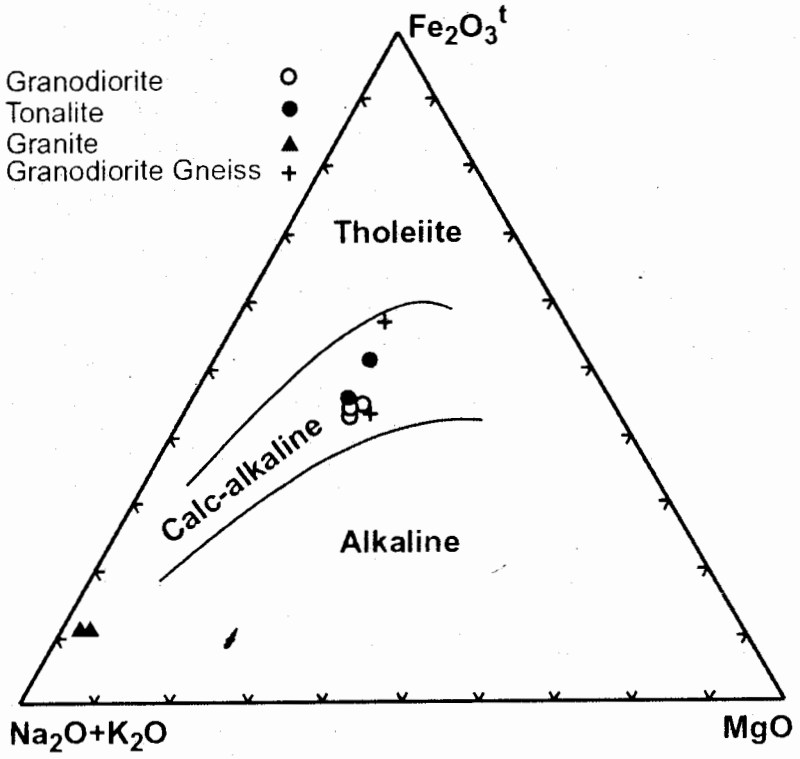

Figure 4. A-F-M diagram for the basement rocks of Madhyapara area shows calc-alkaline affinity (after Barker and Arth, 1976).

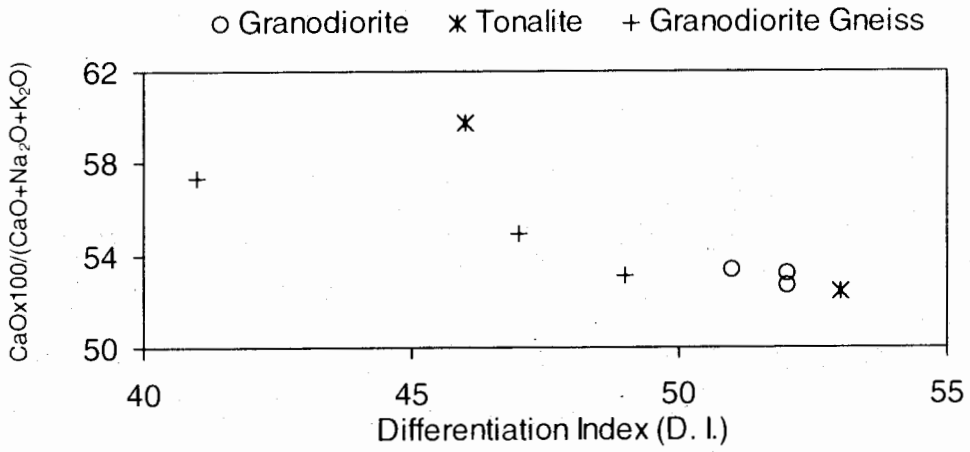

Figure 5. Correlation diagram of $(CaOx100)/(CaO+Na_2O+K_2O)$ for the TG suite of the Basement Complex.

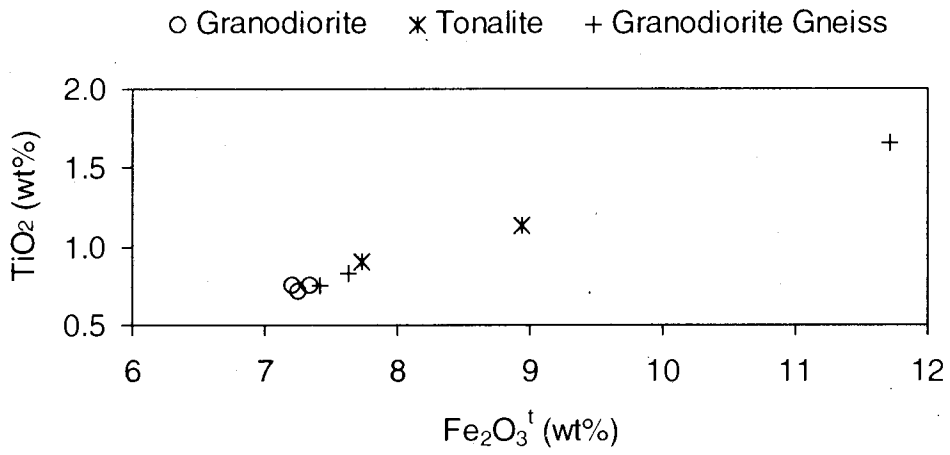

Figure 6. Correlation diagram of TiO_2 vs. $Fe_2O_3^t$ for the TG suite of the Basement Complex (after Islam, et al., 1997).

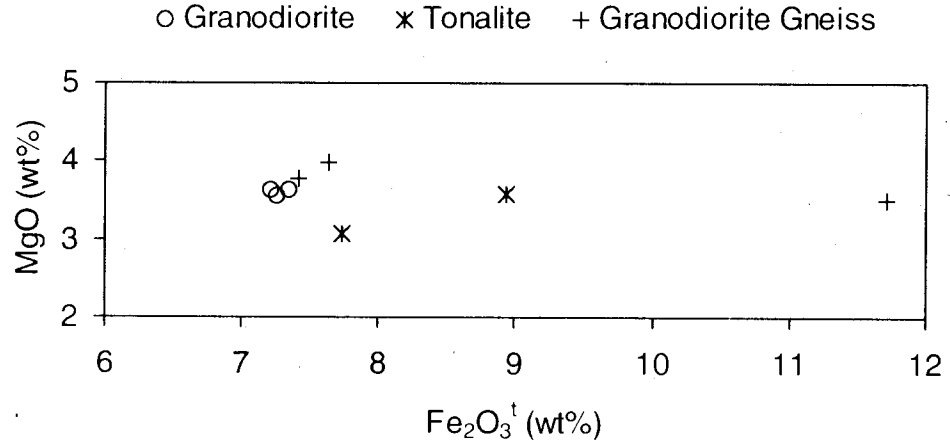

Figure 7. Correlation diagram of MgO vs. $Fe_2O_3^t$ for the TG suite of the Basement Complex (after Islam, et al., 1997).

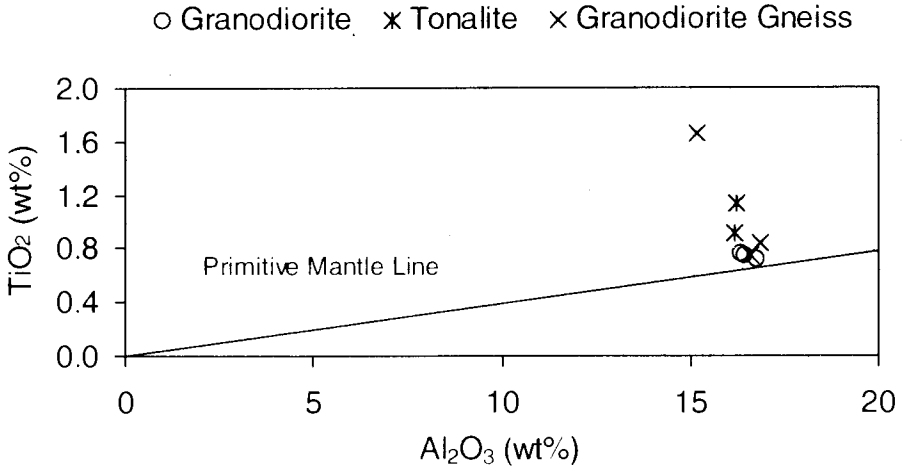

Figure 8. Correlation diagram of TiO_2 vs. Al_2O_3 for the TG suite of the Basement Complex (after Balakrishnan, et al., 1990).

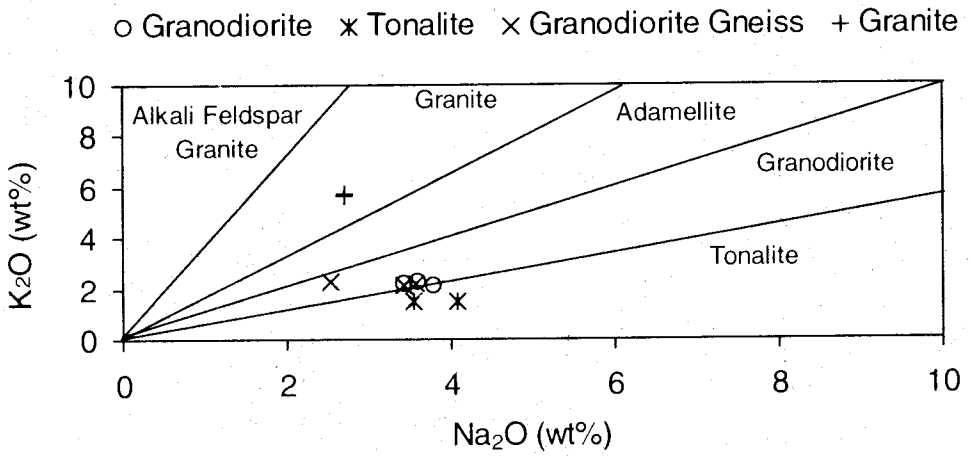

Figure 9. Plot of Na_2O vs. K_2O for the basement rocks of Madhyapara area (after Harpum, 1963).

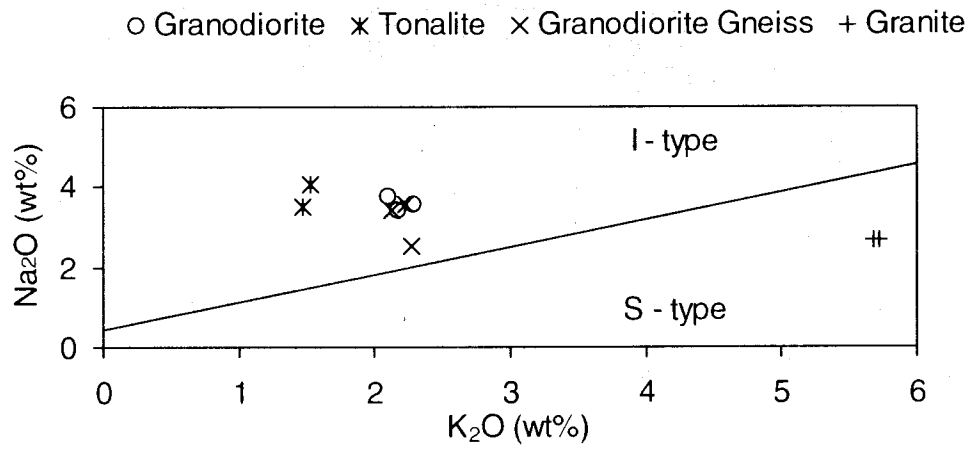

Figure 10. Plot of K_2O vs. Na_2O for the basement rocks of Madhyapara area (after Agrawal, 1999).

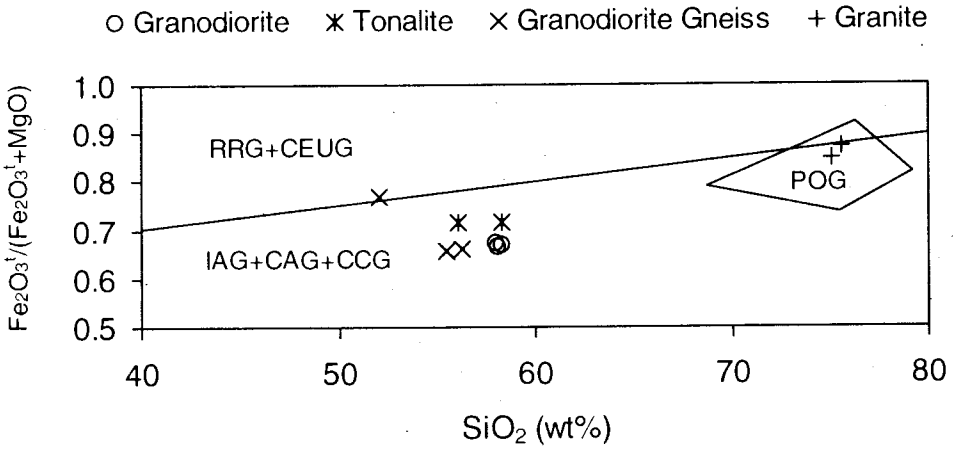

Figure 11. Plot of SiO_2 vs. $Fe_2O_3^t/(Fe_2O_3^t+MgO)$ for the basement rocks of Madhyapara area (after Maniar and Piccoli, 1989).

Alkali feldspar constitutes 37% and is represented by microcline, microcline-perthite and orthoclase while commonly occurs as subhedral megacrysts. Both graphic and perthitic textures are common in these phases. Plagioclase constitutes 33% of the rock. It is generally subhedral, medium-coarse-grained. Sericitic alteration is however, not uncommon in plagioclase. Quartz (upto 27%) is an abundant felsic mineral of the adamellite. It is usually medium-grained and subhedral to anhedral. Biotite (1%) is mainly subhedral and light to dark brown in color. It also shows bending at places. Few anhedral green to greenish brown pleochroic hornblende grains are also present. Zircon, sphene and some opaque varieties are the common accessory.

QUARTZ-MONZONITE

Quartz-monzonite is fine to medium-grained holocrystalline and hypidiomorphic granular in texture. Plagioclase (39%) is sodic (An_{11}%) in composition and usually anhedral, medium-coarse-grained. Both orthoclase and microcline constitute 36% of the rock. These are fractured and show partial alteration to sericite. Subhedral to anhedral, fine-medium-grained quartz (19%) occurs within the interstices of feldspar. Biotite (2.4%) is the main mafic mineral. It is generally fractured and shows chlorite tint. Few green to dark green pleochroic hornblende grains are also noticed. Zircon, sphene and opaque occur as accessories.

GEOCHEMISTRY

The major elements analyses of seven core samples of the Basement Complex of boreholes BH 2 and BH 5 were carried out X-ray Fluorescence Spectrometry (XRF) method at the department of Geoscience, Shimane University, Japan. The analyses of three core samples of borehole GDH 35, however, performed by using Inductively Coupled Plasma Atomic Emission Spectroscopy (ICP-AES) method, at the department of Earth and Space Sciences, University of Science and Technology, China. The major elements of different rock types of the Basement Complex of Madhyapara are presented in Table 2. SiO_2 is 56 to 58 % in tonalites, 58 % in granodiorites, 52 to 56 % in granodiorite gneiss and 75 % in granites. In Harker variation diagram (Harker, 1909) TiO_2, MgO, CaO and P_2O_5 gradually decrease and Al_2O_3, Na_2O and K_2O increase with increasing SiO_2 in the TG suite implying fractionated nature of magma (Fig. 3). To identify the type of magma the AFM discrimination diagram (Barker and Arth, 1976) used which pointed out that the TG suite and gneissic rocks plot in the calc-alkaline field and granitic rocks occupy the alkaline corner (Fig. 4). The TG suite and gneissic rocks are metaluminous (A/CNK < 1) and granites are peraluminous (A/CNK > 1), (Table 1). The ratio (CaO*100)/(CaO + Na_2O + K_2O) when plotted against differentiation index (D. I.) for the TG suite and gneissic rocks shows a negative trend (Fig. 5). The negative correlation suggests preferential entry of CaO over total alkali in the early mafic phases, possibly pyroxene or amphibole. Correlation of $Fe_2O_3^t$ vs. TiO_2 and MgO shows positive trend (Fig. 6 and 7) indicate that the TG suite and gneissic rocks is consistently controlled by hornblende and biotite (Islam, *et al.*, 1997).

During partial melting of a source region the minerals in which Al_2O_3 is an essential structural constituent (ESC) is present, then the Al_2O_3 content in the melt is fixed (Sun and Hanson, 1975). In minerals like plagioclase or garnet, Al_2O_3 is an essential structural constituent. The Al_2O_3 abundance of melts in equilibrium with the above minerals is determined by equilibrium distribution coefficient (K_d) and will not vary as a function of extent of melting. Whereas, if there is no residual phase in which Al_2O_3 is an ESC, the Al_2O_3 content in melts will vary as a function of extent of partial melting just like an incompatible trace element. Thus in a suite of rocks representing different extents of partial melting, by studying the variation in Al_2O_3 abundance one can infer about the presence of phases like garnet or plagioclase in residue (Balakrishnan *et al.* 1990).

The TG suite of the basement rocks plotted in Al_2O_3-TiO_2 diagram (Fig. 8). The corresponding mantle values are also plotted in the diagram. All samples of the TG suite and gneissic rocks plot above the primitive mantle line. TiO_2 abundance shows a wide range compared to virtually constant Al_2O_3 abundance. From this, it can be infer that an aluminium-bearing phase was present either in the residue or as one of the fractional crystallization phases that had equilibrated with the melt representing the TG magmas.

Plots in the Harpum (1963) diagram the TG suite is concentrated in the field of granodiorite and tonalite whereas the intruded granitic rocks plot in the field of granite (Fig. 9). The K_2O/Na_2O is on average 0.61 and 0.39 in granodiorite and tonalite respectively. The high K_2O/Na_2O ratio (average 2.12) in the granitic rocks suggests formation of granite by anatexis of pelitic rocks. In the Na_2O versus K_2O plot (Agrawal, 1999) the TG suite and gneissic rocks fall in the field of I-type and the granites fall in the S-type field (Fig. 10).

DISCUSSION AND CONCLUSIONS

The TG suite and gneissic rocks of the Basement Complex of Madhyapara area are holocrystalline, hypidiomorphic granular in texture having an interlocking arrangement of the mineral constituents. Quartz and plagioclase shows frequent interlocking arrangement indicating their simultaneous crystallization over a long span of time. The presence of minerals like pyroxene, hornblende, biotite and relatively high content of MgO, TiO_2, $Fe_2O_3^t$, CaO

suggest their formation from a mafic source. The TG suite is calc-alkaline, metaluminous and I-type granitoid while granites are alkaline, peraluminous and S-type granitoid.

In the APQ diagram (Maniar and Piccoli, 1989) to ascertain the tectonic environment of the basement rocks show that the TG suite and gneissic rocks occupy the continental arc granitoid (CAG) field whereas the granitic rocks concentrate in the post-orogenic granitoid (POG) field (Fig. 2). The chemical data SiO_2 vs. $Fe_2O_3'/Fe_2O_3'+MgO$ (Maniar and Piccoli, 1989) also support the above result (Fig. 11). The trend line (Lameyra and Bowden, 1982) shows that the TG suite of the basement rocks of Madhyapara is medium K-calc-alkaline granodiorite (Fig. 2). Calc-alkali series usually do not manifest pronounced increases in Fe/Mg ratio. On the other hand a greater abundance of intermediate magma (diorite-tonalite) is characteristics of this series (Bose, 1997). The calc-alkaline nature of the basement rocks of Madhyapara area suggests that the primary magmas were produced in a subduction related environments (Abdel-Rahman, 1990). The decrease of TiO_2, MgO, CaO and P_2O_5 with the increase of SiO_2 is attributed to fractionation of ferromagnesian minerals. It is likely thought that the TG suite had been derived through fractionation of clinopyroxene and hornblende. Chappell and White (1974) recognized granitoids of crustal type (S-type) and mantle type (I-type). The alumina saturation index of the granites are > 1 and genetically they are classified as S-type granites which interpreted to originate from lower to upper crust and the metaluminous TG suite of Madhyapara belongs to I-type granitoid pluton interpreted to originate from upper mantle to lower crust (Chappell and White, 1974).

In view of mineralogical and geochemical study it is suggested that the TG suite and gneissic rocks of the Archean Basement Complex of Madhyapara area might have been resulted by partial melting from a mafic source magma. The coarse-grained granites are the partial melting products derived from pre-existing metasediments, injected through the fractures of the TG suite at later stage and are thus younger than the TG suite.

ACKNOWLEDGMENTS

This paper is a part of the doctoral thesis (Ph.D.) of the first author. Authorities of Madhyapara Hard rock Mining Co. Ltd. are highly acknowledged for providing samples and for permission to publish this paper. Dr. Chowdhury M. Kamruzzaman, Manager of the same organization helped to have core samples and necessary basic information regarding the Basement Complex. Authors are indebted to Prof. Md. Rafiqul Islam, Director (Retd.), Research and Publication, University Grant Commission, Bangladesh for providing valuable suggestions and stimulating discussions to improve the original manuscript.

REFERENCES

Abdel-Rahman, A.M. 1990. Petrogenesis of Early-Orogenic Diorites, Tonalites and Post-Orogenic Trondhjemites in the Nubian Shield. Jour. Petrol., v.31, Part 6, p. 1285-1312.

Agrawal, S. 1999. Geochemical discrimination diagrams: a simple way of replacing eye-fitted field boundaries with probability based classifier surfaces. Jour. Geol. Soc. India. v.54, p. 335-346.

Balakrishnan, S., Hanson, G.N. and Rajamani, V. 1990. Pb and Nd isotope constraints on the origin of high Mg and tholeiitic amphibolites, Kolar Schist Belt, South India. Contrib. Mineral. Petrol., v.107, p.272-292.

Barker, F. and Arth, J.G. 1976. Generation of trondhjemitic-tonalitic liquids and Archean bimodal trondhjemite basalt suites. Geology., v.4, p.596-600.

Bose, M.K. 1997. Igneous Petrology. The World Press Private Limited, Calcutta. 568 p.

Chappell, B.W. and White, A.J.R. 1974. Two contrasting granite types. Pacific Geol., v.8, p.173-174.

Harker, A. 1909. The natural history of igneous rocks. Macmillan. Co., New York. 384 p.

Harpum, J.R. 1963. Petrogenetic classification of granitic rocks in Tanganiyka by partial chemical analysis. Rec. Geol. Surv. Tanganiyka., v.10, p.80-88.

Islam, R., Bist, K.S., Chaudhuri, B.K., Rawat, B.S. and Purohit, K.K. 1997. Geochemistry and petrogenesis of Hanuman Tibba Granite of Kullu Valley, Himachal Himalaya. Jour. Geol. Soc. India. v.49, p.13-21.

Lameyre, J. and Bowden, P. 1982. Plutonic rock types series: discrimination of various granitoid series and related rocks. Jour. Vol. Geotherm. Res., v.14, p.169-186.

Maniar, P.D. and Piccoli, P.M. 1989. Tectonic discrimination of granitoids. Bull. Geol. Soc. America., v.101, p.635-643.

Streckeisen, A.L. 1973. Plutonic rocks: classification and nomenclature recommended by the I. U. G. S. Subcommission on the systematic of Igneous Rocks. Geotimes., v.18, Part 10, p.26-30.

Sun, S.S. and Hanson, G.N. 1975. Origin of Ross Island basanitoids and limitations upon the heterogeneity of mantle sources for alkali basalts and nephelinites. Contrib. Mineral. Petrol., v.52, p.77-106.

Thornton, C.P. and Tuttle, O.F. 1960. Chemistry of igneous rocks 1: Differentiation index. Am. Jour. Sci., v.258, p.664-684.

Manuscript received Dec. 24, 2000
Revised Manuscript received March 12, 2001
Accepted March 13, 2001

ACTA MINERALOGICA PAKISTANICA
Volume 11 (2000)

Article Reference AMP11.2000/035-044/ISSN0257-3660

CHEMISTRY OF CHLORITE AND BIOTITE IN THE CALC-SILICATE ROCKS AT MINIKI GOL, CHITRAL, PAKISTAN: AN INDICATOR OF HYDROTHERMAL ALTERATION

MOHAMMAD ZAHID[1] AND CHARLIE J. MOON[2]
[1] Department of Geology, University of Peshawar
[2] Department of Geology, University of Leicester, LE1 7RH, UK

ABSTRACT

The chlorite and biotite have been found within the calc-silicate rocks, mica quartzite and schist of the Jurassic Arkari Formation and associated leucogranite at Miniki Gol of Chitral, northern Pakistan near the Pak-Afghan border within the eastern Hindu Kush. The chemistry of the chlorite and biotite of the scheelite-bearing calc-silicate quartzite is markedly different from that of barren calc-silicate quartzite, schist and leucogranite. Both the chlorite and biotite from calc-silicate quartzite are Mg-rich and signify hydrothermal alteration in the study area. The aluminum content in the chlorite and biotite and the low level of Ti in the biotite also correspond to the hydrothermal activity at the Miniki Gol.

INTRODUCTION AND GENERAL GEOLOGY

The chemistry of chlorite and biotite can provide some constraints on the genesis of the enclosing rocks. The structure of biotite is flexible and can accept a large amount of cations and even anions, depending on the mineral assemblages (Labotka 1983). The chemistry of the hydrothermal biotite and chlorite is different from the igneous and metamorphic biotite and chlorite (Dymek 1983, Brimhall 1977, Brimhall et al. 1985). The chemical composition of the biotite also correlates generally with the grade of metamorphism (Dymek 1983). The composition of the chlorite and biotite can indicate a hydrothermal activity at Miniki Gol, Chitral, Northern Pakistan.

The study area at Miniki Gol lies within the eastern Hindu Kush range near the Pak-Afghan border (Figs. 1A-B). The area between the Pak-Afghan border and the Reshun fault is mainly composed of metasediments of Devonian to Jurassic in age (Pascoe 1924, Calkins et al. 1981, Pudsey et al. 1985, Buchroithner and Gamerith 1986). Leake et al. (1989) separated the metasediments to the northwest of Shoghor Limestone into three lithostratigraphic formations, Sewakht, Lutkho and Arkari Formations (Fig. 1B).

The Arkari Formation is composed of garnet-mica schist, phyllite, calc-silicate quartzite, tourmalinite and a thick unit of marble. The scheelite-bearing calc-silicate rock represents a skarn-type mineral assemblage. This rock is composed of clinozoisite, quartz, calcic-amphibole, plagioclase, chlorite, biotite, calcite, sphene, garnet and scheelite. The calc-silicate patches and lenses are located within the mica schist about 400 m away from Miocene leucogranites (Fig. 2). The area has undergone at least two episodes of deformation accompanied with metamorphism of upper-amphibolite grade.

Chlorite and biotite occur in the barren calc-silicate quartzite, scheelite-bearing calc-silicate quartzite, mica quartzite and schist of the Arkari Formation at Miniki Gol. Biotite has been found in the exposed leucogranite whereas chlorite is rare in the leucogranite. The present study deals with the mineral chemistry of the chlorite and biotite that have not been analysed in the past in detail. The chemistry of the chlorite and biotite from all the above-mentioned lithologies has been analysed and

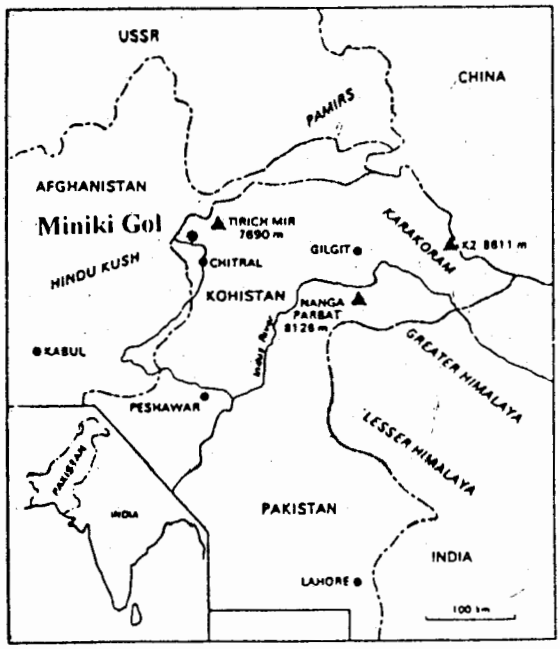

(A)

Figure 1.
(A) Topographic framework of N. Pakistan showing the location of study area (after Fletcher 1985).
(B) Geological map of the Garam Chashma area showing Arkari Formation that hosts tungsten mineralization (after Leake et al. 1989).

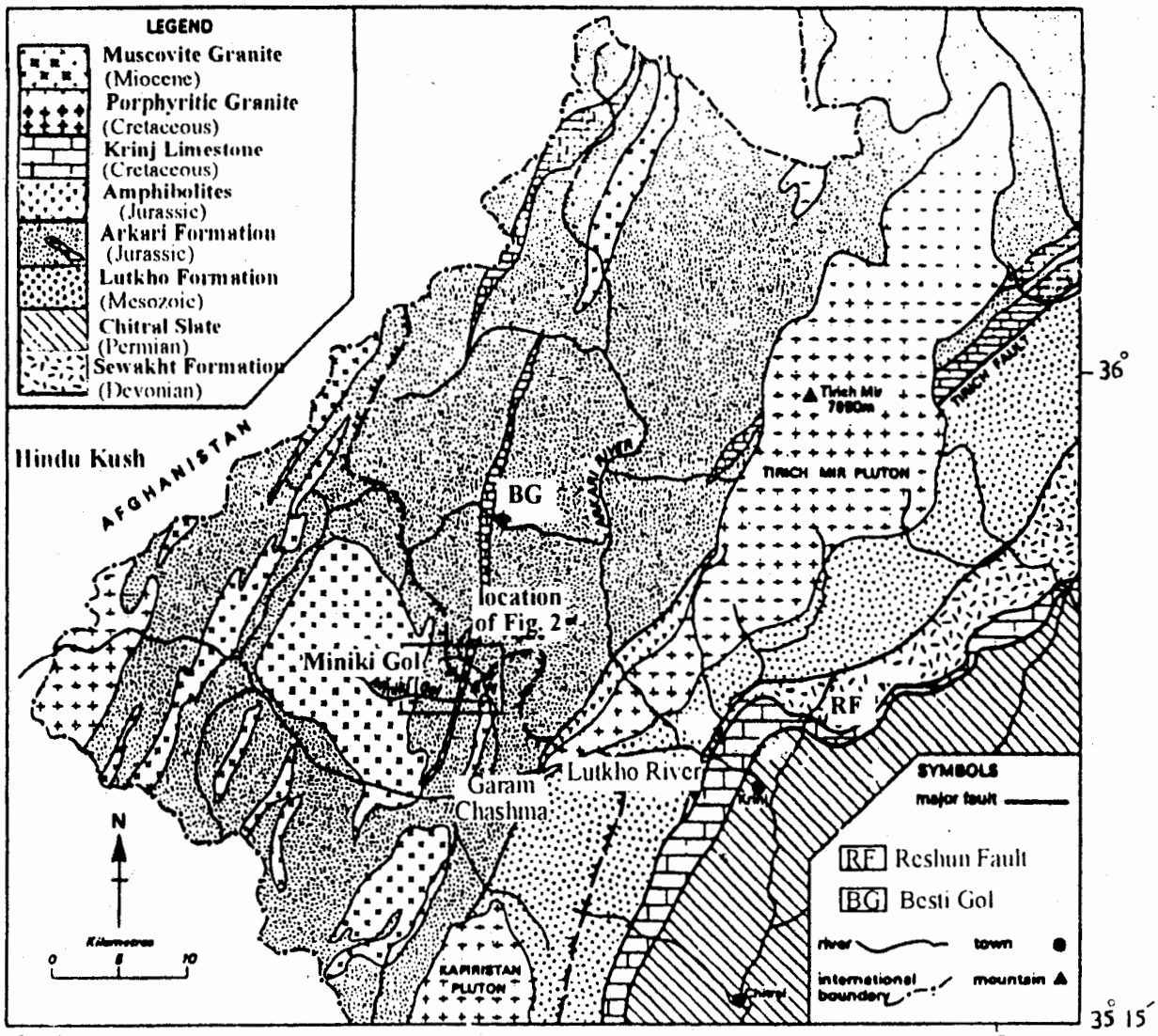

(B)

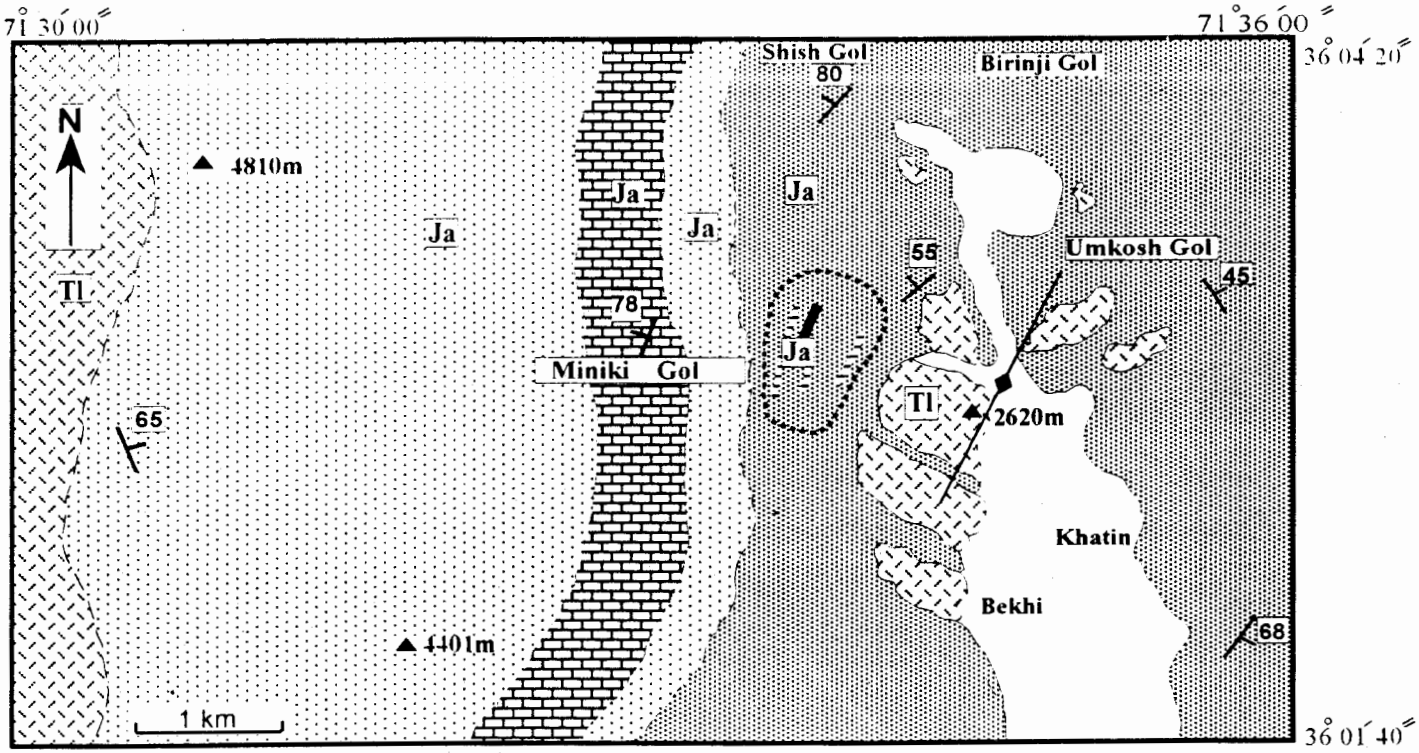

LEGEND

Tl Tertiary Leucogranite

Ja Jurassic Arkari Formation

Key to symbols

Alluvium | Calc-silicate quartzite | Tourmalinite | Scheelite mineralisation | Inferred contact

Phyllite | Marble | Mica schist | Contact | Anticline | Bedding

Figure 2. Simplified geological map of the Miniki Gol and surrounding area.

compared with each other.

ANALYTICAL TECHNIQUES

The analyses were performed through Jeol Superprobe model JXA-8600 with an on-line computer for ZAF corrections. Quantitative analyses were obtained using wavelength dispersive system under the following operating conditions: 15 kV accessory voltage; $30x10^{-9}$ A probe current; 20 (2x10) seconds peak, 10 (2x5) seconds negative background and 10 (2x5) seconds positive background counting times. The diameter of the X-ray beam varied according to the type, nature and grain size of the analysed phase. 5 mm diameter was used for most of the silicate phases.

The silicate phase were analysed for major and minor oxides such as SiO_2, TiO_2, Al_2O_3, FeO (total), MnO, MgO, CaO, Na_2O, K_2O and Cr_2O_3.

The following standards were used during these microprobe analyses: wollastonite (natural for Si, and Ca); rutile (natural for Ti); jadeite (natural for Al and Na); magnetite (synthetic for Fe); rhodonite (natural for Mn); MgO (synthetic for Mg); microcline (natural for K). The accuracy of the ZAF correction is generally better than 2%.

MINERALOGY

CHOLRITE

Chlorite has been found as small flakes or laths and lies at an angle to the main schistosity. Chlorite fibers replace biotite, actinolite and even clinozoisite in the calc-silicate quartzite, where additional Fe and Mg in chlorite are probably provided by the associated amphibole. These secondary chlorites exhibit grey birefringence compared with schist, giving blue coloration in transmitted light.

Microprobe data for chlorite are listed in Table 1, summarising the result of 46 representative points analysed within ten samples. The number of cations in the unit cell was calculated on the basis of 28 oxygen, assuming the total iron as Fe^{+2}. The Si deficiency in the tetrahedral coordination is compensated by Alz (tetrahedral alumina), whereas the unassigned alumina is placed in the octahedral site (Aly) {Table 1}. Chlorite in schist of the area under consideration is different clearly from the calc-silicate quartzite. The composition of the former falls in the field of ripidolite, whereas the later plots between the field of ripidolite and brunsvigite (Fig. 3A) of Foster (1962). Chlorite of the Miniki Gol calc-silicate quartzite is relatively rich in silica as compared to the chlorite in the schist (Table 1). Low value of Al_2O_3 of chlorite is noted in the calc-silicate quartzite compared to the schist. Similarly, the level of FeO in chlorite is higher in the schist than in scheelite-bearing calc-silicate quartzite. In contrast, MgO value in chlorite is low in the schist (up to 13.69 wt %) compared with those of scheelite-bearing calc silicate quartzite (up to 17.16 wt %) {Table 1}.

Chlorite from the calc-silicate quartzite exhibits low Alz values in contrast to those of the schist (Table 1). This level of Alz is compatible with the chlorite from igneous rocks (Bailey 1988, Abdel-Rahman 1995). The chlorites in the investigated area occupy two different positions on the diagram {Alz vs. $Fe^{2+}/(Fe^{2+} + Mg)$} but plot within the compositional field of metamorphic rocks (Fig. 3 B). Most of the analyses of chlorites from Miniki Gol calc-silicates quartzite fall within the field of Pan-African Nubian igneous chlorite (Fig. 3B) of Abdel-Rahman (1995).

BIOTITE

Biotite from the calc-silicate quartzite occurs as minute flakes exhibiting a feathery appearance and seems to be secondary. In comparison, it occurs in schist as bands defining primary schistosity. Biotite in the scheelite-bearing rocks is also associated with clinozoisite. Biotite is one of the dominant constituents in the schist and mica quartzite but also has been found in the leucogranite and calc-silicate quartzite at Miniki Gol.

A summary of microprobe data of 136 analyses from 9 sample in the studied biotite is given in the (Table 2). Structural formula was calculated on the basis of 22 oxygen, assuming total Fe as Fe^{+2}. The following are the main characteristics of the biotite at Miniki Gol.

- Most of the mica analyses have $(Fe/(Fe+Mg) \geq 0.33)$, that is compatible with biotite reported by Deer et al. (1962) although, some analyses plot on the boundary of phlogopite and biotite (Fig. 4A)
- Compositional variation exists within the biotite from schist and calc-silicate quartzite whereas biotite from leucogranite is homogenous in composition.
- The chemistry of biotite in the scheelite-bearing calc-silicate quartzite is different from that of the barren calc-silicate quartzite.
- Biotite in the scheelite-bearing quartzite contains relatively high levels of SiO_2 and MgO compared with those of barren calc-silicate quartzite, mica quartzite, schist and leucogranite respectively.
- Low values of Al_2O_3, FeO and TiO_2 in the biotite of scheelite-bearing calc-silicate quartzite have been found compared with other investigated rocks (Table 2).

TiO_2 content in the analysed biotite from the Miniki Gol scheelite-bearing calc-silicate quartzite is very low and corresponds to hydrothermal biotite (Dymek 1983), indicating hydrous activity in the study area. Biotite contains low Al-content in the scheelite-bearing quartzite (Fig. 4A). A low level of Al_2O_3 has also been reported in many skarns (cf. Robert 1972). The low Al-content and high Si in the scheelite-bearing quartzite reflect high silica activity in these rocks. In contrast, the Al_2O_3 content in the Miniki Gol schist is high, which is considered as typical value of the Al-rich regionally

Table 1. Microprobe analyses of chlorite from schist (ZC 1, ZC 2, ZC 9, ZC 25 and ZC 46), mica quartzite (ZC 4A), barren calc-silicate quartzite (ZC 27, ZC 32 and ZC 50) and scheelite-bearing calc-silicate quartzite (ZC 65A) at Miniki Gol. *= Total Fe is considered as FeO; $Fe^{\#} = Fe^{2+}/(Fe^{2+} + Mg)$.

Sample	Major Oxides											Cations per 28 oxygen atoms											
No.	SiO_2	TiO_2	$A_{l2}O_3$	Cr_2O_3	FeO*	MnO	MgO	CaO	Na_2O	K_2O	Total	Si	Ti	Alz	Aly	Cr	Fe^{2+}	Mn	Mg	Ca	Na	K	$Fe^{\#}$
ZC1	24.06	0.05	24.29	0.04	27.72	0.1	11.97	0.01	0.07	0.02	88.33	5.088	0.008	2.912	3.143	0.007	4.902	0.018	3.773	0.002	0.029	0.006	0.565
ZC1	24.09	0.04	24.3	0.02	27.7	0.09	11.73	0.01	0.04	0.01	88.03	5.107	0.007	2.893	3.18	0.003	4.912	0.016	3.707	0.002	0.017	0.002	0.57
ZC1	24.22	0.09	24.33	0.03	28	0.09	11.86	0	0.03	0.01	88.66	5.105	0.015	2.895	3.15	0.004	4.936	0.016	3.726	0	0.012	0.002	0.57
ZC1	24.23	0.06	24.36	0.04	27.95	0.12	11.83	0.01	0.02	0.01	88.63	5.106	0.009	2.894	3.157	0.007	4.927	0.021	3.716	0.002	0.008	0.002	0.57
ZC2	24.48	0.08	23.21	0.05	26.16	0.14	13.55	0.02	0.02	0.01	87.72	5.177	0.012	2.823	2.961	0.008	4.627	0.025	4.271	0.004	0.008	0.002	0.52
ZC2	24.41	0.08	23.37	0.03	25.99	0.14	13.64	0.02	0.01	0	87.69	5.158	0.012	2.842	2.978	0.004	4.592	0.025	4.296	0.004	0.004	0	0.517
ZC2	24.43	0.05	22.98	0.06	26.24	0.1	13.69	0.01	0.01	0.02	87.59	5.177	0.008	2.823	2.917	0.01	4.65	0.018	4.324	0.002	0.004	0.006	0.518
ZC9	24.27	0.07	23.71	0.07	27.66	0.01	12.41	0.01	0.01	0.01	88.23	5.134	0.011	2.866	3.047	0.011	4.894	0.002	3.913	0.002	0.004	0.002	0.556
ZC9	24.56	0.04	23.44	0.03	27.46	0.01	12.71	0.02	0.02	0.01	88.3	5.183	0.007	2.817	3.014	0.004	4.847	0.002	3.998	0.004	0.008	0.002	0.548
ZC9	23.85	0.1	23.14	0.02	27.16	0.03	12.1	0.01	0.01	0	86.42	5.153	0.017	2.847	3.045	0.003	4.908	0.006	3.896	0.002	0.004	0	0.557
ZC9	24.35	0.09	23.78	0.05	27.49	0.01	12.47	0.01	0	0.05	88.3	5.142	0.015	2.858	3.061	0.008	4.855	0.002	3.926	0.002	0	0.013	0.553
ZC9	24.22	0.09	23.84	0.05	27.35	0.02	12.56	0.01	0	0.02	88.16	5.121	0.015	2.879	3.061	0.008	4.836	0.003	3.958	0.002	0	0.006	0.55
ZC9	24.5	0.06	23.44	0.05	27.35	0.05	12.53	0.01	0	0.02	88.01	5.187	0.01	2.813	3.035	0.008	4.842	0.009	3.954	0.002	0	0.006	0.55
ZC9	24.16	0.06	23.77	0.07	27.63	0.02	12.28	0.02	0.01	0.02	88.04	5.124	0.01	2.876	3.067	0.011	4.901	0.003	3.883	0.004	0.004	0.006	0.558
ZC9	24.05	0.1	23.13	0.03	26.75	0.02	12.44	0.02	0	0	86.54	5.174	0.016	2.826	3.04	0.006	4.813	0.003	3.989	0.004	0	0	0.547
ZC25	24.6	0.08	23.71	0.01	26.7	0.02	12.9	0.02	0.13	0.13	88.3	5.176	0.012	2.824	3.056	0.001	4.698	0.003	4.047	0.004	0.053	0.035	0.537
ZC25	25.19	0.07	22.54	0.02	26.5	0.11	13.17	0	0	0.03	87.63	5.331	0.011	2.669	2.955	0.003	4.691	0.02	4.155	0	0	0.008	0.53
ZC25	23.78	0.07	23.67	0.03	27.24	0.04	12.46	0.01	0.01	0.01	87.32	5.083	0.011	2.917	3.045	0.006	4.869	0.007	3.969	0.002	0.004	0.002	0.551
ZC25	24.21	0.03	23.02	0.03	27.22	0.1	12.49	0.01	0.01	0	87.12	5.187	0.004	2.813	3.000	0.006	4.876	0.018	3.988	0.002	0.004	0	0.55
ZC27	25.97	0.04	21.97	0	28.61	0.38	11.59	0.04	0.06	0.05	88.71	5.487	0.007	2.513	2.958	0	5.056	0.068	3.65	0.009	0.025	0.013	0.581
ZC27	25.86	0.01	21.98	0.01	29.13	0.35	11.76	0.05	0.05	0.01	89.21	5.447	0.001	2.553	2.903	0.001	5.132	0.063	3.693	0.011	0.02	0.002	0.582
ZC27	27.27	0.03	22.47	0.01	26.33	0.36	10.22	2.72	0.03	0.01	89.45	5.663	0.004	2.337	3.162	0.001	4.573	0.064	3.164	0.605	0.012	0.002	0.591
ZC27	27.03	0.03	22.33	0	26.57	0.34	10.64	2.28	0.03	0.01	89.26	5.628	0.004	2.372	3.108	0	4.627	0.06	3.303	0.508	0.012	0.002	0.583
ZC46	24.23	0.07	23.1	0.03	28.76	0.2	11.24	0.04	0.01	0.02	87.7	5.198	0.011	2.802	3.039	0.006	5.16	0.036	3.594	0.009	0.004	0.006	0.589
ZC46	24.51	0.06	22.85	0.06	29.09	0.21	11.03	0.01	0.02	0.02	87.86	5.254	0.01	2.746	3.028	0.01	5.215	0.038	3.525	0.002	0.008	0.006	0.597
ZC46	25.99	0.06	21.92	0.03	27.98	0.22	10.5	0.04	0.17	0.08	86.99	5.58	0.01	2.42	3.127	0.006	5.024	0.04	3.361	0.009	0.071	0.022	0.599
ZC4A	28.26	0.09	21.47	0.04	26.43	0.52	10.82	0.02	0.02	0.6	88.27	5.915	0.015	2.085	3.211	0.007	4.627	0.092	3.376	0.004	0.008	0.16	0.578
ZC4A	26.57	0.1	21.57	0.04	27.74	0.59	11.22	0.02	0.03	0.26	88.14	5.63	0.016	2.37	3.017	0.007	4.916	0.106	3.545	0.004	0.012	0.071	0.581
ZC4A	26.02	0.02	21.12	0.04	28.15	0.63	11.66	0.03	0.02	0.02	87.71	5.562	0.003	2.438	2.883	0.007	5.032	0.114	3.715	0.007	0.008	0.006	0.575
ZC4A	29.28	0.05	20.65	0.03	27.03	0.5	10.21	0.05	0.16	0.62	88.58	6.114	0.008	1.886	3.197	0.004	4.721	0.088	3.179	0.011	0.065	0.165	0.598
ZC32	25.94	0.09	22.1	0.04	21.58	0.29	16.99	0.04	0.01	0	87.08	5.386	0.015	2.614	2.795	0.007	3.748	0.052	5.258	0.009	0.004	0	0.416
ZC32	26.05	0.07	22.23	0.01	21.7	0.38	17.16	0.09	0.02	0.03	87.74	5.374	0.011	2.626	2.779	0.001	3.744	0.066	5.277	0.02	0.008	0.008	0.415
ZC50	29.01	0.01	19.55	0.01	21.75	0.42	16.78	0.06	0.03	0.33	87.95	5.952	0.001	2.048	2.679	0.001	3.732	0.073	5.132	0.013	0.012	0.086	0.421
ZC50	29.27	0.01	19.33	0.02	21.81	0.39	16.82	0.09	0.03	0.32	88.09	5.992	0.001	2.008	2.657	0.003	3.734	0.067	5.133	0.02	0.012	0.084	0.421
ZC50	30.62	0.02	18.34	0.01	20.87	0.4	16.15	0.11	0.04	0.65	87.21	6.294	0.003	1.706	2.737	0.001	3.587	0.069	4.948	0.025	0.016	0.17	0.42
ZC65A	26.43	0.07	21.54	0.01	21.38	0.38	16.62	0.07	0.07	0.05	86.62	5.513	0.011	2.487	2.808	0.001	3.73	0.067	5.168	0.016	0.028	0.013	0.419
ZC65A	26.63	0.09	21.52	0	21.51	0.39	16.73	0.1	0.07	0.08	87.12	5.524	0.015	2.476	2.786	0	3.732	0.068	5.173	0.022	0.028	0.021	0.419
ZC65A	26.69	0.03	21.65	0.01	21.04	0.41	17.05	0.06	0.02	0.1	87.06	5.524	0.004	2.476	2.806	0.001	3.642	0.072	5.261	0.013	0.008	0.027	0.409
ZC65A	26.36	0.01	21.68	0	21.23	0.37	16.77	0.08	0.06	0.05	86.61	5.495	0.001	2.505	2.821	0	3.702	0.065	5.211	0.018	0.025	0.013	0.415
ZC65A	26.38	0	21.69	0.03	21.35	0.41	17.02	0.01	0.04	0	86.93	5.480	0	2.52	2.791	0.004	3.709	0.072	5.271	0.002	0.016	0	0.413
ZC65A	26.6	0.05	21.17	0	21.09	0.39	16.88	0.15	0.04	0.01	86.38	5.554	0.008	2.446	2.764	0	3.683	0.069	5.254	0.034	0.016	0.002	0.412
ZC65A	26.16	0.03	21.07	0.05	21.56	0.43	16.67	0.03	0.11	0.07	86.18	5.501	0.004	2.499	2.725	0.008	3.792	0.076	5.226	0.007	0.045	0.019	0.421
ZC65A	26.4	0.04	21.93	0.04	21.64	0.4	16.81	0.01	0.02	0.01	87.30	5.466	0.007	2.534	2.817	0.007	3.746	0.071	5.188	0.002	0.008	0.002	0.419
ZC65A	25.95	0.08	21.67	0.02	21.64	0.37	16.6	0.12	0.06	0.02	86.53	5.433	0.012	2.567	2.781	0.003	3.789	0.066	5.181	0.027	0.025	0.006	0.422
ZC65A	26.04	0.08	21.6	0.03	21.61	0.38	16.58	0.24	0.13	0.07	86.76	5.441	0.012	2.559	2.761	0.004	3.777	0.067	5.164	0.054	0.053	0.019	0.422
ZC65A	25.88	0.06	21.58	0.01	21.87	0.44	16.7	0.14	0.13	0.05	86.86	5.411	0.009	2.589	2.73	0.001	3.825	0.078	5.205	0.031	0.053	0.013	0.424

Table 2. **Statistical microprobe analyses of the investigated biotite: Schist (ZC 2, ZC 9 and ZC 61), scheelite-bearing calc-silicate quartzite (ZC 65A), barren calc-silicate quartzite (ZC 4), mica quartzite (ZC 4A and ZC 6), and leucogranite (ZM 3 and ZM 52). *= Total Fe is considered as FeO; Fe* =Fe^{2+}/ (Fe^{2+}+ Mg); n = Number of analyses in each sample; Sd^1= standard deviation.**

Sample No.	n	Stat. Para-meters	Major Oxides										Cations per 22 oxygen atom									
			SiO_2	TiO_2	Al_2O_3	FeO*	MnO	MgO	CaO	Na_2O	K_2O	Total	Si	Ti	Al	Fe^{+2}	Mn	Mg	Ca	Na	K	Total	Fe#
ZC2	5	Min.	34.44	1.17	19.56	19.29	0.03	9.1	0	0.21	6.43	94.33	5.231	0.134	3.421	2.396	0.004	2.066	0	0.062	1.246	15.39	0.513
		Max	37.66	1.53	20.4	20.69	0.06	11.01	0.02	0.28	8.36	98.12	5.512	0.168	3.652	2.629	0.008	2.493	0.004	0.083	1.624	15.45	0.545
		Mean	36.46	1.4	19.94	20.01	0.04	10.07	0.01	0.26	7.84	96.03	5.442	0.157	3.508	2.498	0.005	2.241	0.002	0.075	1.493	15.42	0.527
		Sd^1	1.27	0.14	0.37	0.62	0.01	0.68	0.01	0.03	0.8	1.66	0.118	0.014	0.087	0.089	0.002	0.155	0.001	0.008	0.146	0.02	0.012
ZC9	24	Min.	35.01	1.31	19.08	20.7	0	7.94	0	0.22	7.41	93.26	5.386	0.15	3.447	2.69	0	1.814	0	0.065	1.435	15.36	0.58
		Max	36.84	1.51	19.98	22.12	0.07	8.87	0.02	0.33	8.36	96.81	5.494	0.173	3.595	2.826	0.009	2.008	0.004	0.099	1.636	15.49	0.607
		Mean	35.59	1.41	19.61	21.54	0.03	8.31	0.01	0.26	8.11	94.87	5.441	0.163	3.533	2.754	0.003	1.893	0.002	0.078	1.583	15.45	0.593
		Sd^1	0.39	0.06	0.25	0.36	0.02	0.22	0.01	0.03	0.21	0.71	0.028	0.006	0.038	0.04	0.002	0.046	0.001	0.009	0.044	0.03	0.008
ZC61	6	Min.	35.68	2	17.47	17.67	0.25	9	0	0.06	8.9	93.8	5.506	0.232	3.133	2.24	0.032	2.056	0	0.018	1.72	15.4	0.509
		Max	37.28	2.76	17.89	19.97	0.36	9.98	0.32	0.55	9.57	96.19	5.65	0.32	3.237	2.517	0.047	2.295	0.052	0.162	1.878	15.58	0.546
		Mean	36.21	2.53	17.66	19.01	0.28	9.27	0.06	0.16	9.34	94.53	5.545	0.292	3.188	2.435	0.037	2.117	0.01	0.048	1.826	15.5	0.535
		Sd^1	0.73	0.29	0.16	0.82	0.04	0.37	0.13	0.19	0.24	0.87	0.057	0.034	0.035	0.107	0.005	0.089	0.021	0.056	0.061	0.062	0.016
ZC65A	35	Min.	37.33	0.46	14.53	12.66	0.14	14.61	0	0.09	8.21	90.52	5.754	0.053	2.644	1.61	0.018	3.302	0	0.026	1.588	15.44	0.315
		Max	39.61	0.67	15.8	14.13	0.25	16.21	1.52	0.43	9.67	94.59	5.898	0.075	2.823	1.762	0.032	3.608	0.247	0.126	1.838	15.73	0.34
		Mean	38.6	0.6	15.26	13.41	0.2	15.62	0.12	0.19	9.23	93.22	5.816	0.068	2.711	1.69	0.025	3.508	0.019	0.056	1.775	15.67	0.325
		Sd^1	0.53	0.05	0.23	0.27	0.02	0.38	0.27	0.07	0.36	1.14	0.032	0.006	0.037	0.034	0.003	0.058	0.044	0.021	0.056	0.05	0.006
ZC4	4	Min.	37.21	1.16	17.1	16.13	0.33	12.28	0	0.08	8.45	94.12	5.613	0.132	3.04	2.03	0.042	2.774	0	0.023	1.633	15.53	0.419
		Max	37.85	1.52	17.4	17.27	0.38	12.79	0.19	0.11	9.74	96.06	5.639	0.172	3.054	2.189	0.048	2.832	0.031	0.033	1.874	15.64	0.441
		Mean	37.43	1.41	17.2	16.56	0.36	12.5	0.08	0.1	9.32	94.95	5.628	0.16	3.048	2.082	0.045	2.8	0.012	0.028	1.788	15.59	0.426
		Sd^1	0.3	0.17	0.14	0.49	0.02	0.22	0.08	0.01	0.59	0.81	0.013	0.019	0.006	0.073	0.003	0.024	0.013	0.004	0.106	0.05	0.01
ZC4A	16	Min.	36.1	1.76	17.08	19.73	0.34	7.94	0	0.05	8.79	94.33	5.575	0.203	3.085	2.479	0.044	1.785	0	0.015	1.719	15.32	0.575
		Max	38.51	2.28	18.26	20.86	0.44	8.32	0.33	0.48	9.91	96.36	5.806	0.261	3.24	2.673	0.057	1.907	0.054	0.14	1.934	15.56	0.591
		Mean	36.85	2.01	17.73	20.29	0.39	8.17	0.05	0.13	9.64	95.25	5.632	0.231	3.193	2.594	0.051	1.862	0.008	0.038	1.879	15.49	0.582
		Sd^1	0.69	0.11	0.27	0.39	0.03	0.13	0.08	0.1	0.28	0.55	0.074	0.013	0.044	0.063	0.004	0.035	0.013	0.03	0.058	0.073	0.005
ZC6	9	Min.	34.98	2.14	16.34	17.58	0.08	6.16	0.03	0.09	8.27	91.76	5.551	0.243	2.933	2.217	0.011	1.384	0.005	0.026	1.59	15.15	0.536
		Max	39.78	2.77	17.74	20.12	0.2	9.45	0.54	1.48	9.57	95.84	5.997	0.316	3.152	2.599	0.026	2.132	0.087	0.433	1.946	15.61	0.616
		Mean	37.39	2.42	17.26	19.24	0.16	8.74	0.12	0.33	9.21	94.86	5.686	0.277	3.095	2.449	0.02	1.982	0.02	0.096	1.788	15.41	0.554
		Sd^1	1.48	0.19	0.47	0.73	0.04	1	0.16	0.46	0.4	1.27	0.156	0.022	0.067	0.116	0.005	0.231	0.027	0.133	0.099	0.15	0.024
ZM3	20	Min.	34.65	1.65	18.81	22.72	0.46	3.83	0	0.05	8.92	93.21	5.475	0.197	3.494	2.996	0.062	0.902	0	0.015	1.794	15.32	0.758
		Max	36.04	1.98	19.79	25.33	0.63	4.3	0.03	0.15	9.56	95.52	5.585	0.235	3.678	3.323	0.085	1.006	0.005	0.045	1.933	15.52	0.775
		Mean	35.2	1.81	19.22	24.11	0.54	4.08	0.01	0.09	9.28	94.34	5.536	0.214	3.563	3.171	0.072	0.958	0.002	0.027	1.863	15.41	0.768
		Sd^1	0.3	0.07	0.27	0.77	0.04	0.15	0.01	0.03	0.21	0.79	0.036	0.009	0.048	0.1	0.006	0.032	0.002	0.008	0.039	0.07	0.004
ZM52	17	Min.	34.89	1.68	18.68	23.22	0.49	3.86	0	0.03	8.57	93.06	5.519	0.199	3.464	3.055	0.065	0.902	0	0.009	1.719	15.27	0.764
		Max	36.22	1.96	19.57	24.37	0.63	4.04	0.33	0.21	9.51	94.52	5.699	0.232	3.627	3.22	0.084	0.952	0.056	0.064	1.915	15.42	0.776
		Mean	35.3	1.83	19.19	23.73	0.55	3.98	0.05	0.1	9.21	93.95	5.563	0.217	3.565	3.127	0.074	0.936	0.008	0.03	1.851	15.37	0.77
		Sd^1	0.29	0.08	0.21	0.31	0.04	0.05	0.08	0.04	0.26	0.39	0.039	0.009	0.036	0.041	0.005	0.013	0.014	0.013	0.053	0.042	0.003

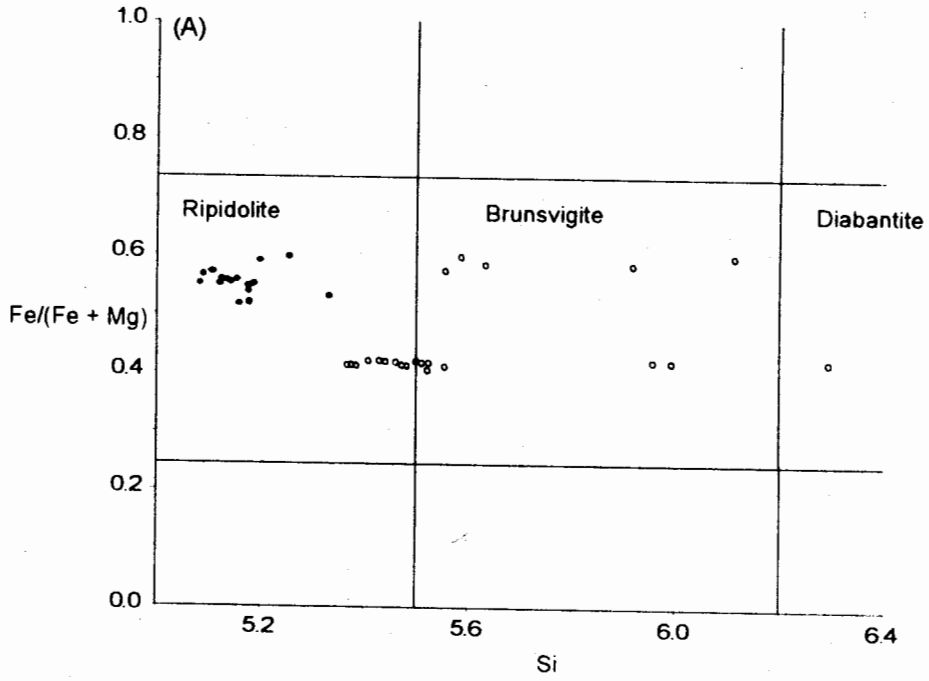

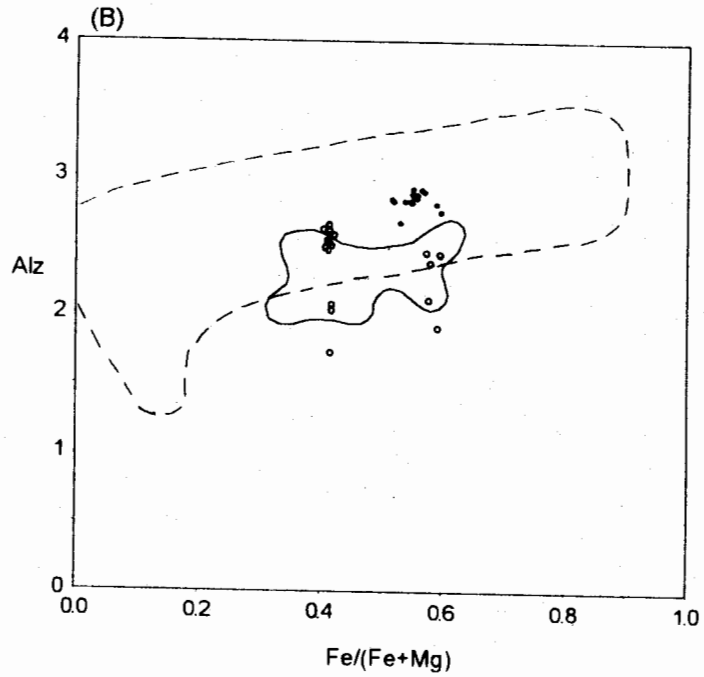

Figure 3. **(A)** Compositional variations of the studied chlorites on the classification scheme of Foster (1962). Open circles = chlorites from calc-silicate quartzite; solid circles =chlorites from schist. **(B)** Plot of Alz vs. Fe/(Fe+Mg) of the Miniki Gol chlorites. The dashed line indicates the field of metamorphic chlorites after Bailey (1988), and the solid line shows the field of Nubian shield igneous chlorites after Abdel-Rahman (1995). Total Fe is considered as Fe^{+2}.

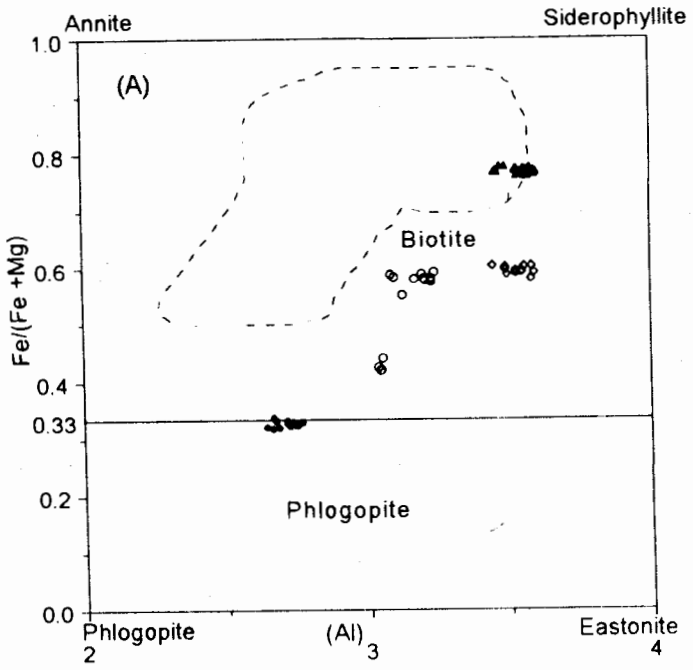

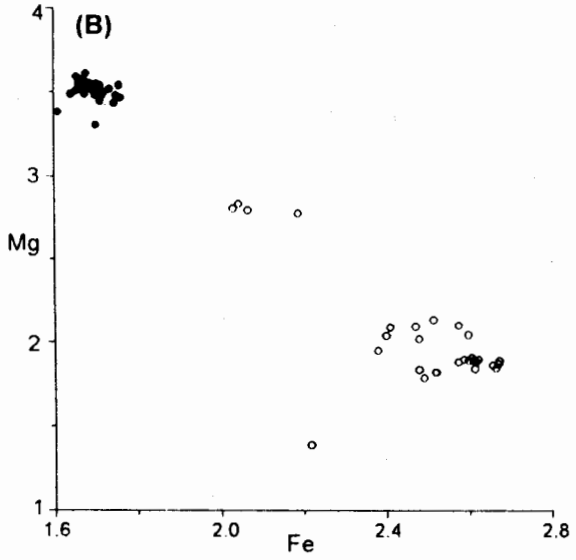

Figure 4. **(A)** Miniki Gol biotite composition in terms of Fe /(Fe+Mg) vs. Al cation. The dashed line indicates the field of Japanese I-series granite superimposed on the plot after Lalonde and Bernard (1993). Solid circle = scheelite-bearing calc-silicate quartzite; Open circle = Barren quarzite; Solid triangle = Leucogranite; Open rhomb = schist. Total Fe is considered as Fe^{+2}.

metamorphosed schist (Robert 1972).

When plotted on the diagram of $Fe^{2+}/(Fe^{2+}+Mg)$ vs. total Al cation (Fig.4 A), most of the analyses from leucogranite fall in the field of ilmenite (I-series granite) of Lalonde and Bernard (1993). The Fe-depletion trend is noted in the biotite from leucogranite to the biotite of scheelite-bearing quartzite at study area (Fig. 4 A). The Fe deficiency in the biotite of W-bearing calc-silicate quartzite is compensated by Mg and the negative correlation between these two cations acknowledge the substitution (Fig. 4B).

DISCUSSION

The calc-silicate rocks at Miniki Gol composed of calcic-amphibole, clinozoisite, chlorite, biotite, sphene, calcite, anorthite, grossular garnet, diopside and scheelite. This mineral assemblage represents a metasomatic skarn environment.

Both the chlorite and biotite from the scheelite-bearing calc-silicate quartzite at Miniki Gol are Mg-rich unlike other lithologies in the area. The composition of these minerals seems to be markedly affected by metasomatic activity. The high level of Mg in the biotite and chlorite (especially in the scheelite-bearing quartzite) seems to be the function of hydrothermal activity in these rocks. In general, hydrothermal biotite is more Mg-rich than igneous biotite (Brimhall et al. 1977). The present data in terms of $Fe^{2+}/(Fe^{2+}+Mg)$ ratio of the biotite from the scheelite-bearing quartzite are compatible with the biotite of W-bearing calc-silicate at Var (France), which is considered to be of metasomatic origin (Sonnet et al. 1985) and consistent with the Morocco skarn-related stratiform-scheelite-biotite mineralisation (Cheilletz 1985).

The Ti value of the studied biotite is also consistent with the hydrothermal biotite of Butte, Montana (Brimhall 1977, Brimhall et al. 1985). The low total of the biotite from the scheelite-bearing quartzite also points to H_2O-rich phases in the study area (Table 2). The concentration of TiO_2 in the Miniki Gol biotite sampled from schist and mica quartzite generally corresponds with the amphibolite-grade of metamorphism (Dymek 1983). However, high grade does not correlate with the Ti-content in the low-grade metamorphosed rock and the phyllitic slate such as ZC 61 that has high content of TiO_2 (2.76 wt %).

The Miniki Gol leucogranite can be considered as peraluminous and S-type granite. Its mineralogy and mineral chemistry of biotite and muscovite together with the aluminum saturation index are consistent with a two-mica leucogranite. The high Al-content (Fig. 4 A), of biotite from leucogranite also reflects directly the peraluminosity of the host magma (Lalonde and Bernard 1993). Peraluminous magma has been ascribed to the fractional crystallisation (Ringwood 1974), metasomatic loss of alkalis (Martin and Bowden 1981) and anatexis or assimilation of pelitic metasediments (Chapell and White 1974).

The occurrence of low aluminum content particularly Alz in chlorite, from the calc-silicate quartzite, compared to the schist (Table 1), indicates igneous-related hydrothermal activity at Miniki Gol and surrounding area. This level of Alz is compatible with the chlorite from igneous rocks (Bailey 1988, Abdel-Rahman 1995). The Miniki Gol leucogranite and its protolith rocks (metasediments) have undergone a certain degree of metsomatic activity. The chloritization (i.e. growth of chlorite at the expense of biotite) and the partial sericitization of the plagioclase within the leucogranite and associated pegmatite also demonstrate the role of hydrothermal fluids in these rocks.

CONCLUSIONS

- It is concluded tentatively that the biotite and chlorite chemistry of the calc-silicate rocks at Miniki Gol, Chitral, has been altered by hydrothermal activity.
- The chemistry of the chlorite and biotite of the scheelite-bearing calc-silicate quartzite is significantly different from that of barren calc-silicate quartzite, schist and leucogranite.
- Both the chlorite and biotite from calc-silicate quartzite are Mg-rich that suggest hydrothermal activity in these rocks.
- The aluminum content in the chlorite and biotite and the low level of Ti in the biotite also consistent with the hydrothermal alteration within both the leucogranite and calc-silicate quartzite at the Miniki Gol.

ACKNOWLEDGMENTS

The Association of Commonwealth Universities in UK financed this study. Mr. Colin Cunnighan prepared the polished thin sections whereas Mr. Rob Wilson performed the probe analyses in the Department of geology, University of Leicester.

REFERENCES

Abdel-Rahman, A. M., 1995. Chlorites in a spectrum of igneous rocks: mineral chemistry and paragenesis. Min. Mag. 59, p. 129-141.

Bailey, S. W., 1988. Chlorites: structures and crystal chemistry. *In*: hydrous phyllosilicates (exclusive of micas). S. W. Bailey (eds), Min. Soc. America, Rev. in min. 19, p. 347-403.

Brimhall, G. H. Jr., 1977. Early fracture-controlled disseminated mineralisation at Butte Montana. Econ. Geol.72, p. 37-59.

Brimhall, G. H., Agee, C. and Stoffregen, R., 1985. The hydrothermal conversion of hornblende to biotite. Can. Min. 23, p. 369-379.

Buchroithner, M. F. and Gamerith, H., 1986. On the geology of the Tirich Mir area, central Hindu Kush (Pakistan). Jb. Geol. B.

A.128, p. 367-381.
Calkins, J. A., Jamiluddin, S., Bhuyan, K. and Hussain, A., 1981. Geology and mineral resources of the Chitral-Partsan area, Hindu Kush Range, Northern Pakistan. U. S. Geol. Surv. Prof. Paper, 716-G, p. 33.
Chappell, B. W. and White, A. J. R.., 1974. Two contrasting granite types. Pac. Geol. 8, p. 173-174.
Cheilletz, P. A., 1985. Les minéralisations stratiformes à scheelite-biotite du Djebel Aouam (Maroc Central). Exemple de skarn d,infiltration dévelopé par remplacement de séries sédimentaires gréso-pélitiques. Bull. De Min. 108, p. 367-376.
Deer, W. A., Howie, R. A. and Zussman, J., 1962. Rock-forming minerals, sheet silicates. Vol.3, Longman, London.
Dymek, R. F., 1983. Titanium, aluminium and interlayer cation substitutions in biotite from high-grade gneisses, West Greenland. Am. Min. 68, p. 880-899.
Fletcher, C. J. N., 1985. Gold, antimony and tungsten mineralisation in the Chitral District, Northwest Frontier Province, Pakistan. Report for Sarhad Development Authority, Peshawar.
Foster, M. D., 1962. Interpretation of the composition and a classification of the chlorites. US. Geol. Sur. Prof. Paper. 414-A, p. 1-33.
Labotka, T. C., 1983. Analysis of the compositional variations of biotite in pelitic hornfelses from northeastern Minnesota. Am. Min. 68, p. 900-914.
Lalonde, A. E. and Bernard, P., 1993. Composition and color of biotite from granites: two useful properties in the characterization of plutonic suite from the Hepburn internal zone of Wopmay orogen, Northwest Territories. Can. Min. 31, p. 203-217.
Leake, R. C., Fletcher, C. J. N., Haslam, H. W., Khan, B. and Shakirullah., 1989. Origin and tectonic setting of stratabound tungsten mineralisation within the Hindu Kush of Pakistan. J. Geol. Soc. London, 146, p. 1003-1016.
Martin, R. F. and Bowden, P., 1981. Peraluminous granites produced by rock-fluid interaction in the Ririwai nonorogenic ring-complex, Nigeria: mineralogical evidence. Can. Min.19, p. 65-82.
Pascoe, E. H., 1924. General report of the Geological Survey of India for the year 1923. India Geol. Surv. Rec. 55.
Pudsey, C. J., Coward, M. P., Luff, I. W., Shackleton, R. M., Windley, B. F. and Jan, M. Q., 1985. Collision zone between the Kohistan arc and the Asian plate in NW Pakistan. Trans. Roy. Soc. Edinburgh, 76, p. 463-479.
Ringwood, A. E., 1974. The petrological evolution of island arc system. J. Geol. Soc. London, 130, p. 183-204.
Robert, F. M., 1972. Stability of biotite: a discussion. Am. Min. 57, p. 300-316.
Sonnet, P., Verkaeren, J. and Crevola, G., 1985. Scheelite bearing calc-silicate gneisses in the Provence crystalline basement (Var, France). Bull. De Min. 108, p. 377-390.

Manuscript received September 29, 2000
Revised Manuscript received April 6, 2001
Accepted April 6, 2001

ACTA MINERALOGICA PAKISTANICA
Volume 11 (2000)

Article Reference AMP11.2000/045-059/ISSN0257-3660

PETROGRAPHY AND MICROFACIES ANALYSIS OF EOCENE WAKAI LIMESTONE, SOUTHWEST, MAKRAN, PAKISTAN

MOHAMMAD AHMAD FAROOQUI[1], MURTEZA BOUSTANI[2] AND KHALIL-UR-REHMAN[1]

[1] Centre of Excellence in Mineralogy, University of Balochistan, Quetta. Pakistan
[2] Department of Earth Sciences, Quaid-e-Azam University, Islamabad, Pakistan

ABSTRACT

Petrographic analysis of seventeen, randomly collected, samples from seven scattered outcrops of Eocene Wakai Limestone (Nisai Formation) revealed that they are composed of 7-85% ($\bar{x}$ = 49.82%) carbonate skeletal and non-skeletal grains, 30-90% ($\bar{x}$ = 41.24%) micrite matrix, 0-30% ($\bar{x}$ = 5.82%) sparite matrix and trace amount of extra clast of sparry calcite and sub-rounded far traveled detrital quartz. The allochems belong to Discocyclina, Nummulites, Assilina, Lokhartia, miliolids, Alveolina, red algae, Operculina, Ranikothalia, Rotalia/ rotaliidae, Orbitolites, Coskinolina/Fallotella, textulariidae, echinoid, ostracod, bryozoa, planktons and some unidentified fauna. The petrography revealed that these carbonate rocks represent four microfacies with in Wakai Limestone. *Microfacies -1* is Discocyclinid-Nummulitid packstone to occasionally wackestone (Discocylinid-Nummulitid packed to occasionally sparse biomicrite) representing shallow water depth (up to 25 m) with normal marine water salinity and weak to moderate energy conditions. *Microfacies-2* is Alveolinid-Miliolid wackestone/packstone to grainstone (Alveolinid-Miliolid sparse to packed biomicrite to biosparit) representing very shallow (<10 m deep), warm, semi-restricted lagoonal, close to shore, environment with weak to moderate current/wave activity and low energy conditions. *Microfacies-3* is mudstone to intraclastic wackestone (micrite to sparse intraclastic biomicrite) representing comparatively deeper marine environment where terrigenous material was also being deposited, and *Microfacies-4* is Red algal wackestone to packstone/grainstone (Red algal sparse to packed biomicrite/sparite) that represents warm, shallow marine, near fore-shore (15-25 m deep) environment with normal marine salinity, low energy conditions and moderate wave and current activities.

INTRODUCTION

The geology of Makran is dominated by subduction related tectonics and sedimentation since Cretaceous (White 1979). The rocks in Makran region are mostly composed of deep marine turbidites and volcanics. The Eocene Wakai Limestone is a comparatively indistinct lithologic unit exposed at seven different locations in western Makran near Pakistan-Iran border (Fig.1) but encompasses important information about the depositional history prior to the deposition of flysch (turbidite) sediments in the Makran Flysch Zone (Baluchistan Geosyncline of HSC 1961). The formation was first recognized as lithologic unit by Blandford (1876) and was formally mapped as lithostratigraphic unit by HSC (1961), during their reconnaissance geological survey, as small isolated lenticular outcrops exposed in two separate areas of Makran. One is between Kohi-e-Wakai and the Shiraz, a prominent peak at the Iran border, and second is Siahan Range north of

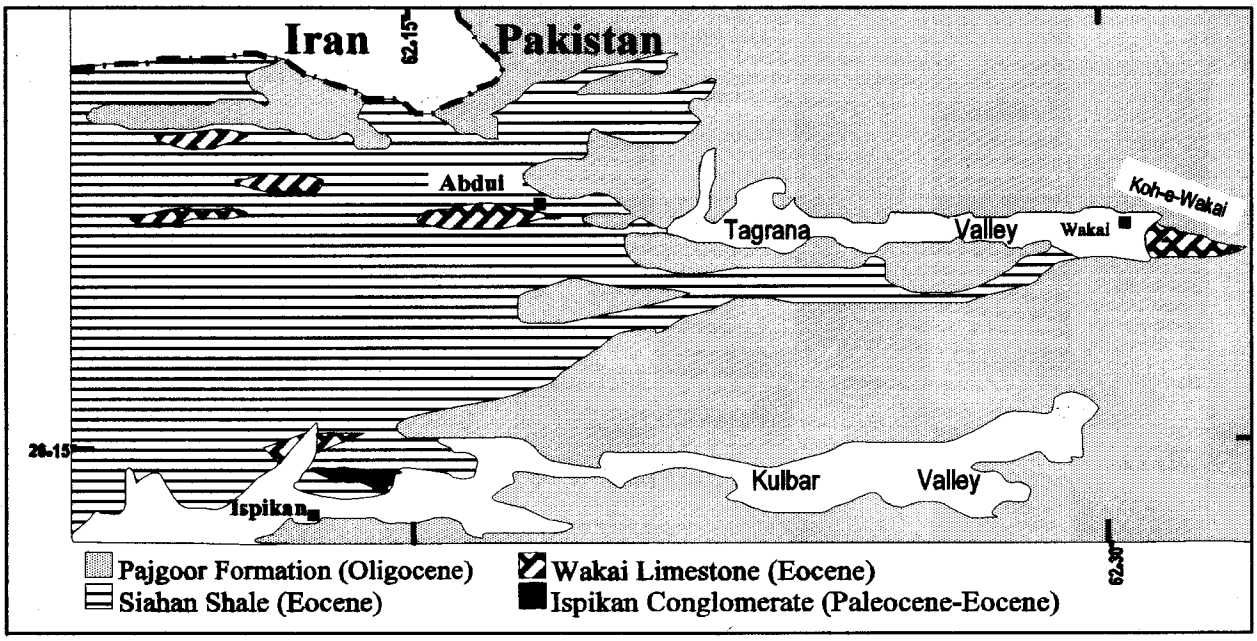

Figure 1. Generalized map of part of western Makran showing outcrops of Eocene Wakai Limestone and other stratigraphic units exposed in the area. For simplicity the topographic, stratigraphic and structural features are omitted.

Grawag. In this paper random samples from the seven outcrops of Wakai Limestone exposed between Koh-e-Wakai and Shiraz are studied. Blanford (1876) reported that limestone similar to the Wakai in lithology, age and mode of occurrence is exposed in many small areas in neighbouring parts of Iran. The thickness of the formation at Koh-e-Wakai is approximately 50 meters but it is thicker in some other localities. Cheema et al., (1977) redefined the stratigraphic nomenclature and lumped this and other Eocene rocks such as Eocene Limestone (Blandford 1879), SpinTangi Limestone (Vredenburg 1909), Nummulitic Beds (Davies 1930), Wakabi Limestone (HSC 1961), Upper part of Jakker and Jumboro Group (HSC 1961), and few other rock units of the eastern margin of Makran-Khojak Flysch Zone (Fig. 2) together and designated them as Nisai Formation that has been accepted by the Stratigraphic Committee of Pakistan (Fatmi 1977).

The Wakai Hill (*Koh-e-Wakai*)-type locality of Wakai Limestone (Fig. 3), in the valley of Tagrana *Kaur* (river) is composed entirely of this limestone. The limestone is fine grained and partly argillaceous, dark gray on fresh surface and weathers light to dark gray. The bedding is generally indistinct and at some places bedding can be deduced from orientation of discoid foraminifera. Reefoid characters appear near the base at the eastern end of the hill, and some of the beds contain limestone breccia that may be calcarenite or autoclastic breccia. Small variations in the internal stratigraphy from place to place are restricted to change in the bed thickness or degree of brecciation. The upper contact of the Wakai Limestone with the Siahan Shale is faulted or sheared. Near Grawag and west of the Nihing River the limestone appears to be interbedded with lower part of the Siahan Shale (HSC 1961). Previous workers have assigned Early to Middle Eocene ages for the most part of the Wakai Limestone, however few fossils of Paleocene have also been reported (HSC 1961, Shah 1977). Few workers have studied the Eocene carbonate rocks of Upper Indus Basin such as Sakesar Limestone (Boustani and Khawaja 1997), Kohat Formation (Iqbal, Pers. Comm) and Chargali Formation (Mujtaba, Pers. Comm.). However, no microfacies studies have been carried out on the Eocene carbonate rocks of Balochistan Basin. This study is the first and preliminary attempt to identify the microfacies of Wakai Limestone and to interpret their depositional environments.

PETROGRAPHY

Seventeen samples collected randomly from various small, isolated, and lenticular outcrops of the Wakai Limestone have been studied in detail. Following the nomenclature and classification of limestones of Dunham (1962) and Folk (1962), the detailed petrographic analysis showed that out of 17 samples, nine are packstone-wackestone (biomicrite), three are wackestone-grainstone (biomicrite-biosparite), three are intraclastic wackestone (intraclastic biomicrite) and two are wackestone-packstone (biomicrite-sparite).

The rock samples are light to medium gray and

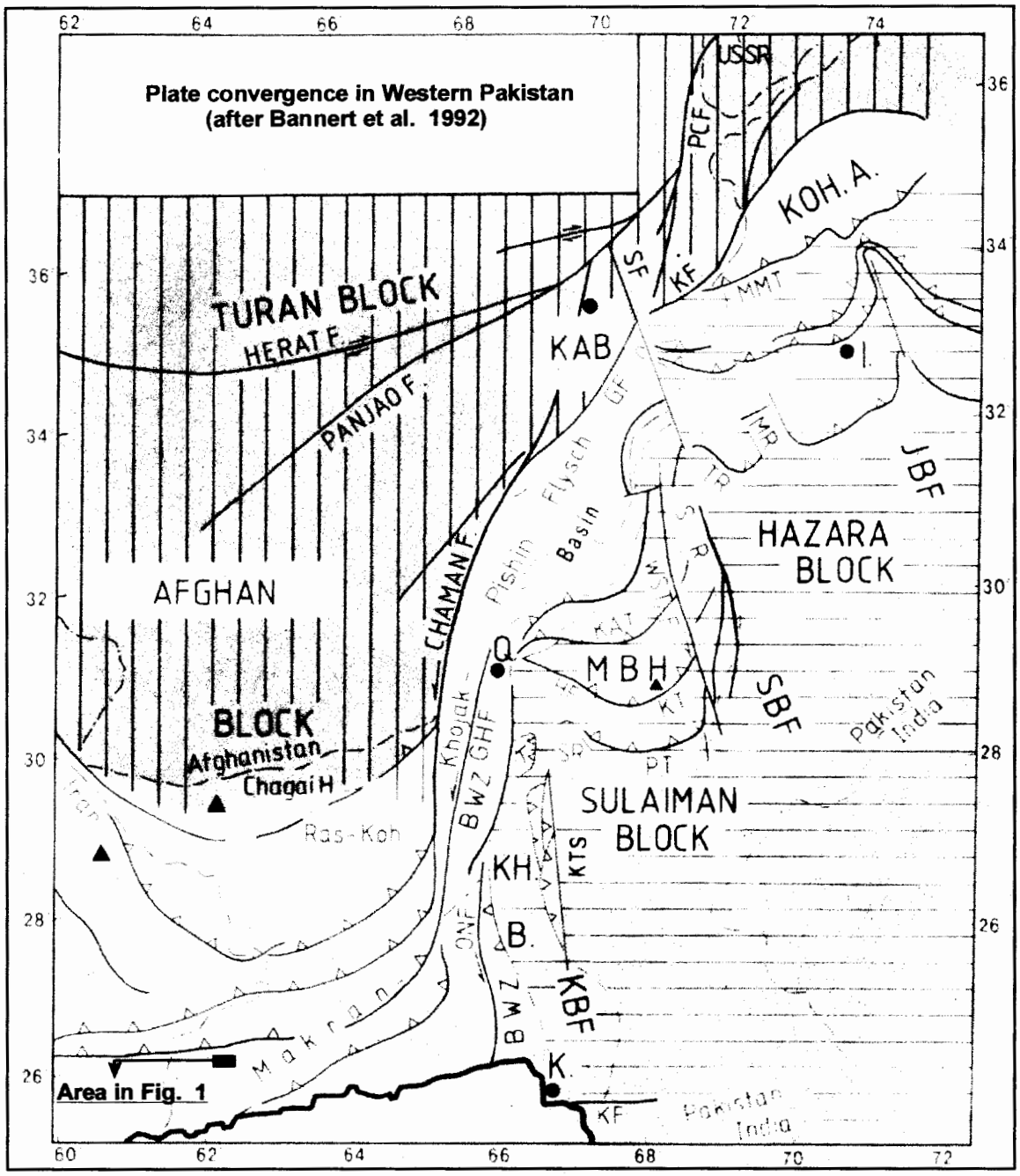

Figure 2. Plate Boundaries in Pakistan showing location of various tectonics zones and major faults. BWZ: Bela-Waziristan Ophiolites Zones; GF: Gardez Fault; GHF: Ghazband Fault: HF: Harani Fault; Herat F: Herat Fault; I: Islmabad; JBF: Jhelum Basement Fault; K: Kalat Plateau; K.: Karachi; KAB: Kabul Block and Kabul; KAT: Karahi Thurst; KBF: Kirther Basement Fault; KF: Kumar Fault; KHB: Khuzdar Block; KOH.A: Kohistan Island Arc Complex; KT: Karmari Thurst; KTS: Kirther Thrust Sheets; KUF: Kach Fault; MBH: Marri-Bugti Hills; MMT: Main Mantle Thurst; MR:Mianwali Re-entrant; ONF: Ornach-Nal Fault; PCF: Panjpir Fault; PT: Pirkoh Thurst; SBF: Sulaiman Basement Fault; SR: Sibi Re-entrant; SR: Sulaiman Range; SF: Sarobi Fault ;TR: Tank Re-entrant; WSTF: Western Sulaiman Transform Fault.

composed of micrite, sparite, and intraclasts with abundant macro and microfossils, and secondary sparry calcite. Microscopic examination revealed that the rocks are comprised of 30-90% ($\bar{x}$ = 41.24%) micrite matrix, 0-30% ($\bar{x}$ = 5.82%) sparite matrix, and 7-85% ($\bar{x}$ = 49.82%) carbonate skeletal and non-skeletal grains. Trace amount of extra clast of sparry calcite and detrital quartz is also present. The allochems are mostly bioclasts that derived from Discocyclina, Nummulites, Assilina, Lokhartia, miliolids, Alveolina, red algae, Operculina, Ranikothalia, Rotalia/rotaliidae, Orbitolites, Coskinolina/Fallotella, textulariidae, echinoid, ostracod, bryozoa, planktons and some unidentified fauna. The Nummulites and Discocyclina are generally larger in size than miliolids. About 20-30 percent allochems are complete showing little transportation. Rest of the bioclasts are present in the form of debris showing some transportation. Other than complete fossils, a large number of broken pieces of shells (fossil debris) are also present. Most of the shell fragments belong to the species mentioned above, however, some broken shells could not be identified positively because of their smaller size and unrecognizable textural features. Hence they have been treated as intraclasts.

The allochems of limestone are formed by chemical or biochemical precipitation within the basin of deposition, but which reorganized into discrete aggregated bodies and for the most part have suffered some transportation e.g. ooids, skeletal particles and pellets (Folk 1959). In Wakai Limestone these allochems are skeletal and derived mostly from benthic foraminifera and unknown species of various organisms. Most of the samples are composed of 70 to 90% skeletal allochems making a major component of the Wakai Limestone. The cement in most of the Wakai Limestone samples is neomorphic spar. Spar crystals are characterized by light grey to colourless, irregular intercrystalline boundaries, irregular crystal size distribution and small patches of intra-crystalline micrite. Most of this cement is developed around the fossil fragments. In a few samples almost colorless, clear and coarse grained (large crystals) syntaxial overgrowth cement occurs in the pore spaces. These crystals are elongated where the larger axis makes 90° angle with the boundary of the pore.

MICROFACIES AND PALEOENVIRONMENTS

Four microfacies have been recognized with in the Wakai Limestone. They have been named following the limestone classification schemes of Dunham (1962) and Folk (1962). They include 1) Discocyclinid-Nummulitid packstone to occasionally wackestone (Discocylinid-Nummulitid packed to occasionally sparse biomicrite), 2) Alveolinid-Miliolid wackestone/packstone to grainstone (Alveolinid-Miliolid sparse to packed biomicrite to biosparite), 3) Mudstone to ntraclastic wackestone (Micrite to sparse intraclastic biomicrite), and 4) Red algal wackestone to packstone/grainstone (Red algal sparse to packed biomicrite/sparite).

MICROFACIES-1

This is the most dominant microfacies and more than half of the studied samples (53%) belong to this microfacies. The allochems constitute 30-85% of the rock volume with a mean of 57%. As the name suggests the major allochems are Nummulites and disocyclinids (Fig 4a,b) of larger benthic foraminifers. Nummulites are common to abundant and present in all the samples of this microfacies. They range in size from 1 to 6.5 mm with an average of 3 mm. They are whole to broken whereas in some of them the outer whorl is abraded. They have medium to thick wall structures and are lensoidal in shape. Discocyclinids are common in abundance and present in 78% of the samples of this microfacies. They are whole to broken, lensoidal and discoidal in shape. Their size ranges from 1 to 6 mm with a mean of 3 mm. Like discocyclinidae, Assilina are also present, though rare, in 78% of the samples. They range in size from 1.5 to 7mm, but usually are 3.5 mm. Assilina are whole to broken and lensoidal in shape. They have commonly thick wall structures.

Other minor fauna are rare to common Rotalia/smaller rotaliidae (Fig. 4c) in 56% of the samples that are <0.32 mm in size and lensoidal in shape. They are mostly whole to rarely broken. These are followed by rare to common (unidentified but most probably the juvenile of) nummulitidae and Rotaliidae that are <0.32 mm in size. Rare miliolidae (in 44%), Ranikothalia (Fig. 4d), Operculina and red algae (in 22% of samples) along with traces of echinoid fragments (in 56%), textulariidae, ostracod, bryozoa and planktons are present in 22% of the samples of this microfacies. Most of the fossil chambers are filled with micrite similar to micrite matrix. In a few samples the micrite is quite darker than the micrite matrix. Ocassionally the chambers are filled with sparite or micrite and sparite together The broken shells are commonly angular to subangular and range from 30 to 70% of the biota with a mean of 47%. In some samples the larger benthic fauna (e.g. Nummulites or Discocyclina) are vaguely oriented.

Other allochems are intraclasts and peloids. Intraclasts are present in 33% of the samples and are commonly micritic in composition. They range from 0.18 to 0.8mm in size and are angular to subangular and rarely sub-rounded. They constitute 2% of the rock volume. Peloids are present in 22% of the samples and range in abundance from 4 to 6% of the rock volume. They are rounded and slightly darker than the micrite matrix and range from 0.2 to 0.5 mm in size.

Burrows are present in some of the samples. They range from 1.8 to 2.8 mm in size. They are nearly rounded and filled with clotted micrite, peloids,

Figure 3. Wakai Hill (Koh-e-Wakai), the type locality of the Eocene Wakai Limestone. The view is approximately 400m (L to R). To the left and right of the hill are the turbidites of Panjgoor Formation.

microspar and some intraclasts and bioclasts (fossil fragments). They are filled with dark gray micrite and the light gray micrite matrix.

Boring in some of the larger benthic fauna such as Nummulites, Assilina and Discocyclina were observed (Fig. 5) which range in size from 0.35 to 0.6 mm. They are oval to rounded in shape with an opening towards the inner chambers. These borings are filled with micrite & rarely micro sparite in the form of patches. The matrix is micritic and ranges from 15 to 60% of the rock volume with a mean of 35%, whereas minor sparite constitute 1 to 4% of the matrix.

Dolomite rhombs are present in 22% of the samples. They constitute about 10% of the rock volume. The rhombs commonly occur in the matrix but also rarely occur in the fossil chambers (Fig. 6). They range in size from 0.05 to 0.15 mm, having both cloudy and clear centers.

Depositional Environment of Microfacies-1

Nummulitids lived in a wide range of environments ranging from the fore-bank to bank and back bank environments (Arni 1965). They are believed to have been living within few centimeters of the soft bottom mud (Blondeau 1972). According to Lehmann (1970) they survived in non-turbid marine water with normal salinity. Different workers have interpreted different depths, for example Reiss and Hottinger (1984) reported a range of 20m to 130m depth for nummulitids. Hottinger and Dreher (1977) reported the nummulitids with flatter tests from greater depths than those having more spherical forms. Assilina is believed to depict the same depositional environment as Nummulites (Lehmann 1970). It can substitute Nummulites in the fore-bank facies (Arni 1965; Hottinger 1974).

Discocyclinids represent typical fore-reef facies (Henson 1950) whereas Luterbacher(1970), Blondeau (1972), and Sartorio and Venturini (1988) inferred them to represent fore-slope environment. Majid and Veizer (1986) have reported the presence of common Discocyclina on the slopes and their abundance at the shelf margin. The associatiion of Discocyclina with Nummulites, Assilina and Asterocyclina is believed to be in deeper environment (Buxton and Pedley 1989).

The above discussion leads to the conclusion that probably these are off shore deposits. The medium to thick wall structure and lensoidal shape in Nummulitids, Assilina and most of discocyclinids indicate comparatively a shallow depth (up to 25m) of deposition. The associated subordinating fauna such as Rotalia/ rotaliidae, Operculina, Ranikothalia, red algae, overall indicates a normal marine environment. Presence of both whole and broken/abraded skeletal grains suggests that some reworking of the grains has taken place, especially amongst the Nummulites. Abrasion and breakage due to weak or moderate currents rather than wave action are considered to be responsible for the generation of angular to sub-angular bioclasts and intraclasts and

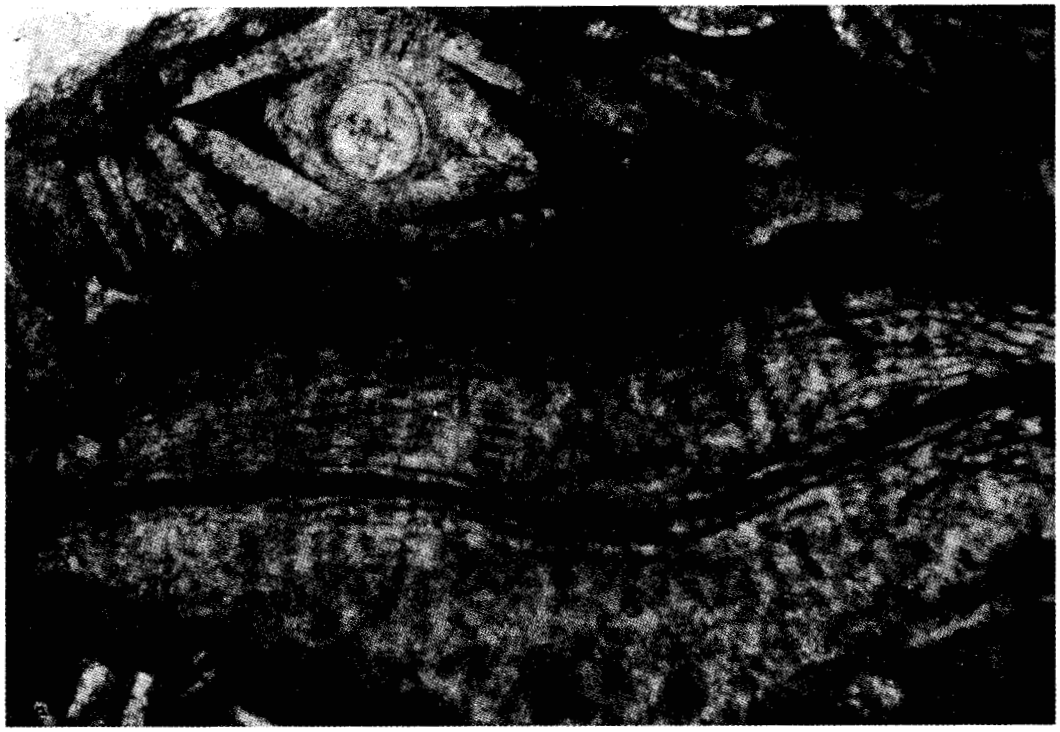

Figure 4a. Discocyclina (lower) and Nummulites (upper left) of the Microfacies-1 of Wakai Limestone (Sample No. WK-1, PPL, 40x).

Figure 4b. Nummulites (centre) and Discocyclina (upper left) of the Microfacies-1 of Wakai Limestone (Sample No. WK-1, PPL, 40x).

Figure 4c. Rotaliidae (lower left) and Discocyclina (center lower) and unidentified faunal debris of the Microfacies-1 of Wakai Limestone (Sample No. WK-5, PPL, 40x).

Figure 4d. Operculina (centre) and unidentified faunal debris of the Microfacies-1 of Wakai Limestone (Sample No. WK-1, PPL, 40x).

Figure 5. Assilina (left half) , Operculina (center) and part of a Discocyclina (extreme right) of the Microfacies-1 of Wakai Limestone (Sample No. WK-5, PPL, 40x). Note oval shaped two borings in the thick shell wall of Assilina with openings towards the central chamber.

Figure 6. Dolomite rhombs in nummulites chamber. Microfacies-1 of Wakai Limestone (Sample No. WK-2, PPL, 100x).

orientation of the grains in these micritic rocks. Micrite might have settled down from suspension during periods of minimal wave or current activity.

The large size boring on Nummulites (Fig. 5), Discocyclina or Assilina are due to either sponges or mollusks. As the sponges are absent in this microfacies, mullusks may be responsible for the boring. This has been concluded due to the presence of some larger size peloids that may belong to the unpreserved gastropods.

MICROFACIES-2

This microfacies represents 18% of the total studied samples. The total allochemical constituents range from 43 to 59% of the rock volume with a mean of 52%. The microfcies contain common to abundant miliolidae (Fig. 7a) and common alveolinidae (Fig. 7b) in all the samples as major faunal constituents.

The miliolids are usually whole and range in size from 0.25 to 0.6 mm. They are commonly globular in shape and rarely slightly elongated with thick to medium shell wall. The alveolinids are both rounded and elongated, whole to broken with medium to thick wall structures. Some have abraded outer whorl. They range in size from 0.5 to 2.5 mm with a mean of 1.7 mm. Chambers of both the miliolids and alveolinids are mostly filled with microspar, whereas in others these are partially filled with either or both sparite and micrite.

Rare amount of the other subordinating fauna which are most probably juvenile of Nummulites and rotaliidae are found in all the samples. They are <0.3 mm in size. Rare Rotalia/smaller Rotaliidae are present in 65% of the samples. They range in size from 0.23 - 0.26 mm and are lensoidal in shape. Rare to common, whole and broken Orbitolites ranging from 2-4 mm are present in 35% of the samples. Traces of whole Coskinolina, texlulariidae and echinoid fragments are also present.

Other allochems are intraclasts and peloids that are present in all the samples. Intraclasts range from 1 to 7% of the rock volume with a mean of 4.5%. They are commonly angular to subangular, rarely subrounded and micritic, exhibiting both darker and lighter tone than micrite matrix. They range in size from 0.1 to 1.3 mm, commonly 0.3 mm. Peloids range in abundance from 2 to 5% of the rock volume with a mean of 3.5%. They are rounded to slightly elongated and usually darker or sometimes the same colour as that of micrite matrix. They range in size from 0.03 to 1 mm ($\bar{x}$=0.15 mm).

Martix is composed of micrite and sparite that ranges from 40 to 54% with a mean of 46%. The micrite is medium to dark gray and ranges from 15 to 48% of the rock volume with an average of 31%. Sparite is the minor constituent of the matrix that ranges from 6 to 10%. Where the sparite is dominant and reaches up to 30%, the rock becomes grainstone (biosparite).

Depositional Environment of Microfacies-2

Miliolids and associated Alveolina and Orbitolites are most common in lagoons and reef areas in recent environments (Hallock and Glenn 1986). Many workers have carried out environmental interpretation of miliolids in carbonate rocks (e.g. Trave et al. 1996, Drzewiecki and Simo 1997; Gomez-Perez et al. 1999). They all consider the miliolids to be representing open or restricted platform conditions varying from beach, tidal flat, lagoon or reef environments. According to Hottinger (1974) miliolids are the only bottom dwellers found in hypersaline environments, whereas alveolinids are usually absent. In restricted shelf with normal salinity, Orbitolites and Alveolina are the characteristic fauna accompanied by valvulinids and/or miliolids.

Absence of any evaporitic feature and the presence of Alveolina in all the samples suggest that hypersaline conditions did not prevail. The minor associated fauna of this microfacies such as juveniles of Nummulites and rotaliidae Rotalia/smaller Rotaliidae also indicate normal marine salinity. The presence of rare Coskinolina strongly supports the idea of a very shallow, warm, semi restricted lagoonal environment where deposition took place somewhere close to the shore (land) probably at a depth of less than 10m. Sartorio and Venturini (1988) in their Tertiary (Eocene) depositional model have suggested very shallow, inner most lagoonal depositional environment (near the shore) for miliolids and Coskinolina.

The dominance of micrite as matix suggest low energy environment and weak to moderate current activity. The dominance of sparite in some parts of the matrix that produced grainstone and the presence of angular to subangular intraclasts and skeletal fragments (such as broken and abraded Allveolina) also suggest weak to moderate current activity.

MICROFACIES-3

About 17% of the studied samples represent this microfacies. Intraclasts (Fig. 8) are exclusively the major allochems in this microfacies. They range from 7% to 25 % of the rock volume with an average of 17% . These are angular to subangular and <1 mm in size. These are at places micritic in composition and appear clayee with light brown colour. Most of these intraclasts may be the skeletal fragments of larger nummulitidae (Numulites and/or Assilina). In one mudstone sample the intraclasts are needle shaped laths filled with sparite (Fig. 9).

Matrix ranges from 72 to 90% of the rock volume with a mean of 81%. It is light to medium gray and micritic in composition. Sparite constitute few (i.e. 2-4%) percent of this matrix. About 1 to 2% quartz grains (Fig. 10) alongwith 1% scattered dolomite rhombs are also present in mudstone samples. Quartz grains are medium sand size, non-udulose monocrsytalline, and sub-rounded to sub-angular.

Depositional Environment of Microfacies-3

The depositional environment of this microfacies in

Figure 7a. Miliolidae (right)in Microfacies-2 of Wakai Limestone (Sample No. WK-16, PPL, 40x). Note a fracture, filled with sparry calcite, that has divided the sample into two (upper and lower) halves

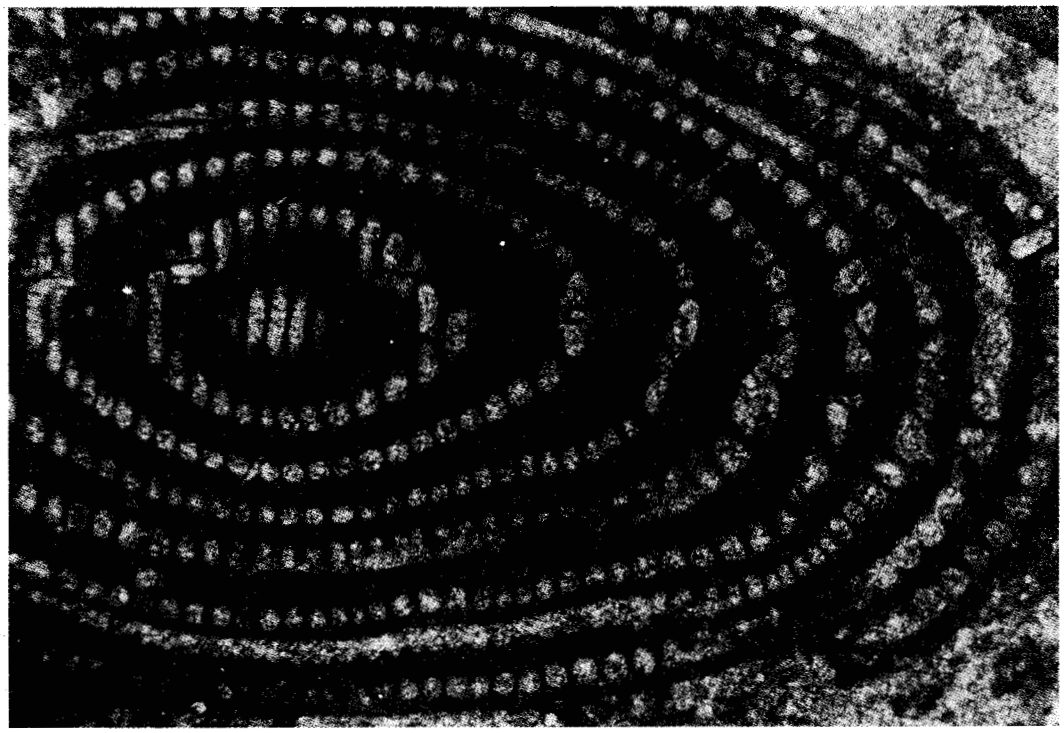

Figure 7b. Oval shaped Alveolina of the Microfacies-2 of Wakai Limestone (Sample No. WK-5, PPL, 40x).

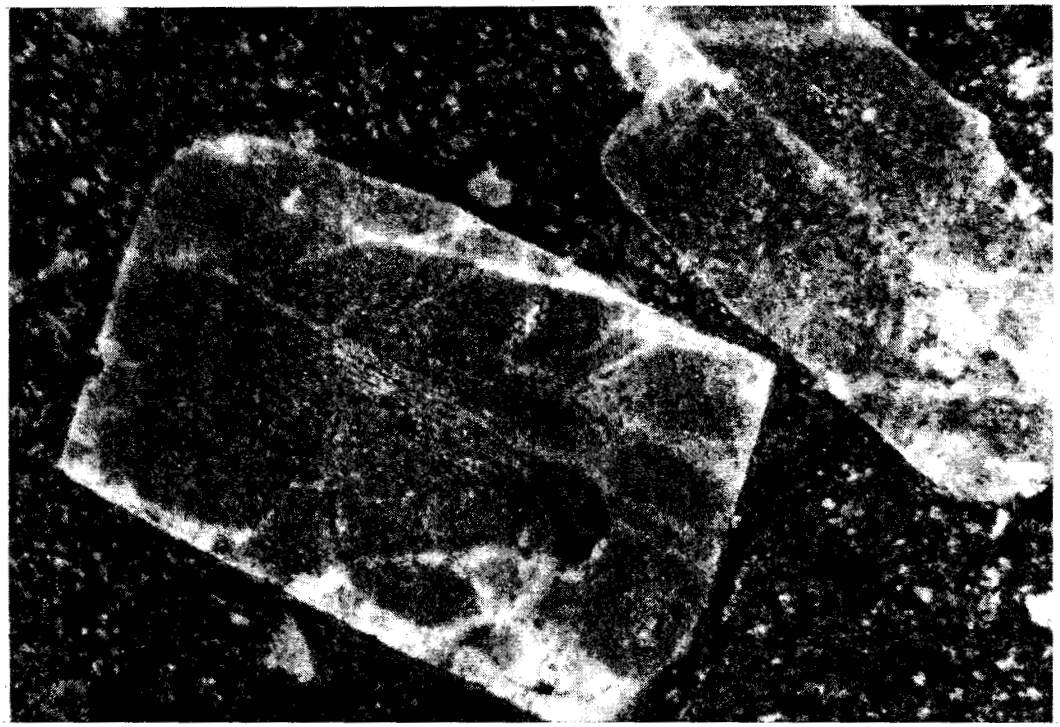

Figure 8. Angular intraclasts of sparite in micrite matrix of the Microfacies-3 of Wakai Limestone (Sample No. WK-21B, PPL, 40x).

Figure 9. Needle shaped laths of sparite in the wacxkestone of the Microfacies-3 of Wakai Limestone (Sample No. WK-B1, PPL, 40x).

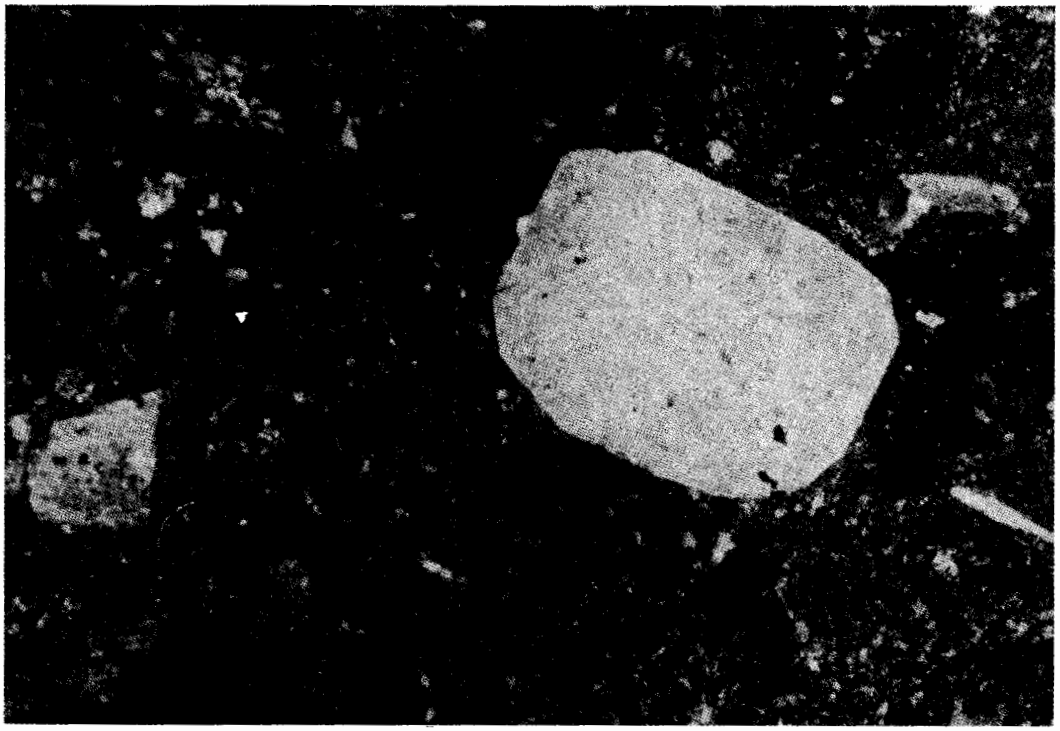

Figure 10. Subangular to subrounded monocrystalline, non-undulose quartz grain in the micrite of the Microfacies-3 of Wakai Limestone (Sample No. WK-21A, PPL, 40x).

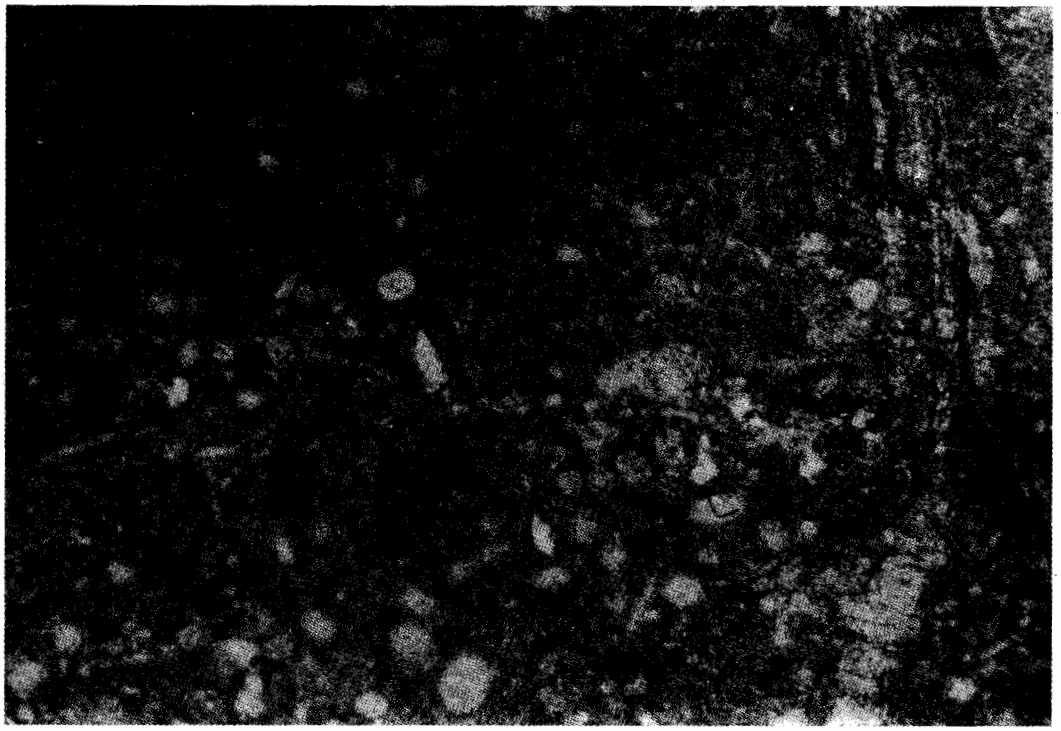

Figure 11. Micritic mudstone and wackestone of the Microfacies-3 of Wakai Limestone. Note that lower half is wackestone which gradually changes into micrite. (Sample No. WK-B1, PPL, 40x).

which intraclasts were originated from numulitidae has already been discussed in Microfacies-1. The size and shape of these intraclasts indicate that they were derived from a place relatively farther from the depositional site. If these are of nummulitidae origin then their reduced size indicates transportation by moderate current activity as no whole larger benthic fauna have been observed. Beside these, the presence of far-travelled, rounded (up to 3 %) quartz grains also indicates the influx of terrigenous material into the depositional site from distant provenance. In one sample micritic mudstone gradually changes into wackestone (Fig. 11). This indicates the change in depositional environment. Some circular (rounded), probably skeletal grains are present in the matrix, but could not be confidently identified as skeletal or diagenetic structure. The authors believe that this microfacies is of comparatively deeper environment, however, no firm conclusion can be drawn because of inadequate number of samples and difficulties in faunal identification.

MICROFACIES-4

This microfacies constitute 11% of the studied samples. The bioclasts are represented by abundant red algae (Fig. 12) that are whole to broken and range in size from 1 to 3 mm. These red algae (rhodolites) are of branching and crustose type (Lithophyllum), usually spherical to ellipsoidal in shape. Most of the red algal conceptacles are filled with micrite.

Other minor bioclasts are rare, unidentified, smaller benthic, <0.22 mm in size, traces to rare miliolidae and ostracods. The ostracods have thin to thick shells and are usually broken. Remaining allochems are intraclasts and peloids. Intraclasts represent 4% of the rock volume and are angular to subrounded. They range in size from 0.1 to 0.3 mm. Peloids constitute 1-3% of the rock volume. They are rounded to elongated in shape and range in size from 0.035 to 0.07 mm.

The matrix constitute 40-42% of the rock volume, in which 25-33% is micrite and 7-17% sparite. In thin sections there are patches where sparite is more dominant than micrite.

Depositional Environment of Microfacies-4

Red algae and their depositional environment are extensively discussed by Bosellini and Ginsburg (1971), Adey and MacIntyre (1973), Bosence (1983), and Marrack (1999). The shape and size of red algae (rhodolites) along with the associated biota are considered important depositional indicators. Different genera of red algae (Coralline) have been reported from tropical, temperate and polar regions. They represent variable water depth ranging from intertidal to as deep as 200m. The Rhodolites have been reported from different depositional settings such as lagoons, bays, reefs, off shore banks and open marine shelves (Bosellini and Ginsburg 1971; Adey and MacIntyne 1973).

The genera Lithophyllum identified in this study is

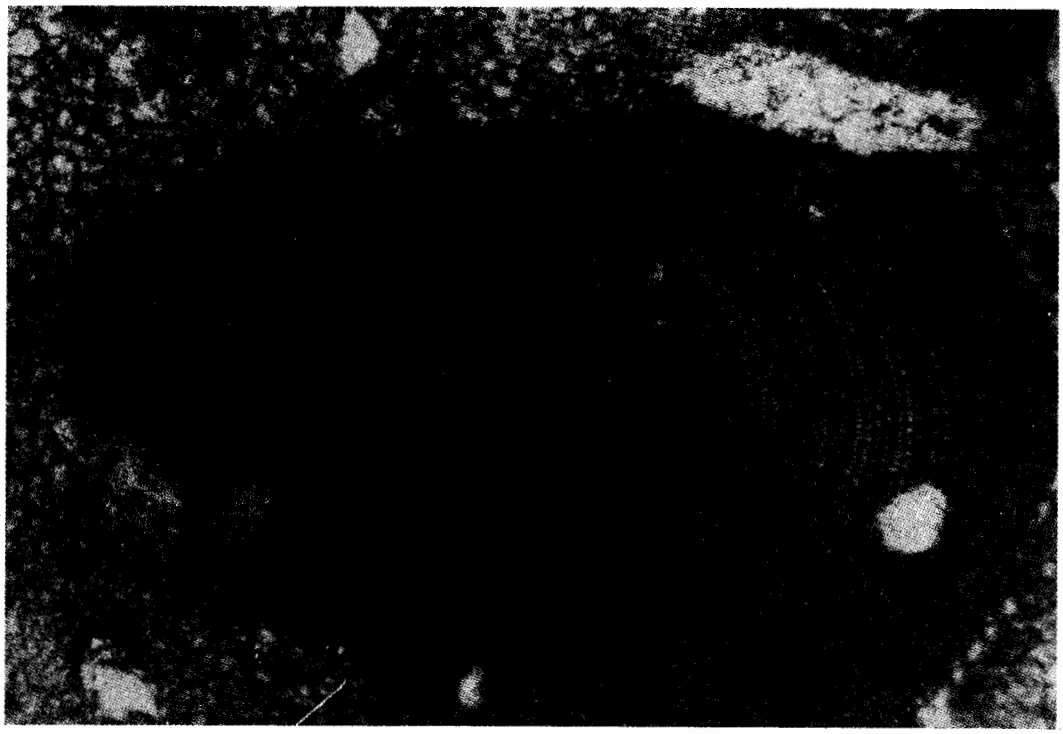

Figure 12. Red algae (Lithophyllum) in Microfacies-4 of the Wakai Limestone (Sample No. WK-5, PPL, 40X).

considered to be primarily warm water crustose coralline (Adey and MacIntyne 1973). The deeper water rhodolites tend to be discoidal rather than spherical in shape (Bosellini and Ginsburg 1971). Marrack (1999) observed that spherical, densely branched forms are more abundant where wave action is more frequent at a depth of 4-5 m, whereas sparsely branched ones become abundant in the deeper portions of wave beds and in tidal current influenced areas. The laminar coating on red algae are reported to be concentrated in sandy chanels (Bosellini and Ginsburg 1971).

The shape and the type of red algae (rhodolites) in this microfacies and the above discussion leads to the interpretation that this microfacies was developed in shallow marine environment some where near the fore-shore at the depth of 15 to 25m. The salinity was mostly normal marine. Micrite matrix indicates low energy environment whereas dominance of sparite in some parts and presence of angular to subrounded intraclasts and broken red algae leads to the conclusion in favour of moderate water energy created by waves or currents.

CONCLUSIONS

Preliminary petrograhic analysis of the Eocene Wakai Limestone of southwestern Makran, Pakistan revealed that these carbonate rocks were formed in very shallow to moderately deep carbonate platform environment where water salinity was normal and energy conditions were low to moderate. Four distinct carbonate microfacies have been identified within Wakai Limestone. *Microfacies-1* is Discocyclinid-Nummulitid packstone to occasionally wackestone (Discocylinid-Nummulitid packed to occasionally sparse biomicrite) that represents shallow water depth (up to 25 m) with normal marine water salinity and weak to moderate energy conditions. *Microfacies-2* is Alveolinid-Miliolid wackestone/packstone to grainstone (Alveolinid-Miliolid sparse to packed biomicrite to biosparite) that represents very shallow (<10 m deep), warm, semi-restricted lagoonal environment, close to shore with moderate to weak current/wave activity and low energy conditions. *Microfacies-3* is Mudstone to intraclastic wackestone (micrite to sparse intraclastic biomicrite) that indicates comparatively deeper marine environment where terrigenous material was also being deposited, and *Microfacies-4* is Red algal wackestone to packstone/ grainstone (Red algal sparse to packed biomicrite/ sparite) that represents warm, shallow marine, near fore-shore (15-25 m deep) environment with normal marine salinity, low energy conditions and moderate wave and current activities.

The Wakai Limestone records a comparatively short period of stable environment, during Eocene. During this period low energy and shallow water conditions allowed the precipitation of carbonates with a little input of terrigenous material in to the basin. After Eocene the basin started subsiding allowing the rapid deposition of thick deep marine turbidites. For better understanding of Eocene paleoenvironment in Balochistan Basin, more systematic petrographic and geochemical studies are needed. Such study would help develop a comprehensive model for depositional and tectonic environments prevailed during Eocene in Balochistan Basin.

REFERENCES

Adey, W.H., and MacIntyre, I.J., 1973. Crustose coralline algae, A re-evolution in the geological sciences: Geological Society of America Bulletin, v. 84, p. 883-904.

Arni, P., 1965. L' evolution des Nummulites en tant que facteur de modification des depots littoraux: Coll. Inter. Micropal. Dakar, Memo. BRGM, No. 32 (1963), p. 7-20.

Bannert, D, Cheema, A., and Schäffer, U., 1992. The structural development of the Western Fold Belt Pakistan; Geol. Jb. B80, Hannover, p. 3-60.

Bathurst, R.G.C., 1975. Carbonate sediments and their diagenesis: Developments in Sedimentology, 2nd ed., Elsevier, Publishing Co, Amsterdam, 658 p.

Blandford, W.T., 1876. On the geology of Sind, Rec. Vol. 9, Geological Survey of India, p. 8-22.

Blandford, W.T., 1879. The geology of western Sind, Mem. Vol. 17, Geological Survey of India, p. 1-196.

Blondeau, A., 1972. Les Nummulites: De L' Enseignement, A La Recherche, Sciences De La Terre, Paris Librairie Vuibert Boulevard Saint-German, 63, 254 p.

Bosellini, A., and Ginsburg, R.N., 1971. Form and internal structure of recent algal nodules (rhodolithes) from Bermuda: Geology, v. 79, p. 669-682.

Bosence, D.W.J., 1983. The occurrence and ecology of recent rhodoliths, A review. In: Coated grains (Ed. Peryt, T.M.), Springer-Verlag, Berlin Heidelberg, p. 225-242.

Boustani, M, Khawaja, A.A., 1997. Microfacies studies of Sakesar Limestone, Centyral Salt Range Pakistan: Geological Bulletin, v. 30, p. 131-142.

Buxton, M.W.N., and Pedley, H.M., 1989. Short paper, A standardized model for Tethyan carbonate ramps: Journal of Geological Society of London, v. 146, p. 746-748.

Cheema, M.R., Raza, S.M., and Ahmad, H., 1977. Cenozoic. *In*: Shah, S.M.I. (ed.) Stratigraphy of Pakistan; Geological Survey of Pakistan, Quetta, Mem. 12, p. 56-97.

Davies, L.M., 1937. The Eocene beds of the Punjab Salt Range: Geol. Surv. India, Mem. Palaeonto. India, News Series, v. 24, No. 1, p. 1-79.

Davies, L.M., 1930. The genus *Dictyoconus* and its allies: a review of the group, together with a description of three new species

from the lower Eocene beds of northern Baluchistan: Royal Society of Edinburgh, Trans. V. 56, pt. 2, No. 20, p. 485-506.
Drzewiecki, P.A., and Simo, J.A., 1997. Carbonate platform drowning and oceanic anoxic events on a Mid-Creta
Dunham, R.J., 1962. Classification of carbonates rocks (Ed. Ham, W.E.). AAPG Bull. Mem. 1, Tulsa, p. 108-123.
Fatmi, A.N., 1977. Mesozoic. In: Stratigraphy of Pakistan (Ed. Shah, S.M.I.), Geological Survey of Pakistan, Quetta, Mem., 12, p. 29-54.
Folk, R.L., 1959. Practical petrographic classification of limestones: AAPG Bull. v. 43, 38 p.
Folk, R.L., 1962. Spectral subdivision of limestone types. In: Classification of Carbonate Rocks (Ed. Ham, W.E.), AAPG Bull. Mem. 1, p. 68-84.
Gómez-Pérez, I., Fernández-Mendiola, P., and Garcia-Mondejar, J., 1999. Depositional architecture of a rimmed carbonate platform (Albian, Gorbea, west Pyrenees): Sedimentology, v. 46, p. 337-356.
Hallock, P., and Glenn, E.C., 1986. Larger Foraminifera: A tool for Paleoenvironmental Analysis of Cenozoic Carbonate Depositional Facies. PA
Henson, F.R.S., 1950. Cretaceous and Tertiary reef formations and associated sediments in Middle East: AAPG Bull. v. 34, p.215-238.
Hottinger, L., 1974. Alveolinids, Cretaceous-Tertiary Larger Foraminifera: (ESSO Production Research-European Laboratory), Basle, Switzerland, 84 p. Pl. 1-106.
Hottinger, L., and Dreher, D., 1977. Differentiation of protoplasm in Nummulitidae (Foraminifera) from Elat, Red Sea: Marine Biology, v. 25(1), p. 41-61.
Hunting Survey Corporation, 1961. Reconnaissance Geology of part of West Pakistan: A Colombo Plan Cooperation Project, Toronto, Canada. 550 p.
Lehmann, R., 1970. Early Tertiary Foraminifera Nummulites and Assilina: (ESSO Production Research-European Laboratories), 103 p.
Luterbacher, H.P., 1970. Environmental distribution of early Tertiary Microfossils, Tremp Basin, North-eastern Spain: (ESSO Production Research- European Laboratories) Switzerland, 48 p., Plate 1-18.
Majid, H.A., and Veizer, J., 1986. Depositional and chemical diagenesis of Tertiary Carbonates, Kirkuk oil field, Iraq: AAPG Bull. v. 70, No. 7, p.898-913,
Marrack, E.C., 1999. The relationship between water motion and living rhodolith beds in the southwestern Gulf of California, Mexico: PALAIOS, v. 14, p. 159-171.
Reiss, Z., and Hottinger, L., 1984. The Gulf of Aquaba, Ecological Micropaleontology, Ecological Studies: Springer-Verlag, Berlin Heidelberg, New York, and Tokyo, v. 50, 354 p.
Sartorio, D., and Venturini, S., 1988. Southern Tethys Biofacies: Agip, Stratigraphic Department, 235 p.
Shah, S.M.I., 1977. Stratigraphy of Pakistan: Geological Survey of Pakistan, Quetta, Mem. No. 12, 138 p.
Trave, A., Serra-Kiel, J., and Zamarreno, I., 1996. Paleoecological interpretation of transitional environments in Eocene carbonates (NE Spain): PALAIOS, v. 11, p. 141-160.
Vredenburg., E. W., 1909. Report on the geology of Sarawan, Jhalawan, Makran, and the state of Lasbela. Records Vol. 38, part 3, Geol. Surv. India., 189-215 Calcutta.
White, R.S., 1979. Deformation of the Makran Continental Margin: *In* Farah, A. and Dejong, K.A. (eds.), Geodynamics of Pakistan: Geological Survey of Pakistan, p. 357-372.

Manuscript received November 5, 2000
Revised Manuscript received April 12, 2001
Accepted April 13, 2001

ACTA MINERALOGICA PAKISTANICA
Volume 11 (2000)

Article Reference AMP11.2000/061-082/ISSN0257-3660

A NEW APPRAISAL OF THE LITHOSTRATIGRAPHY OF THE SPERA RAGHA-URGHARGAI REGION, WESTERN SULAIMAN FOLD BELT, PAKISTAN

AKHTAR MOHAMMAD KASSI[1], ABDUL SALAM KHAN[2] AND MOHAMMAD SARWAR[2]
[1]Department of Geology, University of Balochistan, Quetta, Pakistan
[2]Centre of Excellence in Mineralogy, University of Balochistan, Quetta, Pakistan

ABSTRACT

The Spera Ragha-Urghargai region, comprising part of the western Sulaiman Thrust-Fold Belt, is divisible into two lithostratigraphic domains: a) the Spera Ragha-Chinjun area and: b) the Urghargai-Mazu Ghar area, on the basis of sharply contrasting lithostratigraphic characters of their Middle Cretaceous-Eocene successions. The underlying succession of the Triassic Wulgai Formation, Jurassic Loralai Limestone and Upper Jurassic-Middle Cretaceous Parh Group and the indiscriminately overlying succession of the Miocene-Pliocene Siwalik Group, however, have comparable lithostratigraphic characters. The division line between the two domains is a thrust zone, which we consider as continuation of the Bibai Thrust Zone.

Within the Spera Ragha-Chinjun area the Middle Cretaceous Bibai formation comprises only the *in-situ* basic volcanic rocks which disconformably underlie the Upper Cretaceous Fort Munro Formation. The succession also include the Upper Cretaceous Moro Formation, Pab Sandstone, Paleocene Dungan Formation and Eocene Ghazij and Kirthar Formations. Stratigraphic succession of the Urghargai-Mazu Ghar area, among other formations, include the Jurassic Loralai Limestone, which has a thrusted lower contact with the Paleocene Dungan Formation of the Spera Ragha-Chinjun area, and Upper Cretaceous Mughal Kot Formation, which transitionally and conformably overlies the volcaniclastic succession of the Bibai formation. Also a new lithostratigraphic unit of ?Pleistocene-Sub-Recent age, the "Spezendai breccia", has been described for the first time. It is suggested that the Middle Cretaceous-Paleocene succession of the Urghargai-Mazu Ghar area was formed in deep marine environment far away from the succession of the Spera Ragha-Chinjun area, which developed in marginal shallow marine environments, and was later on juxtaposed by tectonic transport along the Bibai Thrust.

INTRODUCTION

The Spera Ragha-Chinjun and Urghargai-Mazu Ghar areas (Figs.1 and 2) are located within the western Sulaiman Thrust-Fold Belt (Bender and Raza 1995, Kazmi and Jan 1997) east of the Gogai Nappe (Kazmi 1979, Niamatullah et al.1988). The area comprises succession of rocks ranging in age from Triassic to Recent (Table 1, 2). Stratigraphic succession of the Spera Ragha-Chinjun area (Table 1) includes the Triassic Wulgai Formation, Jurassic Loralai Limestone, the Lower-Middle Cretaceous Parh Group, Bibai formation, Upper Cretaceous Fort Munro Formation, Moro Formation and Pab Sandstone, Paleocene-Lower Eocene Dungan Formation, Eocene Ghazij Formation and Kirthar Formation and the Miocene-Pliocene

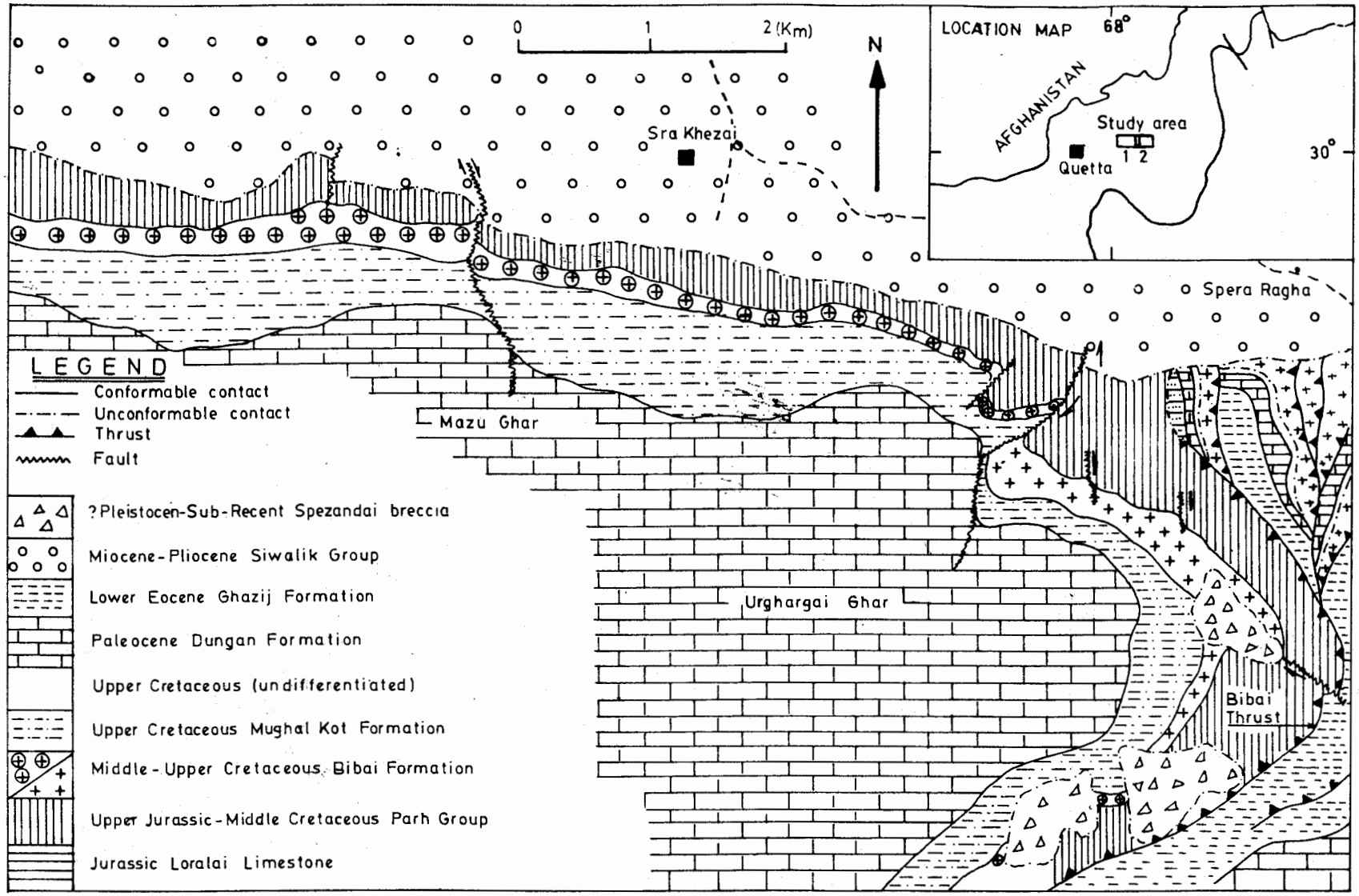

Figure 1. Geological map of the Spera Ragha-Chinjun and Urghargai-Mazu Ghar area.

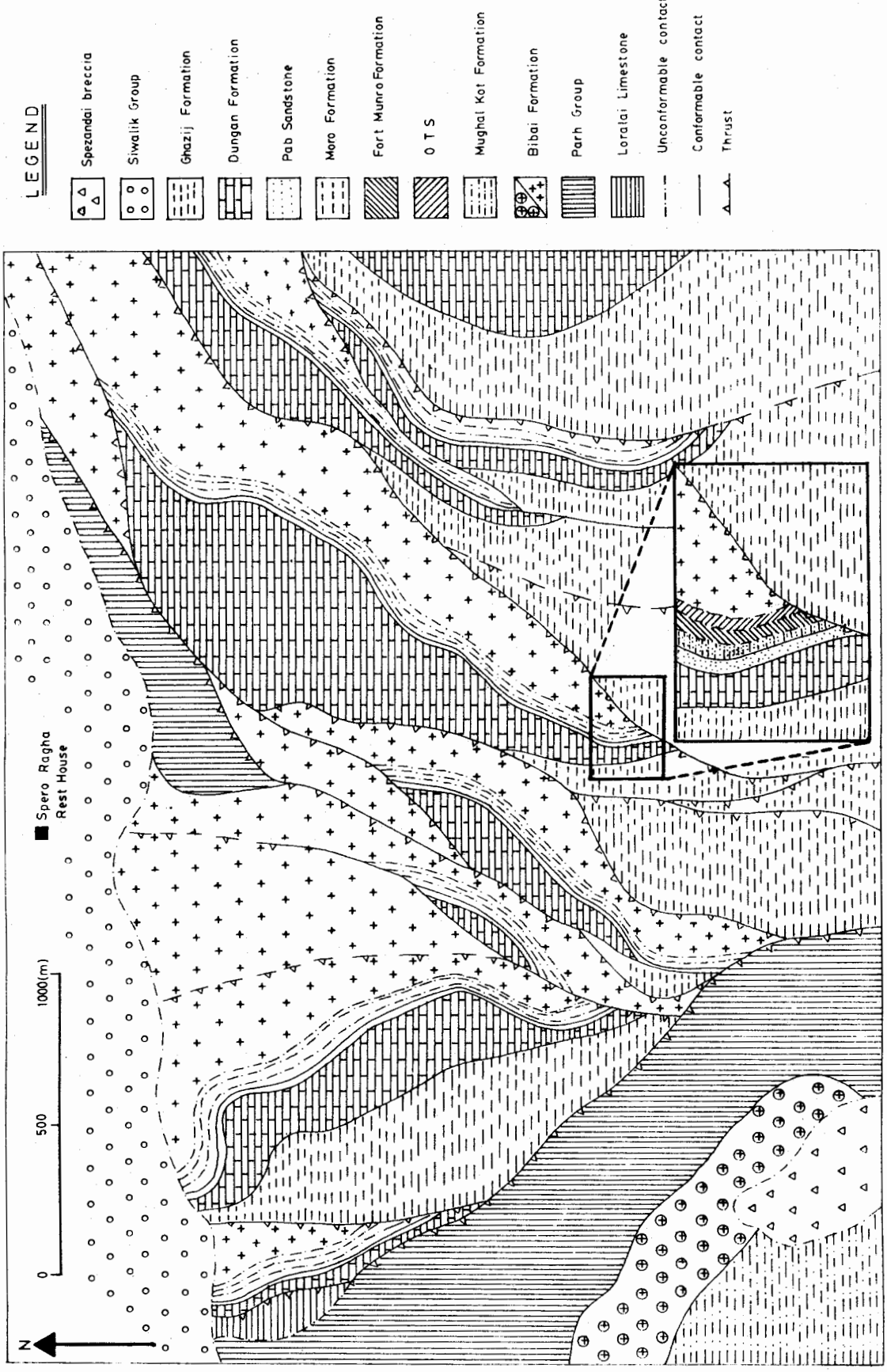

Figure 2. Enlarged geological map of part of the Spera Ragha area.

Table 1. Stratigraphic succession of the Spera Ragha-Chinjun area.

Age	Group/Formation		General Lithology
Recent	Alluvium		Sandstone, mudstone, conglomerate.
Pliocene	Siwalik Group	Dhok Pathan Formation	Cyclic alternations of moderate brown to light brown claystone and pale brown to light brown sandstone
Miocene	Siwalik Group	Nagri Formation	Sandstone with minor intercalations of conglomerate
***Angular Unconformity**			
Upper Eocene	Kirthar Formation		Pinkish grey, highly fossiliferous, limestone.
Lower Eocene	Ghazij Formation		Olive grey shale with sandstone and limestone
Paleocene to Lr. Eocene	Dungan Formation		Medium grey, thick bedded, massive to nodular limestone
Upper Cretaceous (Middle to Upper Maestrichtian)	Pab Sandstone		Light brownish grey and cream quartzose sandstone
	Moro Formation		Light brownish grey, medium to thick bedded limestone (calcarenite) interbedded with dark brownish grey shales
	Disconformity		
	Fort Munro Formation		light olive grey, nodular, biomicritic .limestone
	Disconformity		
	Oxidized Transitional Succession		Bluish grey, highly fossiliferous and arenaceous limestone, conglomerate, sandstone and gypseferous shale, oxidized at several levels
Nonconformity			
Middle Cretaceous: Campanian to E. Maestrichtian	Bibai formation		In-situ basic volcanic rocks
Middle Cretaceous: Berremian to Sentonian)	Parh Group	Parh Limestone	Cream coloured, bio-micritic limestone, medium to thick bedded
Early Cretaceous (Lower Albian to Cenomanian)	Parh Group	Goru Formation	Alternations of pale, olive and greyish red coloured bio-micritic limestone and shale
Late Jurassic to Early Cretaceous (Neocomian)	Parh Group	Sember Formation	Dark brownish grey and light greenish grey belemnitic shale.
Disconformity			
Jurassic	Loralai Limestone		Light brownish grey limestone, possessing ammonites with subordinate shale
Triassic	Wulgai Formation		Shale rhythmically interbedded with limestone
Base not exposed			

*The angular unconformity is between the underlying rocks of Triassic-Eocene age and overlying Miocene Nagri Formation.

Siwalik Group. The Urghargai-Mazu Ghar area (Table 2) include the Jurassic Loralai Limestone, Lower-Middle Cretaceous Parh Group, Middle-Upper Cretaceous Bibai formation and Mughal Kot Formation, Paleocene-Lower Eocene Dungan Formation, Lower-Middle Eocene Ghazij Formation and the Miocene-Pliocene Siwalik Group. Both of these areas contain several lithostratigraphic units / formations which have not been mentioned or described by earlier workers (Hunting Survey Corporation (HSC) 1960, Kazmi 1955, 1979, 1988, 1995, Kazmi and Jan 1997). They include the Loralai Limestone, Fort Munro Formation, Moro Formation, Pab Sandstone, Fort Munro Formation, Mughal Kot Formation and Kirthar Formation. Also another lithostratigraphic unit, arbitrarily named as the "Spezendai breccia", has been first time described. Sharp contrasts exist between the Middle Cretaceous-Eocene successions of the Spera Ragha-Chinjun and Urghargai-Mazu Ghar areas.

The present paper provides first description of some of the newly discovered lithostratigraphic units and some other formations which have not been recognized or described before. Colours of the various rock types have been determined by comparing their fresh hand specimens with the Rock Colour Chart (G.S.A. 1980) and Munsell Notation Numbers assigned to their colours, which are given in brackets. Also the contrasts within the lithostratigraphy of the Spera Ragha-Chinjun and

Table 2. Stratigraphic succession of the Urgharghai-Mazu Ghar area.

Age	Group/Formation		General Lithology
Recent	Alluvium		Sandstone, mudstone, conglomerate.
Sub-Recent	Spezendai breccia		Thick bedded limestone-breccia.
****Angular Unconformity**			
Pliocene	Siwalik Group	Dhok Pathan Formation	Cyclic alternations of moderate brown to light brown claystone and pale brown to light brown sandstone.
Miocene	Siwalik Group	Nagri Formation	Sandstone with minor intercalations of conglomerate.
***Angular Unconformity**			
Lower Eocene	Ghazij Formation		Olive grey shale with sandstone and limestone.
Paleocene to Lower Eocene	Dungan Formation		Thick bedded, massive, nodular limestone with minor sandstone and shale in lower part.
Upper Cretaceous (Upper Maastrichtian)	Mughal Kot Formation		Mudstone, siltstone and shale with intercalations of quartzose sandstone.
Mid. to Up. Cretaceous (Campanian to Middle Maastrichtian)	Bibai formation		Mudstone, ash, volcanic conglomerate, volcanic breccia, sandstone and pillow lava.
Mid. Cretaceous (Berremian to Sentonian)	Parh Group	Parh Limestone	Cream coloured bio-micritic limestone, medium to thick bedded.
Early Cretaceous (Lower Albian to Cenomanain)	Parh Group	Goru Formation	Alternations of bio-micritic limestone and of pale, olive and greyish red coloured shale.
Late Jurassic to Early Cretaceous (Neocomian)	Parh Group	Sember Formation	Brownish grey and light greenish grey coloured belemnitic shale.
Disconformity			
Early Jurassic	Loralai Limestone		Light brownish grey coloured limestone, possessing ammonites, with subordinate shale.
Thrust (Base not exposed)			

*Angular unconformity shown in this position is between the underlying Triassic-Eocene succession and overlying Miocene Nagri Formation.
**Angular unconformity shown in this position is between the underlying Parh Group, Bibai formation, Mughal Kot Formation and overlying Spezendai breccia.

Urghargai-Mazu Ghar areas have been discussed.

LITHOSTRATIGRAPHY

SPERA RAGHA-CHINJUN AREA

The stratigraphic succession of the Spera Ragha-Chinjun area (Table 1) bigins with the Triassic **Wulgai Formation**, the name adopted (Williams 1959) for the Triassic rocks of the Sulaiman Thrust-Fold Belt (Bender and Raza 1995) after the village of Wulgai near Muslimbagh. The formation comprises dark grey and dark brownish grey shale interbedded with thin to thick bedded dark grey limestone. Within the Spera Ragha-Chinjun area (Figs. 1 and 2, Table 1) the formation comprises dominantly shale interbedded with minor proportion of limestone with several dolerite sills and dykes in between. The formation is divisible into shale-dominant and rhythmically interbedded limestone and shale packages. Where sills and dykes are present, the shale has been backed and metamorphosed to slate grade. Near the sills and dykes the limestone beds have been re-crystallized and converted to marbles (Fig. 3). Sills and dykes have clear chilled margins. Within the rhythmically interbedded limestone and shale packages thickness of shale range from 4 cm to 310 cm and thickness of limestone / marble beds range from 5 cm to 100 cm. Thickness of sills and dykes is up to several metres. Shale is medium dark grey (N4) to dark grey (N3), highly fissile and deformed. The limestone/ marble is medium grey (N5), medium light grey (N4) and light grey (N7). It possess grading, parallel lamination, cross-lamination and sole marks. Where converted to marble these sedimentary structures are not clearly observed. The sills and dykes are medium light grey (N6) to medium grey (N5) and mostly doleritic. Within the Rud Malazai area the upper contact of the formation is

Figure 3. Photograph showing the limestone interbedded with shale succession of the Wulgai Formation, Rud Malazai area (Grid ref. 538 692). Note that limestone horizon has been recrystallized and converted to marble and shale is highly cleaved.

Figure 4. View of the Goru Formation, Urghargai-Mazu Ghar area (Grid ref. 616616).

conformable with the Loralai Limestone, whereas, its base is not exposed. Elsewhere, various types of ammonites such as *Helorites, Jovites, Pararcestes, Aretocelites* and *Halobia* have been reported which indicate Early to Late Triassic age (Williams 1959, HSC 1960, Fatmi 1977).

The Jurassic **Loralai Limestone** of Williams (1959), now considered as a member of the Shirinab Formation (Kazmi 1995), is widely developed in Loralai District where it forms prominent hills. Within the Spera Ragha-Chinjun area (Figs. 1 and 2, Table 1) the Loralai Limestone is light brownish grey (5YR6/1), medium grey (N5) and medium dark grey (N4). It is nodular with very thin shale partings. Limestone is generally very finely crystalline, in places oolitic and very coarse intraclastic. It contains various species of ammonites, on the basis of which Woodward (1959), HSC (1960) and Fatmi (1977 have assigned an Early Jurassic age to the Loralai Limestone. The formation is disconformably overlain by the Sember Formation of the Parh Group.

The **Parh Group** (HSC 1960) has been sub-divided into the Sember Formation, Goru Formation and Parh Limestone (Table 1, 2). The **Sember Formation** was introduced by Williams (1959) after the Sember Pass in the Maree -Bugti Hills of the Sulaiman Thrust-Fold Belt. The formation consists black silty shale with interbeds of black siltstone, nodular, rusty weathering, arenaceous limestone and sandstone. In the lower part sandy shale is present which is rich in Belemnite. Within the Spera Ragha-Chinjun area (Figs. 1 and 2, Table 1, 2) several tens of metres thick, dark grey, brownish grey and light greenish grey shale is present where Belemnites are found. Elsewhere, beside Belemnites, a rich assemblage of Foraminifera and ammonites have been reported (Fatmi 1968, 1972, 1977), which suggest a Late Jurassic to Early Cretaceous (Neocamian) age for the Sember Formation. The Sember Formation is conformably and transitionally overlain by the Goru Formation.

The name **Goru Formation** was assigned (Williams 1959) to the rocks included (Oldham 1892) in the upper part of his "Belemnites Beds". The Goru Formation comprises interbedded limestone, shale and siltstone. Limestone is bio-micritic, thin bedded, light to medium grey and olive grey. The interbedded shale and siltstone are grey, greenish grey and maroon (Fig. 4). Within the Spera Ragh-Chinjun area (Figs.1 and 2, Table 1) shale is brownish grey (5YR4/1) and greenish grey (5GY6/10), whereas, limestone is light greenish grey (5GY8/1), light olive grey (5y6/1) and greenish grey (5GY6/1). Shale is interbedded with thin to medium thick bedded bio-micritic limestone and is dominant in lower part. However, the frequency of limestone beds gradually increases upward. Limestone contain micro-planktonic foraminifera. Fritz and Khan (1967) and Allemann (1979) have recognized Foraminifera from the Bangu Nala in the Quetta region which include *Globigerinelloides, G. breggiensis, G. caseyi, Rotaliporatricinensis, R. appennenica, R. brotzeni* etc. On the basis of these an Early Cretaceous (Albian to Cenomanian) age has been assigned. Its upper contact with the Parh Limestone is transitional and conformable.

The name **Parh Limestone** was given (Vredenburg 1909, Williams 1959) to the prominent white limestone of the Cretaceous succession. It is a hard, light grey, white, cream and olive green, bio-micritic limestone which is commonly thin to medium bedded (Fig. 5). The formation is laterally persistent and widely distributed in the Kirthar-Sulaiman Thrust-Fold Belt. Within the Spera Ragha-Chinjun area (Figs. 1 and 2, Table 1) the Parh Limestone is white (N9), very light grey (N8), light grey (N7), bio-micritic and regularly bedded. Red to pink coloured chert bands and nodules are also present. Bed thickness range from 5 cm to 35 cm. The formation is rich in micro-Foraminifera of *Globotruncana sp.* The HSC (1960), Gigon (1962) and Allemann (1979) have described various types of micro-Foraminifera and assigned a Middle Cretaceous (Berremian to Santonian) age to the formation. Within the Spera Ragha-Chinjun area upper contact is transitional and conformable with the *in-situ* volcanic rocks of the Bibai formation.

The name **Bibai formation** was assigned by Kazmi (1955,1979) to the *in-situ* basic volcanic rocks and associated volcaniclastic succession which overlies the Parh Limestone in the Kach-Ziarat valley and Spera Ragha-Urghargai-Chinjun area. Within the Spera Raga-Chinjun area (Figs. 1 and 2, Table 1) the *in-situ* volcanic rocks are dominant (Fig. 6). They are dark grey in colour and mostly basaltic in composition. Numerous sills and dikes are also present within the in-situ volcanic rocks. The rocks contain zeolite and calcite in the form of filled vesicles and veins. Texture is generally very fine grained and porphyritic. Phynocrysts are visible with the naked eye and hand lense. It also shows amygdaloidal texture. Flow banding is also present in some localities. Thickness of the *in-situ* volcanic rocks reaches up to several hundreds metres. The intercalated biomicritic limestone interbedded with lava flows in lower part of the formation resemble with the Parh Limestone and contains micro-Foraminifera of mainly *Globotrancana sp.* On the basis of various fossils found within the mudstone and intercalated bio-micritic limestone in the Kach-Ziarat area, Kazmi (1955) assigned a Middle Cretaceous (Campanian to Early Maastrichtian) age to the formation. On the basis of K-Ar dating Sawada et al. (1995) have proposed 71.4 +3.4 Ma to the *in-situ* volcanic rocks of the Spera Ragha-Chinjun area. Within the Spera Ragha-Chinjun area the Bibai formation is nonconformably overlain by an Oxidized Transitional Succession (Fig. 7).

The arbitrarily named **"Oxidized Transitional Succession"** (Figs. 1, 2, 7, Table 1) has been described first time and separately because of the diversity of its

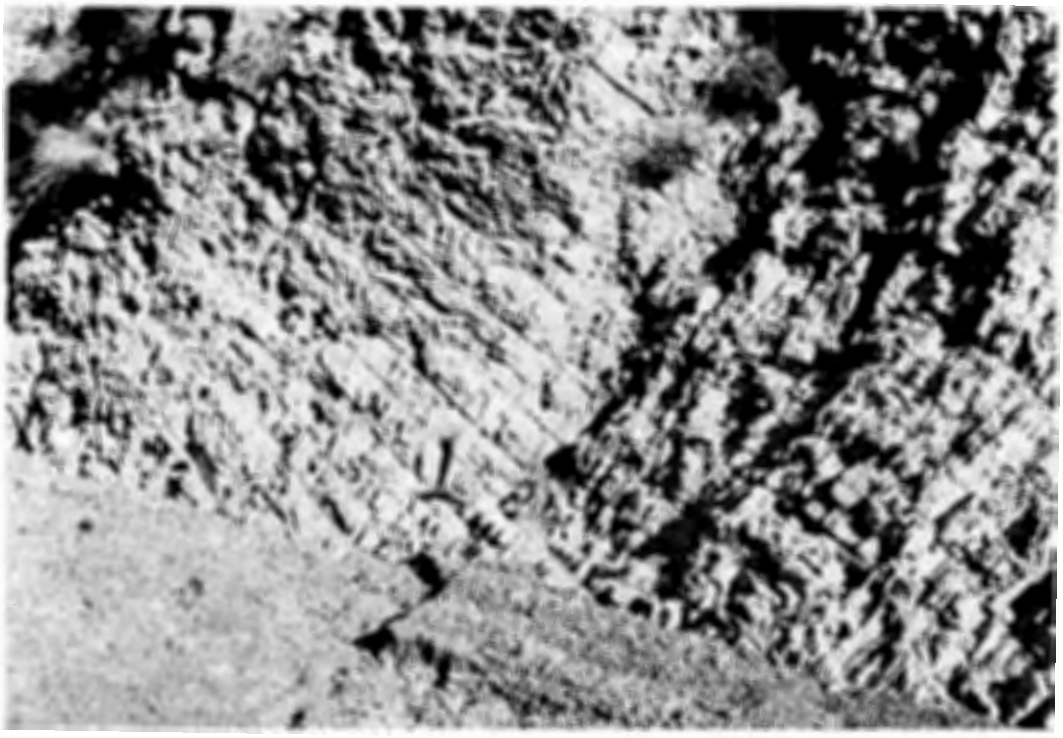

Figure 5. Close-up view of the regularly bedded Parh Limestone, Urghargai-Mazu Ghar area (Grid ref. 608 619).

Figure 6. Sill within the *in-situ* volcanic rocks of the Bibai Formation, Lel Gat section, Spera Ragha-Chinjun area (Grid ref. 628 622).

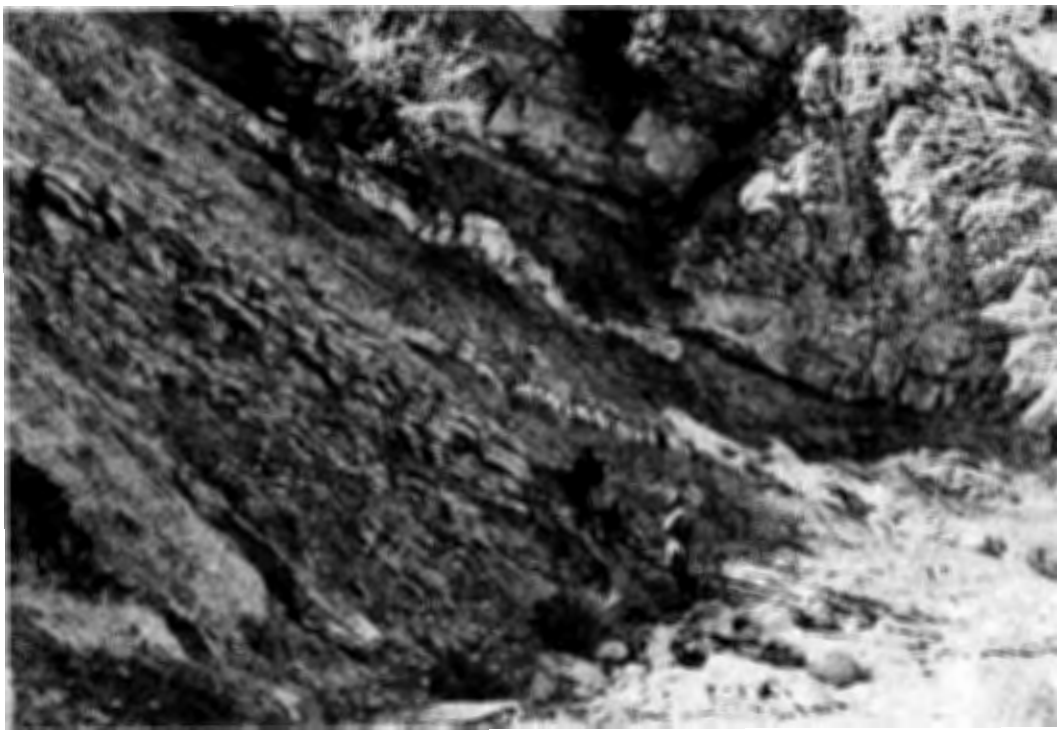

Figure 7. Close-up view of the Bibai Formation, Oxidized Transitional Succession and Fort Monro Formation, Lal Gat section, Spera Ragha-Chinjun area (Grid ref. 828 622).

Figure 8. Photograph of the sharp erosional and disconformable contact between the Fort Monro Formation and Moro Formation, Lal Gat section, Spera Ragha-Chinjun area (Grid ref. 628622).

lithological characters, presence of various oxidized horizons and considerable thickness (up to 10 m). We recognized this succession, arbitrarily, proposed its name and reference section in the Lel Gat Nala, 1 km southwest of Spera Ragha Rest house. The Oxidized Transitional Succession comprises limestone, sandstone, siltstone, gypsiferous shale and volcanic conglomerate (Fig 7). The limestone is partly fossiliferous and nodular and partly silty to arenaceous. Nodular limestone is abundant in upper and middle part of the succession, where its thickness range between 5 to 25 cm. Shale, siltstone and conglomerate are highly oxidized at six different levels within the succession. It is medium light grey (N6) and light brownish grey (5YR6/1), highly fossiliferous containing pelecypod, brachiopods, gastropods and foraminifera. Shale is yellowish brown and commonly contain network of gypsum veins. Conglomerate is generally brownish grey, highly oxidized and contain clasts of basaltic fragments. Sandstone of brownish grey colour is present in the upper part of the succession within two up to 150 cm thick horizons. On the basis of its stratigraphic position we proposed Middle Cretaceous (Early to Middle Maastrichtian) age to the succession. The Oxidized Transitional Succession is disconformably overlain by the Fort Munro Formation.

The **Fort Munro Formation** of HSC (1960) and Williams (1959) has been recognized in the Spera Ragha-Chinjun area for the first time (Figs. 1, 2 and 7, Table 1). It is recognizable on the basis of its stratigraphic position and lithological characters. The formation comprises limestone of light olive grey (5Y6/1), brownish grey (5YR6/1) and medium grey (N5) colours. It is thick bedded, massive to nodular, very hard and compact. Its thickness in Lel Gat section of the Spera Ragha area is 8 m. During the field work we found *Orbitoids* in it, however, detailed bio-stratigraphy is yet to be carried out. Elsewhere, *Omphalocyclus macropora, Orbitoid sp. Actinosiphon, Punjabensis* and *Siderolites* have been reported (Williams 1959, HSC 1960, Marks 1962), on the basis of which a Late Cretaceous (Middle to Upper Maastrichtian) age has been assigned to the formation. Its upper contact is disconformable with the Moro Formation (Fig. 8).

The name **Moro Formation** was assigned by the HSC (1960) to a specific Upper Cretaeous after the Moro River. Within the Spera Ragha-Chinjun area (Figs. 1 and 2, Table 1) the formation has been recognized for the first time where it is 10 m thick. It comprises light brownish grey (5YR6/1), brownish grey (5YR4/1), medium grey (N5) and medium dark grey (N4) coloured calcarenite limestone interbedded with shale. The limestone is dominant lithology in lower part, however, the proportion of limestone decreases upward. Forminifera, bivalves and gastropods are highly abundant within this formation. Elsewhere, the HSC (1960) has reported *Orbitoids, Siderolites* and various species of *Globotruncana* and assigned an Upper Cretaceous (Upper Maastrichtian) age to the formation. It is conformably and transitionally overlain by the Pab Sandstone.

The term **Pab Sandstone**, introduced by Vredenburg (1908) and Williams (1959), has been derived from the Pab Range of the Kirthar Thrust-Bold Belt. Within the Spera Ragh-Chinjun area (Figs. 1 and 2, Table 1) we recognized the formation for the first time. Here it comprises quartzose sandstone of very fine to fine grained, well sorted, sub-angular to sub-rounded texture. It is light brownish grey (5YR6/1), light brown (5YR6/4), very light grey (N8) and light grey (N7). It shows well developed cross-bedding and is generally medium to thick bedded (Fig. 9). Thickness of the formation in Lal Gat section of the Spera Ragha area is 7 m. Elsewhere, Vredenburg (1908), Williams (1959) and HSC (1960) have reported *Orbitoids* from the formation and have assigned an Upper Cretaceous (Upper Maastrichtian) age. Its upper contact with the Dungan Formation is transitional and conformable.

Williams (1959) redefined the term **Dungan Formation** from its original name of the Dungan Limestone (Oldham 1890). Within the Lel Gat section of the Spera Ragha area (Figs. 1 and 2, Table 1) the formation comprises hard and compact limestone of light brownish grey (5YR6/1), pinkish grey (5YR8/1), medium light grey (N6) and medium grey (N5) colours. Its lower portion is comparatively thin bedded where bed thickness range between 20 to 35 cm. Its upper part is thick bedded, massive and nodular. Some of the beds in lower part are highly arenaceous. Thickness of the Dungan Formation in Lel Gat section is 25 m. The formation is very rich in various types of fauna which include forminifera, bivalves, gastropods and echinoderms. Elsewhere, the HSC (1960), Lathif (1964), Iqbal (1969) and Allemann (1979) have reported various species of foraminifera (*Fascioloids, Nummulites* and *Muscellnea*), gastropods, bivalves, brachiopods, echinoderms and cephalopods, on the basis of which a Paleocene to Lower Eocene age has been assigned to the formation. Its upper contact with the Ghazij Formation is transitional and conformable.

The Ghazij Group of Oldham (1890) was re-defined as the **Ghazij Formation** by Williams (1959). Within the Spera Ragha-Chinjun area (Figs. 1 and 2, Table 1) the formation consists dominantly shale with subordinate sandstone and arenaceous limestone. Shale is medium light grey (N4), greenish grey (NGY 6/1) and light olive grey (5Y6/1). It is mostly gypsiferous, fissile and carbonaceous. Sandstone is light olive grey (5Y6/1), medium grey (N5), light brownish grey (5YR6/1) and brownish grey (5YR4/1). It is moderately to poorly sorted, medium to coarse grained and normally cross-stratified. The arenaceous limestone is light brownish

Figure 9. Photograph showing cross-bedding within the Pab Sandstone at the Lel Gat section, Spera Ragha-Chinjun area (Grid ref. 628 622).

Figure 10. Photograph showing contact of the light grey sandstone of the Nagri Formation with the reddish brown claystone of the Dhok Pathan Formation in the study area (Grid ref. 616 625).

grey (5YR6/1) with abundant shell fragments. Near the Spezendai village of the Spera Ragha-Chinjun area the Ghazij Formation has been deformed and imbricated, therefore, it is difficult to estimate its thickness. Elsewhere, various faunas has been reported which include foraminifera, gastropods, bivalves, echioides, algae, plant fragments, leave prints and vertebrate bones (Eames 1952, HSC 1960, Latif 1964, Iqbal 1969, Kassi and Kakar 1998, Ginsberg 1998) on the basis of which the formation has been assigned and Early Eocene age. Its upper contact with the Kirthar Formation is transitional and conformable.

The **Kirthar Formation** (Noetling 1903) is equivalent of the Spintangai Limestone of Oldham (1890). Within the Spera Ragha-Chinjun area (Figs. 1 and 2, Table 1) the formation is highly disturbed. Its discontinuous and broken fragments are present on top of the Ghazij Formation near the Spezendai village within the Bibai Thrust Zone. Here the formation consists interbedded limestone and shale. It is light olive grey (5Y6/1) and light brownish grey (5YR6/1). It is highly fossiliferous with abundant mollusks, brachiopods, echioides and foraminifera. From the Kirthar Range the HSC (1960) has reported various species of foraminifera which include *Lepidocyclina dilatata, Nummulites fichteli and N. intermedius*. Also gastropods, bivalves, echioides and vertebrate remains have been reported by Oldham (1890), Vredenburg (1908), Pilgrim (1940), Eames (1952), HSC (1960), Lathif (1964) and Iqbal (1969), on the basis of which the formation has been assigned a Middle to Late Eocene age. Near the Spezendai village it is exposed in the highly disturbed Bibai Thrust Zone in which the Sember Formation of the Parh Group of the Urghargai-Mazu Ghar area has been thrusted over the Kirthar Formation.

The **Siwalik Group** in Balochistan comprises the Nagri, Dhok Pathan and Soan Formations, which have been well developed within the Sibi-Zarghun trough and Spera Ragha-Kach region. Here the lower part of the Siwalik Group such as the Chinji Formation has not been developed. The Hunting Survey Corporation (1960) and Kazmi and Raza (1970) have named it as "Sibi Group" and "Urak Group" respectively. Within the Spera Ragha-Urghargai region (Figs. 1 and 2, Table 1) only the middle part of the Siwalik Group, i.e. the Nagri and Dhok Pathan Formations, have been developed.

The name **Nagri Formation** was given (Lewies 1937) to the second member of the Siwalik Group which has been accepted as such by the Stratigraphic Committee of Pakistan. Within the Balochistan area, it was named as the "Uzda Pusha Sandstone" of the Sibi Group and Urak Group (HSC 1960, Kazmi and Raza 1970). Within the Spera Ragha-Chinjun area (Figs. 1 and 2, Table 1) the formation is composed mostly of sandstone with minor conglomerate. Sanstone is fine to very coarse grained, poorly sorted and partly conglomeratic. It is light brownish grey (5YR6/1), light olive grey (5GY6/1), medium light grey (N6) and light greenish grey (5GY8/1) (Fig.10). A variety of sedimentary structures such as parallel-lamination, cross-lamination, ripples marks, sole marks, load casts and associated flame structures and convolute lamination are commonly present. Rarely intercalations of minor claystone and siltstone are also present. Various types of vertebrate bones and wood fossils have observed (Duperon et al. 1996, Durrani 1997, Durrani et al. 1997). The Oil and Gas Development Corporation of Pakistan (1965) assigned a Middle to Late Miocene age to the formation. In the Bohr Tangai, Rudgai Basin, Ziarat District, paleomagnetic studies of the Nagri Formation suggest an age of up to15-16.5 Ma (Durrani 1997, Durrani et al 1997a, Durrani et al 1997b). The formation overlies various rocks of older age (Triassic to Eocene) with angular discordant (Fig. 11).

The **Dhok Pathan Formation** was named by Cotter (1913) which was adopted as such by the Stratigraphic Committee of Pakistan. It is represented by the "Shin Matai Shale" of the Sibi Group and Urak Group (HSC 1960, Kazmi and Raza 1970). Within the Spera Ragha-Chinjun area (Figs. 1 and 2, Table 1, 2) the formation is composed of red coloured shale and sandstone. The formation comprises hundreds of metres thick succession of many cycles of alternating claystone and sandstone horizons. Claystone, however, is dominant in proportion. It is moderate brown (5YR5/6), whereas, sandstone is greyish orange pink (5YR7/2), pale brown (5YR5/2) and light brown (5YR6/4) (Fig. 10). Sandstone is medium to fine grained, generally well sorted and pebbly in places. Within the sandstone horizons thickness of the sandstone beds varies from 3 cm to 150 cm. However, thickness of the complete sandstone and claystone cycles reach up to several tens of meters. Various sedimentary structures such as parallel lamination, cross-bedding, ripple marks, sole marks, load casts and convolute bedding are commonly present. A variety of rich vertebrate fauna has been recorded from the Dhok Pathan Formation of the Kohat-Potwar Province. The fossils include *Indarctos salmontanus, Arctamphicyon lydekkeri, Ictitcherium indicum, Mastodon browni, Dicorhypochoerus titanoides, Pechyportax tatiden,* and *Vardhokpathanesis* (Pasco 1963) on the basis of which an Early to Middle Pliocene age has been assigned. Within the Bohr Thangai section of the Rudgai Basin, Ziarat District, Balochistan, paleomagnetic studies of the lower part of the Dhok Pathan Formation suggest 15 to14.8 Ma (Durrani 1997, Durrani et al 1997a, Durrani et al. 1997b). The Dhok Pathan Formation has a transitional and conformable lower contact (Fig. 10) with the underlying Nagri Formation while its upper contact is not present in the study area.

Figure 11. Photograph of the Khatakai nala, east of the Hari Chand, Urghargai-Mazu Ghar area showing (from right to left) succession of the Parh Limestone, Bibai Formation, Mughal Kot Formation and Dungan Limestone, all unconformably underlying the Miocene Nagri Formation of the Siwalik Group.

Figure 12. View of the Urghargai Ghar showing continuous succession of the Bibai formation, Mughal Kot Formation and Dungan Formation, Urghargai-Mazu Ghar area (Grid ref. 610 615).

The Pliocene-Pleistocene Soan Formation (Urak Conglomerate of HSC (1960) and Kazmi and Raza (1970)), which is the uppermost unit of the Siwalik Group, is well developed within the Sibi-Zarghun Trough but not developed in the Spera-Chinjun region.

URGHARGAI-MAZU GHAR AREA

Stratigraphic succession of the Urghagai-Mazu Ghar area (Fig. 1, Table 2) starts with the **Loralai Limestone** which has been described in previous section. Within the Urghargai-Mazu Ghar area (Fig. 1, Table 2) the Loralai Limestone has been recognized for the first time. Here the Loralai Limestone is exposed in a several meters thick, wedge-shaped, outcrop which is tectonically disturbed. It comprises nodular limestone of medium dark grey and brownish grey colour which is generally micritic. Several species of ammonites were collected from the Loralai Limestone of the Urghargai-Mazu Ghar area. The Loralai Limestone of the Urghargai-Mazu Ghar area (Fig. 1, Table 2) has a thrusted lower contact with the Dungan Limestone of the Spera Ragha-Chinjun area. Its upper contact with the Sember Formation is not clearly exposed, however, it is envisaged to be disconformable.

Lithological characters of formations of the **Parh Group** of the Urghargai-Mazu Ghar area (Fig. 1, Table 2) are comparable with those of the Spera Ragha-Chinjun area, which have been described in the previous section.

The **Bibai formation** of the Urghargai-Mazu Ghar area (Fig. 1, Table 2), has contrasting lithological characters to those of the Spera Ragha-Chinjun area, discussed in previous section. Within the Urghargai-Mazu Ghar area the Bibai formation mainly comprises mudstone of olive grey (5Y4/1), brownish grey (5YR4/1) and light brownish grey (5YR6/1) colour (Fig. 12). In its lower part intercalations of the pillow lava (Fig. 13), volcanic breccia, sandstone, siltstone, volcanic conglomerate (Fig. 14) and bio-micritic limestone arre present. The mudstone, conglomerate and breccia is of medium dark grey (N4), brownish grey (5YR4/1), dark grey (N3), medium grey (N5), medium light grey (N6) and light olive grey (5Y6/1) colours. Thickness of the sandstone range from 3 to 125 cm. It is mostly fine grained with some beds of medium to very coarse grained. In some localities rhythmic alternations of sandstone and shale are present which contains sedimentary structures such as grading, parallel-lamination, cross-lamination and sole marks, which are characteristics of turbidites. The volcanic conglomerate is up to several meter thick. Rock fragments within the conglomerate and breccia are mostly basaltic, however, granite, granodiorite, rhyolite, limestone, sandstone and fossil fragments are also present. Boulders, cobbles and pebbles are angular to well rounded. Their maximum clast size reaches up to 120 cm. Mediu n to coarse grained volcanic sand serves as matrix. The formation is highly fossiliferous. Mudstone succession is rich in gastropods, brachiopods and bivalves. Foraminifera and various type of mollusks are also present within some of the conglomerate horizons. The bio-micritic limestone, interbedded with volcaniclastic succession in the lower part, contain profusion of micro-foraminifera of *globotruncan* family on the basis of which Kazmi (1955, 1979) assigned a Cretaceous (Campanian to Middle Maastrichtian) age to the formation. The Bibai formation in Urghargai-Mazu Ghar area (Fig. 1, Table 2) has conformable and transitional lower contact with the Parh Limestone of the Parh Group (Fig. 15), while, its upper contact is conformable and transitional with the Mughal Kot Formation (Fig. 12).

The **Mughal Kot Formation** was introduced by Williams (1959) to the strata between the Parh Limestone and Pab Sandstone near Mughal Kot. Section exposed along the Zhob-Dera Ismail Khan road (Lat. 31° 26' 52" N; Long. 70° 02' 58" E), between 2-5 km west of the Mughal Kot post, and an adjacent stream has been designated as the type section of the formation by (Williams 1959). Within the Urghargai-Mazu Ghar area (Fig. 1, Table 2) we report and describe this formation for the first time. Here it is composed of thin to medium bedded sandstone packages which are rhythmically alternating with siltstone and shale (Fig. 16). Colour of the sandstone is light brownish grey (5YR6/1) and light olive grey (5Y6/1) and those of siltstone and shale is light brownish grey (5Y6/1), medium grey (N5) and medium light grey (N6), which weathers brownish grey (5YR4/1). Sandstone is fine to medium grained, moderately to well sorted and highly qurtzose. Sandstone and siltstone contains sedimentary structures such as grading, parallel lamination, cross-lamination and sole marks (Figs. 17 and 18). Estimated thickness of the formation is 200 m. No body fossils were observed in this formation. However, bioturbation, which is very intense at certain levels, is very common. Within the Sulaiman Thrust-Fold Belt Williams (1959) has reported *Omphalocyclus sp.* and *Orbitoids sp.* Marks (1962) has reported *Siderolites, Calcitrapoides, Orbitoides and Tissoticompressa.* On the basis of these fossils an Upper Cretaceous (Upper Maastrichtian) age has been assigned. The formation in Urghargai-Mazu Ghar area is conformably and transitionally overlain by the Dungan Formation (Figs. 1 and 12).

The **Dungan Formation** of the Urghargai-Mazu Ghar area (Fig. 1, Table 2) has contrasting lithological characters to that of the Spera Ragha-Chinjun area described in the previous section. Within the Urghargai-Mazu Ghar area it is composed of light grey to light brownish grey, coarsely crystalline bio-sparitic limestone, which is generally nodular and interbedded with brownish grey shale and sandstone in lower part. The limestone is highly fossiliferous which possess

Figure 13. Photograph showing pillow structures within the Bibai formation, of the Urghargai-Mazu Ghar area (Grid ref. 594 622).

Figure 14. Photograph showing the volcanic conglomerate and sandstone of the volcaniclastic succession of the Bibai formation, Urghargai-Mazu Ghar area, west of Spera Ragha.

Figure 15. Close-up view of the transitional contact between the Parh Limestone and Bibai formation, Urghargai-Mazu Ghar area (Grid ref. 610 615). Mughal Kot Formation is also visible at the background.

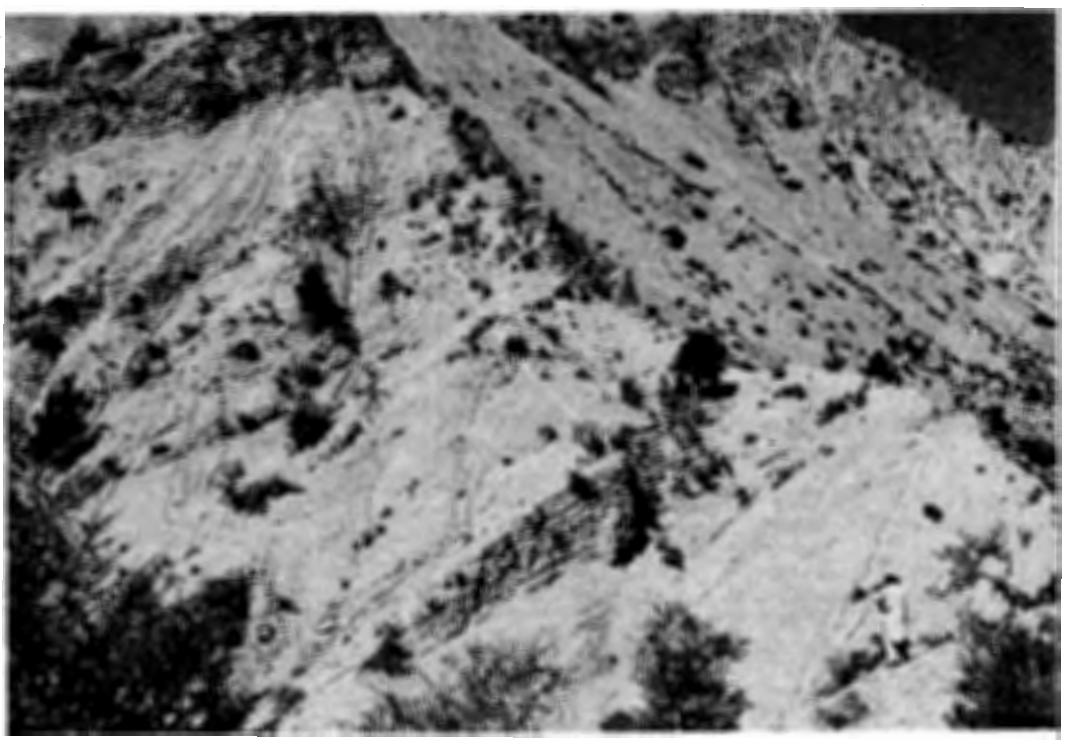

Figure 16. Photograph showing very fine sandstone/siltstone-dominant and shale-dominant peckages within the Mughal Kot Formation of the Urghargai-Mazu Ghar area (Grid ref. 613 609).

bivalves, brachiopods, gastropods, echinoderms and foraminifera. Beds of sandstone and arenaceous limestone possess parallel lamination, cross-lamination and hummocky cross-stratification. Within the Urghargai-Mazu Ghar area the Dungan Formation is 250-300 m thick. The formation is conformably and transitionally overlain by the Ghazij Formation.

The **Ghazij Formation** of the Urghargai-Mazu Ghar area (Fig. 1, Table 2) is exposed in Saro Nala west of the Urghargai-Mazu Ghar area. Its lithological characters are similar to that of the Spera Ragha-Chinjun area. However, its upper contact, which in the Spera Ragha-Chinjun area is with the Kirthar Formation, is not known in the Gogai area to the west of the Urghargai-Mazu Ghar and disturbed by the Gogai Thrust.

Characters of the **Nagri Formation** and **Dhok Pathan Formation** of the **Siwalik Group** have been discussed in previous section, however, it is noteworthy that the Siwalik Group, being younger (Miocene-Pliocene) indiscriminately overlies, with angular unconformity, the older (Triassic-Eocene) succession of the Spera Ragha-Chinjun area as well as the Urghargai-Mazu Ghar area (Fig. 1, Tables 1, 2).

The name **Spezendai breccia** has been arbitrarily proposed by us to the hard and compact breccia that overlies, with angular unconformity, the Mughal Kot Formation, Bibai formation and Parh Group near the Spezendai village (Figs. 1 and 19, Table 2), west of the Spera Ragha Resthouse. It is a several meters thick, well indurated, hard, compact, breccia which is composed of very poorly sorted angular limestone fragments of light brownish grey (5YR6/1), medium grey (N5) and medium light grey (N6) colour. The limestone fragments have been derived exclusively from the Dungan Formation, most probably by a downslope avalanche from the Urghargai Ghar. The breccia is composed of granule to boulder size fragments, the maximum clast size of which reaches up to over 1 m. As the breccia is hard, compact and shows minor tilt, we propose a ?Pleistocene-Sub-Recent age.

DISCUSSION

From the foregoing description of lithostratigraphy of the Spera Ragha-Urghargai region (Fig.1, Table 1, 2) of the western Sulaiman Thrust-Fold Belt, it is clear that sharp contrasts exist between the two successions which also need further explanation and discussion. Following points are be considered:

1) There are several formations/lithostratigraphic units within the region which have not been mapped and/or described before by early workers (HSC 1960, Kazmi 1955, 1979, 1995, Kazmi and Jan 1997, Khan (W. 1994) who have discussed the stratigraphic succession of the area. The HSC (1960) have given the impression that throughout the Spera Ragha-Urghargai region the Parh Group (Lower-Middle Cretaceous) is overlain directly by the Dungan Formation (Paleocene) and also they have referred to the Bibai formation of Kazmi (1955, 1979) as the "Parh-related volcanics". Kazmi (1955, 1979, 1984, 1988, 1995, 1997), has introduced and described the Bibai formation but did not provide further details of the formations and/or lithostratigraphic units which are present between the Bibai formation and Dungan Formation. During our field work of the Spera Ragha-Urghargai region we observed some other formations / lithostratigraphic units, between the Bibai formation and Dungan Formation which had not been mentioned before. They include the Fort Munro Formation, Moro Formation, Pab Sandstone and Kirthar Formation within the Spera Ragha-Chinjun area (Fig.1, Table 1) and Loralai Limestone and Mughal Kot Formation (Fig.1, Table 2) within the Urghargai-Mazu Ghar area. The Mughal Kot Formation of the Upper Cretaceous age, although being a very thick succession (up to 200 m) of mudstone, siltstone and quartzose sandstone, which overlie volcaniclastic succession of the Bibai formation and underlie the Dungan Formation, has not been mapped and/or described (HSC 1960, Kazmi 1955, 1979, 1984, 1988, 1995, Kazmi and Jan 1997). Furthermore, two new lithostratigraphic units have also been discovered. The first named, arbitrarily, as the "Oxidized Transitional Succession" nonconformably overlies the *in-situ* volcanic rocks of the Bibai formation and exposed in the Lel Gat section of the Spera Ragha-Chinjun area (Figs. 1 and 2, Table 1). The second, "Spezendai breccia", named after the Spezendai village, overlies the Mughal Kot Formation, Bibai formation and Parh Group with angular unconformity. It is a hard, compact and flat-lying limestone breccia of ?Pleistocene-Sub-Recent age has been mistakenly shown as the Dungan Formation by the HSC (1960). It is further pointed out that in the Spera Ragha-Chinjun area, near the Spezendai village, the HSC (1960) have mapped a large area as the Parh Group which actually comprises the Eocene Ghazij and Kirthar Formations.

2) Description of the lithostratigraphy of the region shows that the Middle Cretaceous-Eocene successions (Table 1, 2), i.e. between the Parh Limestone and Siwalik Group of the Spera Ragha-Chinjun area and Urghargai-Mazu Ghar area are sharply contrasting. Within the Spera Ragha area the *in-situ* volcanic rocks of the Bibai formation, Oxidized Transitional Succession, Fort Munro Formation, Moro Formation, Pab Sandstone, Dungan Formation, Ghazij Formation and Kirthar Formation represent the succession. The succession also indicate three depositional breaks, i.e. a nonconformity between the *in-situ* volcanic rocks of the Bibai formation and Oxidised Transitional Succession, and two disconformities between the Oxidized Transitional succession, Fort Munro Formation and Moro Formation. The Middle Cretaceous-Eocene succession of the Urghargai-Mazu Ghar area, on the

Figure 17. Photograph showing close-up view of the flysch succession of the Mughal Kot Formation of the Urghargai-Mazu Ghar area (Grid. Ref. 610 615), showing parallel and cross-lamination within the sandstone horizons.

Figure 18. Photograph showing thin bedded distal turbidites of the very fine sandstone/siltstone interbedded with shale package of the Mughal Kot Formation, Urghargai-Mazu Ghar area (Grid ref. 608 613).

Figure 19. Photograph showing the contact of the Bibai formation with the flat-lying Spezandai breccia, Urghargai-Mazu Ghar area (Grid ref. 626 603).

contrary, comprises volcaniclastic rocks of the Bibai formation, Mughal Kot Formation, Dungan Formation and Ghazij Formation. It is noteworthy that lithological characters of the Bibai formation and Dungan Formation of the two domains also have contrasting lithological characters. The Bibai formation of the Spera Ragha-Chinjun area (Fig.1, Table 1) comprises only the *in-situ* basaltic volcanic rocks, the top of which shows an erosional and non-depositinal surface, whereas, that of the Urghargai-Mazu Ghar area comprises mudstone, sandstone, volcanic conglomerate, volcanic breccia and minor amount of pillow lava in its lower part. Also its upper contact with the overlying Mugha Kot Formation is transitional and conformable showing no depositional break in between. The Dungan Formation of the Spera Ragha-Chinjun area is only a 25 m thick, hard and compact limestone that transitionally and conformably overlies the Pab Sandstone, whereas, the Dungan Formation of the Urghargai-Muzu Ghar is over 200 m thick, the lower part of which is composed of shale interbedded with limestone and minor sandstone, while upper part is a hard and compact limestone. Also it conformably and transitionally overlies the Mughal Kot Formation. Succession of the Spera Ragha-Chinjun area also include sheared limestone fragments of the Kirthar Formation which overlie the Ghazij Formation within the Bibai Thrust Zone, west of the Spenzendai village. The Kirthar Formation has not been reported anywhere within the Gogai Thrust Zone west of the Urghargai-Muzu Ghar area (HSC 1960, Kazmi 1955, 1979, Niamatulla et al. 1988) as well as within the Bibai Thrust Zone.

3) The Middle Cretaceous-Paleocene succession of the two stratigraphic domains also indicate sharply contrasting depositional environments. The Spera Ragha-Chinjun area mainly comprises shallow marine limestone-dominant (with minor quartzose sandstone) succession containing profusion of shallow marine mollusks and foraminifera. The succession also contain three depositional breaks in between which snuggest emergence related with episodes of sea-level fluctuations. Thus succession of the Spera Ragha-Chinjun area indicate a marginal shallow marine depositional environment. On the contrary, the Middle Cretaceous-Paleocene succession of the Urghargai-Mazu Ghar area comprises mudstone, siltstone, sandstone and volcanic conglomerate which possess characters of turbidites and associated gravity-flow deposits (Kassi et al. 1993, Khan (A.T.)1998, Khan (A.T.) et al. 1998, Khan (A.T.) et al. 1999, Khan (A.T.) et al. 2000). This succession does not show any depositional break in between. The overall succession appears to have been deposited in deep marine environments where depositional breaks and sub-aerial exposure are not

indicated. Characters of the clasts within the volcanic conglomerate and volcanic breccia suggest that source area of the volcaniclastic succession of the Bibai formation of the Urghargai-Mazu Ghar area was an emergent volcanic island similar in character to that the *in-situ* volcanic rocks of the Spera Ragha-Chinjun area. Similar proposals have been put forward regarding the source terrain for the Bibai formation of the Kach-Ziarat valley (Khan, A.T. 1998, Khan, A.T. et al. 1998, Khan A.T. et al. 1999, Khan, A.T. et al. 2000). We conclude that the Middle Cretaceous-Paleocene succession of the Urghargai-Mazu Ghar area was deposited in deep marine environments, far away west-northwestward from that of the a marginal marine succession of the Spera Ragha-Chinjun area. In a later stage, during the Oligocene times, the deep marine succession of the Urghargai-Mazu Ghar area, along with the underlying succession of the Parh Group, was tectonically emplaced along the Bibai Thrust over the marginal marine succession of the Spera Ragha-Chinjun area.

4) The division line between the two contrasting stratigraphic successions of the Spera Ragha-Chinjun and Urghargai-Mazu Ghar areas (Fig. 1, Tables 1, 2) is a thrust zone, which we consider as continuation of the Bibai Thrust Zone. It indicates thrusting of the Sember Formation (in one locality a wedge of the Loralai Limestone) and the overlying Cretaceous-Eocene succession of the Urghargai-Mazu Ghar area over the Ghazij Formation (near Spezendai village over the Kirthar Formation) of the Spera Ragha-Chinjun succession. Generally the Bibai Thrust Zone in the Kach-Ziarat valley shows thrusting of the Parh Group and overlying satrata over the Ghazij Formation, however, in some localities, e.g. near Kach Levy Post and Spezendai village, sheared limestone fragments of the Kirthar Formation are present within the thrust zone which suggest that the Bibai Thrust occurred after the deposition of the Upper Eocene Kirthar Formation during the Oligocene times. Kazmi (1979) and Niamatullah et al. (1988), however, have proposed a Late Eocene to Oligocene age for the emplacement of both the Gogai and Bibai Thrusts. While their notion may be plausible for the Gogai Thrust, as no Kirthar Formation has been reported from the Gogai area, it is clearly not so for the Bibai Thrust.

CONCLUSIONS

The Spera Ragha-Chinjun region of the western Sulaiman Belt is divisible into two lithostratiigraphic domains, namely the Spera Ragha-Chinjun area and the Urghargai-Mazu Ghar area, on the basis of contrasting lithological characters of their Middle Cretaceous-Eocene succession. The division line between the two domains being the Bibai Thrust. Several formations / lithostratigraphic units, which had never been reported before, were recognized and described for the first time in both of the two domains. Also two new lithostratigraphic units have been discovered, arbitrarily named and described, the "Oxidized Transitional Succession" in the Spera Ragha-Chinjun area and the "Spezendai breccia" in the Urghargai-Mazu Ghar area. Lithological characters, fossils and sedimentary facies of the succession suggest that they were deposited in contrasting depositional environments. The Spera Ragha-Chinjun succession was deposited in the marginal shallow marine environment, whereas, the Urghargai-Mazu Ghar succession in the deep marine environment. The two successions of different depositional environments were later juxtaposed in Oligocene by west-southeastward tectonic transport along the Bibai Thrust.

REFERENCES

Allemann, F., 1979. Time of emplacement of the Zhob Valley Ophiolites and Bela Ophiolites, of Balochistan, *In* Farah, A. and DeJong, K. A., (eds.), Geodynamics of Pakistan: Geological Survey of Pakistan, Quetta, p. 215-242.

Bender, F. K. and Raza, H. A., (eds.), 1995: Geology of Pakistan: Gebruder Borntreager, p. 11-22.

Blandford, W. T., 1876. On the geology of Sind: Geol. Surv. India Recs. Calcutta, 9, p. 8-22.

Cotter, G. de P., 1933. Geology of part of the Attock District, west of Longitude 72° 45' E: India Geol. Surv. Mem., 55, p. 63-161.

Duperon, J., Laudoueneix, M.D. and Durrani, K.H., 1996. Occurrence of Bombacoxylon owenii (Carr.) Gottwald in Cenozoic of Pakistan - History and importance of this species: Palaeontographica Abt. B, 239, Lfg. 1-3, p. 59-75.

Durrani, K. H., 1997. Estude Stratigraphique et Sedimentologique du "Siwaliks" Dans La Region de Zarghun, Quetta, Balochistan, Pakistan: Ph.D thesis (Mem. no. 17/1997), University of Orleans, France (unpubl.).

Durrani, K. H., Kassi, A. M. and Kakar, D. M., 1997a. Siwaliks of the Zarghun-Rudgai area east of Quetta, Pakistan: Acta Mineralogica Pakistanica, 8, p. 106-109.

Durrani, K.H., Yan, C. Courme, M.D. and Kassi, A.M., 1997b. Age determination of Rudgai-Sibi basin (NE Balochistan, Pakistan): a preliminary magnetostratigraphic study and its tectonic implications: Earth and Planetary Sciences, 325, p. 11-18.

Eames, F. E., 1952. A contribution to the study of Eocene in Western Pakistan and Western India: Part A, The Geology of Standard Section in the Western Punjab and in the Kohat District: Part B, Description of the Faunas of certain Standard Sections and their bearing on the classification and correlation of the Eocene in Western Pakistan: Quart. Jour. Geol. Soc. London, 107, Pt. 2, p. 159-200.

Fatmi, A.N., 1968. The paleontology and stratigraphy of the Mesozoic rocks of the western Kohat, Kalachitta, Hazara and Trans-Indus Salt Ranges, West Pakistan. Ph.D. thesis (Unpubl.), Univ. Wales, 409 p.

Fatmi, A.N., 1972. Stratigraphy of the Jurassic and Lower Cretaceous rocks and Jurassic ammonites from the northern areas of West Pakistan: Bull (Geol.) British Museum Natural History, 20, 7: p. 299-380.

Fatmi, A. N., 1977. Mesozoic: *In* Shah, S. M. I., (ed.), Stratigraphy of Pakistan: Geol. Surv. Pakistan, Mem., 12, p. 28-56.

Fritz, E. B. and Khan, M. R., 1967. Cretaceous (Albiab-Cenomanian) planktonic foraminifera in Bangu Nala, Quetta Division, West Pakistan: U. S. Geol. Surv. Proj. Rept. (IR), PK-36, Washington, 16 p.

Gigon, W. O., 1962. Upper Cretaceous Stratigraphy of the Well Giandari-I and its correlation with the Sulaiman and Kirthar Ranges, West Pakistan - E. C. A .F. Symp. Dir. Petrol. Res., Asia and Far East, Tehran, p. 248-282.

Ginsburg, L., Durrani, K.H., Kassi, A.M. and Welcomme, J.P., 1999. Discovery of a new Anthrchobbunidae (Tethytheria, Mammalia) from the Lower Eocene lignite of Kach-Harnai area in Balochistan, Pakistan: Earth and Planetary Sciences, 328, p. 1-5.

Hunting Survey Corporation, 1960. Reconnaissance Geology of part of West Pakistan: A Colombo Plan Cooperation Project, Toronto, Canada. 550 p.

Iqbal, M. W. A., 1966. Mega-Fauna from the Ghazij Shale (Lower Eocene), Quetta - Shahrig area, West Pakistan: Geol. Surv. Pakistan Mem., 7, 45p.

Iqbal, M. W. A., 1969). Mega-fauna from the Ghazij Formation (Lower Eocene), Quetta-Sharigh Area, West Pakistan: Geol. Surv. Pak. Mem. Palaeontlogica Pakistanica, 5, 27p.

Kakar, D. M. and Kassi, A. M., 1997. Lithostratigraphy, Sedimentology and Petrology of the Ghazij Formation, Sor Range area, Quetta District, Pakistan: Acta Mineralogica Pakistanica, 8, p. 73-85.

Kassi, A. M., Khan, A. S., Kakar, D. M., Qureshi, A. R., Durrani, K. H. and Khan, H., 1993.Preliminary Sedimentology of part of the Bibai Formation, Ahmadun-Gogai Area, Ziarat District, Balochistan: Geol. Bull. Punjab Univ., 28, p. 73-80.

Kazmi, A. H., 1955. Geology of the Ziarat-Kach-Zardalu area of Balochistan: D.I.C. thesis, Imperial College of Science and Technology, London (Unpubl.), 157 p.

Kazmi, A. H., 1979. The Bibai and Gogai Nappes in the Kach-Ziarat area of northeastern Balochistan: *In* Farah, A. and DeJong, K. A., (eds.), Geodynamics of Pakistan: Geological Survey of Pakistan, Quetta, p. 333-340.

Kazmi, A. H., 1984. Petrology of the Bibai Volcanics, northeastern Balochistan: Geol. Bull. Univ. Peshawar, 17, p. 34-51.

Kazmi, A. H., 1988. Stratigraphy of the Dungan Group in Kach-Ziarat area, northeastern Balochistan: Geol. Bull. Univ. Peshawar, 21, p. 117-130.

Kazmi, A. H., 1995. Sedimentary Sequence: *In* Bender, F. K. and Raza, H. A., (eds.), Geology of Pakistan: Gebruder Borntraeger, p. 61-124.

Kazmi, A.H. and Jan, Q., 1997. Geology and tectonics of Pakistan: Graphic Publishers, Karachi.

Kazmi, A. H. and Raza, S. Q., 1970. Water supply of Quetta Basin, Balochistan, Pakistan: Geol. Surv. Pak. Recs. 20, Pt. 2, 114p.,

Khan, A.T., 1998. Sedimentology and petrology of the volcaniclastic rocks of the Bibai formation, Ziarat District, Balochistan, Pakistan: Ph.D. thesis (Unpubl.), Centre of Excellence in Mineralogy, University of Balochistan, Quetta.

Khan, A.T., Kassi, A.M. and Khan, A.S., 1998. Volcaniclastic sediments of the Upper Cretaceous Bibai Formation, Kach-Ziarat valley, Balochistan: Acta Mineralogica Pakistanica, 9, p. 117-22.

Khan, A.T., Khan, A.S. and Kassi, A.M., 1999. Petrography, geochemistry and provenance of the volcanic conglomerate and sandstone of the Upper Cretaceous Bibai formation, Kach-Ziarat valley, Balochistan: Acta Mineralogica Pakistanica, 10, p. 103-123.

Khan, A.T., Kassi, A.M. and Khan, A.S., 2000. The Upper Cretaceous Bibai Submarine Fan (Bibai formation), Kach-Ziarat valley, western Sulaiman Thrust-Fold Belt, Pakistan: Acta Mineralogica Pakistanica, 11, p. 1-24 (this volume).

Khan, W., 1994. Geology, geochemistry and tectonic setting of the volcanic rocks of Chinjun and Ghunda Manra areas, northeastern Balochistan, Pakistan: Ph.D. dissertation (unpubl.), University of Iowa, 257p.

Latif, M. A., 1964. Variation in abundance and morphology of pelagic forminifera in the Paleocene-Eocene of the Rakhi Nala, West Pakistan: Punjab Univ. Geol. Bull., 4, p. 29-109.

Marks, P., 1962. The Abbotabad Formation: a new name for Middlemis's Infra-Rrias: Punjab Univ. Bull. 2, p. 56.

Niamatullah, M., Durrani, K. H., Qureshi, A. R., Khan, Z., Kakar, D. M., Jan, M. R. and Ghaffar, A., 1989. Emplacement of the Bibai and Gogai Nappes, northeast of Quetta: Geol. Bull. Univ. Peshawar, 22, p. 153-158.

Noetling, F., 1903. Ubergang zwischen Kreide und Eozan in Balochistan: Centralbl. Mineral. Geol. Palaeont., (Schweizerbart) Stuttgart. 4, p. 514-523,

Oldham, R. D., 1890. Report on the geology and economic resources of the country adjoining the Sind-Pishin railway between Sharigh and Spintangi and the country between it and Khattan: India Geol. Surv. Recs., 23, Pt. 3, p. 93-109.

Oldham, R.D., 1892. Report on the Geology of the Thal Chotiali and part of the Mari country: Geol. Surv. India, Rec., 25, p. 18-29.

Otsuki, K., Anwar, M., Mengal, J. M., Brohi, J. A., Hohino, K., Fatmi, A. N. and Okimura, Y., 1989. Break-up of Gondwanaland and emplacement of ophiolitic complex in Muslim Bagh area of Balochistan: Geol. Bull. Univ. Peshawar, 22, p. 103-126.

Pilgrim, G. E., 1913. The correlation of the Siwaliks with mammal horizons of Europe: Geol. Surv. India Rec., 43, Pt. 4, p. 264-326.

Pilgrim, G.E., 1940. Middle Eocene mammals from northwest India: Zool. Soc. Lond. Proc. Ser. B., 110, 1-2: p. 127-152.

Sawada, Y., Siddiqui, R. H. and Khan, S. R., 1995. K-Ar Ages of the Mesozoic Igneous and Metamorphic Rocks from the Muslim

Bagh area, Pakistan: Proc. Geosci. Colloq., 12, p. 73-90.

Vredenburg, E. W., 1908. The Cretaceous Orbitoides of India: Geol. Surv. India, Recs., 36, p. 171-213.

Vredenburg, E. W., 1909. Mollusca of the Ranikot Series - introductory note on the stratigraphy of Ranikot Series: Geol. Surv. India Mem. Paleont. Indica, New Series, 3 (1), p. 5-19.

Williams, M. D., 1959. Stratigraphy of the lower Indus basin, West Pakistan: Proc. 5th World Petroleum Congress, New York, Sec. 1, 19, p. 337-391.

Woodward, J.E., 1959. Stratigraphy of the Jurassic System, Indus Basin: Stand. Vacuum Oil Co., (Unpubl. Rep.), p. 2-13.

Manuscript received December 20, 2001
Revised Manuscript received March 15, 2001
Accepted March 16, 2001

ACTA MINERALOGICA PAKISTANICA
Volume 11 (2000)

Article Reference AMP11.2000/083-091/ISSN0257-3660

PRELIMINARY SEDIMENTOLOGY OF THE NEWLY DISCOVERED UPPER CRETACEOUS MUGHAL KOT FORMATION, URGHARGAI-MAZU GHAR AREA, WESTERN SULAIMAN THRUST-FOLD BELT, PAKISTAN

AKHTAR MOHAMMAD KASSI[1], ABDUL SALAM KHAN[2] AND MOHAMMAD SARWAR[2]
[1]Department of Geology, University of Balochistan, Quetta, Pakistan
[2]Centre of Excellence in Mineralogy, University of Balochistan, Quetta, Pakistan

ABSTRACT

The Upper Cretaceous Mughal Kot Formation has been recognized, mapped and described first time within the Urghargai-Mazu Ghar area of the western Sulaiman Thrust-Fold Belt. It is composed of thin to medium bedded sandstone, rhythmically alternating with siltstone/shale. Sandstone and siltstone contain sedimentary structures such as grading, parallel lamination, cross-lamination and sole marks. The lower part comprises a succession of classic turbidites, possessing Bouma Tabcde, Tbcde, Tcde, Tde sequences showing frequent amalgamation. The upper part comprises alternations of shale-dominant and siltstone-dominant packages, which also possess characters of turbidites. In these packages Bouma sequence like Tcde and Tde are common. Within the Mazu Ghar area near Hari Chand, the formation composed of shale and siltstone dominant successions with minor proportion of arenaceous limestone showing grading, parallel and cross-lamination and intense bioturbation.

The succession comprising classic Bouma sequences are proximal turbidites deposited by high concentration turbidity currents. Frequent amalgamation, erosive bases, lenticular morphology and rip up mud clasts indicate that the sandstone dominant succession is a deposit of submarine channels. The shale/siltstone dominant packages of facies are distal turbidites deposited by low concentration turbidity currents. The shale dominant packages, which show intense bioturbation, are deposits of a combination of very low energy turbidity currents and pelagic/hemi-pelagic sedimentation. These facies indicate deposition in calm conditions away from the source area. The alternating shale-dominant and siltstone-dominant packages of the Mughal Kot Formation may reflect transgressive and regressive events and sea level fluctuations. The transitional shift from the deep marine turbidite succession of the Mughal Kot Formation upward to the shallow marine succession of the Dungan Limestone, without any depositional break in between, suggest an overall regressional trend of the sea.

INTRODUCTION

The Urghargai-Mazu Ghar area (Figs. 1 and 2; Kassi et al., this volume) is located within the western Sulaiman Thrust-Fold Belt (Bender and Raza 1995, Kazmi and Jan 1997) northeast of the Gogai Nappe (Kazmi 1979, Niamatullah et al. 1989). The area comprises a rock succession (Table 2; Kassi et al. this volume) which include the Triassic Wulgai Formation, Jurassic Loralai Limestone, the Lower-Middle Cretaceous Parh Group, Middle-Upper Cretaceous Bibai formation and Mughal Kot Formation, Paleocene-Lower Eocene Dungan Formation, Lower-Middle Eocene Ghazij Formation and the Miocene-Pliocene Siwalik Group. Within the Urghargai-Mazu Ghar area the Upper Cretaceous succession, specially the Mughal Kot

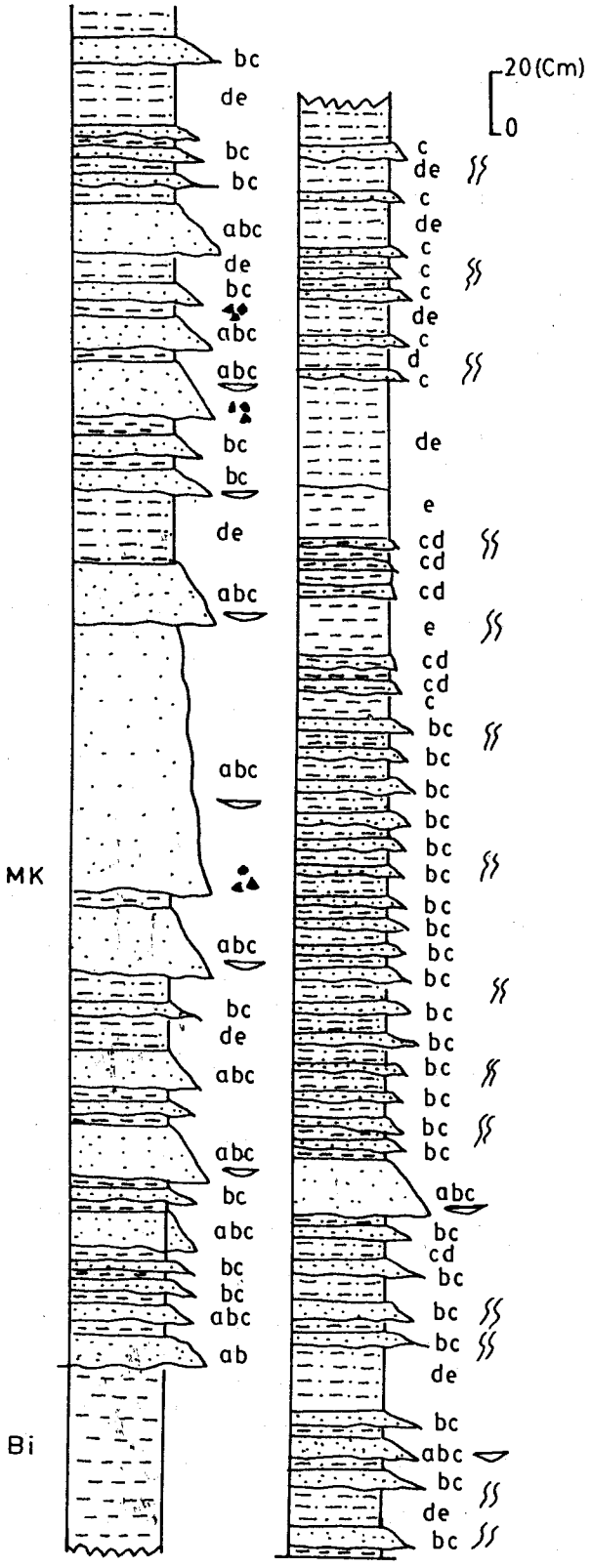

Figure 1. Sedimentary log of lower part of the Mughal Kot Formation within the Urghargai-Mazu Ghar area (Grid ref. 608 613). Legend as in Fig. 1 of Kassi et al. (this volume). The *a,b,c,d,*and *e* are the units of the Bouma (1962) sequence.

Formation has not been described by any worker before (Hunting Survey Corporation [HSC] 1960, Kazmi 1955, 1979, 1988, Kazmi and Jan 1997). Its lithological characters are described (Kassi et al. this volume), however, the present paper first time describes its preliminary sedimentology.

SEDIMENTOLOGY

DESCRIPTION

The Mughal Kot Formation in the Urghargai-Mazu Ghar area comprises siltstone, mudstone, shale and minor proportion of quartzose sandstone (Fig. 12, Kassi et al. this volume). The formation is composed of sandstone/siltstone dominated and shale dominated packages (Figs. 1 and Fig. 12; Kassi et al. this volume) which show intense bioturbation (Fig. 2). In lower part a succession of the rhythmic alternations of quartzose sandstone and shale are present (Figs. 1 and 3) in which the sandstone possesses grading, parallel lamination, cross-lamination, load casts and sole marks (Figs. 4-6). This is a succession of classic turbidites possessing Bouma Tabcde, Tbcde, Tcde, Tde sequences. Most of these turbidite horizons also show frequent amalgamation and various kinds of sole marks (Figs. 5, 6 and 7). Upper part of the formation comprises alternations of shale-dominant and siltstone-dominant packages, which also possess characters of turbidites (Figs. 7 and 8). However, in these packages Bouma sequence like Tcde and Tde are common. Within the Mazu Ghar area near Hari Chand (Fig. 7), the Mughal Kot Formation comprises shale and siltstone dominant successions with minor proportion of arenaceous limestone, which shows grading, parallel and cross-lamination and intense bioturbation (Fig. 2). In some localities the arenaceous limestone possess hummocky cross-stratification (Fig. 9).

INTERPRETATION

Interpretation of facies and facies associations is mainly based on their classification and description by Mutti and Ricci Luchi (1975), Pickering et al. (1986) and Shanmugam and Moiola (1988). The rhythmic alternation of sandstone and mudstone beds, and the range of the associated sedimentary structures like grading, sole marks and Bouma sequences (Bouma 1962) indicate their deposition by turbidity currents. These characters resemble the facies C 2.3 of the organized sand-mud couplets of Pickering et al. (1986), indicating dilute to moderately high concentrated turbidity currents and grain-by-grain deposition from suspension and by traction transport. Muddy upper divisions are the product of low concentration turbidity currents and/or hemipelagic/pelagic sedimentation or rapid deposition of mud-rich turbidity currents. The succession showing grading, classic Bouma sequences like Tabcde, Tbcde and flute marks at the base of

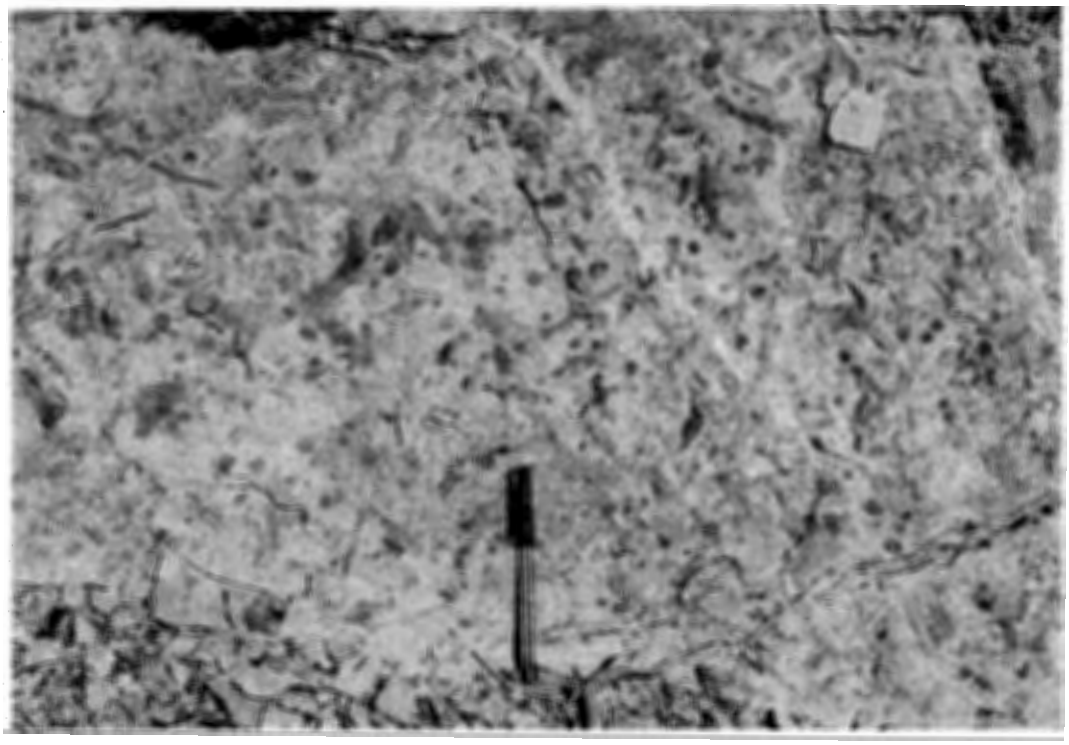

Figure 2. Photograph showing intense bioturbation within the arenaceous limestone horizons of the Mughal Kot Formation, Urghargai-Mazu Ghar area west of Spera Ragha Guest House.

Figure 3. Photograph showing the flysch succession of the Mughal Kot Formation of the Urghargai-Mazu Ghar area (Grid Ref. 610 615), showing sandstone interbedded with shale.

Figure 4. Photograph showing close-up view of the flysch succession of the Mughal Kot Formation of the Urghargai-Mazu Ghar area (Grid. Ref. 610 615), showing parallel and cross-lamination within the sandstone horizons.

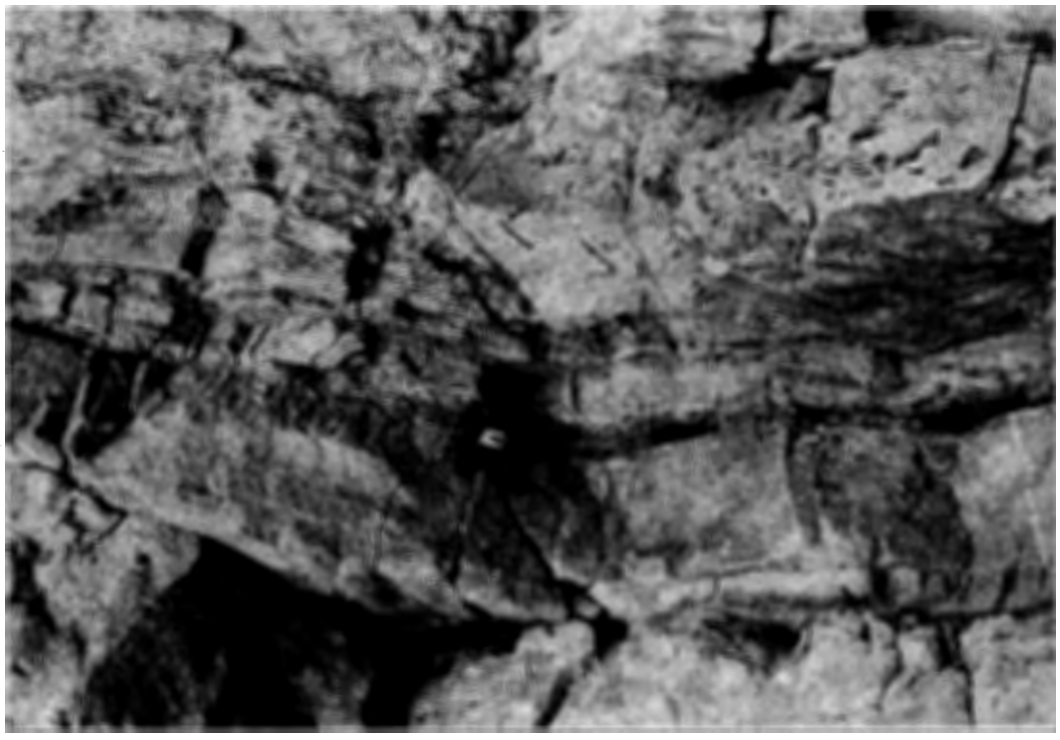

Figure 5. Photograph showing close-up view of the flysch succession of the Mughal Kot Formation of the Urghargai-Mazu Ghar area (Grid. Ref. 610 615), showing parallel and cross-lamination within the sandstone horizons and flute marks at their base.

Figure 6. Photograph showing flute marks at the base of the sandstone horizons of the Mughal Kot Formation of the Urghargai-Mazu Ghar area (Grid. Ref. 610 615).

sandstone (Figs. 3-5 and 7) indicate proximal turbidites deposited by high concentration turbidity currents. Frequent amalgamation, lenticular morphology, erosive bases and rip up mud clasts indicate that the sandstone dominant succession is a deposit of submarine channels.

The shale/siltstone dominant packages of facies (Figs. 7 and 18 of Kassi et al., this volume) show distal turbidites deposited by low concentration turbidity currents. The shale dominant packages, which show intense bioturbation, are deposits of a combination of very low energy turbidity currents and pelagic/hemi-pelagic sedimentation. These facies represents the facies classes D and E of Pickering et al. (1986). Facies D is deposited partly by low-concentration turbidity currents, and partly by grain-by-grain deposition and traction. Facies E which comprises the structure less and mottled shale is deposited by mud-rich very low-concentration turbidity currents and lateral transfer of hemipelagic/ pelagic material by ocean currents where settling occurs from suspension. This facies indicates deposition of mudstone in calm conditions away from the source area. The arenaceous limestone, which also possess characters of turbidites, indicate that the source terrain of quartz was not always available. Presence of the hummocky cross-stratification (Fig. 9) at upper part of the succession suggest influence and reworking by the storm waves. The alternating shale and siltstone-dominant packages of the Mughal Kot Formation may reflect sea level fluctuations. However, the transitional shift from the deep marine turbidite succession of the Mughal Kot Formation upward to the shallow marine succession of the Dungan Limestone, without any depositional break in between, suggest an overall regressional trend of the sea. Paleocurrent directions observed in the Urghargai Ghar section (Gr. Ref. 608 613) based on sole marks indicate a paleocurrent flow generally from SE to NW.

DISCUSSION

There are several lithostratigraphic units within the Spera Ragha-Chinjun and Urghargai-Mazu Ghar region which have not been mapped and/or described before by early workers (HSC 1960, Kazmi 1955, 1979, 1984, 1988, 1995, Kazmi and Jan 1997, Khan (W) 1994). The HSC (1960) has given the impression that throughout the Spera Ragha-Chinjun and Urghargai-Mazu Ghar region the Parh Group (Lower-Middle Cretaceous) is overlain directly by the Dungan Formation (Paleocene) and also they have referred to the Bibai formation of Kazmi (1955, 1979) as the "Parh-related volcanics". Kazmi (1955, 1979, 1984, 1988, 1995), introduced and described the Bibai formation, however, he did not provide any detail of the formations and/or lithostratigraphic units which lie between the Bibai

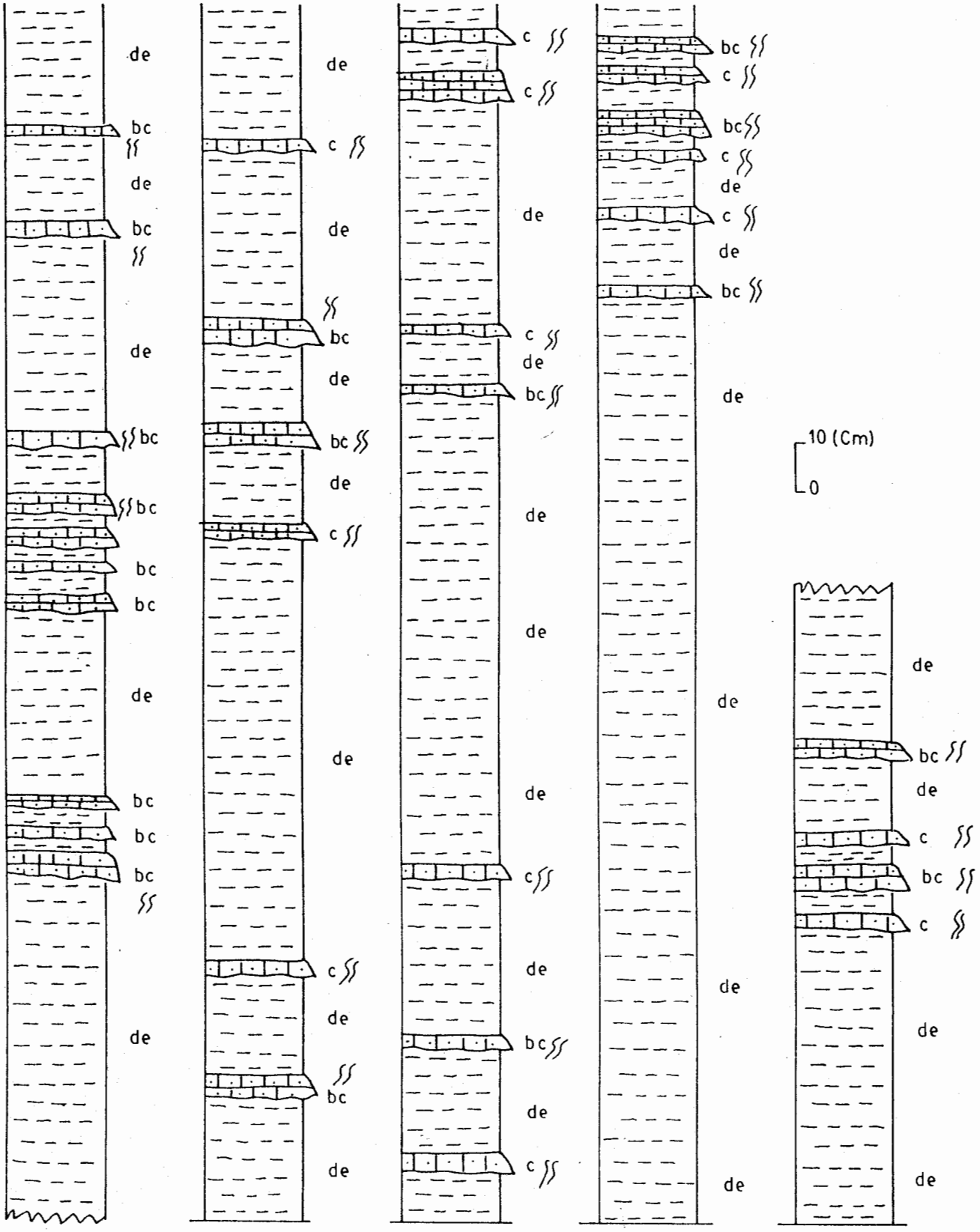

Figure 7. Sedimentary log of the upper part of Mughal Kot Formation within Urghargai-Mazu Ghar area near the Hari Chand village. Legend as in Fig. 1 of Kassi et al. (this volume). The *a, b, c, d,* and *e* indicate units of the Bouma (1962) sequence.

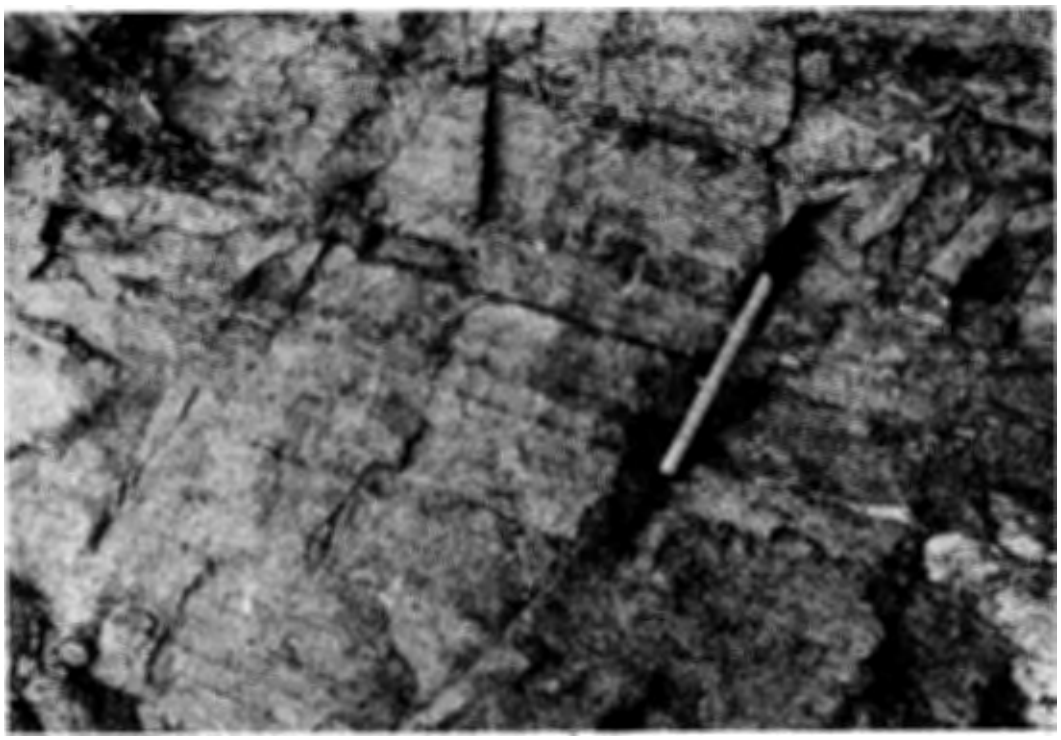

Figure 8. Photograph showing a close-up view of the thin bedded distal turbidites of the very fine sandstone/ siltstone interbedded with shale package of the Mughal Kot Formation, Urghargai-Mazu Ghar area (Grid Ref. 608 613).

Figure 9. Photograph showing hummocky cross-bedding with the arenaceous limestone horizons of the of the Mughal Kot Formation near Hari Chand village.

formation and Dungan Formation. During our field work of the Spera Ragha-Chinjun and Urghargai-Mazu Ghar region we observed some other lithostratigraphic units, between the Bibai formation and Dungan Formation which had not been mentioned before. They include the Fort Munro Formation, Moro Formation, Pab Sandstone and Kirthar Formation within the Spera Ragha-Chinjun area and Loralai Limestone and Mughal Kot Formation (Figs. 1 and 2; Kassi et al., this volume) within the Urghargai-Mazu Ghar area. The Upper Cretaceous Mughal Kot Formation within the Urghargai-Mazu Ghar area, being a thick (>200m) succession of mudstone, siltstone and quartzose sandstone which overlie the volcaniclastic succession of the Bibai formation and underlie the Dungan Formation (Kassi et al. 2000), has not been mapped and/or described before (HSC 1960, Kazmi 1955, 1979, 1984, 1988, 1995, Kazmi and Jan 1997).

The Upper Cretaceous-Palaeocene succession in Kach-Ziarat valley and Urghargai-Mazu Ghar area represent deposition in deep marine conditions where volcaniclastic rocks and turbidites were deposited without any depositional break in between. Within the Kach-Ziarat valley and Urghargai-Mazu Ghar area the volcaniclastic turbidite succession of the Bibai formation was laid down in the form of submarine fan (Kassi et al. 1993, Khan 1998, Khan et al. 1998, Khan et al. 2000) on the slope of hot spot-related volcanos, while the Mughal Kot Formation in Urghargai-Mazu Ghar area, which represents a thick succession of turbidites, is the lateral deep marine equivalent of the Pab Sandstone of the Spera Ragha-Chinjin, Ziarat, Harrnai and Quetta areas. Within the Spera Ragha-Chinjun valley a shallow marine succession of the Fort Munro Formation, Moro Formation, Pab Sandstone and Dungan Formation (Kassi et al. 2000) disconformably overlies the *in-situ* volcanic rocks of the Bibai formation. Whereas, within Quetta and surrounding areas a shallow marine succession of the Hanna Lake limestone, Fort Munro Formation and Dungan Formation disconformably overlies directly the Parh Limestone without showing any sign of the volcanic activity and/or associated volcaniclastic rocks. The Bibai and Mughal Kot Formations of the Kach-Ziarat valley and Urghargai-Mazu Ghar area, being the deep marine equivalent of the shallow marine succession of the Spera Ragha-Chinjun, Ziarat, Harrnai and Quetta areas, were deposited further north-northwestward away from the margin of the Indo-Pakistan Plate and later on juxtaposed by a south-southeastward tectonic transport along the Bibai Thrust during Late Eocene-Oligocene (Kassi et al 2000).

CONCLUSIONS

1) The Mughal Kot Formation is hereby discovered, mapped and described first time in the Urghargai-Mazu Ghar area of the Western Sulaiman Thrust-Fold Belt.
2) It represents flysch succession comprising rhythmic alternations of shale, siltstone and quartzose sandstone, with alternations of sandstone-dominant, siltstone/shale-dominant and shale-dominant packages.
3) The succession possesses characters of turbidites of alternately proximal and distal natures and alternating packages may be related to sea-level fluctuations.
4) The Mughal Kot Formation of the Urgharrgai-Mazu Ghar area is the northwestward deep marine equivalent of the shallow marine succession of the Spera Ragha-Chinjun, Ziarat, Harnai, Shahrig and Quetta areas.

REFERENCES

Bender, F. K. and Raza, H. A., (eds.). 1995. Geology of Pakistan: Gebruder Borntreager, p. 11-22.

Hunting Survey Corporation,. 1960): Reconnaissance Geology of part of West Pakistan: A Colombo Plan Coorporation Project,. Toronto, Canada. 550 p.

Kassi, A. M., Khan, A. S., Kakar, D. M., Qureshi, A. R., Durrani, K. H. and Khan, H., 1993. Priliminary Sedimentology of part of the Bibai Formation, Ahmadun-Gogai Area, Ziarat District, Balochistan: Geol. Bull. Punjab Univ., 28, p. 73-80.

Kassi, A. M., Kaker, D. M., Khan, A. S., Khan, A. T. and Umar, M., 1999. Lithostratigraphy of of the Cretaceous-Paleocene succession in Quetta region, Pakistan: Acta Mineralogica Pakistanica, 9, p. 1-11.

Kassi, A.M., Sarwar, M. and Khan, A.S., 2000. A new appraisal of the lithostratigraphy of the Spera Ragha-Urghargai region, western Sulaiman Belt, Pakistan: Acta Mineralogica Pakistanica, 11 (this volume), p. 61-81.

Kazmi, A. H., 1955. Geology of the Ziarat-Kach-Zardalu area of Balochistan: D.I.C. Thesis, Imperial College of Science andTechnology, London (unpubl.), 157 p

Kazmi, A. H., 1979. The Bibai and Gogai Nappes in the Kach-Ziarat area of northeastern Balochistan: *In* Farah, A. and DeJong, K. A., (eds.), Geodynamics of Pakistan: Geological Survey of Pakistan, Quetta, p. 333-340.

Kazmi, A. H., 1984. Petrology of the Bibai Volcanics, northeastern Balochistan: Geol. Bull. Univ. Peshawar, 17, p. 34-51.

Kazmi, A. H., 1988. Stratigraphy of the Dungan Group in Kach-Ziarat area, northeastern Balochistan: Geol. Bull. Univ. Peshawar, 21, p. 117-130.

Kazmi, A. H., 1995. Sedimentary Sequence: *In* Bender, F. K. and Raza, H. A., (eds.), Geology of Pakistan: Gebruder Borntraeger.

Kazmi, A.H. and Jan, Q., 1997. Geology and tectonics of Pakistan: Graphic Publishers, Karachi. 500 p.

Khan, A.T., 1998. Sedimentology and petrology of the volcaniclastic rocks of the Bibai Formation, Ziarat District, Balochistan, Pakistan: Ph.D. thesis (Unpubl.), Centre of Excellence in Mineralogy, University of Balochistan, Quetta.

Khan, A.T., Kassi, A.M. and Khan, A.S., 1998. Volcaniclastic sediments of the Upper Cretaceous Bibai Formation, Kach-Ziarat valley, Balochistan: Acta Mineralogica Pakistanica, 9, p. 117-122.

Khan, A.T., Khan, A.S. and Kassi, A.M., 1999. Petrology, geochemistry and provenance of the volcanic conglomerate and sandstone of the Upper Cretaceous Bibai Formation, Kach-Ziarat valley, Balochistan: Acta Mineralogica Pakistanica, 10, p. 103-124.

Khan, A.T., Kassi, A.M. and Khan, A.S., 2000. The Upper Cretaceous Bibai Submarine Fan (Bibai Formation), Kach-Ziarat valley, western Sulaiman Thrust-Fold Belt, Pakistan: Acta Mineralogica Pakistanica, 11, p. 1-24.

Khan, W., 1994. Geology, geochemistry and tectonic setting of the volcanic rocks of Chinjun and Ghunda Manra areas, northeastern Balochistan, Pakistan: Ph.D. dissertation (unpubl.), University of Iowa, 257 p.

Marks, P., 1962. The Abbotabad Formation: a new name for Middlemis's Infra-Rrias: Punjab Univ. Bull., no. 2, p. 56.

Niamatullah, M., Durrani, K. H., Qureshi, A. R., Khan, Z., Kakar, D. M., Jan, M. R. and Ghaffar, A., 1989. Emplacement of the Bibai and Gogai Nappes, northeast of Quetta: Geol. Bull. Univ. Peshawar, 22, p. 153-158.

Williams, M. D., 1959. Stratigraphy of the lower Indus basin, West Pakistan: Proc. 5th World Petroleum Congress, New York. Sec. 1, 19, p. 337-391.

Manuscript received December 20, 2000
Revised Manuscript received March 15, 2001
Accepted March 17, 2001

ACTA MINERALOGICA PAKISTANICA
Volume 11 (2000)

Article Reference AMP11.2000/093-103/ISSN0257-3660

LITHOSTRATIGRAPHY AND STRUCTURE OF THE ZHARAI AREA SOUTHWEST OF SOR RANGE, QUETTA DISTRICT, BALOCHISTAN, PAKISTAN

AKHTAR MOHAMMAD KASSI[1], MOHAMMAD UMAR[1], DIN MOHAMMAD KAKAR[1], ABDUL SALAM KHAN[2] AND ABDUL TAWAB KHAN[1]

[1]Department of Geology, University of Balochistan, Quetta, Pakistan
[2]Centre of Excellence in Mineralogy, University of Balochistan, Quetta, Pakistan

ABSTRACT

The Zharai area is located to the southwest of Zarghun-Sibi Trough on the junction of Sulaiman and Kirther Fold-Thrust Belts. Rock succession ranging in age from Jurassic to Recent comprises the Jurassic Chiltan Limestone, Cretaceous Sembar Formation, Goru Formation, Parh Limestone, the newly discovered and arbitrarily named Hanna Lake limestone, Fort Munro Formation and Pab Sandstone; Paleocene-Early Eocene Dungan Limestone, Eocene Ghazij Formation and Kirthar Formation. The Campanian-Early Maastrichtian Hanna Lake limestone, Maastrichtian Pab Sandstone and Sirki Shale member of the Eocene Kirthar Formation have been recognized and described first time within the Zharai area. Both the lower and upper parts of the Paleocene-Early Eocene Dungan Formation are developed. The succession in Zharai area presents five depositional breaks (disconformities). The NNW-SSE - trending rock succession is highly deformed. The Ushbul Thrust, the overturned Sor Range Syncline and numerous wrench faults are the main structural features in the area. The NE-SW trending pattern of wrench faults cut across the NNW-SSE trending succession mostly in sinistral manner. The incompetent Eocene Ghazij Formation in the area serves as a decolma over which various rocks of the Jurassic-Paleocene age have been thrusted.

INTRODUCTION

The Zharai area is located to the southwest of Zarghun Ghar, southwest of the Sor Range and east of Quetta (Fig. 1), on the junction between the Kirthar and Sulaiman Fold-Thrust Belts (Bender and Raza 1995, Kazmi and Jan 1997). The area is very interesting from the stratigraphic and structural point of view, however, after the reconnaissance mapping by the Hunting Survey Corporation (1960), the area has never been mapped in detail. In the nearby Sor Range area, most of the earlier workers have worked on the coal-bearing Eocene Ghazij Formation (Mohsin et al. 1991, Kakar 1993, Kassi and Kakar 1997) and none has studied the older succession and structural aspects of the area.

The present paper provides the first detailed map and describes the lithostratigraphy and major structural features of the Zharai area. A newly discovered lithostratigraphic unit, the Hanna Lake limestone, which disconformably overlies the Parh Limestone and disconformably underlies the Fort Munro Formation, has been mapped and described. Also the Maastrichtian Pab Sandstone and Sirki Shale member of the Eocene Kirthar Formation have also been recognized and mapped first time within the Quetta and surrounding region.

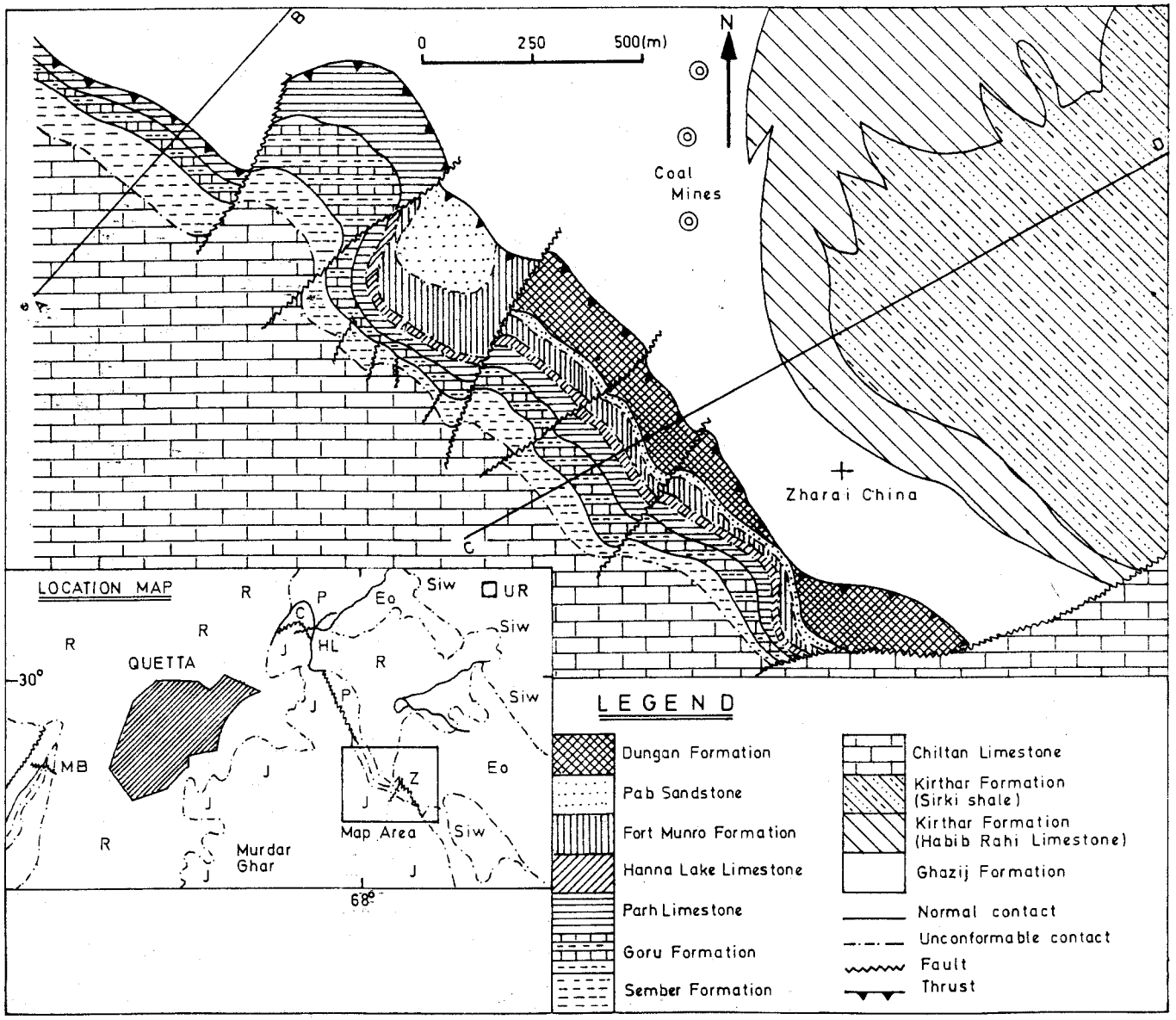

Figure 1.
Location and geological map of the Zharai area. Abbreviations used in the location map include: J= Jurassic, C=Cretaceous, P=Paleo-cene, Eo=Eocene, Siw=Siwaliks, R=Recent, MB=Maree Brewery, HL=Hanna Lake, UR=Urak, Z= Zharai.

Table 1. Stratigraphic succession of the Zharai area of Quetta District.

Age		Group/Formation		General Lithology
Recent		Alluvium		Sandstone, mudstone, conglomerate.
Pliocene-Pleistocene		Siwalik Group	Dhok Pathan Formation	Cyclic alternations of moderate brown to light brown claystone and pale brown to light brown sandstone.
Miocene		Siwalik Group	Nagri Formation	Light brownish and greenish grey sandstone with minor intercalations of conglomerate.
Disconformity				
Late Eocene		Kirthar Formation		*Sirki shale member:* Chocolate to dark brownish grey shale interbedded with arenaceous limestone, highly fossiliferous. *Habib Rahi limestone member:* Limestone, white , cream and pinkish grey, highly fossiliferous.
Early Eocene		Ghazij Formation		Olive grey shale with sandstone and limestone.
Late Paleocene to Early Eocene		Dungan Formation		*Upper Part:* medium grey, thick bedded, massive to nodular limestone. *Lower Part:* Thin to medium bedded nodular limestone interbedded with brownish grey shale.
Cretaceous	Maastrichtian	Pab Sandstone		White, cream and brownish grey, highly quartzose sandstone.
Disconformity				
Cretaceous	Maastrichtian	Fort Munro Formation		Dark grey, thin bedded orbitoidal limestone.
Disconformity				
Cretaceous	Campanian to E. Maastrichtian	Hanna Lake limestone		Dark brownish grey, medium to thick bedded, barely fossiliferous, argillaceous limestone.
Disconformity				
Cretaceous	Berremian to Sentonian	Parh Group	Parh Limestone	White and cream, medium to thick bedded, bio-micritic limestone, possesses pink and red chert nodules and bands.
Cretaceous	Lower Albian to Cenomanian	Parh Group	Goru Formation	Alternation of bluish grey, bio-micritic limestone and pale, olive and greyish red shale.
Late Jurassic to Early Cretaceous (Neocomian)		Parh Group	Sembar Formation	Dark brownish grey and light greenish grey Belemnitic shale
Disconformity				
Jurassic		Chiltan Limestone		Dark brownish grey very thick bedded limestone.
Base not exposed				

LITHOSTRATIGRAPHY

The stratigraphic succession (Table 1) in the Zharai area (Fig. 1, Figs. 4 and 5 of Kassi et al. 1999) comprises the Jurassic Chiltan Limestone, Late Jurassic-Sentonian Parh Group (Sembar Formation, Goru Formation and Parh Limestone), the newly discovered and arbitrarily named Campanian-Maastrictian Hanna Lake limestone, Fort Munro Formation and Pab Sandstone; Paleocene-Early Eocene Dungan Formation, Eocene Ghazij Formation and Kirthar Formation, and Miocene-Pliocene Siwalik Group. In addition to these lithostratigraphic units, four depositional breaks (disconformities) have been recognized in addition to the major unconformity between the fluvial succession of the Miocene Nagri Formation of Siwalik Group and the underlying marine succession of the Eocene Kirthar Formation in the nearby Sor Range Syncline and Zarghun Ghar.

The **Jurassic Chiltan Limestone** (HSC 1960, Fatmi 1977), now considered as the Loralai Limestone member (Kazmi 1995, Kazmi and Jan 1997) of the Shirinab Formation (Williams 1959), in the Zharai area is a dark brownish grey to dark grey, thick bedded and massive limestone. It is mostly very finely crystalline, partly oolitic and barely fossiliferous. Its thickness is several hundreds of meters and base is not exposed in the area. Fossils are rare in the Zarai area, however, elsewhere on the basis of its biostratigraphy (Fatmi 1977), it is considered to be of Middle Jurassic age. Its upper contact with the Sembar Formation is not exposed in the Zharai area, however, in the Maree Brewery section of the Quetta area it is disconformable and marked by a well developed oxidation zone (Fig. 2). Numerous rounded, elliptical and concentric concretions, which are associated with oxidation zone in the Maree Brewery

section are present in the stream detritus of the Zharai area near the contact.

The Late Jurassic-Middle Cretaceous **Parh Group** (HSC 1960) has been sub-divided into the Late Jurassic-Neocomian Sembar Formation, Lower Albian-Cenomanian Goru Formation and Berremian-Sentonian Parh Limestone (Table 1). The **Sembar Formation**, which is the lower most unit of the Parh Group, was introduced by Williams (1959) after the Sembar Pass in the Maree-Bugti Hills of the Sulaiman Fold-Thrust Belt. The formation is pale to yellowish brown silty shale with interbeds of siltstone, nodular rusty weathering arenaceous limestone and sandstone. In the lower part sandy shale is present which is rich in Belemnite. Within the Zharai area (Figs. 1, Table 1) the lower part of the formation is not exposed. It comprises brownish grey and light greenish grey glauconitic and belemnitic shale. Elsewhere, beside Belemnites, a rich assemblage of Foraminifera and ammonites have been reported, which suggest a Late Jurassic-Early Cretaceous (Neocomian) age for the Sembar Formation (Williams 1959, Fatmi 1968, 1972, 1977). The Sembar Formation is conformably and transitionally overlain by the Goru Formation.

The **Goru Formation** (Williams 1959) in the Zharai area (Figs. 1, Table 1) comprises interbedded limestone, shale and siltstone with the frequency of the limestone beds increasing upward. The limestone is light to medium grey and olive grey, thin bedded, bio-micritic and sub-lithographic. The interbedded shale and siltstone are grey, greenish grey and maroon coloured, calcareous, hard and splintery. Limestone contains micro-planktonic foraminifers of the *Globotruncana* group. Williams (1959), Fritz and Khan (1967) and Allemann (1979) have recognized Foraminifera from the Bangu Nala in the Quetta region which include *Globigerinelloides, G. breggiensis, G. caseyi, Rotalipora ticinensis, R. appenninica, R. brotzeni* etc., on the basis of which an Early Cretaceous (Albian to Cenomanian) age has been assigned. Its upper contact with the Parh Limestone is transitional and conformable.

The **Parh Limestone** (Vredenburg 1909, Williams 1959) is the prominent white limestone of the Cretaceous succession. It is light grey, white, cream, commonly thin to medium bedded, sub-lithographic, hard and bio-micritic limestone. The formation is laterally persistent and widely distributed throughout the Kirthar and Sulaiman Fold-Thrust Belts. In the Zharai area (Figs. 1, Table 1) upper part of the Parh Limestone contains two dolomitized horizons (330-480 cm thick) which are light brownish grey to reddish brown, medium to thick bedded (15-60 cm). In the field it appears as a well sorted and medium grained sandstone. However, association of red and pink coloured chert nodules with these horizons, which is a well known character of the Parh Limestone, indicate secondary, late diagenetic, partial or complete dolomitization of the upper part of the Parh Limestone. It is interesting to note that the chert nodules, which are the product of diagenetic processes. The chert nodules predate the process of dolomitization which occurred later on, effecting the limestone only and leaving behind the chert nodules fairly intact. The formation in Zharai area is 30-35 m thick. The formation is rich in species of *Globotruncana*. The HSC (1960), Gigon (1962) and Allemann (1979) have identified various types of foraminifera within the Parh Group and assigned a Early to Late Cretaceous (Berremian to Santonian) age to the formation. In Zharai area the upper contact of the Parh Limestone is disconformable with the overlying Hanna Lake limestone. This disconformity is marked by an oxidized lateritic zone present on the irregular erosional surface of the top-most bed of the Parh Limestone (Fig. 2).

The **Hanna Lake limestone** (Kassi et al. 1999) in the Zharai area (Figs. 1, Table 1) is dull brownish grey, thick bedded, finely crystalline (micritic and biomicritic) and argillaceous. Some parts possess very small-size Foraminifera. This lithostratigraphic unit is clearly distinguishable in Bolan Pass, Gwani Nala, Maree Brewery, Hanna Lake and Zharai sections and ranges in thickness from 3-13 m. Within the Zharai area it is 10 m thick. It is partly the lateral equivalent of the Bibai formation of Kazmi (1955, 1979, 1984, 1988, Kassi et al. 1993, Khan 1998, Khan et al. 1998, 1999, 2000) and Mughal Kot Formation (Williams 1959, Fatmi 1977). Its biostratigraphy is yet to be established, however, on the basis of stratigraphic position its age is proposed as Late Campanian to Early Maastrichtian (Kassi et al. 1999, Kassi et al. *in press*). The formation is disconformably underlain by the Fort Munro Formation.

The **Fort Munro Formation** represents the Fort Munro Limestone member of Williams (1959) and Orbitoides Limestone of Eames (1952) and Allemann (1979). The formation consists of dark bluish grey to dark grey, very hard, nodular, micritic and bio-micritic limestone. In Zharai area the formation is composed of dark grey, nodular, orbitoidal limestone (Fig. 1, Table 1). The formation containing various species of *Orbitoides* such as *Siderolites, Daviesina, Sulcoperenlina and Omphalocycles* (Williams 1959, Allemann 1979), which suggest an Upper Maastrichtian age. In Zharai area it is 17 m thick and is disconformably underlain by the Pab Sandstone and the disconformity is marked by a well defined erosional and oxidized surface.

The **Pab Sandstone** was introduced and described by Vredenburg (1908) from the Pab Range within the Kirthar Fold-Thrust Belt, however, it is also widely exposed in the Sulaiman Fold-Thrust Belt. It is normally composed of brownish grey and cream coloured highly mature quartzose sandstone. The Pab Sandstone, although very thin (1-4 m), is present in Zharai and Hanna Lake sections (Figs. 1, Table 1) where sandstone is light brownish grey to cream coloured, fine to very

Figure 2. Photograph showing the disconformable contact between the underlying Jurassic Chiltan Limestone and overlying Upper Jurassic-Lower Cretaceous Sembar Formation in the Maree Brewery section. Note the brownish grey oxidation zone within the contact zone.

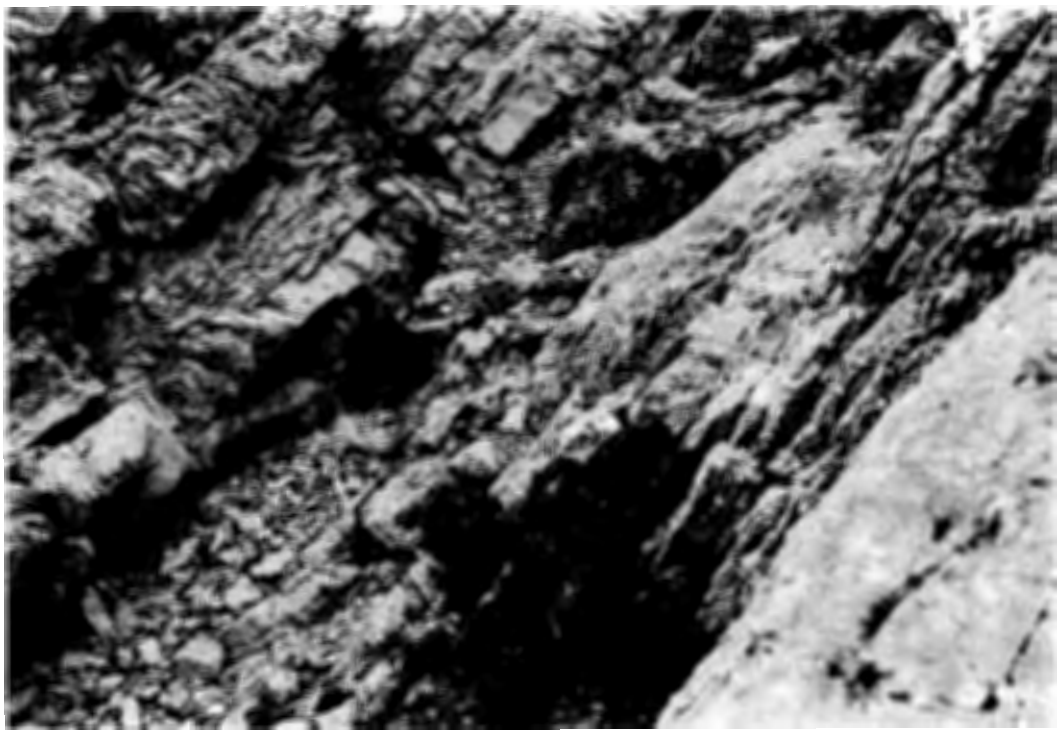

Figure 3. Photograph showing well developed lateritic bed within the disconformable contact between the underlying Parh Limestone and overlying Hanna Lake limestone in Zharai area.

Figure 4. Photograph showing conformable contact between the Habib Rahi limestone member and Sirki shale member of the Eocene Kirthar Formation within the Sor Range Syncline, Zharai area.

Figure 5. Photograph showing close up view of the contact between the Habib Rahi limestone member and Sirki shale member of the Eocene Kirthar Formation within the Sor Range Syncline, Zharai area.

fine grained, well sorted and highly quartzose. Its thickness is 2-4 m in Zharai section and 1-2 m in Hanna Lake section. It pinches out southwestward towards Maree Brewery and Gwani Nala (Kassi et al. 1999, *in press*), however, reappears in Bolan Pass near Dozan Railway Station. On the basis of *Orbitoides* and other foraminifera species (Vredenberg 1908, Williams 1959, HSC 1960) have assigned it an Upper Maastrichtian age. In Zharai area the formation is transitionally and conformably underlain by the Dungan Formation. However, in the Maree Brewery section the formation is missing and the Upper Maastrichtian Fort Munro Formation is directly underlain by the Upper part of the Paleocene Dungan Formation.

The **Dungan Formation** (Oldham 1890, Williams 1959, Fatmi 1977) generally consists of nodular to massive limestone with subordinate marl, sandstone and intra-formational conglomerate. In Zharai area the formation is composed of compact limestone of dark brownish, pinkish grey, brownish grey and buff grey colours which is interbedded with brownish grey shale in lower part. In Zharai section (Figs. 1, Table 1) it is up to 50 m thick and clearly differentiable into **lower part** of brownish grey shale interbedded with light brownish grey nodular limestone and **upper part** of compact limestone. Whereas, the Dungan Formation in Maree Brewery section is only 8 m thick and consists of light grey, compact, hard, thick bedded and highly fossiliferous limestone. The larger foraminiferral assemblage of the formation that comprises *Miscellanea, Alveolina, Glomalveolina, Lockhartia, Ranikothalia, Somalina, Discocyclina, Kathina* suggests its Late Palaeocene-Early Eocene age (Allemann 1979) . As its upper and lower parts are well developed in Zharai area, the age most likely to be Paleocene-Early Eocene. The formation in the Zharai area is conformably underlain by the Ghazij Formation.

The Ghazij Group of Oldham (1890) was re-defined as the **Ghazij Formation** by Williams (1959). Within the Zharai area (Figs. 1, Table 1) the formation consists dominantly shale, sandstone, siltstone, conglomerate, arenaceous limestone and coal seams. Shale is medium light grey, greenish grey and light olive grey, mostly gypsiferous, fissile and carbonaceous. Sandstone is light olive grey, medium grey, light brownish grey and brownish grey. It is moderately to poorly sorted, medium to coarse grained and normally cross-stratified. The arenaceous limestone is light brownish grey with abundant shell fragments. Diversified fauna have been reported from the Ghazij Formation which include Foraminifera, gastropods, bivalves, echinoides, algae, plant fragments, leave prints and vertebrate bones (Eames 1952, HSC 1960, Latif 1964, Iqbal 1966, 1969, Kassi and Kakar 1997, Ginsburg et al. 1999) on the basis of which the formation has been assigned and Early Eocene age. Its upper contact with the Habib Rahi Limestone member of the Kirthar Formation is transitional and conformable.

The **Kirthar Formation** (Noetling 1903, Cheema et al. 1977, Fatmi 1977) is equivalent of the Spintangai Limestone of Oldham (1890). Within the Zharai area (Fig. 1, Table 1) the formation is divisible into the lower **Habib Rahi limestone member** and upper **Sirki shale member** (Fatmi 1977). The Habib Rahi limestone member comprises light pinkish grey and cream coloured, thin to thick bedded, hard, argillaceous limestone (Figs. 4, 5). The upper Sirki shale member is composed of dark brownish grey to chocolate coloured shale interbedded with medium to coarse grained calcareous sandstone. It is highly fossiliferous with abundant mollusks, brachiopods, echinoides and Foraminifera. From the Kirthar Range the HSC (1960) has reported various species of Foraminifera which include *Lepidocyclina dilatata, Nummulites fichteli and N. intermedius*. Also gastropods, bivalves, echinoides and vertebrate remains have been reported by Oldham (1890), Vredenburg (1908), Pilgrim (1940), Eames (1952), HSC (1960), Latif (1964), Meissner and Rehman (1973) and Iqbal (1966, 1969), on the basis of which the formation has been assigned a Middle to Late Eocene age. The formation in the nearby Sor Range Syncline is disconformably underlain by the Nagri Formation of the Siwalik Group.

The Miocene-Pliocene **Siwalik Group** in Balochistan comprises the Nagri, Dhok Pathan and Soan formations, which have been well developed within the Zarghun-Sibi Trough (Table 1). The HSC (1960) and Kazmi and Raza (1970) have named it as the "Sibi Group" and "Urak Group" respectively. Within the Zharai area (Fig. 1, Table 1) only the middle part of the Siwalik Group, i.e. the Nagri and Dhok Pathan formations, have been deposited.

The **Nagri Formation**, which is the second lowermost member of the Siwalik Group, within the Balochistan area has been named as the "Uzda Pusha Sandstone" of the Sibi Group and Urak Group (HSC 1960, Kazmi and Raza 1970). Within the Zharai area (Fig. 1, Table 1) the formation is composed mostly of sandstone with minor conglomerate. Sanstone is fine to very coarse grained, poorly sorted and partly conglomeratic. It is light brownish grey, light olive grey, medium light grey and light greenish grey. A variety of sedimentary structures such as parallel-lamination, cross-lamination, ripples marks, sole marks, load casts and associated flame structures and convolute lamination are commonly present. Rarely intercalations of minor claystone and siltstone are also present. Elsewhere in Zarghun Trough various types of vertebrate bones and wood fossils have been observed (Duperon et al. 1996, Durrani 1997, Durrani et al. 1997a). The Oil and Gas Development Corporation of Pakistan (1965) assigned a Middle to Late Miocene age to the formation. In the Bohr Tangai, Rudgai Basin, Ziarat District, paleomagnetic studies of the Nagri Formation suggest an

age of up to15-16.5 Ma (Duperon et al. 1996, Durrani 1997, Durrani et al. 1997a, Durrani et al. 1997b). In Zharai area the Nagri Formation is conformably and transitionally underlain by the Dhok Pathan Formation.

The **Dhok Pathan Formation** (Cotter 1933) within the Zarghun area is named as the "Shin Matai Shale" of the Sibi Group and Urak Group (HSC 1960, Kazmi and Raza 1970). Within the Zharai area (Fig. 1, Table 1) it is composed of red coloured shale and sandstone. The formation comprises hundreds of metres thick succession of many cycles of alternating claystone and sandstone horizons in which claystone is dominant in proportion. Thickness of the complete sandstone and claystone cycles reach up to several tens of meters. It is moderate brown, whereas, sandstone is greyish orange pink, pale brown and light brown. Sandstone is medium to fine grained, generally well sorted and pebbly at places. Various types of sedimentary structures such as parallel lamination, cross-bedding, ripple marks, sole marks, load casts and convolute bedding are commonly present. Elsewhere a variety of rich vertebrate fauna has been recorded from the Dhok Pathan Formation which include *Indarctos salmontanus, Arctamphicyon lydekkeri, Ictitcherium indicum, Mastodon browni, Dicorhypochoerus titanoides, Pechyportax tatiden,* and *Vardhokpathanesis* (Pasco 1963) on the basis of which an Early to Middle Pliocene age has been assigned. Within the Bohr Tangai section of the Rudgai Basin, Ziarat District, paleomagnetic studies of the lower part of the Dhok Pathan Formation suggest an age of 15 to14.8 Ma (Durrani 1997, Durrani et al. 1997a, Durrani et al. 1997b). Its upper contact with the overlying Soan Formation is not exposed in the study area.

The Pliocene-Pleistocene **Soan Formation**, the Urak Conglomerate of HSC (1960) and Kazmi and Raza (1970), which is the upper most unit of the Siwalik Group, is well developed and thousands of meters thick within the nearby Zarghun Ghar. However, it is not well developed within the Zharai area.

STRUCTURE

The Jurassic-Pliocene succession of the Zharai area and nearby Sor Range Syncline is well exposed along both sides of a thrust which is call here the **Ushbul Thrust** (Figs. 1 and 6). The strata has a general strike of NNW-SSE and dip nearly vertical to overturned. The Jurassic-Paleocene succession (Chiltan Limestone, Parh Group, Hanna Lake limestone, Fort Munro Formation, Pab Sandstone and Dungan Limestone) has been thrusted over the Eocene Ghazij Formation. Succession of the older rocks have been highly deformed, overturned and tightly folded. The south dipping Ushbul Thrust has caused the Cretaceous Parh Group and Paleocene Dungan Formation to overlie the Eocene Ghazij Formation (Figs. 1 and 6). Near the Zharai China the thrust itself is not exposed and the Ghazij and Kirthar formations are highly deformed and overturned. Two kilometers to the northwest of the Zharai China the Parh Group and, at places, the overturned Jurassic Chiltan Limestone directly overlies the Eocene Ghazij Formation (Figs. 1 and 6). Near Zharai China the displacement of the Ushbul Thrust is very minor showing almost normal succession, however, whole of the succession, including the Eocene Ghazij and Kirthar formations in the southern limb of the Sor Range Syncline have been overturned and succession of the Ghazij Formation is highly deformed, crushed and squeezed (Figs. 1 and 6).

The area also possesses a number of wrench faults most of which are oriented in the NE-SW direction. Most of the wrench faults are sinistral while a few are dextral. Out of the six wrench faults mapped in the Zharai area (Fig. 1) only two are dextral. The wrench faults cut across the whole of the Jurassic-Eocene succession including the Ushbul Thrust itself which indicate that the wrench faulting system is a younger feature which occurred later than the folds and thrusts within the final phase of deformation. Some of the wrench faults, such as those near the Ushbul Khand east of the Zharai China (Fig. 1), are large scale showing a left-lateral displacement of up to 800 m.

DISCUSSION

Within the Zharai and surrounding area the rock succession ranging in age from Jurassic-Pleistocene is well exposed. However, it has not been mapped on a larger scale and contain several geological features which have not been reported before.

The Hanna Lake limestone is first time established as a separate lithostratigraphic unit which is a 3-13 m thick and bears distinct lithological characters and stratigraphic position. It is a dull brownish grey limestone which disconformably overlies the upper dolomitized part of the Parh Limestone and disconformably underlies the Fort Munro Formation. In the Zharai area a 10-30 cm thick lateritic horizon is present between the upper most bed of the Parh Limestone and the disconformably overlying Hanna Lake limestone (Fig. 3). On the basis of its distinct characters, stratigraphic position, disconformable upper and lower contacts and fairly tabular form, it has been proposed as a distinct lithostratigraphic unit (Kassi et al. 1999, Kassi et al. *in press*) and the Hanna Lake locality (30°01'E; 67°03N) designated as its type section because of its easily accessible outcrop. The Hanna Lake limestone is exposed at several other outcrops in the Zharai China (29°06'E; 67°06'), Maree Brewery (29°07'E; 66°08'), Gwani Nala (29°01'E; 67°01') and Bolan Pass near Dozan Railway Station. It is partly the lateral equivalent of the Bibai formation (Kazmi 1955, 1979, Kassi et al. 1993, Khan 1998, Khan et al. 1998,1999, 2000) and Mughal Kot Formation (Williams 1959, HSC 1960, Fatmi 1977). However, its lithological

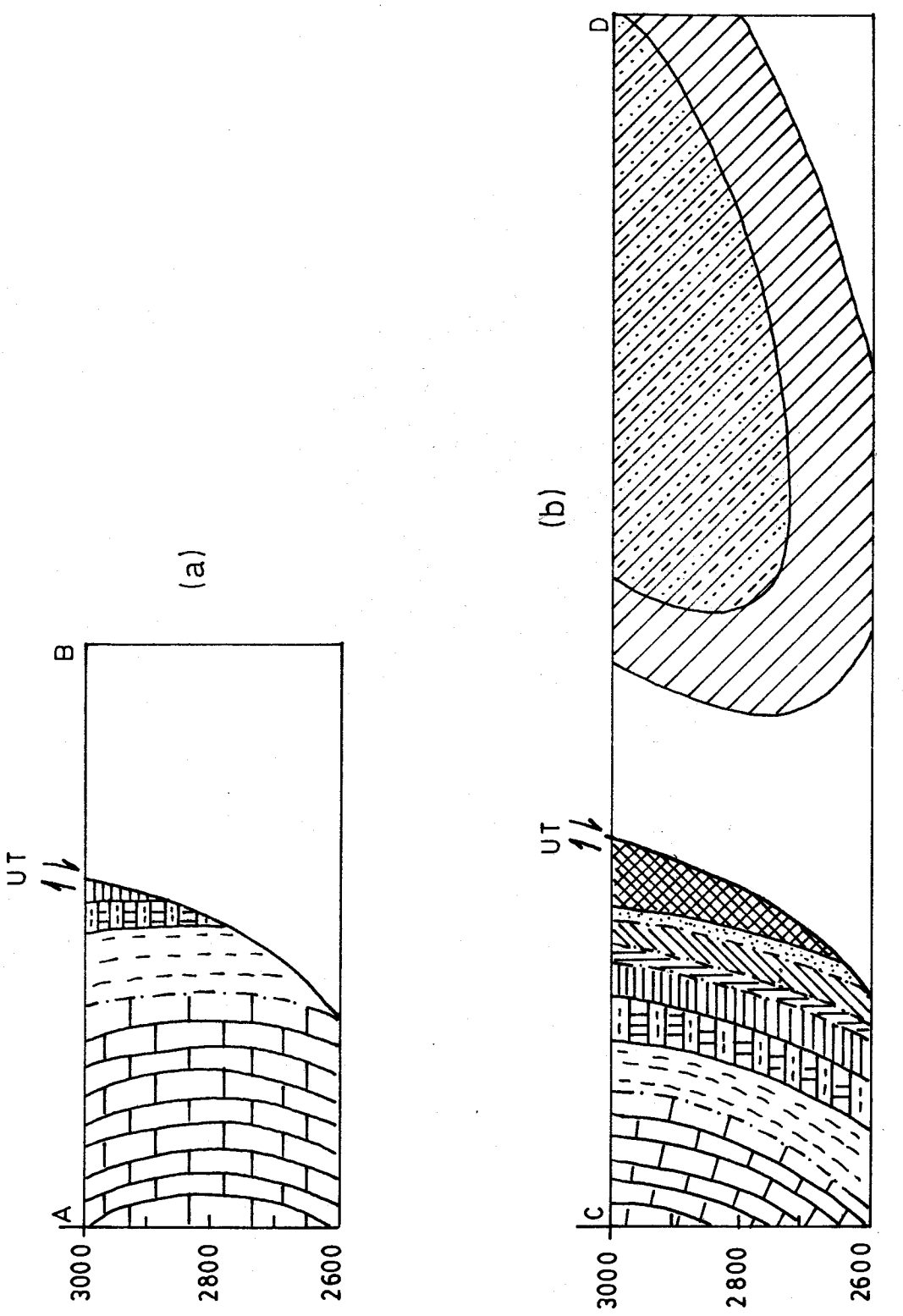

Figure 6. Schematic sections along line A-B and C-D of the of the map area showing position of the Ushbul Thrust (UT). Legend as in Figure 1.

characters are very much different from those of the Bibai and Mughal Kot formations, which mainly comprises shale, mudstone, arkosic and quartzose sandstone, minor proportion of grey argillaceous limestone and basic volcanic rocks and associated volcaniclastic sedimentary succession (volcanic conglomerate, volcanic breccia, sandstone and mudstone) respectively.

Within the Quetta and surrounding area the Maastrichtian Pab Sandstone was never recognized and/or mapped by any worker before. However, the Pab Sandstone, although very thin (only 1-4 m), is clearly distinguishable within the Zharai and Hanna Lake areas. It pinches out to the southwest in the Maree Brewery

section where a disconformity exists between the Maastrichtian Fort Munro Formation and the Paleocene-Early Eocene Dungan Formation (Kassi et al. 1999, Kassi et al. *in press*). Also in the Gwani Nala section, east of the Spezend, the Pab Sandstone is not present, however, it again re-appears in the Bolan Pass area near the Dozan Railway Station.

The two easily distinguishable members of the Kirthar Formation, the Habib Rahi limestone member and the Sirki shale member, are well exposed within the core of the nearby Sor Range Syncline. Previous workers (Mohsin et al.1991) have mapped these units as the Nari and Gaj formations of Oligocene age which is erroneous and misleading because not only its lithological characters resemble with the Sirki Shale member of the Eocene Kirthar Formation but also its Eocene age has been confirmed by the presence of various species of Eocene *Nummulites*, (Kakar 1993, Kassi and Kakar 1997, L. Huttnger and A.A. Butt, pers. Comm.).

Within the Sor Range Syncline the Miocene Nagri Formation and Pliocene Dhok Pathan Formation of the Siwalik Group are also present. However, its upper most unit, the Upper Pliocene-Pleistocene Soan Formation, which is several hundreds of meters thick within the nearby Zarghun Ghar to the north-northeast, has not been developed in the Sor Range Syncline. This stratigraphic contrast reflects its tectonic implications which suggests that the Sor Range Syncline may have been tectonically raised during the Upper Pliocene times after the deposition of the Dhok Pathan Formation further deposition of the Soan Formation during the Upper Pliocene-Pleistocene did not occur in the Sor Range Syncline. The raising of the Sor Range Syncline may have been related to tectonism along the Ushbul Thrust which is a complicated tectonic feature causing progressively thrusting of the succession of the Jurassic Chiltan Limestone, Cretaceous Parh Group and overlying Late Cetaceous-Paleocene strata over the Eocene Ghazij Formation as well as overturning, deformation and squeezing of the incompetent succession of the Eocene Ghazij and Kirthar formations. The whole of the deformed Jurassic-Eocene succession, along with the earlier Ushbul Thrust in turn has been displaced by the wrench faults mostly in a sinistral manner.

CONCLUSIONS

1) The Zharai area comprises the Jurassic-Pliocene succession, which also includes the newly established Campanian to Early Maastrichtian Hanna Lake limestone and first time recognized and mapped Maastrichtian Pab Sandstone. The previously considered Oligocene Nari and Gaj Formations are now mapped and described as the Sirki Shale member of the Eocene Kirthar Formation. Also the Upper Pliocene-Pleistocene Soan Formation of the Siwalik Group, which is well developed within the nearby Zarghun Trough, has not been deposited in the Sor Range Syncline, which implies that the Sor Range Syncline might have been raised tectonically prior to deposition of the Upper Pliocene-Pleistocene Soan Formation causing termination of its deposition within the Sor Range Syncline.

2) The area comprises interesting structural features like the NNW-SSE trending Ushbul Thrust which have caused the older Jurassic-Cretaceous succession to overlie the Eocene Ghazij Formation and overturn the Jurassic-Eocene and younger succession within the Zharai area and nearby Sor Range Syncline. Several NE-SW trending wrench faults, mostly sinistral, have in turn laterally displaced the Jurassic-Eocene succession as well as the Ushbul Thrust itself during a later deformation.

REFERENCES

Allemann, F., 1979. Time of emplacement of the Zhob Valley Ophiolites and Bela Ophiolites, of Balochistan, *In* Farah, A. and DeJong, K. A., (eds.), Geodynamics of Pakistan: Geological Survey of Pakistan, Quetta, p. 215-242.

Bender, F. K. and Raza, H. A., (eds.), 1995. Geology of Pakistan: Gebruder Borntreager, p. 11-22.

Cheema, M. R., Raza, S. M. and Ahmad, H., 1977. Cenozoic: *In* Shah, S. M. I. (ed.), Stratigraphy of Pakistan: Geol. Surv. Pakistan, Quetta, Mem., 12, p. 56-98.

Cotter, G. de P., 1933. Geology of part of the Attock District, west of Longitude 72° 45' E: India Geol. Surv. Mem., 55, p. 63-161.

Duperon, J., Laudoueneix, M.D. and Durrani, K.H., 1996. Occurrence of *Bombacoxylon owenii* (Carr.) Gottwald *In* Cenozoic of Pakistan - History and importance of this species: Palaeontographica Abt.Stuttgart. B, 239, Lfg. 1-3, p. 59-75,

Durrani, K. H., 1997. Estude Stratigraphique et Sedimentologique du "Siwaliks" Dans La Region de Zarghun, Quetta, Balochistan, Pakistan: Ph.D thesis (Mem. no. 17/1997), University of Orleans, France (unpubl.).

Durrani, K. H., Kassi, A. M. and Kakar, D. M., 1997a. Siwaliks of the Zarghun-Rudgai area east of Quetta, Pakistan: Acta Mineralogica Pakistanica, 8, p. 106-109.

Durrani, K.H., Yan, C. Courme, M.D. and Kassi, A.M., 1997b. Age determination of Rudgai-Sibi basin (NE Balochistan, Pakistan. a preliminary magnetostratigraphic study and its tectonic implications: Earth and Planetary Sciences, 325, p. 11-18.

Eames, F. E., 1952. A contribution to the study of Eocene in Western Pakistan and Western India: Part A, The Geology of Standard Section in the Western Punjab and in the Kohat District: Part B, Description of the Faunas of certain Standard Sections and their bearing on the classification and correlation of the Eocene in Western Pakistan: Quart. Jour. Geol. Soc. London, 107, Pt. 2, p. 159-200.

Fatmi, A.N., 1968. The paleontology and stratigraphy of the Mesozoic rocks of the western Kohat, Kalachitta, Hazara and Trans-Indus Salt Ranges, West Pakistan. Ph.D. thesis (Unpubl.), Univ. Wales, 409p.

Fatmi, A.N., 1972. Stratigraphy of the Jurassic and Lower Cretaceous rocks and Jurassic ammonites from the northern areas of West Pakistan: Bull (Geol.) British Museum Natural History, 20, 7: p. 299-380.

Fatmi, A. N., 1977. Mesozoic: *In* Shah, S. M. I., (ed.), Stratigraphy of Pakistan: Geol. Surv. Pakistan, Mem., 12, p. 28-56.

Fritz, E. B. and Khan, M. R., 1967. Cretaceous (Albiab-Cenomanian) planktonic Foraminifera in Bangu Nala, Quetta Division, West Pakistan: U. S. Geol. Surv. Proj. Rept. Washington. (IR), PK-36, 16p.

Gigon, W. O., 1962. Upper Cretaceous Stratigraphy of the Well Giandari-I and its correlation with the Sulaiman and Kirther

Ranges, West Pakistan - E. C. A .F. Symp. Dir. Petrol. Res., Asia and Far East,Tehran. p. 248-282.
Ginsburg, L., Durrani, K.H., Kassi, A.M. and Welcomme, J.P., 1999. Discovery of a new *Anthrchobbunidae* (Tethytheria, Mammalia) from the Lower Eocene lignite of Kach-Harnai area in Balochistan, Pakistan: Earth and Planetary Sciences. 328, p. 1-5.
Hunting Survey Corporation, 1960. Reconnaissance Geology of part of West Pakistan: A Colombo Plan Cooperation Project, Toronto, Canada. 550 p.
Iqbal, M. W. A., 1966. Mega-Fauna from the Ghazij Shale (Lower Eocene), Quetta - Shahrig area, West Pakistan: Geol. Surv. Pakistan Mem., 7, 45p.
Iqbal, M. W. A., 1969. Mega-fauna from the Ghazij Formation (Lower Eocene), Quetta-Sharigh Area, West Pakistan: Geol. Surv. Pak. Mem. Palaeontlogica Pakistanica, 5, 27p.
Kakar, D. M., 1993. Structure and sedimentology of the coal-bearing Ghazij Formation, Sor Range area, Quetta District, Pakistan: M. Phil thesis, Centre of Excellence in Mineralogy, University of Balochistan, Quetta (unpubl.)
Kassi, D. M. and Kakar, A. M., 1997. Lithostratigraphy, sedimentology and petrology of the Ghazij Formation, Sor Range area, Quetta District, Pakistan: Acta Mineralogica Pakistanica, 8, p. 73-85.
Kassi, A. M., Khan, A. S., Kakar, D. M., Qureshi, A. R., Durrani, K. H. and Khan, H., 1993. Preliminary Sedimentology of part of the Bibai Formation, Ahmadun-Gogai Area, Ziarat District, Balochistan: Geol. Bull. Punjab Univ., 28, p. 73-80.
Kassi, A. M., Kakar, D. M., Khan, A. S. and Umar, M., 1999. Lithostratigraphy of the Cretaceous-Paleocene succession in Quetta region, Pakiatan: Acta Mineralogica Pkistanica, Vol. 10, p. 1-9.
Kassi, A. M., Khan, A. S., Khan, A. T., Kakar, D. M. and Farooqui, M. A. (*in press*): Lateral variations within the Upper Cretaceous - Paleocene succession, Quetta-Ziarat region, Western Sulaiman Belt, Pakistan, and their tectonic implications: Geologica Vol. 5.
Kazmi, A. H., 1955. Geology of the Ziarat-Kach-Zardalu area of Balochistan: D.I.C. thesis, Imperial College of Science and Technology, London (unpubl.), 157 p.
Kazmi, A. H., 1979. The Bibai and Gogai Napes in the Kach-Ziarat area of northeastern Balochistan: *In* Farah, A. and DeJong, K. A., (eds.), Geodynamics of Pakistan: Geological Survey of Pakistan, Quetta, p. 333-340.
Kazmi, A. H., 1984. Petrology of the Bibai Volcanics, northeastern Balochistan: Geol. Bull. Univ. Peshawar, 17, p. 34-51.
Kazmi, A. H., 1988. Stratigraphy of the Dungan Group in Kach-Ziarat area, northeastern Balochistan: Geol. Bull. Univ. Peshawar, 21, p. 117-130.
Kazmi, A. H., 1995. Sedimentary Sequence: *In* Bender, F. K. and Raza, H. A., (eds.), Geology of Pakistan: Gebruder Borntraeger, 414 p.
Kazmi, A.H. and Jan, Q., 1997. Geology and tectonics of Pakistan: Graphic Publishers, Karachi. 500 p.
Kazmi, A. H. and Raza, S. Q., 1970. Water supply of Quetta Basin, Balochistan, Pakistan: Geol. Surv. Pak. Quetta. Recs. 20, Pt. 2, 114 p.
Khan, A.T., 1998. Sedimentology and petrology of the volcaniclastic rocks of the Bibai formation, Ziarat District, Balochistan, Pakistan: Ph.D. thesis (Unpubl.), Centre of Excellence in Mineralogy, University of Balochistan, Quetta.
Khan, A.T., Kassi, A.M. and Khan, A.S., 1998. Volcaniclastic sediments of the Upper Cretaceous Bibai Formation, Kach-Ziarat valley, Balochistan: Acta Mineralogica Pakistanica, 9, p. 117-22.
Khan, A.T., Khan, A.S. and Kassi, A.M., 1999. Petrology, geochemistry and provenance of the volcanic conglomerate and sandstone of the Upper Cretaceous Bibai formation, Kach-Ziarat valley, Balochistan: Acta Mineralogica Pakistanica, 10, p. 103-123.
Khan, A.T., Kassi, A.M. and Khan, A.S., 2000. The Upper Cretaceous Bibai Submarine Fan (Bibai formation), Kach-Ziarat valley, western Sulaiman Thrust-Fold Belt, Pakistan: Acta Mineralogica Pakistanica, 11, p. 1-24.
Latif, M. A., 1964. Variation in abundance and morphology of pelagic Foraminifera in the Paleocene-Eocene of the Rakhi Nala, West Pakistan: Punjab Univ. Geol. Bull., 4, p. 29-109.
Meissner, C. R. and Rahman, H., 1973. Geological map and cross-section of the Kohat-Quadrangle, Pakistan, Scale 1: 250,000: U.S. Geol. Surv. Pak. Prof., 716-D.
Mohasin, A. K., Asif, N. R., Memon, A.R., Saleem, M. and Khan, A.L., 1991. Coal resources of the Sor Range Block, Sor Range-Degari Coal Field, Balochistan, Pakistan: Inf. Release Geol. Surv. Pakistan. No. 463.
Noetling, F., 1903. Ubergang zwischen Kreide und Eozan in Balochistan: Centralbl. Mineral. Geol. Palaeont., (Schweizerbart) Stuttgart, 4, p. 514-523
Oldham, R. D., 1890. Report on the geology and economic resources of the country adjoining the Sind-Pishin railway between Sharigh and Spintangi and the country between it and Khattan: India Geol. Surv. Recs., 23, Pt. 3, p. 93-109.
Pilgrim, G.E., 1940. Middle Eocene mammals from northwest India: Zool. Soc. Lond. Proc. Ser. B., 110, 1-2: p. 127-152.
Vredenburg, E. W., 1908. The Cretaceous Orbitoides of India: Geol. Surv. India Recs., 36, p. 171-213.
Vredenburg, E. W., 1909. Mollusca of the Ranikot Series - introductory note on the stratigraphy of Ranikot Series: Geol. Surv. India Mem. Paleont. Indica, New Series, 3 (1), p. 5-19.
Williams, M. D., 1959. Stratigraphy of the Lower Indus basin, West Pakistan: Proc. 5th World Petroleum Congress, New York, Sec. 1, 19, p. 337-391.

Manuscript received January 25, 2001
Revised Manuscript received March 15, 2001
Accepted March 17, 2001

ACTA MINERALOGICA PAKISTANICA
Volume 11 (2000)

Article Reference AMP11.2000/105-118/ISSN0257-3660

AGE AND TECTONIC SETTING OF THE RAS KOH OPHIOLITES, PAKISTAN

EDWIN GNOS[1], MEHRAB KHAN[2], KHALID MAHMOOD[2], IGOR MARIA VILLA[3] AND ABDUL SALAM KHAN[2]

[1] Mineralogisch-Petrographisches Institut, Baltzerstrasse 1, 3012, Bern, Switzerland
[2] Centre of Excellence in Mineralogy, University of Balochistan, Quetta, Pakistan.
[3] Mineralogisch-Petrographisches Institut, Gruppe fur Isotopengeologie, Erlachstrasse 9a, 3012 Bern, Switzerland.

ABSTRACT

The serpentinized peridotites with preserved subophiolitic metamorphic sole present in the Ras Koh Range, Pakistan, were identified as relics of an ophiolite nappe emplaced onto a Jurassic/Cretaceous island are sequence Initial emplacement was dated with hornblendes from the metamorphic soles at 108.7±0.3 Ma to 111.0±1.0 Ma ($^{39}Ar/^{40}Ar$.). The final emplacement onto the island arc sequence occurred between Campanian and Paleocene, and was followed by accretion of the island arc to the Eurasian plates and subaereal exposure of the ophiolite. Both the ophiolite and the Paleocene/Eocene sedimentary cover were intruded by calcalkaline to subalkaline tonalite-diorite-gabbro magmas, related to north-directed subduction magmatism A biotite and hornblende separate from the main intrusions yielded argon isochrone ages of 46.0±0.5 and 48.4±1.2 Ma. Due to its analogies, the Ras Koh range is viewed as the western, less eroded continuation of the Spin Boldak-Kohistan-Ladakh-Tibet island arc offset by ~800 km along the Chaman-Nushki fault system during the India-Eurasia collision. Uplift of the Ras Koh range started in Late Oligocene/Miocene and was caused by extrusion of the Helmand Block and shortening in he region west of the Chaman fault. This translated into southward thrusting and ramping of the Ras Koh range, possibly over a hidden micro continental block located beneath the Hamun-I-Maskhel depression.

INTRODUCTION

Ophiolites mark boundaries between different continental plates and/or island arcs, and their emplacement indicates the time point of large scale tectonic reorganization. Dating of metamorphic rocks from the basal shear zone below ophiolites gives the age of initial intra oceanic thrusting (subduction), and the obtained cooling ages overlap with age results from the crustal sequence of the ophiolite (e.g. Hacker et al. 1996). Shear sense determination in the basal peridotite mylonites allows reconstruction of emplacement direction (e.g. Boudier et al. 1982). Initial thrusting of an ophiolite nappe over the continental edge is manifested by the formation of a foreland basin (e.g. Robertson et al. 1987) and may be associated with shelf collapse (e.g. Beck et al. 1996). The final ophiolite obduction is bracketed by the youngest sediments underlying the ophiolite nappe, and the youngest sedimentary rocks overlying the ophiolite. The time lapse between initial and final emplacement is typically in the order of 10-20 Ma (e.g. Hacker et al. 1996), indicating that closure of a large ocean like the Neo-Tethys is associated with multiple switching from choked to new subduction zones.

The relictic ophiolite studied here is located in the

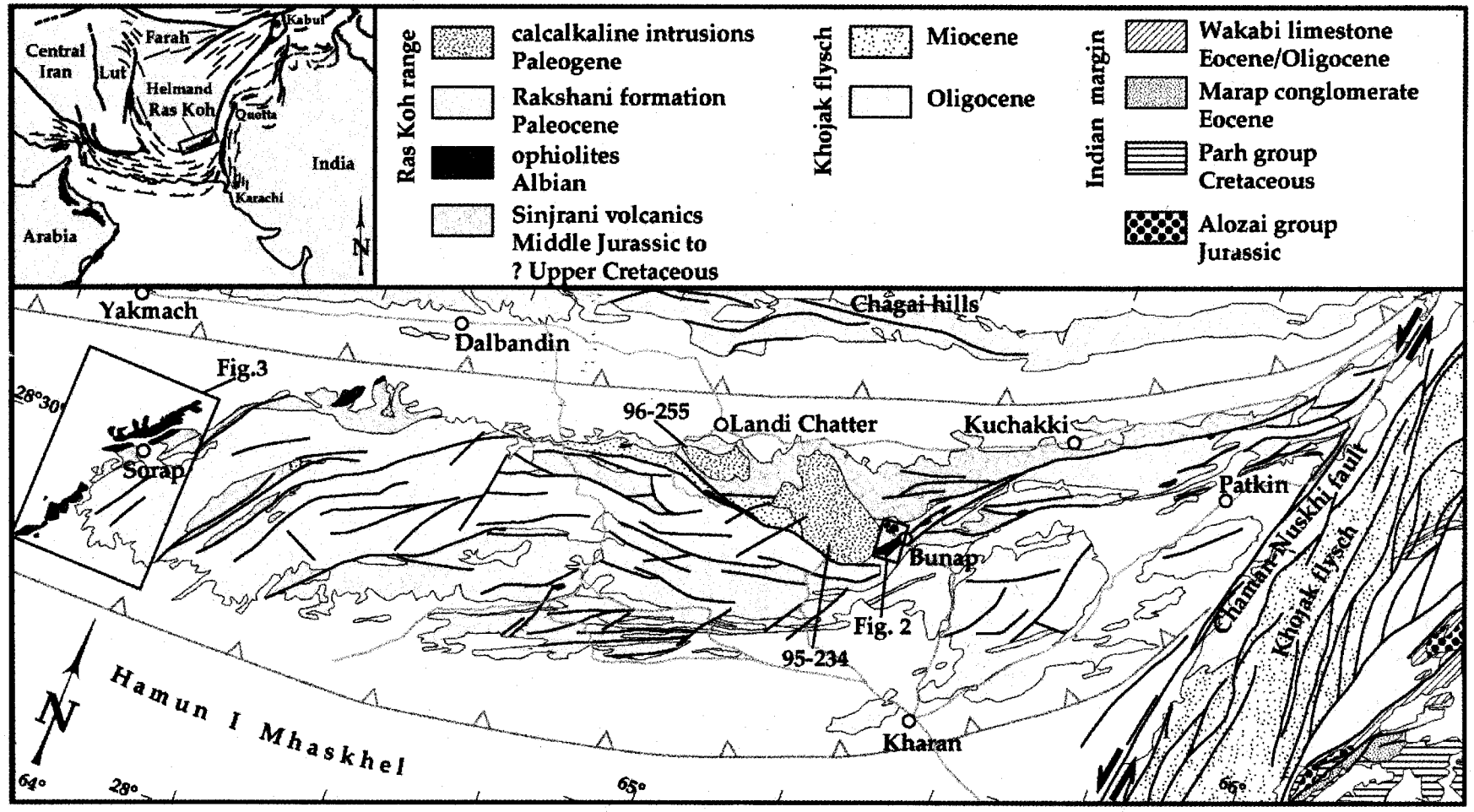

Figure 1. Overview map of the Ras Koh range, based on Hunting Corporation (1960) and Bakr (1964). For location of the range see the inset. Note the steep, north dipping foliation paralleling the main fault system and generel trend of the range. A second fault system is parallel to the sinistral Chaman- Nushki fault system which separates the Ras Koh Range from the Oligocene/ Miocene Khojak flysch and elements of the Indian passive margin. All main structures are related to Himalayan tectonics. The two sample numbers locate the dated plutonic rock samples.

Ras Koh range in Balochistan, Pakistan. This range forms a topographic high (up to 3000 m) located at the northern rim of the Hamun-I-Mashkhel depression and south of the active volcanic arc in the Chagai hills of the Helmand Block (Fig. 1). The Ras Koh and Chagai ranges are separated by the Dalbandin trough which provides the main connection between Quetta and the Iran (Fig. 1). The Ras Koh range bends at its eastern end north into the active Chaman-Nushki left lateral strike slip fault. At its western end it disappears below the sands of the Hamun-I-Mashkhel basin.

Several authors proposed that the southern part of the Makran is an exceptional example where oceanic crust is uplifted due to the underplating of thick flysch material and crustal shortening (e.g. Jakob and Quittmeyer 1979, Pavlis and Bruhn 1983). However, it rests unclear if there are hidden micro continental blocks below the central or northern part of the Makran flysch as it was observed in Iran (McCall and Kidd 1982). The later is supported by the fact that the arc-trench gap between the subduction zone in the Gulf of Oman and the active arc in the Chagai Hills is conspicuously wide, and where normally a forearc depression develops, stands the Ras Koh range with its mountains exceeding the altitude of the active arc.

Although some gravel roads enter the range, many areas are not accessible by car and access tracks to the western end of the range are continuously covered by moving sand dunes.

GEOLOGY OF THE RAS KOH RANGE

The geology of parts of the eastern Ras Koh range was described by Vredenburg (1901). He recognized volcanic material, Cretaceous to Eocene sedimentary rocks and Eocene or younger igneous intrusions crosscutting the marine strata. A more detailed study was published by Bakr (1958, 1962, 1964) who produced an excellent 1:100'000 geologic map of the western half of the range. Bakr's (1964) work includes a stratigraphic correlation chart between his own formation names and those of Hunting Survey Corporation (1960) who used different formation names. Hunting Survey Corporation (1960) produced three 1:250'000 overview maps covering the whole Ras Koh range (Hunting Survey Corporation and Geological Survey of Pakistan 1958a, 1958b, 1958c). Hunting Corporation (1960) also newly defined the calcalkaline Cretaceous Kuchakki volcanic group consisting of andesitic agglomerates, lavas and tuffs, the Bunap ultramafic intrusions, the Paleocene Rakshani Formation, the Eocene Kharan limestone and the late Eocene Pishi Formation. According to the models of that time, Hunting Corporation (1960) and Bakr (1964) considered the Bunap peridotites as magmatic intrusions related to the tonalites and diorites which intrude the Paleocene Rakshani formation. Their suggested Eocene or younger peridotite intrusion age is thus obviously too young. Because many of the formations were stratigraphically not well defined, Shah (1977) merged the Kuchaki volcanic group with the Sinjrani volcanic group exposed in the Chagai hills, and redefined the Kharan limestone and the Pishi Formation as parts of the Kharan Formation. However, few work has been published using the recommended newer stratigraphic names and some correlations remain questionable. For consistency, in this study we have used the nomenclature of Hunting Surv. Corp. (1960).

The high topography of the Ras Koh range is relatively young, and was caused by south-west extrusion of the Helmand block along the Chaman-Nushki and the Harirud faults in middle Oligocene, and ramping along a series of north-dipping faults (e.g. Bannert, et al. 1992). One of these thrusts is probably located along the southern boundary of the Ras Koh range largely obscured by the sands of the Balochistan desert. Recent tectonic activity along the south-eastern rim of the range was shown by Nakata et al. (1991).

The whole Ras Koh range shows schistosity paralleling the main fault/thrust system and the trend of the range. Sericite schists are typical developed in he Rakshani Formation in the central and eastern part of the range. Metamorphism and deformation are weaker in the western parts of the range.

KUCHAKKI FORMATION

The Kuchakki Formation is the oldest unit exposed in the Ras Koh range (Fig. 1). It includes basaltic to andesitic pillow lavas and flows, agglomerates and volcanic conglomerates, tuffs, cherts and limestone lenses (Hunting Survey Corporation 1960). This survey assumed an Late Cretaceous age of the Kuchakki Formation as determined for the Sinjrani volcanic group of the Chagai arc. Siddiqui et al. (1995) studied radiolarian cherts of the Kuchakki formation and found Middle Jurassic to Late Cretaceous radiolarian assemblages; they proposed that one assemblage could be as young as Early Coniacian to Early Santonian. Since the ophiolites were thrusted over the Kuchakki formation exact dating of the youngest sedimentary rocks beneath the ophiolite would constrain the final emplacement of the ophiolite.

A recent chemical study by Siddiqui et al. (1996) revealed that the volcanic rocks of the Kuchakki formation have tholeiitic chemistry with an island arc signature.

RAS KOH OPHIOLITES

Two main ophiolite areas can be distinguished in the Ras Koh range. These are the strongly serpentinized harzburgite outcrorps in the Bunap area and the fairly weathered outcrops in the Sorap area at the western end of the range (Fig. 1). Many small serpentinite outcrops occurring dispersed over the range are similar to the Bunap serpentinites. Most outcrops are fault/thrust

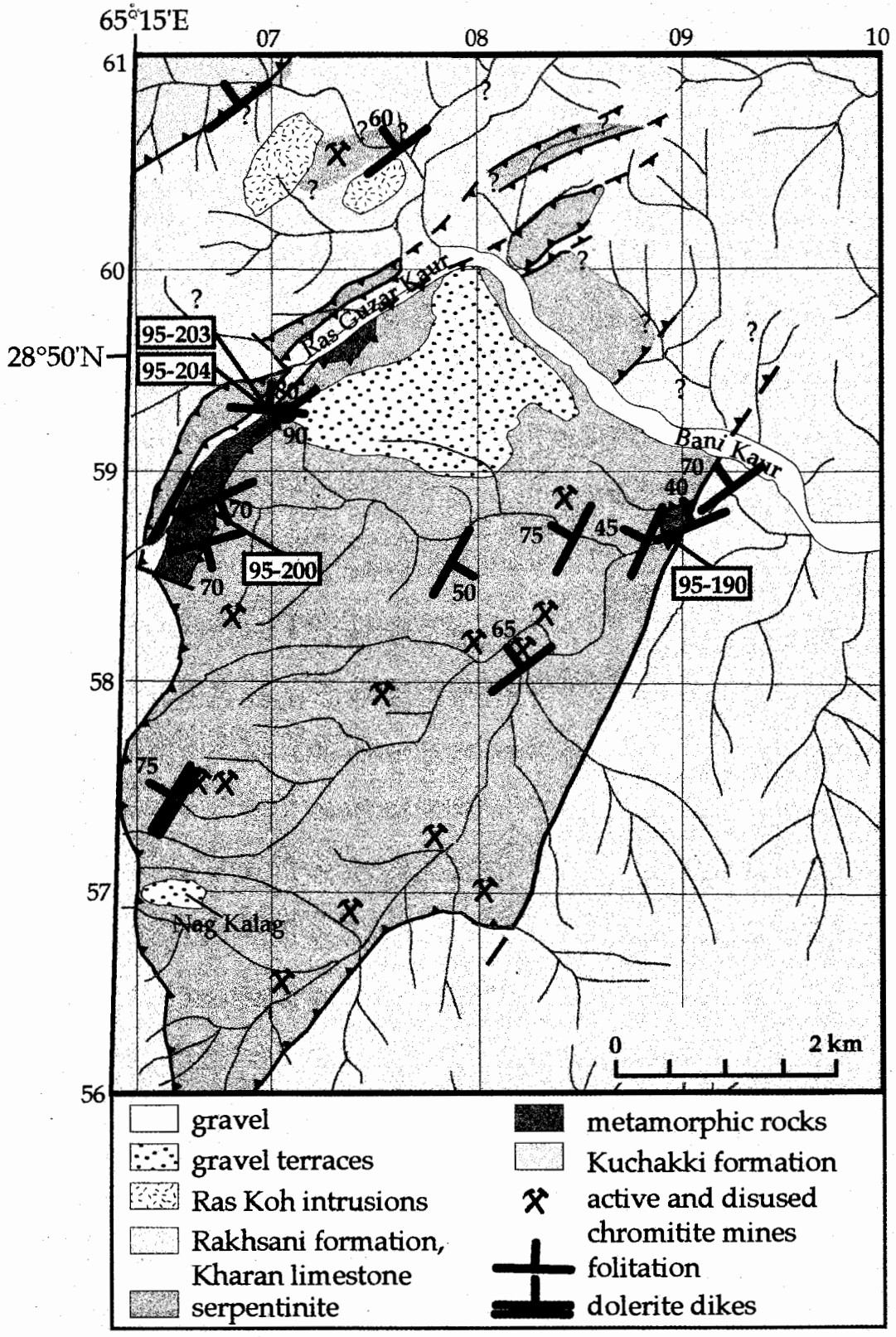

Figure 2. Geological map of the main ultramafic body of the Bunap area. For location see Fig.1. The ophiolite forms the central part of a syncline bordered on both sides by subophiolitic metamorphic rocks, which become dissected by normal faults. The numbers locate the dated metamorphic sole samples.

bound and occur aligned along faults paralleling the main trend of the range. Red conglomerates containing basalt and chert pebbles occur associated with the serpentinites at several localities and indicate Late Cretaceous subaereal exposure and weathering of the ophiolite before the deposition of the (?)Maastrichtian-Paleocene siliciclastic Rakshani formation. These undated red conglomerates are for example exposed at the following coordinates: 29°09.22'/65°42.62; 29°04.62/65°40.56; 28°48.54'/65°15.58'.

BUNAP AREA

The ophiolite outcrops of the Bunap area (earlier Bunap intrusion; Hunting Survey Corporation 1960) consist of strongly faulted, folded ad nearly completely serpentinized harzburgites which contain(ed) small chromitite deposits (Fig. 2). Low-grade (~34%), massive chromite ore is presently mined at one locality north of the main massif (Fig. 2) At some localities dunite/ harzburgite banding may be recognized. The peridotites were intruded by dm to meter sized doleritic dikes, and some dikes underwent transformation into amphibolites in an early stage. The dikes became folded, boudinage, and partially or completely rodinitized during the serpentinization. The largests peridotite outcrop in the Bunap area forms the core of a syncline (Fig. 2), bordered on both sides by metamorphic sole rocks and the Kuchakki formation. A description of smaller outcrops to the east of the study area was published by Siddiqui et al. (1995). Most other serpentinite outcrops are fault-bound, and exposures occur concentrated along a line extending from the Patkin over Bunap to the Landi Chatter area (Fig. 1). Locally (e.g. N 28°33.47; E 64°44.43') pillow lavas are found associated with the serpentinite outcrops. The relationship between the two rests unclear and it is possible that the pillow lavas are part of the underlying Kuchakki formation.

Although subophiolitic metamorphic soles are well exposed at three localities north and south of the main Bunap ophiolite massif (Fig. 2), mylonitic peridotites normally present at the base of ophiolite napes, have only been recognized at two localities. Samples from these localities were completely serpentinized and lineation and shear sense (emplacement direction) could not be determined. The largest metamorphic sole sequence is found at the northern end of the main serpentinite outcrop where it locally also contains garnet-diopside amphibolites and medium to coarse grained dark amphibolites. The amphibolites at the contact to the peridotite underwent rodingitization and silicification and commonly form an approximately half a meter thick out weathering band. Some amphibolite layers contain biotite/phlogopite or muscovite.Most of the outcrop area consists of banded black to greenish amphibolites with up to 2m thick inlayers of banded impure calcite-marbles and cm to m-sized layers of quartzo-feldspatic and quartz-muscovite gneisses. With exception of a few small slivers all preserved metamorphic rocks indicate amphibolite/granulite facies peak metamorphic assemblages.

Three amphibolite and one muscovite bearing quartzo-feldspatic rock from these metamorphic soles were selected for $^{39}Ar/^{40}Ar$ analysis. The locations are indicate in Fig. 2.

SORAP AREA

Ophiolitic outcrops at the western end of the Ras Koh range cover the transition from upper mantle to lower crustal section of an ophiolite sequence. We found harzburgites, dunites, large conspicuous serpentinized wehrlitic intrusions and some small, outcrops of isolated layered gabbros in the sand dunes at the northern end of the massif (Fig. 3). The mantle/curst transition zone (Moho), is nowhere exposed. Low-grade disseminated to nodular chromitite ore is presently mined at three localities (Fig. 3). Since neither metamorphic sole nor the upper parts of a classic ophiolite sequence (Participants 1972) were found we can only assume from its similar tectonic position above the Kuchakki volcanics that the outcrops of the Sorap area are the tectonically less affected equivalents of the Bunap ophiolite. Gabbroic outcrops similar to the Sorap area are also present at the northern border of the range southwest of Dalbandin (Bakr 1964; Fig. 1). We could not find any suitable lithology for 39Ar-40Ar dating.

THE LATE CRETACEOUS? - PALEOCENE RAKSHANI FORMATION

The siliciclastic Rakshani formation consists according to Hunting Survey (1960) of shales, sandstones and subordinate conglomerates and limestones of marine origin. Volcanic material is also common. This formation covers the Kuchakki formation and the Ras Koh ophiolite. Conglomerate layers indicate erosion from nearby highs and most of the materials that compose the shales and sandstones derived probably from a northern source (Helmand Block).

$^{39}Ar/^{40}Ar$ DATING

Three hornblendes and one muscovite concentrates from the Bunap metamorphic soles (Fig. 2) and an amphibole and biotite concentrate from the Ras Koh intrusions (Fig. 1) were pre-separated magnetically and gravimetrically, and the concentrates handpicked. The samples were step-heated in a double-vacuum resistance oven connected to a MAP 215-50 mass spectrometer at Berne University using Taylor Creek sanidine(Duffield and Dalrymple 1990) as monitor. Age results are summarized in Table 1 and are graphically displayed in Fig. 4 and 5

The ophiolitic sample least affected by alteration is hornblende concentrate 95-203 (Fig. 4) which gave a plateau age of 108.7±0.3 Ma and an isochron age of

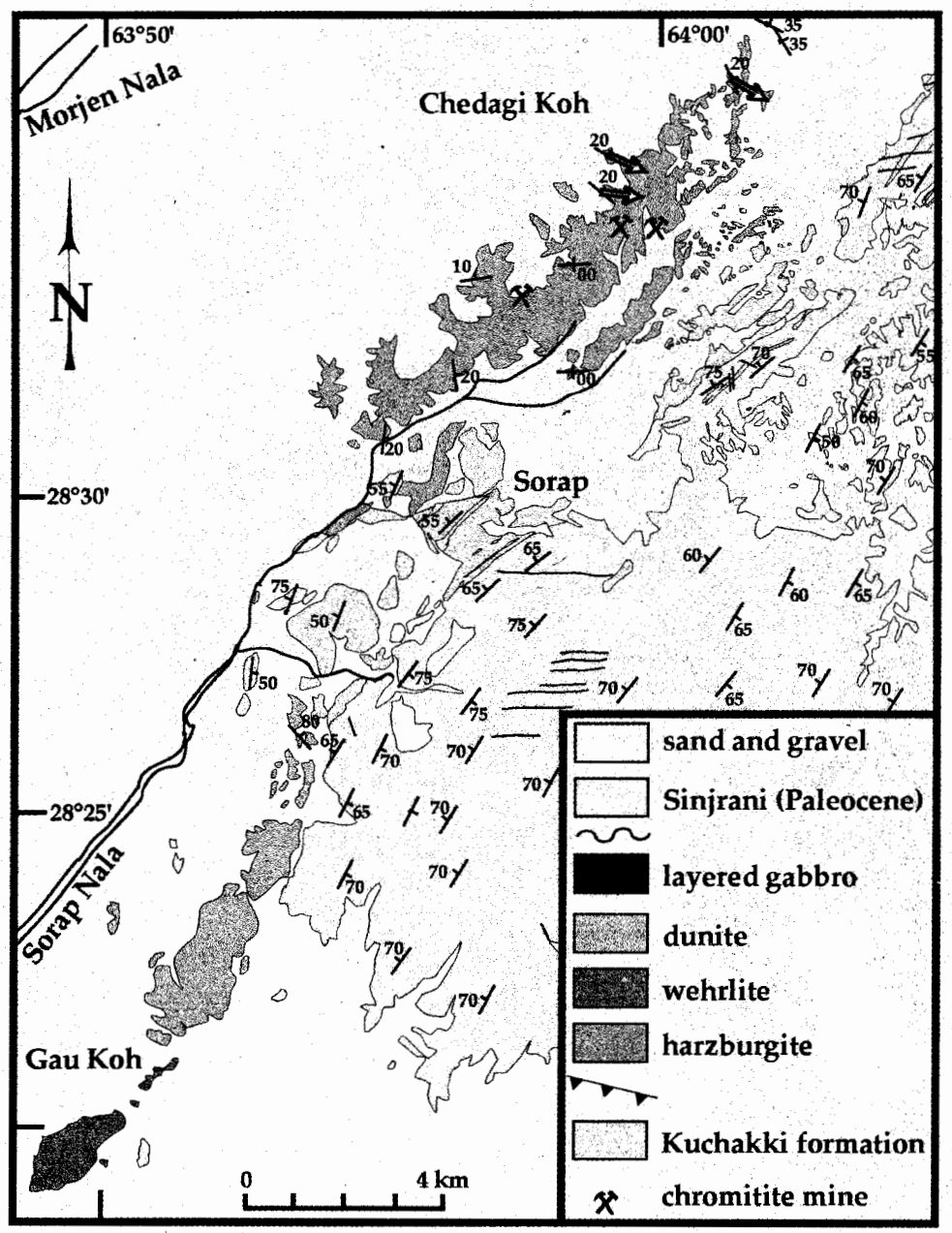

Figure 3. Geological map of the Sorap massif at the western end of the Ras Koh range. For location see Figure 1. Note the structural trend in the well preserved peridotites and layered gabbros (two small outcrops at the northern end) which is completely independent from the regional trend.

Table 1. **$^{39}Ar/^{40}Ar$ results of metamorphic minerals from the Bunap subophiolitic metamorphic sequence.**

Sample	Mineral	Latitude	Longitude	Ar* [ml/g]	K[Wt%]	Ca[Wt%]	Al[ppm]	t Pri[Ma]
EG95-190	Hornblende	28° 29.72'	65° 16.77'	3.3447E-08	0.20	4.46113	6	~110
EG95-200	Hornblende	28° 49.55'	65° 15.04'	2.2664E-08	0.18	4.46433	15	111.0±1.0
EG95-203	Hornblende	28° 49.83'	65° 15.26'	5.6650E-08	0.31	4.61694	20	108.7±0.3
EG95-204	Muscovite	28° 49.83'	65° 15.26'	1.7909E-07	2.76	0.90915	19	~110-116

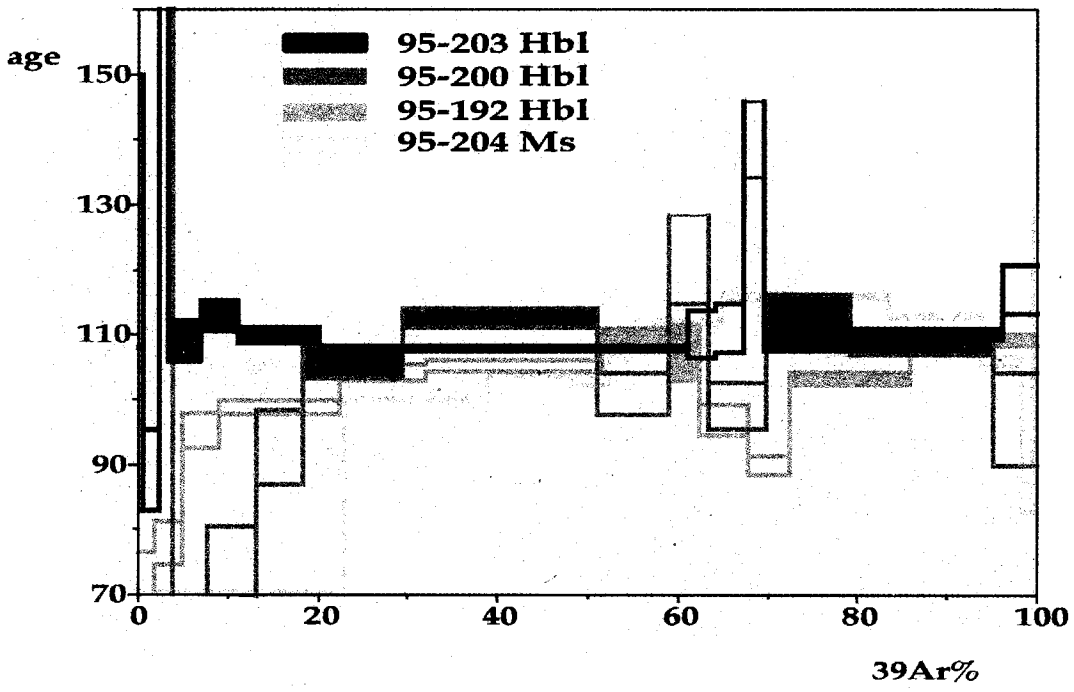

Figure 4. Age spectra of amphiboles and white mica from the metamorphic sole rocks of the Bunap area. See Figure 2 for location.

107.5±0.9 Ma with an initial $^{40}Ar/^{36}Ar$ of 299±3

The spectra of amphiboles 95-2000 and 95-192 (Fig. 4) both are internally discordant; the chemical information on Ca CI and K from the Ar isotopes (cfr. Boriani and Villa 1997) shows that both analyzed concentrates were chemically heterogeneous, and consisted of a primary amphibole formed around 110 Ma and a second-generation (alteration) phase formed around 70-80 Ma.

The muscovite concentrate 95-204 (Fig. 4) yielded a convex shaped age spectrum with the oldest steps at 116 Ma. Such spectra are typical for white mica mixtures (Wijbrans and McDougall (1986). As the oldest steps (116 Ma) give a similar age as the amphiboles, it is possible that primary white mica grew during the formation of the sole (possibly incorporating some excess Ar). The very low K content of 2.79% clearly shows that the muscovite was altered; the Ca-Cl-K correlation systematics point to several different alteration phases. It may be possible that one alteration episode was related to deformation during a late stage of ophiolite emplacement, and a subsequent one (t<70 Ma) to subaerial weathering.

The two mineral concentrates from the Ras Koh intrusions yielded homogeneous spectra (Fig. 5). Amphibole concentrate 96-655 gave a plateau age of 48.4±0.52 Ma and an isochron age of 48.4±1.17 Ma. The result from biotite 95-234 are 45.89±0.45 Ma (plateau) and 46.03±0.46 Ma (isochron).

We correlate the age results from the metamorphic sole rocks with ophiolite emplacement at ~108 Ma and subsequent alteration no earlier than Late Cretaceous. It is still unclear whether this alteration was a single event (late emplacement, accretion of the island arc to Eurasia) or if the fluid circulation took place gradually and therefore has no precise tectonic counterpart. The two Middle Eocene cooling (intrusion) ages from the Ras Koh plutons confirm the stratigraphic observation of Bakr (1964).

DISCUSSION AND TECTONIC MODEL

The presence of well developed metamorphic soles leave little doubt that the serpentinite outcrops in the Bunap area are the relicts of a once larger ophiolite nappe which was emplaced onto an Jurassic-Cretaceous island arc. The ~110 Ma ages from the metamorphic sole show that the Ras Koh ophiolite is neither a part of the Semail-Zagros suture line (~95 Ma; e.g. Hacker et al. 1996) nor belongs it to the Bela Muslim Bagh ophiolite belt of Pakistan (~70 Ma; Mahmood et al. 1995). The ages of this study support the results obtained by Siddiqui et al. (1995) that the underlying Kuchakki formation is older than Upper Cretaceous. The red conglomerates overlying the ophiolite indicate a stage of subeareal exposure before transgression and deposition of the Paleocene Rakshani formation.

The ophiolite and the Kuchakki Formation can

Table 2. **Correlation table displaying characteristics of the island arc and its southern and northern adjoining units. Note the similarities between the Ras Koh range and areas east of it. The Chagai arc is correlated here with the Eurasian magmatic arc, because young magmatism is characteristic for this belt. However, more data are needed to confirm this. The cited references are only examples of the vast literature available.**

Eurasin block	**Helmand**	**Helmand**	**"Hindu Kush"**	**"Pamir"**	**"Tibet"**	**Lhasa**
Volcanic arc along southern rim of Eurasian plates (transhimalayan plutonic belt of Gansser, 1980)	Chagai Cretaceous to Miocene and Neogene (Hunting Survey,1960; Breitzman et al., 1983; Siddiqui et al. 1987)	Arghandab Cretaceous to Eocene and ? Neogene (Debon et al.,1987)	Western,Nuristan 96-89) Ma (Desio et al.,1964), and Oligocene, 26-34 Ma (Debon et al., 1987)	Karakorum 111-109 Ma; Late Cretaceous to Oligocene (Debon et al; 1987)	Karakorum 21 (Parrish and Tirrull, 1989 and Miocene, Allegre.,et al., 1984)	Gangdise belt Cretaceous (120 Ma) to Eocene (41 Ma), Scharer et al.,1984)and 10-15 Ma (Coulon et al., 1986)
island arc	**Ras Koh**	**Spin Boldak**	**East Nuristan**	**Kohistan**	**Ladakh**	**"Tibet"**
Ophiolite cover (siliciclastic to volcanoclastic sediments shed from the Eurasian side).	Rakhshani shallow marine, siliciclastic (Hunting Survey, 1960)	?	?	?	Shallow marine?	Xigaze group (Einsele et al., 1994).
Ophiolite emplaced onto island arc	Bunap ophiolite (this study)	Unnamed Ophiolite Ganss(1970)	?Jalalabad Ophiolite (Griesbach,1982)	Chalt melange (Coward,1986)	Shyok melange (Virdi, 1992)	Xigaze ophiolite (Marcourx et al., 1982; Girardeau et al., 1984)
Stratigraphic age of island arc volcano-sedimentary series	Kuchakki; Jurassic to Cretaceous (Siddiqui et al., 1995)	Jurassic to Cretaceous (Montenat et al.,1979)	?Jurassic? to mid Cretaceous (not dated; Debon et al. 1987)	Drosht and Utror Units; Jurassic to Cretaceous not younger than Albian (Virdi, 1992; Tahirkheli 1982)	Yasin and Rakaposhi units;Jurassic to Cretaceous (Virdi,1992)	not exposed ?Hauterivian to Senonian (Bally et al., 1980)?
Intrusion into island arc sequence (locally crosscutting ophiolite)	Ras Koh intrusions (Middle Eocene, this study)	Spin Boldak intrusions (106-110 Ma)?Eocene (Debon et al.1987)	Eastern Nuristan plutonic complex ? Early Eocene (Trealor et al., 1989)	Kohistan plutonic complex 102-50 Ma Possibly two Phases; second 55-48 Ma (Sullivan et al., 1996)	Ladakh plutonic complex 104-50 and ?37 Ma possibly two phases(Searle et al., 1989)	not exposed
Paleoposition	not known	not known	not known	2-3^0 (Zaman and Torii, 1996)	not known	10-20°N(Possi et al., 1984)
Cretaceous/Tertiary **ophiolite(s) on the Indian plate** located south of the island arc	[(Bela, colliding in future (Alleman 1979)]	Muslim Bagh (Mahmood et al., 1995)	?	?Malakand (Ahmed and Hall, 1981)	Zidat-Sumbo, ophiolite (Virdi, 1992)	serpentinites along Tsangpo suture (Burg,1983)

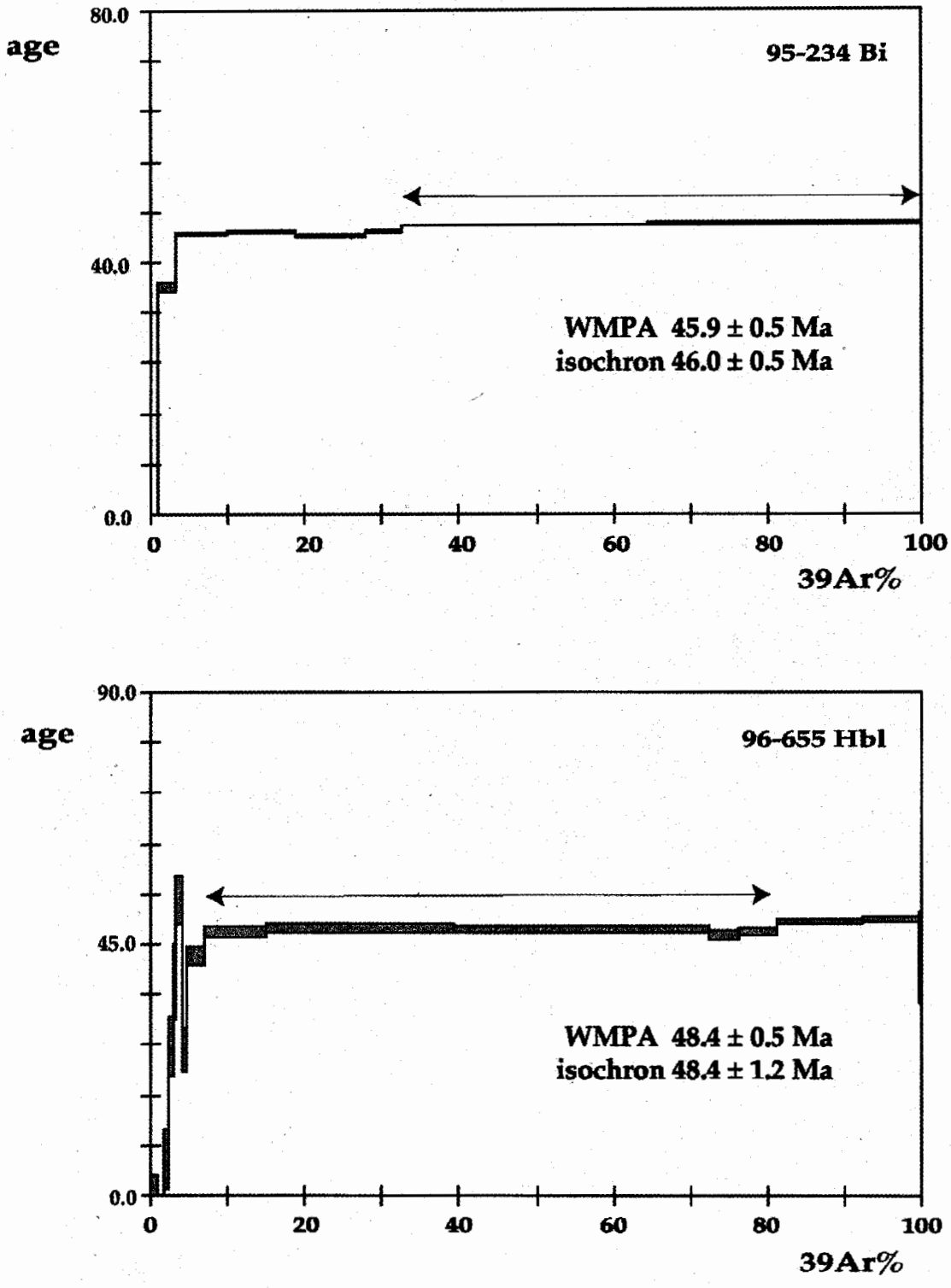

Figure 5. Age spectra of the two mineral separates from the calcalkaline rocks intruding the Ras Koh Range and the Bunap ophiolite. See Figure 1 for location.

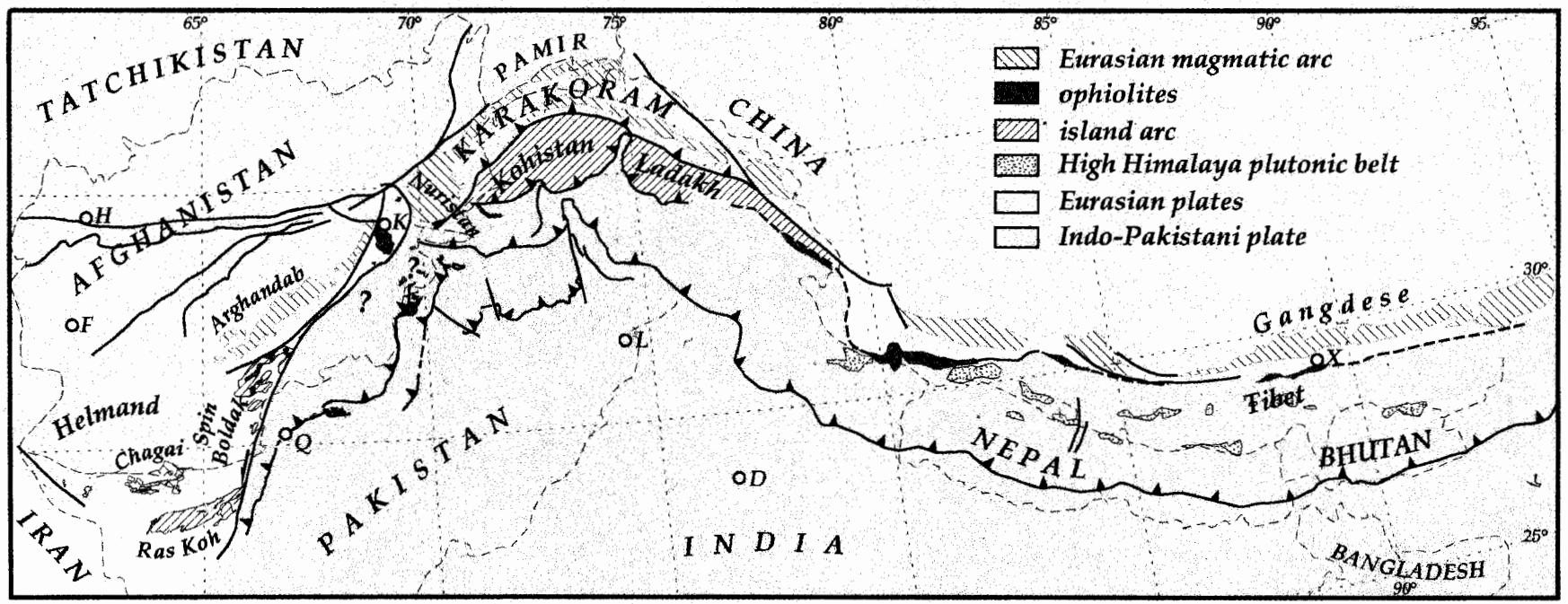

Figure 6. Tectonic overview map showing the magmatic arc marking the southern rim of the Eurasian plates, the ophiolite belts and the island arc assemblage. The map was compiled using Hunting et al. (1960), Cassaigneau (1979), Wolfart and Wittekind, (1980), Debon et al., (1987) and LeFort, (1988). Note that the Chagai arc is tentatively correlated with the magamatic arc of the Eurasian plates. It is, however possible that the Chagai hills are also part of the island arc assemblage. D: Delhi, F: Farah, H: Herat, K: Kabul, L: Lahore, Q: Quetta, X; Xigaze

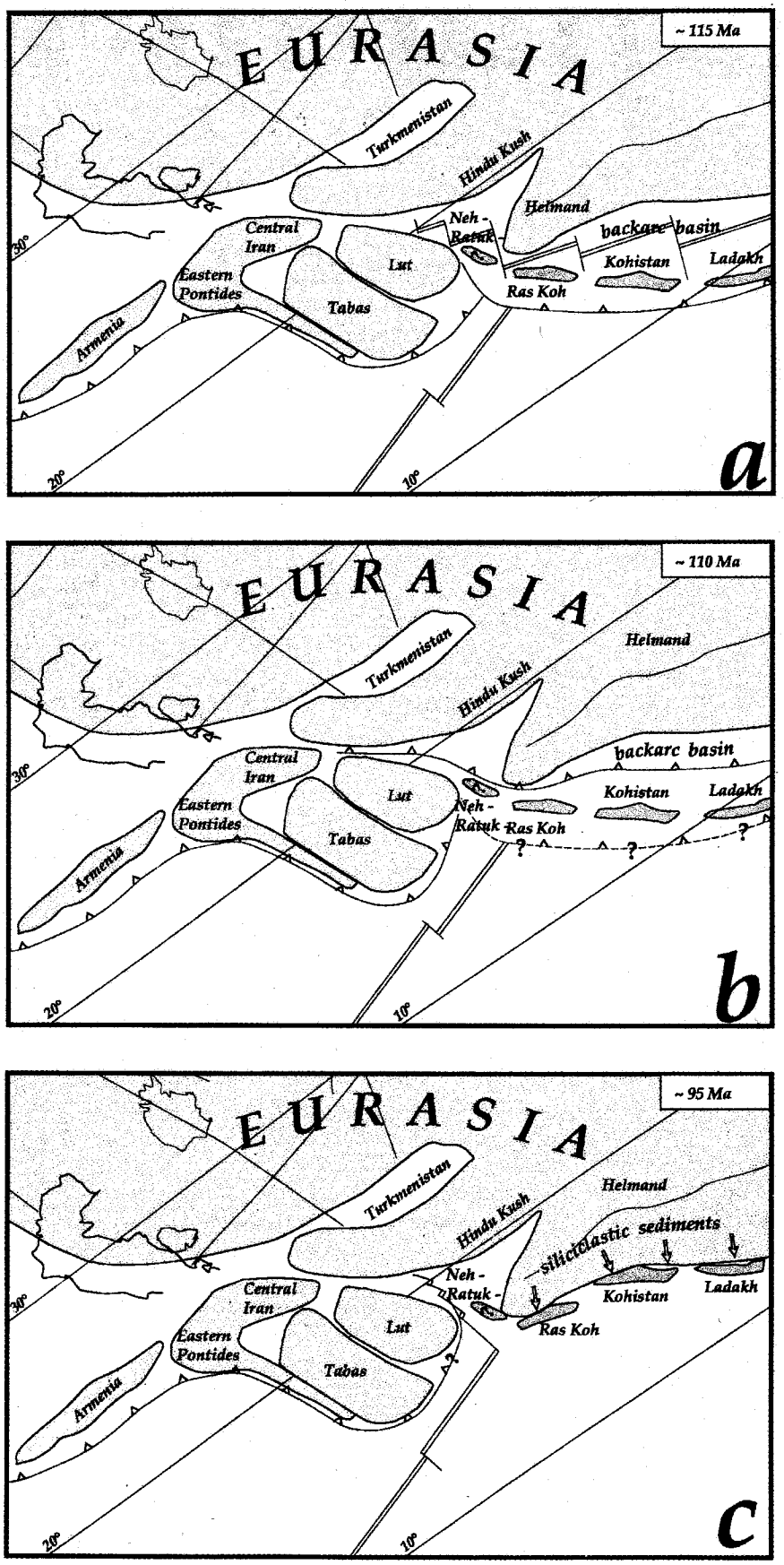

Figure 7.
Paleogeographic reconstruction based on Dercourt et al., 1993. The Ras Koh arc is placed in continuation with the Kohistan-Ladakh island arc.
a) Situation from Jurassic to Neocomian with NeoTethys spreading partially accommodated along an introaceanic subduction zone, possibly with back-arc spreading.
b) Destruction of the backarc basin along a "north-dipping" subduction zone. Ini-tiation of ophiolite emplacement onto the arc, and formation of a magmatic arc along the southern rim of Eurasia.
c) Accretion of the island arc to Eurasia and switch to the Semail-Zagros subduction zone located in the southern part of the closing Neo-Tethys. The siliciclastic sediments covering the accreted island arc and ophiolite sequence arc schematically indicated in this although sedimentation started in Late Maastrichtian only.

be traced discontinuously to the eastern end of the Ras Koh range, where the range bends towards north along the Chaman-Nushki fault. The Jurassic to Albian/Aptian volcano-sedimentary sequence in the Spin Boldak area in Afghanistan and adjoining Pakistan (Montenat et al. 1979; Fig. 6) consists of radiolarian cherts, serpentinites, gabbros (Ganss 1970, Lawrence and Yeats 1979), and Paleocene to Eocene calcalkaline to subalkaline intrusions (Debon et al. 1987). It lies in direct continuation of the Ras Koh range. Offset by the Chaman fault the eastern extension of this belt is probably found in Eastern Nuristan, Kohistan, Ladakh and Tibet (Table 2; Fig. 6) and the belt may continue further east to Sumatra-Java and Borneo (e.g. Dercourt et al. 1986). The Neh Complex in the Zahedan region in Iran (Tirrul et al. 1983) is a possible candidate for the western continuation of the belt. Table2 gives and overview for correlation of the different tectonic units.

Due to the Himalayan collision the exposure level of the different parts of the island arc varies strongly, with the deepest parts exposed in the southern Kohistan and Baltistan area and probably no or few exposures in the Xigaze area in Tibet. The island arc belt is bound by ophiolites to the north and south. The northern ophiolite belt (Bunap-Chalt melange-Shyok melange-Xigaze; Table 2) is here interpreted as the relict of ophiolitic nappes emplaced onto the island arc at approximately 110 Ma. The ophiolites represent old fragment of oceanic lithosphere originally located in a back-arc position between the island arc and the rim of the Eurasian plates (Fig. 7). The north-dipping structures in the Ras Koh range and in the Himalayas also point to thrusting of the island arc beneath the Eurasian continental plates. The emplacement direction of the Bunap ophiolite could not be determined directly during this study. However, emplacement from the north is preferred here, because a similar south-directed emplacement was obtained for the Xigaze ophiolite (Girardeau et al. 1984), and because the southern edge of the Eurasian plates was rimmed by an active magmatic arc at that time (Table 2).

According to results from the Himalayas, accretion of the island arc to the Eurasian plates occurred between 102 and 76 Ma (e.g Treloar et al. 1989). Brackets for the Ras Koh island arc accretion to Eurasia are the initial ophiolite emplacement (~110 Ma) and the Late Cretaceous/Paleocene Rakhshani Formation). If we correlate the undated red conglomerates above the Bunap ophiolite with the shallow water, mainly Maastrichtian biohermal Humai Formation (Vredenburg 1901, Hunting Survey Corporation 1960) of the Chagai Hills, and interpret them as related to the accretion, this indicates accretion between ~110 Ma and 75 Ma. With a better knowledge of the youngest sedimentary rocks beneath the ophiolite it should be possible to narrow down the range of island arc accretion.

In the south, the island arc belt is discontinuously bounded by ophiolites which were first emplaced onto the edge of the Indian plate in Late Cretaceous-Early Tertiary and subsequently, during the Himalayan collision, came into contact with the island arc sequence. The Bela ophiolite (Fig. 1, Gnos et al. *in review*) and the Ras Koh range are not juxtaposed yet because continent collision did not take place in this area.

After accretion, the island arc belt was intruded by Tertiary Andean type magmatic rocks. By comparing geological maps it is obvious that the largest clusters of plutonic rocks are located in the southern rim of the Eurasian plates forming the Chagai-Arghandab-Western Nuristan- Wakan-Karakorum-Gangdise arc (e.g Debon et al. 1987, LeFort 1988; Fig. 6, Table 2). This belt is characterized by subduction magmatism starting at - 120 Ma (Table 2, Fig. 6) and continuing until Eocene, possible composed of two main cycles Because a third Oligocene/Miocene magmatic cycle is also typical for this arc, we tentatively the Chagai hills, where Breitzmán et al. (1983) reported Miocene fission track ages, with the magmatic arc of the Eurasian plates.

Zaman and Torii (1996) obtained paleolatitudes of ~2°S for the Mid-Cretaceous red beds of the Purit, Drosh and Reshun Formations in Chitral. Estimates for the Xigaze ophiolite (Pozzi et al. 1984) are 10-20° N, and Allegre et al. (1984) suggested a Late Cretaceous (80-60 Ma) paleolatitude of 10° and 15° N for South Tibet. The few data indicate that the island arc belt was mostly located at low northern latitudes during the Late Cretaceous. This interpretation is in agreement with the paleogeographic reconstruction in Dercourt et al. (1993) and Fig. 7.

The results from the Ras Koh area indicate the following evolution of the Neo-Tethys:

1) Major plate reorganization at ~110 Ma (Patriat et al. 1982) with development of a new Eurasian-dipping subduction zone. This subduction probably replaced an older accommodation front located at the southern rim of the island arc belt (Figs. 7a,b)

2) Closure of the backarc basin, emplacement of ophiolites onto the island arc, and accretion of the island arc to the Eurasian plates (Figs. 7b,c). Accretion is probably completed by 95 Ma.

3) The closure of the Neo-Tethys continues initiating the Semail-Zagros-Cyprus subduction zone which became chocked at ~75 Ma (e.g. Allemann and Peters 1972).

4) Continued contraction resulted in the formation of the Bela-Muslim Bagh and Masirah subduction zones (Gnos et al. 1997).

5) After a phase of subaereal exposure or transgression by a shallow sea, the accreted island arc ophiolite association becomes covered by siliciclastic sediments from a northern source (Fig. 7c, Table 2).

6) Reactivation of the subduction zone along the southern edge of the Eurasian plates and accreted island arc results in emplacement of the Ras Koh intrusions. The switch of the subduction zone was possibly caused

by chocking of the Bela-Muslim Bagh subduction zone in Early Eocene.

ACKNOWLEDGMENTS

The study was supported by the Schweizerische Nationalfonds (grants 8820-40098 to E. Gnos and 20-40442.94 to J.D. Kramers) for the isotope laboratory. We thank Sardar Gul Mohammed Khan Jogezai, former governor of Balochistan, Prof.Muhammed Khan Raisani and Dr. Abdul Haque (late) of the Centre of Excellence in Mineralogy, University of Balochistan, and Prof.Jan Kramers, University of Berne for their support. Lal Muhammad and the Kharan Levis are thanked for guiding us through the sand dunes and for contacting local people.

REFERENCES

Ahmed, Z.and Hall, A., 1981. Petrology and mineralization of the Sahakot-Qila ophiolite, Pakistan. *In* Gass, I.G., Lippard, S.J. and Shalton, A.W., (eds.), Ophiolites and oceanic lithosphere. Geological Society of London Special Publication, London, p. 241-252.

Allegre, C.J. et al., 1984. Structure and evolution of the Himalaya-Tibet orogenic belt. Nature, 307, p. 17-22.

Allemann, F., 1979. Time of emplacement of the Zhob Valley Ophiolites and Bela Ophiolites, Baluchistan (preliminary report). *In* Farah, A. and DeJong, K.A. (eds.), Geodynamics of Pakistan. Geological Survey of Pakistan, Quetta, p. 215-242.

Allemann, F. and Peters, Tj., 1972. The ophiolite-radiolarite belt of the North-Oman Mountains. Eclogae. Geol. Helv., 65, p. 657-697.

Bakr, M.A., 1958. Geology of part of western Ras Koh Range, Chagai District, Pakistan, J Sci, 1-10:10 p.

Bakr M.A., 1962. Vermiculite deposits in the Doki River area, Western Ras Koh Range, Kalat Division, West Pakistan, Rec. Geological Survey Pakistan, 9, p. 1-7.

Bakr, M.A., 1964. Geology of the Wester Ras Koh range, Chagai and Kharan districts, Quetta and Kalat divisions, West Pakistan: Rec. Geological Survey of Pakistan, 10, 28 p.

Bally, A.W. and others., 1980. Notes on the geology of Tibet and adjacent areas. Report of the American plate tectonics delegation to the People's Republic of China. U.S. Geol. Surv. Open File Rep., Washington D.C., 80-501, p. 1-100.

Bannert, D., Cheema, a., Ahmed, A., and Schafer, U., 1992. The structural development of the Western Fold Belt, Pakistan. Geol Jahrbuch Reihe B, 80, p. 1-60.

Beck, R.A., Burbank, D.W., Sercombe, W.J., Khan, A.M. and Lawrence, R.D., 1996. Late Cretaceous ophiolite obduction and Paleocene India-Asia collision in the westernmost Himalaya. Geodinamica Acta, 9, p. 114-144.

Boriani, A.C., and Villa, I.M., 1997. Geochronology of regional metamorphism in the Ivrea-Verbano Zone and Serie dei Laghi, Italian Alps. Schweiz. Mineral. Petr. Mitt., 77.

Boudier, F., Nicolas, A. and Bouchez, J.L., 1982. Kinematics of oceanic thrusting and subduction from basal sections of ophiolites. Nature, 296, p. 825-828.

Breitzman, L.L., Birnie, R.W. and Johnson, G.D., 1983. Fission-track ages of the Chagai intrusives, Balochistan, Pakistan. Geol. Soc. Am. Bull., 94, p. 253-258.

Burg, J.P. and Vanderhaeghe, O., 1993. Structures and way-up criteria in migmatites, with application to the velay dome (French Massif Central). J. Struct. Geol., 15, p. 1293-1301.

Coulon, C., Maluski, H., Bollinger, C. and Wang, S., 1986. Mesozoic and Cenozoic volcanic rocks from Central and Southern Tibet: 40Ar-39Ar dating petrological characteristics and geodynamical significance. Earth Planet. Sci. Lett., 79, p. 281-302.

Coward, M.P. et al. (Editors), 1986. Collision tectonics in the NW Himalayas. Collision Tectonics, 144. Geological Society of London, Spec. Publ., London, 377-391 p.

Debon, F.,Afzali, H., Le Fort, P., and Sonet, J., 1987. Major intrusive stages in Afghanistan: typology, age and geodynamic setting. Geol Rundschau, 76, p. 245-264.

Dercourt, J., Zonenshain, L.P., Ricou, L.E., and 16 others, 1986. Geological evolution of the Tethys belt from the Atlantic to the Pamirs since the Lias. Tectonophysics, 123, p. 241-315.

Dercourt, J., Ricou, L.E. and Vrielynck, 1993. Atlas Tethys paleoenvironmental maps. Gauthier- Villars, Paris, 307 p.

Desio, A., Tongiorgi, E. and Ferrara, A., 1964. On the geological age of some granites of the Karakorum, Hindu Kush and Badakhshan (Central Asia), Proceedings 22nd International geological Congress, India, p. 479-496.

Duffield, W.A. and Dalrymple, G.B., 1990. The Taylor Creek Rhyolite of New Mexico: a rapidly emplaced field of lava domes and flows. Bull Volcanol., 52, p. 475-487.

Einsele, G., et al., 1994. The Xigaze forearc basin; evolution and facies architecture) Cretaceous, Tibet. Sed. Geol., 90, p. 1-32.

Ganss, O., 1970. Zur Geologie von Sudost-Afghanistan. Geol. Jahrb. Beihefte, 84, p. 1-203.

Gansser, A., 1980. The division between Himalaya and Karakorum. Geol. Bull. Univ. Peshawar 13, p. 9-22

Girardeau, J., Marcoux, J. and Zao, Y., 1984. Lithologic and tectonic environment of the Xigaze ophiolite (Yarlung Zangbo suture zone, Southern Tibet, China), and kinematics of its emplacement. Ecologae Geol. Helv., 77, p. 153-170.

Griesbach, C.L., 1982. The Geology of the Safed Koh. Rec. Geol. Survey India, 25, p. 59-109.

Hacker, B., Mosenfelder, J., and Gnos, E., 1996.Rapid emplacement of the Oman ophiolite: thermal and geochronological considerations. Tectonics, 15, p. 1230-1247.

Hunting Survey Corporation, 1960. Reconnaissance geology of part of western Pakistan: A Colombo Plan Co-operative Project Report: Government of Canada, Toronto, 550 p.

Hunting Corporation and Geological Survey of Pakistan, 1958a. Geological map No.18, Nok Kundi, 30 L-P, 1, p. 253, 440.

Hunting Corporation and Geological Survey of Pakistan, 1958b. Geological map No.19, Kharan Kalat, 34 D-H, 1:253,440.

Hunting Corporation and Geological Survey of Pakistan, 1958c. Geological map No. 23, Ahmed Wal, 34 C-G, 1:253,440.

Jakob, K.H., and Quittmeyer, R. L., 1979. The Makran region of Pakistan and Iran:trench-arc systems with active plate subduction.

In Farah, A. and DeJong, K.A. (eds.), Geodynamics of Pakistan. Geological Survey of Pakistan, Quetta, p. 305-317.

Krumsiek, K., 1980. Zur plattentektonischen Entwicklung des Indo-Iranischen Raumes (Resultate palaomagnetischer Untersuchungen in A118fghanistan). Geotekt. Forsch., 60, p. 1-223.

Lawrence, R.D. and Yeats, R.S., 1979. Geological reconnaissance of the Chaman fault in Pakistan. *In* Farah, A. and DeJong, K.A. (eds.), Geodynamics of Pakistan. Geol. Surv. Pak., Quetta, p. 351-358.

LeFort, P., 1988. Granites in the tectonic evolution of the Himalaya, Karakorum and southern Tibet. Phil. Trans. R. Soc. London, A, 326, p. 281-299.

Mahmood, K., Bouvier, F., Gnos, E., Monie, P. and Nicolas, A., 1995. The emplacement of the Muslim Bagh ophiolite, Pakistan. Teconophysics, 250, p. 169-181.

Marcoux, J. et al., 1982. Preliminary report on depositional sediments on top of volcanic member: the Xigaze ophiolite (Yarlung-Zangbo suture zone, Zizang, China). Ofioliti, 6, p. 31-32.

McCall, G.J.H., and Kidd, R.G.W., 1982. The Makran, southeastern Iran: the anatomy of a convergent plate margin active from Cretaceous to present. Legett, J.K. (Editors), Trench - Forearc Geology, Geol. Soc. London Spec. Publ., Oxford-London, 387-397 p.

Montenat, C. et al., 1979. Un jalon de la Mesogee eocretacee dans la region de Kandahar (Afghanistan). C. R. Acad. Sc. Paris, Serie D, 289, p. 651-654.

Nakata, T., Tsutsumi, H., Khan, S.H. and Lawrence, R.D., 1991. Active faults of Pakistan. Research Center for regional geography, Hiroshima University, Spec. Publ. 21, 141p.

Parrish, R.R. and Tirrul, R., 1989. U-Pb systematics. Geology, 17, p. 1076-1079.

Participants, 1972. Penrose field conference on Ophiolites. Geotimes, 17, p. 24-25.

Patriat, P. et al., 1982. Les mouvements relatifs de L'inde, de l'Afrique et de L'Eurasie. Bull. Soc. Geol. Fr., 7, p. 363-373.

Pavlis, T. L., and Bruhn, R.L., 1983. Deep-seated flow as a mechanism for the uplift of broad forearc ridges and its role in the exposure of high P/T metamorphic terranes. Tectonics, 2, p. 473-497.

Pozzi, J.P. et al., 1984. Paleomagnetism of the Xigaze ophiolite and flysch (Zarlung Zangbo suture zone, Southern Tibet): latitude and direction of spreading. Earth Planet. Sci. Lett., 70, p. 383-394.

Robertson, A.H.F., 1987. Upper Cretaceous Muti formation: transition of a Mesozoic nate platform to a foreland basin in the Oman Mountains. Sedimentology, 34, p. 1123-1142.

Scharer, U., Xu, R. H. and Allegre, C.J., 1984. U-Pb geochronology of Gangdese (Transhimalaya)plutonism in the Lhasa-Xigaze region, Tibet. Earth Planet. Sci. Lett., 69, p. 311-320.

Searle, M.P. and Rex, A.J., 1989. Thermal model for Zanskar Himalaya. J. metamorphic Geol., 7, p. 127-134.

Shah, S. M.I., (ed.) 1977. Stratigraphy of Pakistan: Memoirs of the Geological Survey of Pakistan, Geological Survey of Pakistan, Quetta, 138 p.

Siddiqui, R, H., Kito, N. and Nabi, G., 1995. Radiolarian ages fro Kuchakki volcanic group of Raskoh Arc, Balochistan, Pakistan and its tectonic significance. Proc. Geosci. Colloquium, Geosci. Lab. Geol. Surv. Pak., 12, p. 61-71.

Siddiqui, R.H., 1996. Magmatic evolution of Chagai-Raskoh arc terrane and its implication for porphyry copper mineralization. Geologica, 2, p. 87-120.

Siddiqui, R.H., Hussein, S.A. and Munir, U.H., 1987. Geology and petrography of Eocene mafic lavas of Chagai island arc, Baluchistan, Pakistan. Acta Mineralogica Pakistanica, 3, p. 123-127.

Sullivan, M.A., Saunders, A.D., and Windley, B. F., 1996. The petrology and geochemistry of the Utror and Shamran volcanic formations, Kohistan, NW Pakistan. Abstract, 11th Himalaya-Karakorum-Tibet Workshop (April 29-May 1, 1996), Flagstaff, Arizona, 155 p.

Tahirkheli, R.A.K., 1982. Geology of the Himalaya, Karakorum and Hindu Kush in Pakistan. Geol. Bull. Univ. Peshawar, 15, p. 1-50.

Treloar, P.J. et al., 1989. K-Ar and Ar-Ar geochronology of the Himalayan collision in NW Pakistan: Constraints on the timing of suturing, deformation, metamorphism and uplift. Tectonics, 8, p. 881-909.

Tirrul, R., Bell, I.R., Griffis, R.J. and Camp, V.E., 1983.The Sistan suture zone of eastern Iran. Geol. Soc. Am. Bull., 94, p. 134-150.

Virdi, N.S., 1992. Cretaceous marginal basins of the Indus-Kohistan collision zone-development and evolution. In: A.K. Sinha (Editor), Himalayan orogen and global tectonics. A.A. Balkema, Rotterdam, p. 157-168.

Vredenburg, E., 1901. A geological sketch of the Baluchistan desert and part of eastern Persia. Mem. Geol. Surv. India, 31, p. 179-302.

Wijbrans J.R. and McDougall, I., 1986. $^{40}Ar/^{39}Ar$ of white micas from an Alpine high pressure metamorphic belt on Naxos (Greece): The resetting of the argon isotopic system. Contrib. Mineral. Petrol, 93, p. 187-194.

Zaman, H. and Torii, M., 1996. Paleoposition of the Kohistan-Karakorum composite unit: a paleomagnetic study of the Cretaceous red beds from the eastern Hindukush range of northern Pakistan. Abstract, 11th Himalaya-Karakorum-Tibet Workshop (April 29-May 1, 1996), Flagstaff, Arizona, p. 175.

Manuscript received October 31, 2000
Revised manuscript received April 21, 2001
Accepted April 22, 2001

ACTA MINERALOGICA PAKISTANICA
Volume 11 (2000)

Article Reference AMP11.2000/119-127/ISSN0257-3660

STRUCTURE AND TECTONICS OF KOH-E-MARAN – KOH-E-SIAH FOLD AND THRUST ZONE, DISTRICT KALAT, PAKISTAN.

MOHAMMAD NIAMATULLAH[1], GHULAM NABI[2] AND MEHRAB KHAN[3]
[1]Department of Geology, University of Karachi, Karachi, Pakistan
[2]Department of Geology, University of Balochistan, Quetta, Pakistan
[3]Centre of Excellence in Mineralogy, University of Balochistan, Quetta, Pakistan

ABSTRACT

The Koh-e-Maran and Koh-e-Siah are large northeast trending anticlinal structures cored by the thick bedded and massive Middle Jurassic Chiltan limestone. In the intervening area, Cretaceous Parh Group has been repeated several times where majority of structures are southeast verging except adjacent to Koh-e-Maran where vergence is northwesterly. The vergence of the structures indicates that the tectonic transport is from northwest. Although conjugate sets of strike slip faults are present but the predominance of the sinistral faults is by virtue of location of the area on the northwestern edge of Indian plate. The fault-bend fold geometry of the Koh-e-Maran indicate a staircase pattern of the basal thrust in subsurface. This thrust steps up southeastward over a ramp of Chiltan limestone. The detachments in the region are provided by the Early Jurassic Shirinab Formation in the subsurface and the Early Cretaceous Sembar Formation at the base of the Parh Group.

The exposed thrust zone is a cover deformation above a blind thrust where southeast vergence of structure is a response of Bulldozer effect of Koh-e-Maran thrust sheet in the foreground of the tip point whereas behind this tip point structures are back thrusted. The involvement of the Early Eocene Ghazij formation in thrusting indicates the age of tectonism as post Early-Middle Eocene. An estimate of shortening is about 37 % in the area. Cleavage development in the Parh Group at places indicates some layer parallel shortening as well.

INTRODUCTION

The Koh-e-Maran - Koh-e-Siah fold and thrust zone is located in the northern part of the Kirthar fold and thrust belt, to the east of Mangucher, a village on Quetta-Karachi RCD highway at a distance of about 100 km from Quetta (Fig. 1). This thrust zone was first mapped by the Hunting Survey Corporation (1960) on quarter of an inch to a mile (1:253,440) as a part of reconnaissance survey of the part of West Pakistan. The area is underlain by sedimentary rocks of Middle Jurassic to Early Eocene (Table 1). The oldest rock unit exposed in the area is Chiltan Limestone (Middle Jurassic), a thick bedded limestone unit. This unit is exposed in the cores of northeast trending Koh-e-Maran and Koh-e-Siah anticlinal structures. The Parh Group (Cretaceous) occupies a major part of the intervening zone, which have been repeated several times due to thrusting and folding.

To the southeast of the intervening thrust zone the Dungan formation (Paleocene) and the Ghazij Formation (Early Eocene) are well developed. To the northwest of the zone the Dungan formation is not present at all whereas the Ghazij formation is poorly developed. However, within the thrust zone these two formations are poorly developed (Hunting Survey Corporation, 1960).

In the blind thrust system the overlying cover

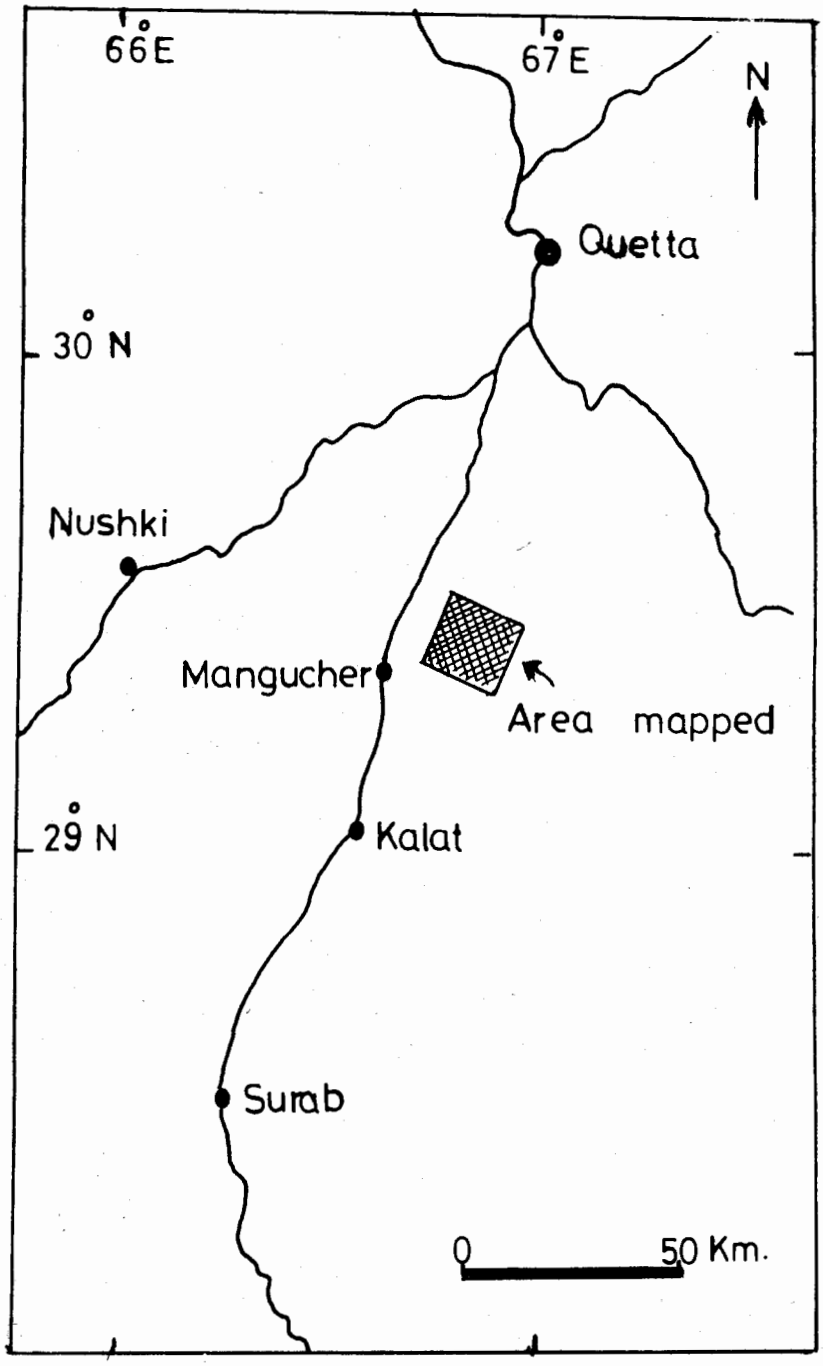

Figure 1. Location map of the Koh-e-Maran - Koh-e-Siah fold and thrust zone.

sequence may deform by fore thrusting as well as by back thrusting (Ferrill and Dunne, 1989). For fore thrusting the cover is pinned to the blind system behind the leading branch line (Fig. 2a). The cover displaces towards the foreland forming upright or foreland verging folds and imbricate fore-thrusts (Marshank and Engelder, 1985; Geiser, 1988). For back-thrusting the cover is pinned at the leading branch or tip line (Fig. 2b) and the cover displaced towards the hinterland with respect to the underlying thrust, facing hinterland verging folds and imbricate thrusts (Suppe 1983, McMechan 1985, Banks and Warburton 1986 and Morley 1986 a, b). For coupling (Fig.2c) the cover is also pinned at the leading branch or tip line, but the cover deforms locally without a regionally consistent transport direction, producing upright and locally

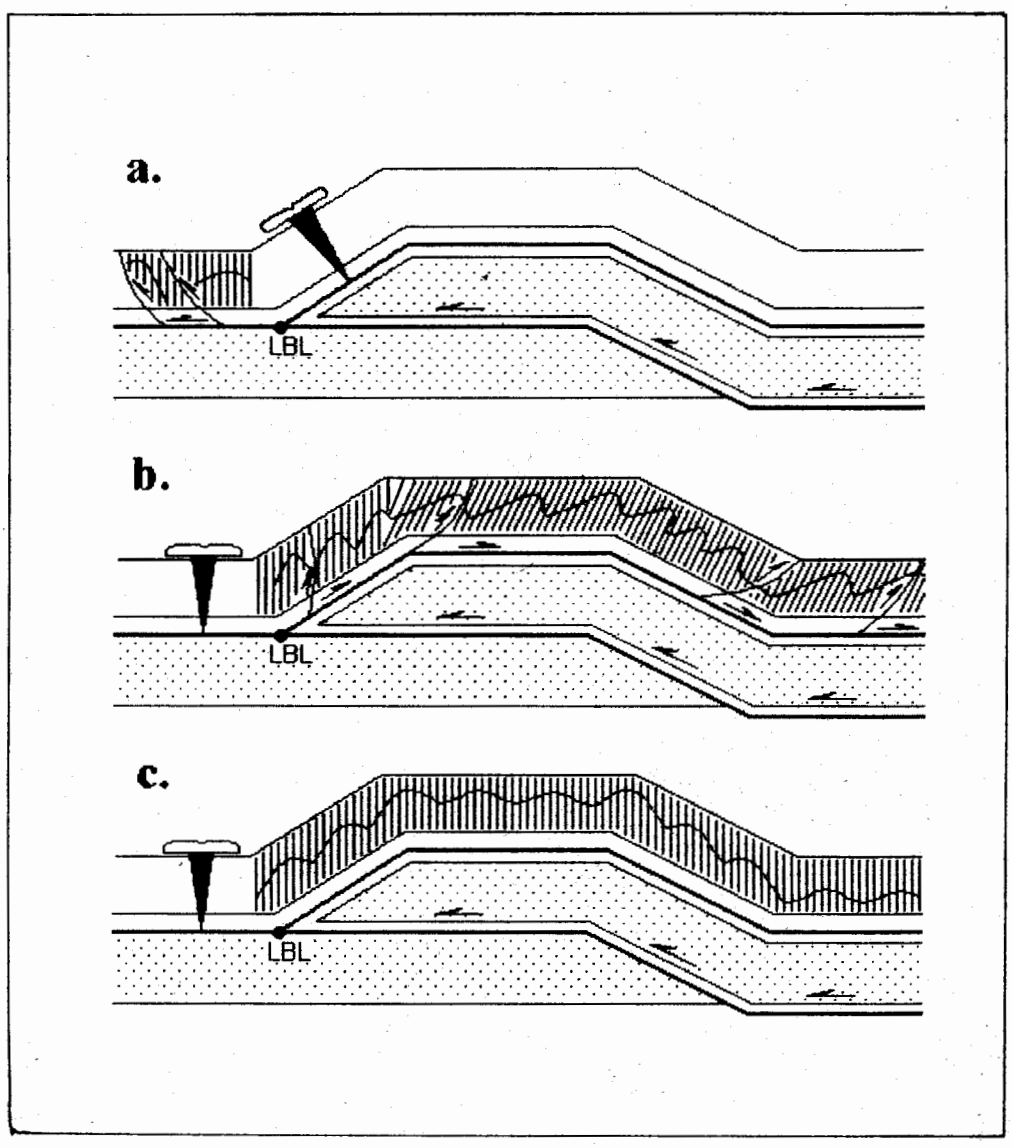

Figure 2. Cover responses to blind thrusting. (a) Fore thrusting, (b) Back thrusting and (c) Coupling. Dashed lines are schematic cover folds, thin lines show cleavage geometry and LBL is leading branch line. After Ferril and Dunne (1989).

Table -1 Stratigraphy of the study area

Formation	Age	Lithology	
Ghazij Formation	Early Eocene	Shale/Sandstone	d3-detachment
Dungan Formation	Paleocene	Limestone/Shale	
Parh limestone	Late Cretaceous	Limestone	
Goru Formation	Late Cretaceous	Limestone/Shale	
Sembar Formation	Early Cretaceous	Shale	d2-detachment
Chiltan Limestone	Middle Jurassic	Limestone	
Shirinab Formation	Early Jurassic	Limestone/Shale	d1-detachment

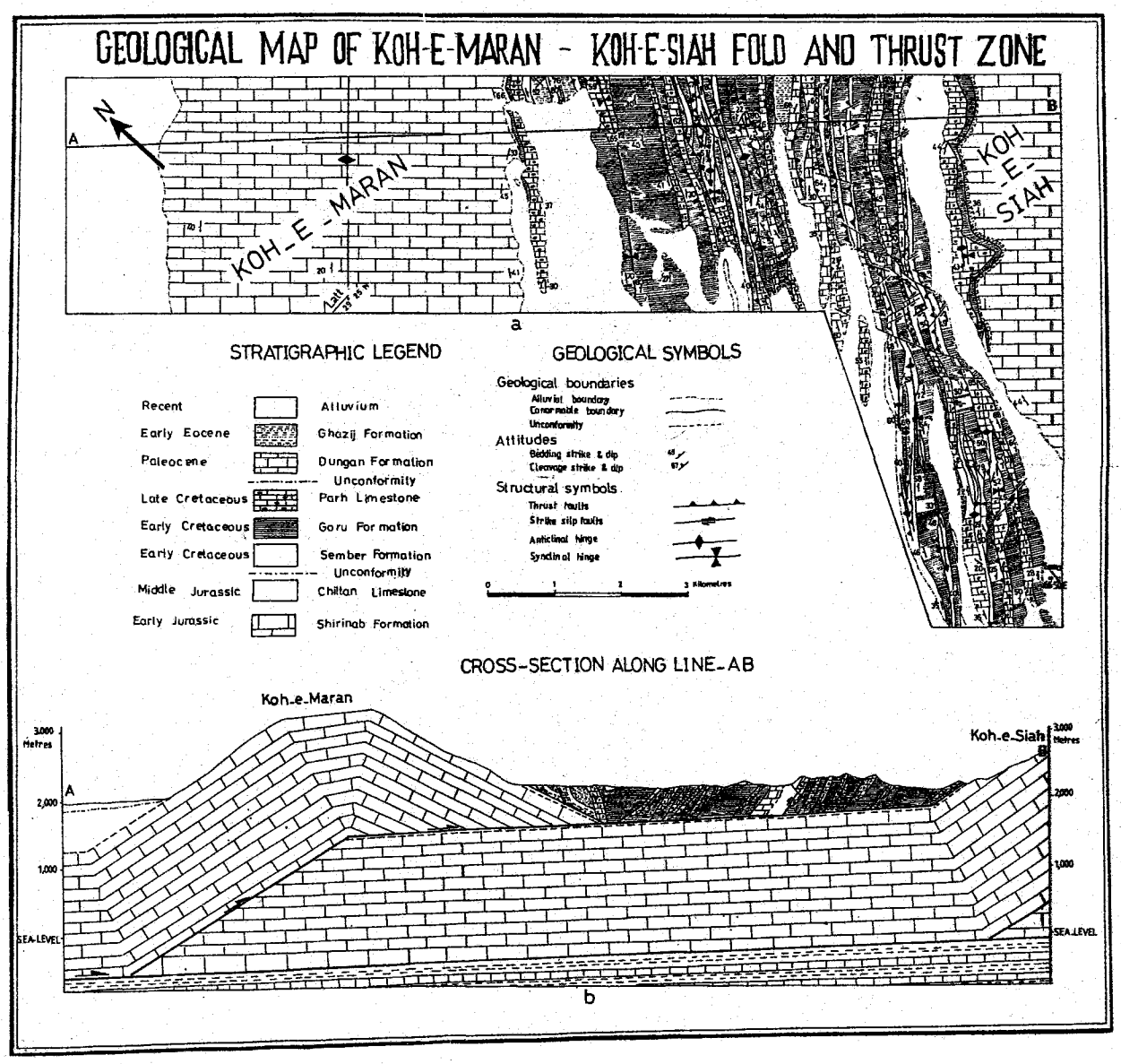

Figure 3. **(a)** Geological map of the Koh-e-Maran - Koh-e-Siah area, **(b)** geological cross section across the area.

verging folds.

Seismic sections are most useful in studying the subsurface structures, particularly in delineating the detachment horizons in the subsurface. In the present study due to the lack of seismic control it was not possible to accurately mark the depth of detachment and subsurface structures and consequently the amount of shortening involved. However, the thickness of the Chiltan Limestone, the most widespread and competent unit has been used to delineate the depth of the lower detachment by area balancing. This has been done because the Early Jurassic Shirinab Formation, a shale limestone sequence probably has provided detachment below the Chiltan Limestone. Whereas the depth of the upper detachment has been determined at the intersection of the forelimb of the Koh-e-Maran anticline with the plane where structural vergence changes from dominantly southeast to northwest in the intervening thrust zone. The Early Cretaceous Sembar Formation, a shale unit has provided detachment above the Chiltan Limestone (Table 1). The amount of shortening has been estimated by line balancing method on balanced cross section using top of the Chiltan Limestone.

The Ghazij Formation which is an excellent detachment horizon in other areas of lower Indus basin (Banks and Warburton 1986, Niamatullah et al. 1989, Bannert et al. 1992) is poorly developed in this thrust zone whereas it is well developed to the east of the area. The area studied probably was at the edge of the sedimentary basin where Ghazij Formation was deposited.

STRUCTURAL ELEMENTS AND STYLE

The Koh-e-Maran - Koh-e-Siah are large northeast trending anticlines cored by massive Chiltan Limestone (Fig. 3a). The Koh-e-Maran anticline is a straight limb sharp-hinged fault bend fold, indicative of a staircase pattern of a blind thrust in subsurface. On the other hand Koh-e-Siah seems to be a fault propagation type fold having a sharp hinge with straight limbs. However, due to later erosion the fault through which the Chiltan Limestone has climbed up and brought in contact with the Parh Group on the southern slope of Koh-e-Siah region, has been exposed due to erosion. Parh Group in turn has been thrusted on the Ghazij Formation.

Mainly Parh Group, repeated several times due to thrusting and folding occupies the region between the two large anticlinal structures. In the imbricate zone majority of structures are southeast verging except in a narrow zone along Koh-e-Maran where structures are locally northwest verging (Fig. 3b).

Within the thrust zone there is a change of structural style along the strike. Thrusting is dominant in the northeastern part, whereas rocks have been equally deformed by thrusting as well as by folding in the southwestern area (Fig. 3a). This change of structural style is attributed probably to the variation in the amount of shortening in parts of the thrust zone. In the northeastern part a greater amount of shortening gave rise to thrusting which is a predominant structural feature of the area.

The structural style of the folds in the intervening zone of Koh-e-Maran – Koh-e-Siah where Parh Group has been repeated several times is different from the large northeast trending Koh-e-Maran – Koh-e-Siah anticlines. Contrary to the folds having kink geometry, the folds in this zone has smoothly curved hinges suggest an absence of fault induced folding. This difference in structural style is probably due to different rheology and overburden at the two places.

SHORTENING ESTIMATES

Shortening has been caused in the area by means of folding as well as thrusting. However, at certain localities the presence of incipient cleavage indicates that a component of layer parallel shortening is also involved. The depth of the lower detachment in the Shirinab Formation has been determined by area balancing through planimetric shortening (Suppe, 1985). This has been done using thickness of the most competent unit, the Chiltan Limestone. Curvimetric shortening of the area has been estimated by line balancing using top of the Chiltan Limestone. The depth of the upper detachment has been delineated at the intersection of the forelimb of the Koh-e-Maran anticline and the plane where vergence changes from dominantly southeast to northwest in the intervening thrust zone. Section balancing across the thrust zone indicates 37 % (4 km) of shortening (Fig. 4).

DISCUSSION

The structural style of the Koh-e-Maran and Koh-e-Siah anticlines indicates staircase pattern of a blind thrust in subsurface. At a lower level detachment d1 is present probably in the early Jurassic Shirinab Formation, a shale-limestone unit (Table 1). This blind thrust steps up on the Chiltan Limestone through a northwest dipping ramp beneath the Koh-e-Maran. Above the Chiltan Limestone the Sembar Formation, a shale unit, provide detachment d2 in the region. The Parh Group and the younger strata, exposed to the south of the northwest-dipping ramp beneath the Koh-e-Maran, have been deformed by southeast moving thrust sheet of the Chiltan Limestone. The Parh Group and younger strata have been repeated several times due to thrusting and folding above detachment d2 between two large anticlines.

In the blind thrust system the overlying cover sequence may deform by fore thrusting as well as by back thrusting. This result in different vergence direction of structures in the cover sequence which in

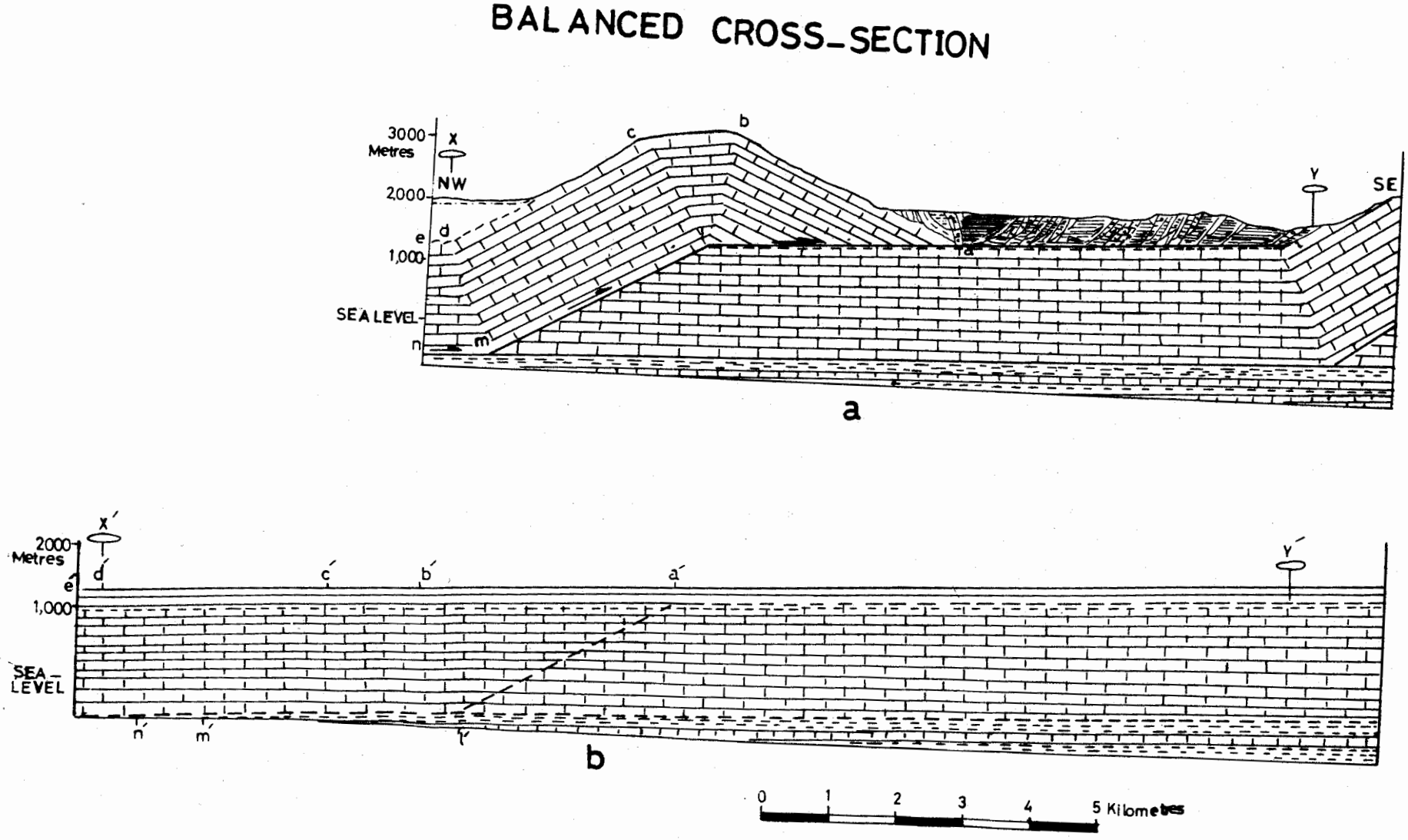

Figure 4. Balanced cross section of the area, **(a)** Deformed-state cross section, **(b)** Restored un-deformed-state cross section.

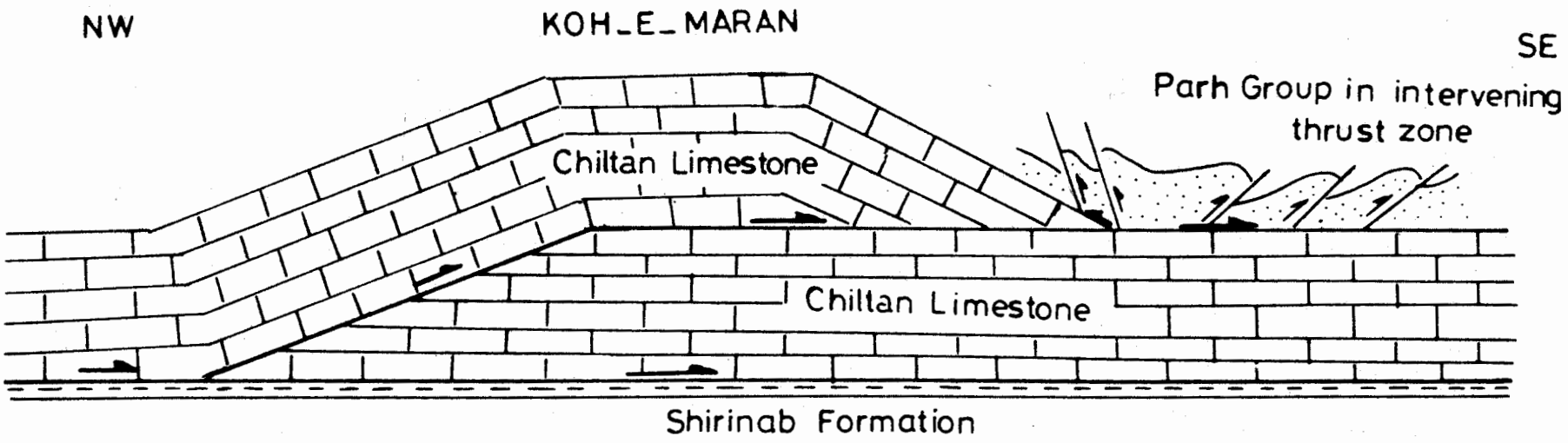

Figure 5. Schematic tectonic model of the area showing mainly fore thrusting in front of the leading branch or tip line with some back thrusting behind the line.

turn depends on that the cover sequence is pinned behind or in-front of branch tip line (Ferrill and Dunne 1989). In complexes where cover sequence is pinned behind the branch tip line, then foreland verging structures develop because of de-coupling of cover sequence towards foreland (see Fig. 2a). Where cover sequence is pinned in front of branch tip line hinterland verging structures develop because of de-coupling towards the hinterland (Fig. 2b).

In the cover deformation between Koh-e-Maran – Koh-e-Siah thrust zone above detachment d2 majority of structures are verging towards foreland. However, in a narrow zone adjacent to the Koh-e-Maran, structures are locally verging towards hinterland. This suggests that in the Koh-e-Maran -Koh-e-Siah thrust zone cover has pinned neither in front of the leading branch or tip line nor behind it. The cover rocks have been displaced in front of tip line towards foreland as well as behind it towards hinterland. It's displacement in the foreground of tip line has developed foreland verging structures whereas backward displacement has developed structures verging towards the hinterland (Fig. 5). The line in the exposed thrust zone which separate foreland verging structures from the hinterland verging structures in the region is the projection of leading branch or tip line. However, deformation in front of the leading branch line is more intense than behind it.

It is argued in this model that while same detachment horizon is present in front of leading branch line on the upper flat as behind leading branch line on the forelimb of the fault bend fold. The difference of angle of detachment is the main cause of formation of dominant foreland verging structures as compare to back verging structures, because it will be comparatively easy to thrust a sheet on a low angle detachment than to push it uphill. This is in contrast to the model that when cover is pinned behind the leading branch line then only fore land verging structures develop (Marshank and Engelder 1985, Geiser 1988). It also is in contrast to the models presented by Suppe (1983), McMechan (1985), Banks and Warburton (1986) and Morley (1986,a,b). According to these authors hinterland verging structures develop if cover is pinned in front of the leading branch line.

CONCLUSION

The northeast trending folds and thrusts manifest tectonism in the northern part of the Kirthar fold belt. Early Jurassic Shirinab Formation and Early Cretaceous Sembar Formation have provided detachments for thin skin tectonism in the region. Southeastward directed tectonic transport has developed southeast-verging structures in the region. Thrusts at deeper levels have staircase pattern with lower detachment in the Shirinab Formation and upper detachment in the Sembar Formation, and northwest dipping ramps cutting through thick, competent Middle Jurassic Chiltan Limestone. Consequently, the larger Koh-e-Maran and Koh-e-Siah have kink geometry and developed as fault induced folds.

Movement of the thick sheets of the Chiltan Limestone in southeast direction has bulldozed cover rock overlying the Sembar Formation into an imbricate zone. As a consequence the Parh Group and younger rocks have been repeated several times in the intervening thrust zone between Koh-e-Maran and Koh-e-Siah. However, in this intervening thrust zone structural style is different than the large anticlines and absence of folds having kink geometry in the zone indicate an absence of staircase pattern of the thrusts. The vergence of the structures in the intervening imbricate zone indicates major thrusting in front of leading branch or tip line, localized back thrusting behind the line is also observed. The predominance of the sinistral strike slip faults over dextral faults in the region is due to its location on to northwestern edge of the Indian plate close to the sinistral Chaman fault.

REFERENCES

Banks, C.J. and Warburton, J., 1986. Passive-roof duplex geometry in the frontal structures of the Kirthar and Sulaiman mountain belts, Pakistan. J. Struct. Geol. 8, p. 229-237.

Bannert, D.Chema, A, Ahmed, A. and Schaffer, U., 1992. The structural development of the western fold belt, Pakistan. Geol. Jb. BS80 , p. 3-60.

Ferrill, D.A. and Dunne, W.M., 1989. Cover deformation above a blind duplex: an example from West Virginia, U.S.A. J. Struct. Geol. 11, p. 421-431.

Geiser, P.A., 1988. The role of kinematics in the construction and analysis of geological cross-sections in deformed terrains; *In* Mitra, G. and Wojtal, S., (eds.) Geometries and Mechanisms of Thrusting, with Special Reference to the Appalachians, Spec. Pub. Geol. Soc. Am., 222, p. 47-76.

Hunting Survey Corporation, 1960. Reconnaissance geology of part of West Pakistan: A. Colombo Plan Cooperative Project, Government of Canada, Toronto, Canada, 550 p.

Marshank, S. and Engelder, T., 1985. Development of cleavage in lime-stones of a fold-thrust belt in eastern New York. J. Struct. Geol. 7, p. 345-359.

McMechan, M.E., 1985. Low-taper triangle-zone geometry: an interpretation for the Rocky Mountain foothills, Pine-Peace River area, British Columbia. Bull. Can. Petrol. Geol. 33, p. 31-38.

Morley, C.K., 1986a. A classification of thrust fronts. Bull. Am. Assoc. Petrol. Geol., 70, p. 12-25.

Morley, C.K., 1986b. Vertical strain variations in the Osen-Roa thrust sheet, northwestern Oslo Fjord, Norway. J.Struct. Geol. 8, p. 621-632.

Niamatullah, M., Durrani, K.H., Qureshi, A.R., Khan, Z., Kakar, D.M., Jan, M.R., Din, M. and Ghaffar, A., 1989. Emplacement of the Bibai and the Gogai Nappes Northeast of Quetta. Geol. Bull. Univ. Peshawar. 22, p. 71-78.

Suppe, J., 1983. Geometry and Kinematics of fault-bend folding. Am.J.Sci. 283, p. 684-721.

Suppe, J., 1985. Principles of Structural Geology. Prentice-Hall, Inc. New Jersey, 537 p.

Manuscript received November 29, 2000
Revised manuscript received April 28, 2001
Accepted April 30, 2001

ACTA MINERALOGICA PAKISTANICA
Volume 11 (2000)

Article Reference AMP11.2000/129-136/ISSN0257-3660

EXPERIMENTAL RESISTIVITY SCANNING APPROACH TO DELINEATE COAL ZONES AND THE BASEMENT IN THAR DESERT OF SINDH, PAKISTAN

NAYYER ALAM ZAIGHAM AND MUJEEB AHMAD
Department of Geology, University of Karachi, Karachi

ABSTRACT

The coal zones encountered in different holes drilled by the Geological Survey of Pakistan in Thar Desert were found to vary in thickness substantially and even some of them were devoid of coal bearing beds. In view of lack of adequate sub-surface geological information regarding the stratigraphic sequences and structures of the Thar sedimentary basin and the basement, often problems were faced in selection of drill sites because of very wide spacings between the bore holes. In order to substantiate the sub-surface geological information in between the widely spaced drilled holes, Vertical Electric Soundings (VES) were experimentally carried out at selected known drilled sites and at places in between them, scanning an average depth of 1,000 feet (about 303 m), based on a theoretical study of coal resistivities of different grades. This study gave encouraging results regarding the sub-surface delineation of dune sand-bedrock contacts, upper and lower limits of thick coal zones, and presence of the basement. The results of VES have also shown layering in the basement indicating bright prospect for the good quality groundwater aquifer(s). It has been concluded that this study would provide adequate sub-surface geological information as a guideline for the future feasibility drilling program to obtain the optimum drilling results.

INTRODUCTION

On the discovery of thick coal zones in Chachro-Dhaklo area (19 meters at Chachro and 16.1 meters at Dhaklo as estimated by the geophysical logs in 1989), the Geological Survey of Pakistan (GSP) extended exploratory drilling program in collaboration with United States Geological Survey (USGS) and John T. Boyd Company (JTB) during 1992-93 and 1993-94 respectively funded by United States Agency for International Development (USAID) for the assessment of coal potentials in the Thar Desert (Fig. 1a).

In two phases, 38 bore holes have been drilled on a very large interval in the Thar Desert (Fig. 1b). These investigations were of reconnaissance nature and resulted in the discovery of about 78 billion metric tonnes of estimated geological reserves of lignite coal (Fassett and Durrani 1994). 25 test holes were drilled at an average spacing of about 22 km, and 13 test holes at an average spacing of about 8 km. Due to large distances between the drilled holes, the correlation of coal zones, establishment of sub-surface stratigraphy and solution to complexity of buried structures became difficult and ambiguous. Considering very wide spacing between the drill holes and associated problems, an application of geophysical technique was considered a pre-requisite for the delineation of sub-surface geological features related with the coal zones and the associated basement conditions.

Thar is a famous desert covering an area of about 200,000 sq km and lies partly in Pakistan and partly in India. About 25% of this desert is in Pakistan in the south-eastern corner of Sindh Province. The Thar Desert has been characterized as one of the most densely

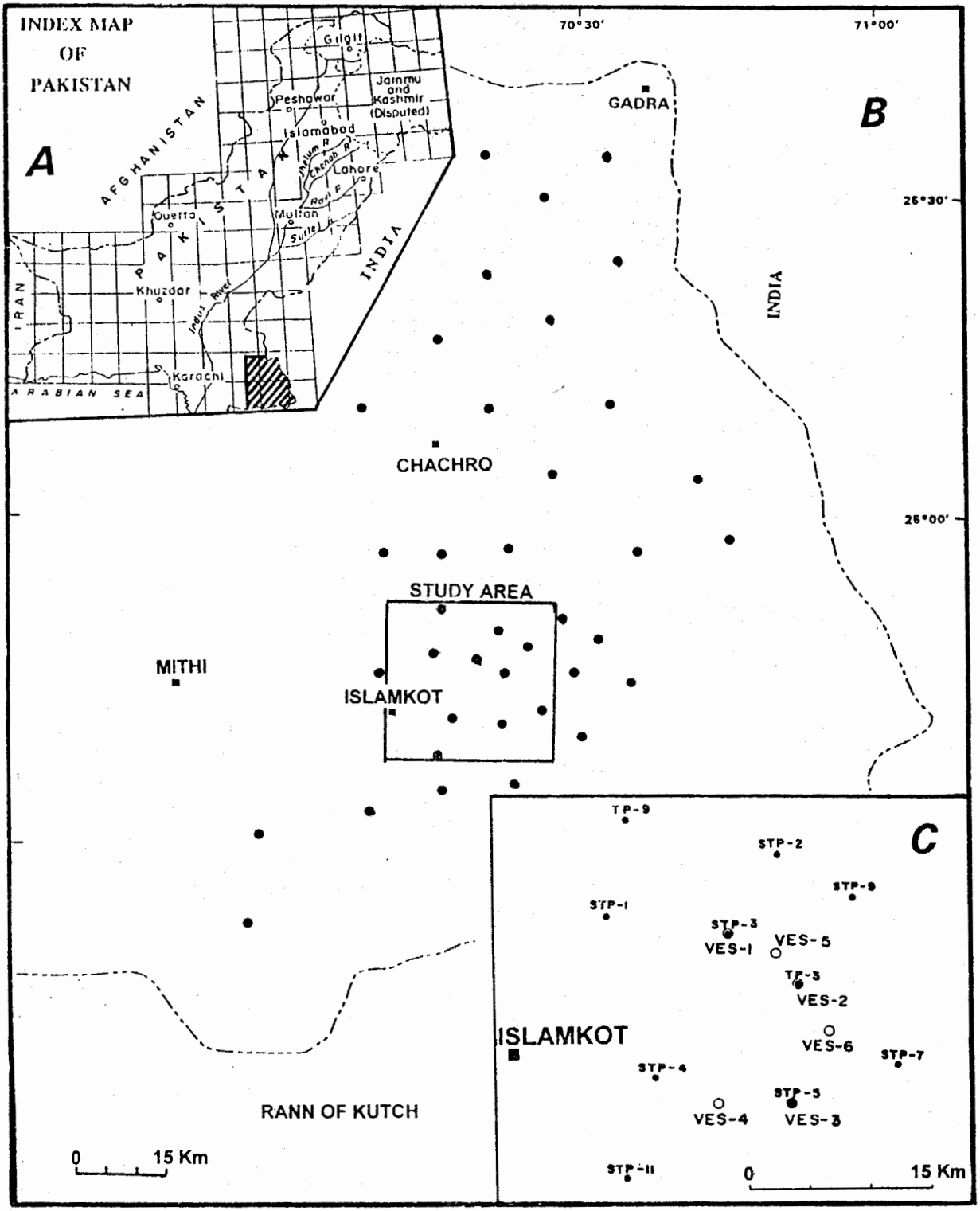

Figure 1. A: Index map of Pakistan, B: locations of the bore holes drilled for the exploration of coal, and C: locations of sites for Vertical Electric Soundings (VES) in the Thar, Sindh Province, Pakistan.

populated deserts in the world. Topographically, the northern and eastern parts of the area are higher with elevations ranging from near sea level in the south to more than 200 meters above sea level in the northeast. The dunes are longitudinal with a north-east trend having relief from tens of meters to 100 meters. These dunes are generally stabilized by scrub vegetation and grasses.. The average annual rainfall ranges from 20 to 30 cm. Mean annual maximum and minimum temperatures are 35°C and 19°C respectively. Maximum daily temperatures commonly exceed 45°C in April through June.

GENERAL GEOLOGY

The only outcropping red-granite basement complex of the Precambrian age surrounded by dunes is found in Nagar Parker, otherwise, the whole area is covered by dune sand to an average depth of 80 meters. The geology of the Thar Desert has been poorly understood due to lack of surface exposures of the prevailing geological sequences. However, Ahmad and Zaigham (1993) have provided a good presentation of the subsurface geology of the Thar Desert. Their work shows that the Thar coal field rests upon a structural platform in the eastern part of the Desert. This platform is underlain by relatively shallow granite basement rocks. The granite basement shows pre-Jurassic rifting which caused the flexure and ultimate development of Thar Basin. For detailed description of the Thar stratigraphy and structural development, the readers are referred to Ahmad and Zaigham (1993).

THEORETICAL ANALYSIS OF RESISTIVITY CHARACTERS OF DIFFERENT COAL TYPES IN RELATION TO THE THAR COAL

The use of geophysical exploration methods in search for economic coal deposits, requires a comprehensive knowledge of the electrical properties of different types of coal. In general, the electrical resistivity depends on the carbon ratio of the coal. Moisture plays a more important role in low quality coals, like Thar coal. In order to study the possible effective parameters to design the present geophysical exploration, a statistical analysis of the most probable values for the resistivity of coals of various grades, as a function of quality, is done with respect to Thar coal. Before taken up the VES investigation in the field, a theoretical analysis of coal resistivity of different grades in relation to Thar coal has also been considered in this paper.

The resistivity is a function of a great number of variables related to a) physical and petrographic characters of the coal, b) mineral composition and c) degree of metamorphism..

The high values of resistivity are reported from coal in completely dry state (Agroskin 1959), and relatively lower values are observed from naturally wet coal (Dakhnov 1951) and air-dried coal (Agroskin and Petrenko 1950). From the published literature it is found that the range of resistivity values for coals is extremely wide with range extending from semiconductor to insulator, even wider than the ranges for ores or for highly resistant rocks.

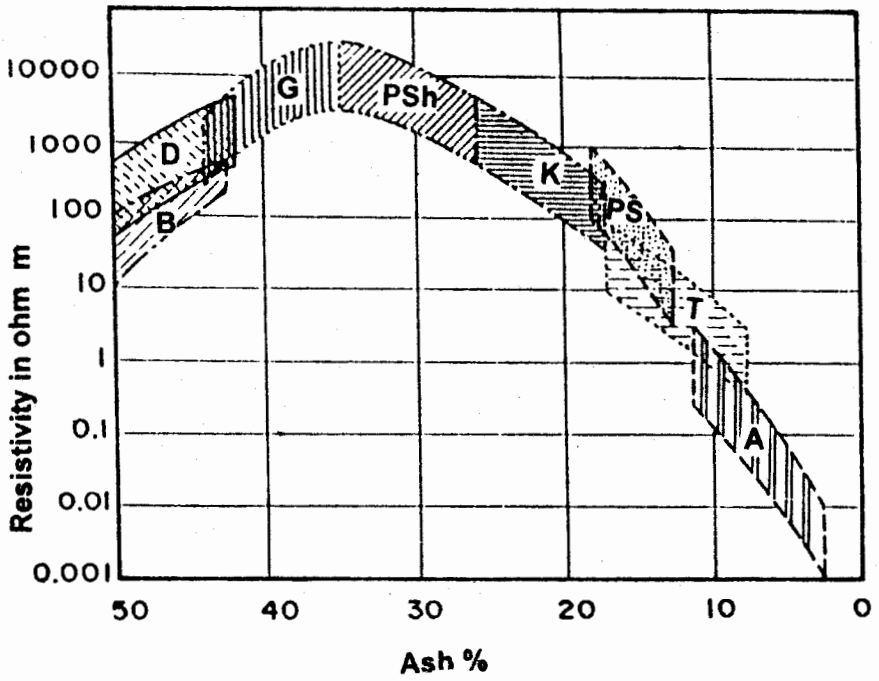

Figure 2.
Graphic plot of the most probable values for the resistivity of coals of various grades as a function of quality against the ash content. B: Brown coal, D: Long-burning coal, G: Gassing coal, PSh: Bituminous coal, K: Coking coal, PS: Super-bituminous coal, T: Sub-anthracite coal, A: Anthracite coal. (Modified after Dakhnov 1962).

The main factor in determining resistivity of a coal is the degree of metamorphism, which causes differences in carbonitization and carbon ratio. With progressive carbonitization, the physical and chemical properties of coal change from those of a brown coal to those of an anthracite. Weakly metamorphosed coals (brown coals) have a rather high resistivity, i.e., 10^{10} to 10^{11} ohm cm when dry, and 10^5 to 10^6 ohm cm when moist. The strong metamorphism leads to the formation of free carbon stringers and a reduction of the organic radicals in the coal causing decrease in the resistivity (Agroskin 1959).

Based on the experimental data (Dakhnov 1962), it is observed that high resistivities are associated with lignitic and bituminous coals (Fig. 2). Thar coal is expected to lie in this range of resistivity values.

A study of Toporets (1958) indicates that the role of carbon ratio in determining the resistivity of coals with various degrees of carbonitization is not uniform. For coals of type D, G, and PSh, the resistivity is decreasing with increasing carbon ratio, while in the case of anthracite, on the other hand, increasing the carbon ratio increases the resistivity. It is noted that not only is the carbon ratio important, but so is the ash content, which is related to the carbon ratio. It is also observed that the kaolinite in a coal with an intermediate degree of carbonitization will markedly decrease the resistivity.

Accordingly, the Thar coal should lie in range of highest resistivities, but the ash content of Thar coal is much less (i.e., 8.83 %; Fassett and Durrani 1994) as compared to proposed model of Dakhnov (1962)which is an anomaly in this case.

In Thar region the quality of coal ranges between lignite-B to lignite-C. In general, the coal zones are underlain and/or overlain by sandstone aquifers. Based on a study of JTB (1994) it is found that the total dissolved salts(TDS) in water samples from different depths in area between Chachro and Islamkot range from 3967 to 6852 mg/l, the pH values vary from 5.57 to 8.36 and the field electrical conductivity is found 4165 to 5900 μmhos/cm (Table 1).

From the present analysis of physical properties of coals, it is inferred that in Thar area relatively high resistivity coal is embedded within rock units of relatively low resistivity values causing a considerable resistivity contrast important for the geophysical exploration.

DEEP RESISTIVITY MEASUREMENTS

On experimental basis, six sites were selected for the deep vertical electric soundings(VES). Three soundings were observed at drill hole sites TP-3, STP-3, and STP-5 in order to correlate the resistivity values with the known subsurface geological units and to observe the effectiveness of the technique. Other three soundings were observed in between these drill holes to study lateral behavior of the coal zone(s) and the basement (Fig. 1c).

Considering the power to detect thin layers, the Wenner electrodes configuration was adopted for the field measurements so as to possibly detect thin coal beds. Scintrex transmitter TSQ-3 and receiver IPR-10 were used to observe the soundings in the field. At each site a depth of about 1,000 feet (about 303 meters) was scanned. The observations were made at 20 feet (about 6 meters) interval.

DISCUSSION OF RESULTS

The resistivity field curve were plotted on bi-log graphs and interpreted qualitatively by the empirical method to determine the possible number of lithologic layers, their tentative depth or thickness, and range of their resistivity values. The tentative information attained through empirical analysis of field curve is used for the quantitative interpretation adopting iteration modeling technique. The iteration modeling program "RESIST VERSION 1.0" of ITC was used to generate multilayered models with respect to the resistivity parameters found in the study area. For this purpose the correlation of resistivity ranges with the lithological

Drill Hole No.	Meters			Field Electrical Conductivity (μmhos/cm)
	Thickness of Sand Tested	Depth to Top of Sand	Interval Tested	
STP-3	12.9	11.6	115.9 to 118.9	4,165
	20.9	185.2	191.6 to 194.6	4,500
STP-7	5.2	137.5	139.2 to 142.3	4,760
	12.3	210.7	213.4 to 216.4	4,270
STP-8	3.7	89.1	88.4 to 91.4	5,900
	9.1	176.4	179.9 to 182.9	4,550

Table-1. Analysis of field electric conductivity in Thar coal deposit area, Sindh, Pakistan (modified after JTB in Fassett and Durrani 1994).

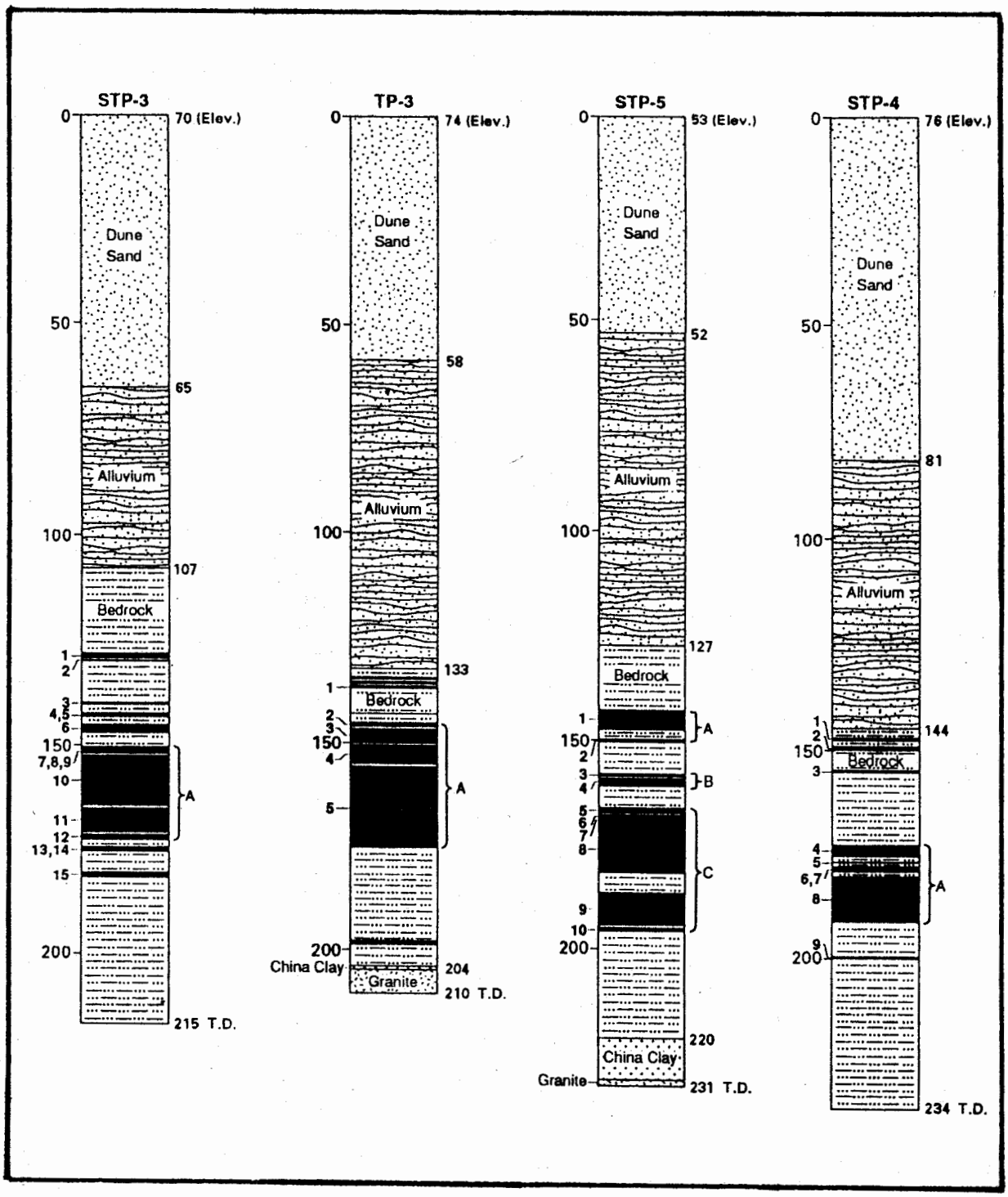

Figure 3. Stratigraphic columns of drill holes STP-3, TP-3, STP-4, and STP-5, Thar Desert, Sindh Province, Pakistan (after Fassett and Durrani 1994).

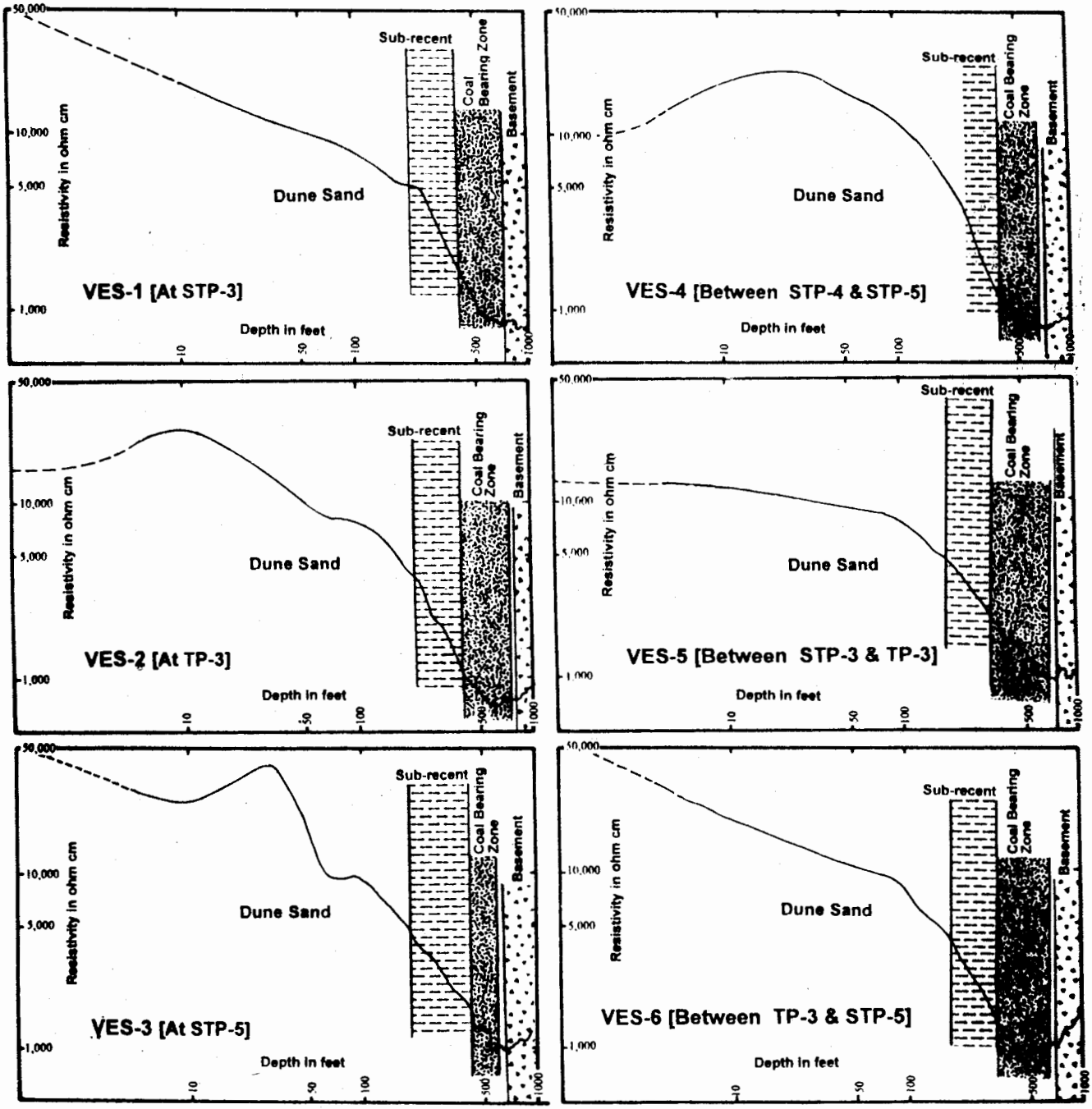

Figure 4. Interpreted zones of subsurface lithological units at sites VES-1, VES-2, VES-3, VES-4, VES-5, and VES-6 in Thar Desert, Sindh Province, Pakistan.

units prevailing in the study area, the bore hole lithological logs of STP-3, TP-3, STP-5, and STP-4 (Fig. 3) have been used.

In general, the field curves show distinct resistivity gradients with respect to major lithologic boundaries. Based on the pattern of resistivity gradient on the field curves in correlation with available bore holes information, four major lithological units are inferred to encounter within an average depth of 1,000 feet (about 303 m), i.e., dune sands, sub-recent sediments, coal bearing formation, and the basement (Fig. 4a and 4b).

ZONE OF DUNE SANDS

Dune sand unit shows an average resistivity range

of 50,000 ohm cm for dry zones, with intercalation of low resistivity layers (1000-10,000 ohm cm) of silty sand with moisture and/or silty clay. The thickness of the dune sand zone is inferred ranging from 180 to 260 feet (or 54.5 to 78.8 m) from site to site. The general resistivity gradient of the field curves indicates that the moisture content increases gradually with respect to increase in depth within dune sand zone. Presence of this moisture is also being reflected by the wide spread arid vegetal growth in the study area of Thar desert under the process of capillary phenomenon. Layers of significant low resistivity values (average 1,000 ohm cm) within Dunesand zone also indicate the possibility of high concentration of salts with moisture. A significant trend of resistivity range from 8,000 to 10,000 ohm cm at an average depth of about 100 feet (or 30.3 m) is inferred to be due to the presence of water aquifer of relatively better quality with limited yield, except at site of VES-1 where this trend is found at a depth of about 200 feet (60.6 m).

ZONE OF SUB-RECENT SEDIMENTS

Overlain by thick zone of Dune-sands, there is a consistent trend of low resistivity gradient observed on each field curve, which extends generally down to an average depth of 400 feet (121 m). This low resistivity zone (100-700 ohm cm) is inferred to correspond with the zone of sub-recent sediments consisting of silt, clay and sand units. In this zone silt and clay dominate over the sand component.

ZONE OF COAL BEARING FORMATION

Based on the bore holes information, it is found that the formation, in which coal is hosted, is dominantly claystone. Sand and silt are found interlaminated as minor constituents. Considering the lithological material of this zone, a trend of low resistivity values was expected similar to the zone of sub-recent sediments. But beneath an average depth of 400 feet (121 m), there is a well marked zone of relatively higher resistivity values with an average value of about 2,500 ohm cm intercalated with layers of low resistivity material (claystone/ siltstone) with average resistivity value of 300 ohm cm)

As discussed earlier under the heading of "Theoretical analysis of resistivity characters of coals", the increase in resistivity values is due to the presence of resistive coal beds hosted in claystone inspite of association of water saturation with main thick coal beds. The field resistivity data supports the theoretical model discussed earlier in this paper. The field curves indicate the presence of thick coal beds corresponding to resistivity values ranging from 1,000 to 3,000 ohm cm, but thin coal units have generally not been reflected on the field curves due to masking effect of dominating low resistivity trend in the area. As per limitation of the exploring technique precise thickness could not be calculated from the field curves. However, tentative limits of the zone of interest have been inferred.

Based on resistivity trends of the field curves, it is also inferred that water aquifers are associated with the main thick coal beds at their bottom parts. The quality is indicated to be saline to brackish. The interpretation of water aquifers and their quality corresponds to the finding of hydrogeological studies done under GSP-JTB-USAID Coal Exploration Program 1993-94. The analysis of water samples of nearby bore holes also shows high percentage of 'Total dissolved salts' which was reported to be 3,967 to 6,852 mg/l (Fassett and Durrani 1994).

THE BASEMENT

A sharp and prominent change of resistivity pattern is found on the field curves reflecting at depths ranging from 670 to 780 feet (203 to 236 m) in the study area. The correlation of resistivity data with the known lithological information obtained from bore holes, it is found that this change of resistivity trend corresponds to the basement rock units, i.e., granite and associated rocks. Resistivity values ranging from 2,000 to 4,000 ohm-cm are inferred to be associated with granite rock unit which encounters at depths between 670 and 780 feet (203 to 236 m) in the study area. The low resistivity layers of 400 to 1,000 ohm cm have also been observed within the basement zone. These low resistivity layers could be due to possible presence of fracture zone water aquifers within thick granite bodies or due to some other low resistive material. In view of non-availability of the geological information from greater depth, proper conclusion is difficult to draw at this stage about this association of low resistivity layers within the basement.

A significant low resistivity trend is also observed just above the basement zone which is inferred to be related with the weathering layer overlain the basement zone corresponding with the china clay beds which have also encountered in the bore holes drilled in the study area for the coal exploration.

CONCLUSIONS

1. The vertical soundings have successfully delineated subsurface contacts between dune sand and alluvium, upper and lower limits of thick coal bearing formations and the basement.
2. VES results show layering in the basement indicating bright prospect for aquifers of relatively better quality in Thar area.
3. This study provides adequate subsurface geological information for the future drilling programs.
4. Resistivity data of Thar may be used for feasibility studies pertaining to coal mines development.

REFERENCES

Agroskin, A.A., 1959. Thermal and electric properties of coals: Metallurgizdat.

Agroskin, A.A., and Petrenko, I.G., 1950. Electrical conductivity of slate and coal on heating: Izv. Akad. Nauk SSSR, Ser. Geol.

Ahmad, M.A., and Zaigham, N.A., 1993. Seismostratigraphy and basement configuration in relation to coal bearing horizons in the Tharparkar Desert, Sindh Province, Pakistan: Geol. Surv. Pak. Record No.100, 26p.

Dakhnov, V.N., 1951. Electrical exploration in oil and gas fields: Gosgeolizdat.

Dakhnov, V.N., 1962. Interpretation of the results of geophysical investigations of well sections: Gostoptekhizdat.

Fassett, J.E., and Durrani, N.A., 1994. Geology and coal resources of the Thar Coal Field, Sindh Province, Pakistan: U.S.Geological Survey Open-file report 94-167, 74p.

Toporets, S.A., 1958. On the electrical conductivity of petrographic ingredients of coals: Dolk. Akad. Nauk SSSR, Vol.118, No1.

Manuscript received September 13, 2000
Revised Manuscript received April 9, 2001
Accepted April 9, 2001

ACTA MINERALOGICA PAKISTANICA
Volume 11 (2000)

Article Reference AMP11.2000/137-138/ISSN0257-3660

[1] PETROLOGY AND PROVENANCE OF ISPIKAN CONGLOMERATE, SOUTHWEST MAKRAN, AND ITS IMPLICATIONS ON THE TECTONIC EVOLUTION OF MAKRAN REGION

KHALIL-UR-REHMAN[2], MOHAMMAD AHMAD FAROOQUI[2] AND AKHTAR MUHAMMAD KASSI[3]

[2]Centre of Excellence in Mineralogy, University of Balochistan, Quetta, Pakistan.
[3]Department of Geology, University of Balochistan, Quetta, Pakistan

ABSTRACT

The Ispikan Conglomerate of southwest Makran is a mixture of medium to coarse grained pebbly sandstone, siltstone, mudstone and numerous beds and lenses of of matrix supported conglomerate. The sandstone of Ispikan Conglomerate is composed of angular to sub angular poorly sorted, immature sandstone with 30% matrix and 5% cement. The detrital modes of sandstone are 72.5% Quartz, 12.62% Feldspar, and 14.85% lithic grains. Monocrystalline and polycrystalline quartz grains are poorly sorted and angular to sub rounded. Feldspar (plagioclase and orthoclase and microcline) grains are moderately sorted and sub rounded to well rounded. Lithic grains are composed of volcanic, plutonic, metamorphic, and sedimentary rocks fragments. VRFs, PRFs and MRFs are moderately sorted and sub-rounded to well rounded whereas SRFs are poorly sorted and very angular to sub-angular. The texture, mineralogy and petrography of detrital modes of sandstone indicate that the source area was located to the north of the depositional site at a relatively short distance. The provenance of the Ispikan Conglomerate was composed of plutonic and volcanic rocks with minor (probably contact) metamorphic rocks.

High K/Rb ratio of the sandstone of Ispikan Conglomerate indicate that the detritus was derived from acid and intermediate source. Rb vs Y+Nb plot suggests that sandstone, plutonic and volcanic clasts from Ispikan Conglomerate originated from the subduction related volcanic arc environment. Based on geochemical signatures the sand grade sediments of the Ispikan Conglomerate are best correlated with continental island arc setting. The chemistry of the andesite clasts of Ispikan Conglomerate is same as that of Ras koh andesite.

Limited paleontological studies on the Ispikan Conglomerate and Middle Eocene Wakai Limestone revealed that the Ispikan Conglomerate contains those fossils (*Nummulites and Discocyclina)* that are also present in Wakai Limestone. These fossils which were recovered form the sandstone component of the Ispikan Conglomerate are detrital and show little transportation Therefore it is concluded that the age of the Ispikan Conglomerate is Late Eocene i.e. younger than Wakai Limestone. This interpretation is different than all previous

[1] *Abstract of the dissertation submitted by K. Rehman for the degree of Master of Philosophy (University of Balochistan) under the research supervision of M.A. Farooqui and A.M. Kassi*

interpretations by various workers.

Ispikan Conglomerate was formed by a localized submarine mass flow (or sediment gravity flow) triggered by slope failure, fast sedimentation rate, or an earthquake. After the placement of Ispikan Conglomerate on the deeper marl facies of the Wakai Limestone, the tectonic status of the forearc basin changed. The basin started subsiding and provided enough space for the accumulation of thick piles of turbidites.

Abstract received December 21, 2000
Accepted December 30, 2000

ACTA MINERALOGICA PAKISTANICA
Volume 11 (2000)

Article Reference AMP11.2000/139-140/ISSN0257-3660

[1]SEDIMENTOLOGY, PETROLOGY AND DIAGENESIS OF MIOCENE-PLIOCENE HINGLAJ FORMATION, KHUZDAR AND BELA DISTRICTS BALOCHISTAN

KHAWAR SUHAIL, ABDUL SALAM KHAN AND MOHAMMAD AHMAD FAROOQUI
Centre of Excellence in Mineralogy, University of Balochistan, Quetta, Pakistan

ABSTRACT

The Miocene to Pliocene Hinglaj Formation comprises a significant Cenozoic strata in the southern Balochistan from Nal to Bela area and extends as far as in the southwest as Ormara, Mekran. The present study sought to document its depositional environment and some petrographic aspects including provenance and diagenesis. The facies distribution of these siliciclastic rocks reflects the complex interaction of tectonic, fluvial and marine processes. The marine processes include wind field, shelf slope, wave propagation and near bottom combined flow kinematics.

Thirteen different facies in the 1443 m thick Nal section and 7 facies in the 3780 m thick Bela section have been recognised on the basis of sedimentary structures and distinct faunal association. The facies of shale, shale with interbedded sandstone, arenaceous limestone and hummocky cross stratified sandstone were deposited on the lower shoreface. Bioturbated sandstone and shale clasted sandstone were deposited on lower shoreface to transition zone, whereas the deposition of low angle cross bedded sandstone, trough cross bedded sandstone and turriform gastropod shell lag facies are interpreted to have been deposited in upper to middle shoreface environment. The herringbone cross stratified sandstone with oyester shell fragments represents swash zone depositional environment.

The detailed facies analyses of the Nal and Bela sections of the Hinglaj Formation indicate foreshore beach and subaqueous deltaic to delta front environments respectively. The Nal and Bela sections have been divided into 7 and 4 zones respectively on the basis of the dominance of transgressive and regressive facies and are termed here as transgressive and regressive complexes. In the Nal section the transgressive complexes involve the shoreface retreat of the topographically higher parts of the beach during storms and continuous reworking of the sediment input by wave action during fair weather conditions. The shoreface retreat storm events produced shell lag beds of turriform gastropod and oyester which characterize the initial transgression and secondary transgression respectively. Shell lag beds are lacking in the Bela area and the transgression involves the continuous reworking of delta front sands. On the other hand the regressive complexes originated during the period of prolonged calm and quiescent intervals accompanied with lower reworking, reduced wave energy, climatic periodicity and sporadic subaerial exposures. The prodelta plumes (Bela area) and shale with thin interbeds of sandstone (Nal area) are the regressive complexes. The top most part of the Bela section

[1] *Abstract of the dissertation submitted by K. Suhail for the degree of Master of Philosophy (University of Balochistan) under the research supervision of A.S. Khan and M.A. Farooqui.*

reflects dry eoline environment also in which the reworking by wind and tidal cutting of the storm emplaced sands in the backshore area took place.

The petrographic analyses indicate that the Hinglaj Formation is composed of 28-88% monocrystalline quartz, 0-15% polycrystalline quartz, 0-13% chert, 0-8% plagioclase feldspar, 0-3% potash feldspar, 0-24% sedimentary rock fragments, 0-17% volcanic rock fragments, 0-4% plutonic rock fragments, 0-2% biotite, 0-3% muscovite, 0-2% heavy minerals including zircon, hornblende, sphene, rutile, epidote, 1-17% opaque minerals, 0-8% shell fragments, 1-35% algae fragments and 0-17% microfossils.

Extensive replacement of the incompetent non detrital constituents, after the pore filling by 15 to 39 % calcite and less commonly upto 15% iron oxide have been identified to be the major diagenetic modifications. The early cementation remained mostly stable through out the post depositional history.

The limited sandstone model data, when plotted on tectonic discrimination ternary diagrams, indicate a granitic provenance most probably the Chagai Magmatic Arc that presently lies in the northwestern part of Balochistan.

Abstract received April 15, 2001
Accepted April 16, 2001

ACTA MINERALOGICA PAKISTANICA
Volume 11 (2000)

Article Reference AMP11.2000/141-142/ISSN0257-3660

[1]GEOLOGY OF THE UPPER CRETACEOUS SUCCESSION, WEST OF SPERA RAGHA, DISTRICT PISHIN, PAKISTAN

MUHAMMAD SARWAR[2], AKHTAR MUHAMMAD KASSI[3], AND ABDUL SALAM KHAN[3]
[2]Centre of Excellence in Mineralogy, University of Balochistan, Quetta. Pakistan
[3]Department of Geology, University of Balochistan, Quetta. Pakistan

ABSTRACT

The study area is part of the western Sulaiman Thrust-Fold Belt, located to the south of Rud Malazai on Topographic map No. 34-N/7. Several new lithostratigraphic units have been identified in the area. On the basis of lithostratigraphy of the Middle Cretaceous to Paleocene succession the area has been subdivided into the Spera Ragha-Chinjun and the Urghargai-Mazu Ghar domains. The dividing line between the two domains is the Bibai Thrust. The Spera Ragha-Chinjun area comprises the Triassic Wulgai Formation, Jurassic Loralai Limestone, Cretaceous Parh Group, Bibai formation (*in-situ* volcanic rocks), an arbitrarily named Oxidized Transitional Succession, Fort Munro Formation, Moro Formation, Pab Sandstone, Paleocene Dungan Formation, Eocene Ghazij Formation and Kirther Formation and the Miocene-Pliocene Siwalik Group. Within the Urghargai-Mazu Ghar area the Triassic to Lower Cretaceous succession is similar to that of the Spera Ragha-Chinjun area, however, the Middle Cretaceous to Paleocene succession, comprises the Bibai formation (volcaniclastic sedimentary rocks), Mughal Kot Formation and Dungan Formation. The Triassic to Eocene successions of both the areas are indiscriminately overlain, with angular unconformity, by the Siwalik Group, which includes the Nagri and Dhok Pathan Formations. Also within the Urghargai-Mazu Ghar area the ?Pleistocene Spezendai breccia overlies, the Bibai and Mughal Kot Formations with angular unconformity.

The Middle Cretaceous to Paleocene succession of the Spera Ragha-Chinjun and Urghargai-Mazu Ghar areas show contrasting sedimentary characters and depositional environments. The Triassic-Jurassic succession of the Wulgai Formation is deep marine distal turbidites which gradually gives way to the shallow marine intraclastic limestone succession of the Loralai Limestone. This, along with the disconformity on top of the Loralai Limestone, shows an overall regressional trend and ultimate emergence. The Upper Jurassic - Lower Cretaceous belemnitic shale of the Sember Formation shows a transgressive shallow marine succession whereas the overlying Lower Cretaceous bio-micritic pelagic limestone and shale succession of the Goru Formation and Parh Limestone indicate continued trend of transgression and deposition in deep marine environment.

In the Spera Ragha-Chinjun area the Middle Cretaceous Bibai formation comprises only the *in-situ* basaltic rocks. They are nonconformably overlain by the shallow marine to transitional marine limestone, shale and sandstone succession of the arbitrarily named Oxidized Transitional Succession (OTS), Fort Munro Formation, Moro Formation, Pab Sandstone and Paleocene Dungan Limestone. This succession shows deposition in marginal marine conditions, which also shows several depositional breaks. This is overlain by the shale and sandstone succession of the Lower Eocene Ghazij Formation, which has been interpreted as deposits of a progradational delta. The Ghazij

[1] *Abstract of the dissertation submitted by M. Sarwar for the degree of Master of Philosophy (University of Balochistan) under the research supervision of A.M. Kassi and A.S. Kahn.*

Formation, in turn, is overlain by the shallow marine limestone succession of the Kirther Formation which indicate another episode of transgression of the sea.

In contrast to the shallow marine succession of the Spera Ragha-Chinjun area the Middle Cretaceous to Paleocene succession of the Urghargai-Mazu Ghar area was deposited in deep marine environments. The volcaniclastic sedimentary succession of the Bibai formation includes turbidites, mudstones, volcanic conglomerate, volcanic breccia and minor amount of pillow lava. These were deposited by gravity flows and high to low concentration turbidity currents of a submarine fan. The overlying Mughal Kot Formation also comprises a flysch-type succession of mudstone, sandstone, siltstone and arenaceous limestone, which are interpreted as turbidites. The lower part of the Dungan Formation, having interbedded shales and arenaceous limestone, is also deeper marine, however, shows an overall regression of the sea.

Thin section studies revealed that limestone of the Moro Formation is bio-clastic arenaceous and composed of quartz and fossil fragments. The Pab Sandstone is well sorted, angular to sub-angular quartz arenite and composed of quartz grains with minor proportion fossil fragments. Sandstone of the Mughal Kot Formation, classified as quartz arenite, is moderately to well sorted, sub-rounded to rounded and composed mostly of quartz grains with minor proportion of sedimentary fragments and opaque minerals. Detritus of sandstones of the Mughal Kot, Pab and Moro formations was derived from a crystalline massif (the Indian Craton), exposed to the southeast of the studied area.

Sandstones of the Nagri Formation and Dhok Pathan formations are moderately to poorly sorted, sub-angular to sub-rounded, grain-supported and composed of mineral grains as well as a variety of rock fragments. They may be classified as sub-lithic arenite and sedimentary arenite and have comparable characters to other studied areas of the Sulaiman and Kirther Fold-Thrust Belt. Their source area was the nearby exposed terrain of the Sulaiman Belt, which is comprised of a variety of sedimentary rocks of Triassic to Eocene age including the Muslimbagh Ophiolites.

Limestone of the Wulgai Formation has been recrystallized to marble. The Loralai Limestone may be categorized as bio-pelsparite and bio-pelmicrit. Limestone of the Goru Formation and Parh Limestone are bio-micritic comprising micro-forminifera and sparitic casts of radiolaria. Limestone of the Oxidized Transitional Succession is grainstone, packstone and bio-pelmicrite containing ooids, pellets and bio-clasts of foraminifera, brachiopod, gastropod and echinoderms. Limestone of the Fort Munro Formation is bio-pelsparite containing pellets and bio-clasts. Limestone of the Moro Formation is arenaceous, containing ooids and bio-clasts of foraminifera, bivalves, gastropods and quartz grains and may be categorized as wackstone and oo-biosparite. Limestone of the Dungan Formation is bio-sparite and composed of bioclasts of foraminifera, echinoderms, gastropods, crinoids' ossicles, brachiopods and bivalves. Limestone of the Ghazij Formation is also bio-sparitic and contains abundant bio-clasts of foraminifera, gastropods, bivalves and coralline algae. Limestone of the Kirther Formation is oo-biosparite containing ooids and bio-clasts of echinoderm, crinoids, brachiopods, coralline algae and foraminifera. The *in-situ* volcanic rocks of the Bibai Formation is porphyritic with phenocrysts of palgioclase and clinopyroxene. Palgioclase laths and minor amount of ferromagnesian minerals occur as groundmass. Amygdales are abundant and filled with zeolites. It may be categorized as amygdaloidal olivine basalt.

The Spera Ragha-Urghargai region shows intense deformation in the form of folds, thrusts, wrench (strike-slip) faults, joints and unconformities. Structures strike in a WNW-ESE direction. The pre-Siwalik succession of the Triassic to Eocene age is comparatively more deformed than the Miocene-Pliocene Siwalik succession, which overlies them with angular unconformity. Major structures include the Gogai-Bibai Syncline, associated Gogai and Bibai Thrusts, the imbricated Bibai Thrust Zone and the Spera Ragha Syncline. A conjugate set of wrench faults and joints are also present. Also the Triassic-Pliocene succession of the Spera Ragha-Urghargai region include three disconformities, a non-conformity and two angular unconformities. The area has suffered from various phases of prolonged and continued deformation, however, the two most notable phases of tectonic deformation being the pre-Siwalik and post-Siwalik phases. Since the division line between the contrasting domains of the Spera Ragha-Chinjun and Urghargai-Mazu Ghar is the Bibai Thrust, it is proposed that successions of the contrasting characters were deposited in different sedimentary environments and later on brought together and juxtaposed by the tectonic transport along the Bibai Thrust during the Late Eocene-Pleistocene. This proposal is based on the fact that the youngest rock succession involved in the Bibai Thrust is the Upper Eocene Kirther Formation and that the Bibai Thrust Zone is concealed under the unconformably overlying Miocene-Pliocene Siwalik Group.

Abstract received April 25, 2001
Accepted April 26, 2001

ACTA MINERALOGICA PAKISTANICA
Volume 11 (2000)

Article Reference AMP11.2000/143-146/ISSN0257-3660

ANNUAL REPORT
(2000)

NATIONAL CENTRE OF EXCELLENCE IN MINERALOGY, QUETTA

ACADEMIC STAFF

Director

Dr. Akhtar Mohammad Kassi, Professor of Geology, University of Balochistan continued working as Acting Director, C.E.M. The appointment of a permanent Director is still awaited. Dr. Kassi is Ph.D. from U.K. and has been teaching geology at the Department of Geology for the last 24 years.

Associate Professors	Specialization	Date of Joining C.E.M.
1. Shamim Ahmad Siddiqui	Economic Geology, Ph.D. (U.S.A.)	01-Jan-1998
2. Abdul Salam Khan	Sedimentology, Ph.D. (U.K.)	01-Jan-1998
3. Jawed Ahmad	Clay Mineralogy, M.Phil. (Univ. of Balochistan)	01-Apr-1980
4. Khalid Mahmood	Ophiolites, Ph.D. (France)	05-Nov-1989
5. Mohammad Ahmad Farooqui	Sedimentary Geology and Tectonics, Ph.D. (U.S.A.)	05-Nov-1989
Assisstant Professors		
6. Mehrab Khan	Ophiolites, Ph.D. (Univ. of Balochistan)	05-Nov-1989
Visiting Professors		
7. Syed Mobasher Aftab	Hydrogeology, Ph.D. (Turkey), Chief Hydrogeologist, P.H.E.D., Government of Balochistan, Quetta.	
8. Din Mohammad Kakar	Sedimentology, M.Phil. (Univ. of Balochistan), Assistant Professor, Geology Department, University of Balochistan, Quetta.	

ADMINISTRATIVE/TECHNICAL STAFF

	Name	Designation	Date of joining C.E.M.
1.	Mirza Manzoor Ahmad	Accounts Officer	07-May-1980
2.	Syed Shahabuddin	Administrative Officer	28-May-1977
3.	Khushnood Ahmad Siddiqui	Senior Technician	13-Jul-1976
4.	Abdul Ghafoor	Assistant Librarian	02-May-1985
5.	Lal Mohammad	Superintendent	12-May-1973
6.	Hussainuddin	Photographer	16-Jun-1981
7.	Syed Rasool Mahjoor	Stenographer	06-Jun-1990
8.	Ghalib Shaheen	Stenotypist	17-Jul-1985

	Name	Designation	Date of joining C.E.M.
9.	Ahmad Khan Mangi	Draughtsman	01-Jul-1981
10.	Musa Khan	Laboratory Supervisor	20-Aug-1977
11.	Sher Hassan	Store Keeper	22-Aug-1977
12.	Mohammad Anwar	Assistant	18-Sep-1973
13.	Juma Khan	Assistant	12-Jun-1985
14.	Ikram Ali	Laboratory Assistant	13-Sep-2000
15.	Hameedullah	Laboratory Assistant	09-Dec-2000
16.	Abdul Malik	Senior Clerk	28-Apr-1987
17.	Manzoor Ahmad	Junior Clerk	26-May-1995
18.	Shabbir Ahmed	Junior Clerk	13-Sep-2000
19.	Mohammad Tariq	Junior Clerk	09-Dec-2000
20.	Ali Mohammad	Driver	17-Jul-1984
21.	Saleh Mohammad	Driver	18-Aug-1990
22.	Ghulam Rasool	Junior Mechanic	20-Aug-1977
23.	Mohammad Rafiq	Peon *(Naib Qasid)*	12-Oct-1978
24.	Sikandar Khan	Peon *(Naib Qasid)*	30-Apr-1976
25.	Atta Mohammad	Peon *(Naib Qasid)*	25-Mar-1986
26.	Abdul Salam	Peon *(Naib Qasid)*	12-Dec-2000
27.	Mohammad Din	Peon *(Naib Qasid)*	12-Dec-2000
28.	Murad Baksh	Peon *(Naib Qasid)*	15-Nov-2000
29.	Abdul Wadood	Chowkidar	26-Jan-1992
30.	Amir Baksh	Chowkidar	11-Sep-2000
31.	Nazir Masih	Janitor	01-Apr-1977

ACADEMIC/RESEARCH ACTIVITIES

Khalil-Ur-Rehman, under the supervision of M.A.Farooqui, and A.M. Kassi has submitted his M.Phil. thesis in December, 2000 and is waiting for evaluation and final examination.

Khawar Suhail, under the supervision of A. Salam and M.A.Farooqui, has submitted his M.Phil. thesis in April, 2001and is waiting for evaluation and final examination.

Muhammad Sarwar, under the supervision of A.M.Kassi, and A. Salam Kahn has submitted his M.Phil. thesis in May 2001 and is waiting for evaluation and final examination.

Muhammad Rahim Jan and Muhammd Zahir, under the supervision of M.A.Farooqui have also completed their M.Phil. research projects and are expected to submit their thesis in July 2001.

By the end of December 2000, the C.E.M had the following two Ph.D. and seventeen M.Phil. students working on various aspects of the geology of Balochistan:

	Student	Supervisor	Co-Supervisor	Project Title
			Ph.D. PROJECTS	
1.	Din Muhammad Kakar	Akhtar M. Kassi	Mohammad Ahmad Farooqui	Geology of the Tertiary Khojak Form-ation of Pishin, Muslimbagh and Chaghi Districts, Balochistan
2.	Ghulam Nabi	Abdul Salam	Jawed Ahmad	Petrography and depositional environment of Ghazij Formation (Eocene) Balochistan.
			M. PHIL. PROJECTS	
1.	Atif Saleem	Khalid Mahmood	Mehrab Khan Baloch	Nature of mafic intrusions in the mantle section of Saplai Tor Ghar Ophiolites related to mantle rocks, Muslim Bagh, Balochistan.

	Student	Supervisor	Co-Supervisor	Project Title
2.	Ahmad Jan	Abdul Salam Khan	Jawed Ahmad	Sedimentological and structural studies of the coal bearing Ghazij Formation near Khost/ Shahrig, Balochistan.
3.	Khalil-Ur-Rehman	Mohammad Ahmad Farooqui	Akhtar Mohammad Kassi	Petrology and provenance of Paleocene (?) Ispikan Conglomerate, SW Makran and its implications on the tectonic evolution of Makran Region.
4.	Mohammad Zahir Kakar	Mohammad Ahmad Farooqui	Din Mohammad Kakar	Depositional environment and Diagen-esis of Lower Cretaceous Sembar Forma-tion, Balochistan.
5.	Syed Ashrafuddin	Mohammad Ahmad Farooqui	Mehrab Khan Baloch	Study of K-T Boundary in the western Sulaiman Foldbelt, Pakistan.
6.	Mohammad Rahim Jan	Mohammad Ahmad Farooqui	--	Geology and mineral resources of part of Makran Coast, Balochistan.
7.	Azhar Hussain	Mohammad Ahmad Farooqui	Khalid Mehmood	Petrology, stratigraphy and lithofacies analysis of Dungan Formation (Paleocene), Sulaiman Foldbelt, Balochistan.
8.	Khawar Sohail	Abdul Salam	Mohammad Ahmad Farooqui	Petrology, sedimentology and diagenesis of Miocene-Pliocene Hinglaj Formation, District Khuzdar and Bela Balochistan.
9.	Hussain Buksh	Mobasher Aftab	Jawed Ahmad	Hydrogeological investigations of Kalat Sub-Basin, Balochistan.
10.	Abdul Hadi	Mobasher Aftab	Mehrab Khan Baloch	Hydrogeological investigation of Pishin Sub-Basin Balochistan.
11.	Arif Ali	Mobasher Aftab	Jawed Ahmad	Assessment of groundwater budget of Mangocher Valley, Balochistan.
12.	Mohammad Sarwar	Akhtar M. Kassi	Abdul Salam	Geology of the area west of Spera Ragha, District Ziarat, Balochistan.
13.	MuhammadUmar	Abdul Salam	Akhtar M. Kassi	Sedimentological studies of Upper Cretaceous Pab Sandstone, Kirther Fold Belt Balochistan.
14.	Abdul Razique	Shamim Ahmed Siddiqi	--	Copper mineralization in Chaghi metal-logenic province, Balochistan.
15.	Muhammad Ishaq	Mehrab Khan Baloch	Khalid Mehmood	Metamorphic rocks associated with Mus-lim Bagh Ophiolites, Balochistan.
16.	Mushtaq Ahmad Pathan	Khalid Mehmood	Mehrab Khan Baloch	Origin and mode of occurrence of chro-mites in the mantle section of Muslim Bagh Ophiolites..
17.	Razzak Abdul Manan	Shamim Ahmed Siddiqi	--	Iron ore deposits of Dilband area, Kalat.

Faculty members continued supervision of their research students. A number of students completed their field studies/work. Following field studies were carried out during 2000:

Research Supervisor	Student	Program of Study	Areas visited
Abdul Salam	Muhammad Umar	M.Phil.	Karkh, Khuzdar, and Bela areas
Mohammad A. Farooqui	Muhammad Rahim Jan	M.Phil.	Prome valley, Panjgoor, Makran
Khalid Mahmood	Mushtaq Ahmad Pathan	M.Phil.	Muslim Bagh

Beside student's research projects, the faculty members remained involved in the following research projects:

	Title of the Research Project	Principal Investigator	Co-Investigators	Funded by
1	Structural & Textural studies of mantle rocks from Muslim Bagh ophiolites.	Khalid Mahmood	Mehrab Khan	UGC
2	Facies distribution, depositional environments and Petroleum prospects of the Foreland Basin sediments, Kirthar fold-belt, Balochistan, Pakistan.	Abdul Salam Khan	Akhtar M. Kassi	PSF
3	Study of Sedimentological and Structural Aspects of Selected Sites in the Makran Accretionary Belt, Pakistan.	Akhtar Mohammad Kassi	A. Salam Khan, M. A. Farooqui and Din Mohammad Kakar	UGC
4	Industrial utilization of Nickel and Manganese deposits associated with Muslim Bagh and Bela Ophiolites., Balochistan	Shamim Ahmed Siddiqi	M.A.Farooqui and Shabbar Atiq (PCSIR)	PCSIR and UGC
5	Sedimentology, geochemistry and geochronology of Quaternary deposits of selected playa lakes, Balochistan.	Muhammad Ahmad Farooqui	Akhtar M. Kassi and A. Salam Khan	UGC
6	Geology, geochemistry, and origin of iron ore deposits, Kalat District, Balochistan	Shamim Ahmed Siddiqi	–	UGC
7	Metamorphic rocks associated with ophiolites	Mehrab Khan	Khalid Mahmood	UGC
8	Hypogene and supergene copper-gold systems around Koh-e-Dalil, Western Chaghi, Balochistan.	Shamin Ahmad Siddiqi.	--	UGC
9	Geology of the Cretaceous-Paleocene succession, Sulaiman Thrust Belt, Pakistan	Akhtar M. Kassi	A. Salam Khan, M.A.Farooqui	UGC
10	Petrology and sedimentology of coal bearing Ghazij Formation, Balochistan	Abdul Salam Khan	Jawed Ahmed	UGC

(UGC; University Grants Commission. PSF; Pakistan Science Foundation, PCSIR; Pakistan Council for Scientific and Industrial Research).

Abdul Salam proceeded to Keele University U.K. in Octoober 2000 under postdoctoral fellowship by the Commonwealth Organization for the year 2000-2001. He is studying the sedimentology of Upper Cretaceous Pab Sandstone, Kirther Foldbelt Pakistan during this fellowship.

M.A. Farooqui has been selected for Fulbright postdoctoral grant to study geochemical aspects of Miocene Diz Formation, Makran, at Utah State University, Logan, Utah, USA. He is expected to start his work in September 2001.

Khalid Mahmood has also been selected for the grant of Postdoctoral Fellowship by the Commonwealth Organization for the year 2001-2002. He will be studying Muslimbagh ophiolites during this fellowship which is expected to start in October 2001.

Akhtar M. Kassi, A. Salam Khan, and Mehrab Khan participated in the Third South Asia Geological Congress (GEOSAS-III) held at Lahore in September 2000 and presented their research findings.

Compiled by M.A. Farooqui

INSTRUCTIONS FOR AUTHORS

Send three unbound copies, not stapled, of the complete manuscript to Editor *Acta Mineralogica Pakistanica*, Centre of Excellence in Mineralogy, University of Balochistan, Quetta Pakistan, along with a computer disk. Create and format your document in WordPerfect 5 or higher (for windows), or MS Word, however, manuscripts saved in any major wordprocessor will also be accepted. Mark the computer disk with the name of the principal author, abbreviated title of the paper, name of the file and the software in which the document was created. We will not retype manuscripts! Except for minor editing, content will be printed as it is received on computer disk or returned to be redone if required. **Please note that manuscripts received without a computer disk shall not be considered for publication.**

Type or laser print manuscripts, single sided, double spaced on A4 size paper including abstract, references, figure captions, appendices and tables. Leave one inch margin on all four sides and do not use extremely small font size. Number all pages beginning with the abstract. Exact format of the title page is unimportant because it will be changed upon computer formatting for electronic typesetting, but supply the following items clearly differentiated in the following order

❶ running head: a descriptive condensation of the title, not exceeding 80 characters, in all capital letters
❷ title, in all capital letters
❸ list of authors, in all capital letters, all in single paragraph, with first names or initials first, with superscripts to identify the addresses
❹ list of addresses, in capital and small letters, superscripted to correspond to the list of authors (use asterisks to indicate current address when different from original address).
❺ the word 'manuscript received' with a generous space for a date stamp

In the text, use the following format for heading

first order headings are **BOLD CAPITAL CENTRED**;

second order headings are ***BOLD ITALIC CAPITALS CENTRED***;

third order headings are left indented **bold Small Letter**

fourth order headings are left indented ***bold Italic Small Letter***

FIGURES: All line figures (maps, drawings etc.) and photographs should be clear, sharp, and legible originals in black and white colours only. Submit figures and photographs as large as possible but no larger than 8½" x 11". Line figures and photographs may be reduced during printing for the prupose of saving space, therefore, lettering on figures should be large enough to be ≥1.5mm when figure is reduced to final width. Photographs should be of superior quality, black and white only, glossy, ideally 5" x 7". If necessary authors should indicate crop lines on photos before submittal. Composite photos, line drawings and multi-part figures must have identifying Roman capital Letters applied firmly and permanently in the upper left corner. Publisher shall not be responsible for such letters falling off during review and production. Identity all figures on the back by authors name and figure number. List figure captions on a separate page or pages at the end of the manuscript. In the text the word *figure* is capitalized and spelled out e.g. Figure 1; it is capitalized and abbreviated when used parenthetically e.g. (Fig. 1). Colour plates and foldouts can only be published if the author bears the full extra cost in advance of publication; contact the Editor for details. All permissions for quotations, photographs, illustrations, etc. are the author's responsibility and should be acknowledged in the paper.

KINDS OF CONTRIBUTIONS

Research Papers Articles dealing with original unpublished research results in the multifaceted field of Earth Sciences covering Economic Geology, Petroleum Geology, Mineral Exploration, Mineralogy, Petrology, Crystallography, Tectonics, Structural Geology, Hydrogeology, Aqueous Geochemistry, Geophysics, Tectonophysics, Geochemistry, Mineral Chemistry, Geochronology, Historical Geology, Environmental Geology, Engineering Geology, Paleontology, Stratigraphy, Sedimentology, Oceanography, Coastal Geology, Marine Geology and Geology Education

Review Articles Articles reviewing the research results, theories, models, or opinions presented in the already published literature.

Book Reviews: Reviews of books useful to the readers of the Acta Mineralogica Pakistanica.

Short Communications Short articles (up to four printed pages) dealing with more personal or opion-oriented viewpoints or observation on any aspect of the Earth Sciences.

Abstracts Abstracts of original unpublished research results shall also be considered for publication. The abstracts should not be longer than two printed page, including figures if any.

Announcements Announcements of events of interest to the readers of Acta Mineralogica Pakistanica.

Please make sure that your contribution/s fulfill the following criteria of scientific publications:
Original data and information,
Clear conceptual approach of analysis,
Useful information from academic and practical considerations, and
Simple style and straight expression

ACTA MINERALOGICA PAKISTANICA

VOLUME 11

2000

CONTENTS

ARTICLES

ABSTRACTS

REPORTS